Interim Report

Jackson State University

Interim Report - Ike Dike Concept for Reducing Hurricane Storm Surge in the Houston-Galveston Region

Bruce A. Ebersole, Thomas C. Massey, Jeffrey A. Melby, Norberto C. Nadal-Caraballo, Donald L. Hendon, Thomas W. Richardson, Robert W. Whalin

Sep 2015

Contents

1 Overview

A consortium of universities and other partners, led by Texas A&M University at Galveston, is investigating the feasibility of a coastal barrier to greatly reduce hurricane-induced coastal flooding in the Houston/Galveston region. In 2008 Hurricane Ike produced considerable storm surge and damage in the area, raising awareness of the flooding threat to the region posed by hurricanes. Had Ike tracked and made landfall 20 to 40 miles farther to the southwest, storm surge in the Houston/Galveston region would have been much more devastating. In support of the feasibility study and as members of the study team, Jackson State University and the U.S. Army Engineer Research and Development Center's Coastal and Hydraulics Laboratory (ERDC) are collaborating to quantify the reduction in flooding that can be expected with a long coastal dike and gate system. This protective measure, called the Ike Dike concept, has been proposed and advanced by the Texas A&M University at Galveston (Merrell 2012). This report presents results from the initial assessment of the Ike Dike's flood mitigation benefits.

Utilizing the latest state-of-the-science coupled computer models for hurricane winds, pressures, waves and storm surge, the study is comparing inundation due to hurricane surge for existing conditions with reduced inundation achieved by a proposed 17 foot high Ike Dike that stretches from Freeport in the west to Sea Pines State Park in the east (at Sabine Pass), which would provide risk-reduction to the entire Galveston Bay area during a severe hurricane. The models were first set up and applied as part of the Federal Emergency Management Agency's (FEMA) Risk MAP study to update coastal flood risk maps for the Texas coast, then adapted and modified for use in the present feasibility study (USACE 2011). These are the same models that have been developed and applied by the U.S. Army Corps of Engineers in their recent assessments of coastal flood risk done for FEMA, the Nuclear Regulatory Commission, and in their internal design of flood-risk-reduction measures, including measures constructed in the New Orleans area.

Initial results documented in this report were derived from a total of 50 hypothetical synthetic hurricane simulations. Twenty-five different hurricanes were simulated for both the existing conditions reflecting a post-Ike (2008) condition and the with-Ike-Dike condition. Twenty-one of the storms involved a very intense, rare, but possible storm having a

900-mb central pressure. Each of those 21 storms had a different path, characterized by one of three general approach directions (south, south-southeast, and southeast). The other 4 storms had varying intensities, central pressures of 900 mb, 930 mb, 960 mb, 975 mb, but were all on a "direct- hit" path approaching from the south-southeast. The direct-hit path involved landfall at the City of Galveston and a storm track along the western shoreline of Galveston Bay.

These 25 storms were chosen as a "bracketing set." They represent a small subset of storms considered in the FEMA Risk MAP project (USACE 2011). The bracketing set was intended to achieve the following objectives: understanding exactly how hurricane storm surge is generated in the region and in different locations within the region for both the existing and with-dike conditions; quantify how high the storm surge can reach for this severe rare hurricane intensity (900 mb central pressure) in those key areas that have the greatest potential for damage and losses; characterize how the peak surge varies from location to location throughout the region for a particular storm and how storm track influences both the surge development process and peak surge. The "direct-hit" storms were selected to provide insights into how storm surge varied as a function of intensity, primarily. The effectiveness of the Ike Dike in reducing storm surge was examined for all storms.

Results from the "direct-hit" were used to assess the reduction in damages/losses associated with the Ike Dike. This economic analysis work is being done by the economics team as part of the feasibility study, work that also is being led by Texas A&M University at Galveston.

In addition to analysis of the bracketing set, ongoing work will involve additional simulations for several "historic" Texas hurricanes: the 1900 Galveston Hurricane, a re-tracked Hurricane Ike and a re-tracked Hurricane Carla, both re-tracked to make landfall at San Luis Pass, which is about 25 miles southwest of Bolivar Roads. The general populace can better relate to historic storms versus synthetic hypothetical storms, and these storms have actually occurred in the past 115 years. The 1900 Galveston Hurricane devastated the City of Galveston. Hurricane Carla in 1961 was the most intense storm, in terms of maximum wind speed just before landfall, to impact the Texas coast, based on the available record since the late 1800's.

Flooding associated with three "proxy" storms will be examined. The three proxy storms will be selected from among hypothetical storms that have been simulated and the historic storms to approximate peak water surface elevations at a small number of points that lie along the western side of the bay associated with the 10-yr, 100-yr and 500-yr average recurrence intervals. Examination of proxy storms will provide an initial probabilistic assessment of economic damages and losses. The proxy storm approach is being adopted as balance between level of effort, technical rigor, and resources available to perform the work (time and funding).

The influence of sea level rise on storm surge and economic damages/losses will be examined for the three historic storms and the three proxy storms. A projected contribution to global sea level rise of 1.5 feet over the next 50 years will be adopted for this sensitivity study. The subsidence contribution to relative sea level rise, which can have significant local variation, will be neglected in this preliminary analysis. The effects of sea level rise will be investigated for both existing and with-dike conditions.

A rigorous assessment of flood risk, and the risk of damage/loss with the Ike Dike in place, requires simulation of a much larger set of storms, characterization of the flooding and economic damage/loss for each storm, and estimation of the probability of occurrence of each storm that is simulated. Despite the valuable insights gained from work involving a relatively small set of hypothetical hurricanes, historic hurricanes, and proxy storms, it does not thoroughly or adequately consider the probability, or likelihood, that a particular hurricane will occur (and the spatial variability in flooding and damages/losses it causes). It does not adequately capture the benefits of the dike for a wide range of hurricanes (and their characteristics), some severe, others not as severe. As such, the work described in this report serves a precursor to a more rigorous effort that is proposed to characterize the probability of flooding for existing conditions and conditions reflecting the dike in place which will involve a much larger set of hypothetical synthetic storms (on the order of 200) having a wider range of characteristics such as intensity, track, forward speed and radius-to-maximum winds.

A proposed plan for the rigorous assessment of flood risk and the risk of damage/losses, is contained in the last chapter of this report.

2 Storm Surge Model Validation for Hurricane Ike

Introduction

The modeling reflected in this report used state-of-the-science coupled computer models for hurricane winds and pressures, waves and storm surge. These are the same models that have been developed and applied by the U.S. Army Corps of Engineers (USACE) to design flood-risk-reduction measures, including measures constructed in the New Orleans area following Hurricane Katrina. The models also were used by the USACE in recent assessments of coastal flooding risk that have been performed for FEMA and the Nuclear Regulatory Commission. The models are run as a coupled modeling system using the USACE Coastal STORM Modeling System (CSTORM-MS). The system is comprised of the following:

a) tropical cyclone Planetary Boundary Layer (PBL) model, Cardone et al. (1992), Cardone et al. (1994), Thompson and Cardone (1996), Cardone and Cox (2009),

b) deep water wave model, WAM, WAMDII Group (1988), Komen et al. (1994), Gunther (2005), Smith et al. (2010),

c) shallow water wave model, STWAVE, Smith et al. (2001), Smith (2007), Smith et al. (2010), Massey et al. (2011), and,

d) storm surge model, ADCIRC, Luettich et al. (1992), Westerink et al. (1992), Blain et al. (1994), Dietrich et al. (2010a and 2010b).

The models were set up and applied to the north Texas coast as part of the FEMA Risk MAP project to update coastal flood risk maps for the entire Texas coast, then adapted and modified for use in the present feasibility study.

One change was made to the wave modeling approach that was originally adopted in the Risk MAP study. In the Risk Map study, the regional north Texas shallow water wave model domain that included the Houston-Galveston region was first simulated with the half-plane version of STWAVE. The half-plane wave model then provided boundary conditions

to a nested wave model within Galveston Bay which was run with the full-plane version of STWAVE. The half-plane version of STWAVE only considers waves approaching the coast in a 180-degree window relative to the coastline, which is a reasonable approximation for the open coast of Texas. In the full-plane model waves can approach from a full 360-degree window, which is required to accurately simulate wave conditions around the periphery of a fully- or semi-enclosed bay, like Galveston Bay. For this feasibility study, in light of computational efficiency advancements made to the CSTORM-MS modeling system, the wave modeling was improved by simulating shallow water waves for the full north Texas regional domain using the full-plane version of STWAVE.

Storm surge simulations of several extreme 900-mb storms included in the original bracketing set of storms, using the original FEMA Risk Map study grid mesh, became numerically unstable. To stabilize the simulations, global slope limiting was applied to all of the bracketing set of storms, for all time steps, to produce the original bracketing set results.

In an effort to reduce the error associated with applying slope limiting globally, on the entire computational domain, a more localized procedure for applying slope limiting was sought and developed. A polygon was created which encompassed the very shallow nearshore open Gulf region (shallower than approximately 10 m water depth), from Sabine Pass to the south of Texas; and it extended inland to the landward side of the natural dune system, encompassing the jetty systems at the passes, and extending into the throats of the passes. These were the areas where model instabilities tended to develop for several of the most extreme hurricanes in the bracketing set. The application of slope limiting was geographically restricted to those areas within the polygon. A trigger also was applied to restrict application of slope limiting to those time steps when the water surface slope exceeded a threshold value.

One other change was made to the model set-up that was applied in the original bracketing set of storm simulations. The bottom friction coefficient on the Louisiana and Texas continental shelves was reduced to enable a better simulation of the wind-driven hurricane surge forerunner that can occur along the Texas shelf for approaching hurricanes. The reduced bottom friction enabled higher along-shelf water velocities to develop under wind forcing, which in turn produced a greater coriolis-driven Ekman setup at the coast, i.e. the surge forerunner. Bottom friction on the continental shelf was reduced to levels that were quite similar to

those used in the FEMA study; and the level of accuracy of forerunner simulation achieved with this revised modeling procedure is quite similar to that achieved in the original FEMA study.

The change in wave modeling approach, while improving the quality of the wave computations, was not expected to significantly alter the computed storm surge. To verify this, and as a check of the revised coupled modeling system's capability to replicate the accuracy of results obtained in the original FEMA Risk Map study, the modeling system was rerun for Hurricane Ike. The re-validation also provided a check on the performance of and influence of the polygon-based application of slope limiting.

Extensive verification of the coupled models was performed in the original Risk MAP study for several historic hurricanes, including Ike. Verification included comparisons between ADCIRC results and high water marks collected by different agencies as well as comparisons between water surface elevation hydrographs computed using ADCIRC and hydrographs measured by the U.S. Geological Survey (USGS), see East et al (2009), by the National Oceanic and Atmospheric Administration (NOAA), by the Texas Coast Ocean Observing Network (TCOON) and by Kennedy et al (2010, 2011).

At present, the economic analysis of damage/losses prevented by the Ike Dike concept relies solely on maximum water surface elevations (still-water elevations) that are simulated with the ADCIRC storm surge model. In light of this fact, the re-evaluation of model accuracy for Hurricane Ike only considered a comparison of computed and measured high water marks.

Computed Maximum Water Surface Elevations for Hurricane Ike

The maximum water surface elevation field (in feet) computed for Hurricane Ike using the ADCIRC model, with the modified modeling procedure, is shown in Figure 2-1. At each computational node of the ADCIRC grid mesh, the maximum water surface elevation is recorded as the simulation progresses and saved to an output file. At the conclusion of the simulation, the maximum elevation file reflects the maximum water surface elevation reached at each and every grid node in the active model domain, regardless of when the maximum occurred during the simulation. Figure 2-1 graphically displays the maximum water surface elevation

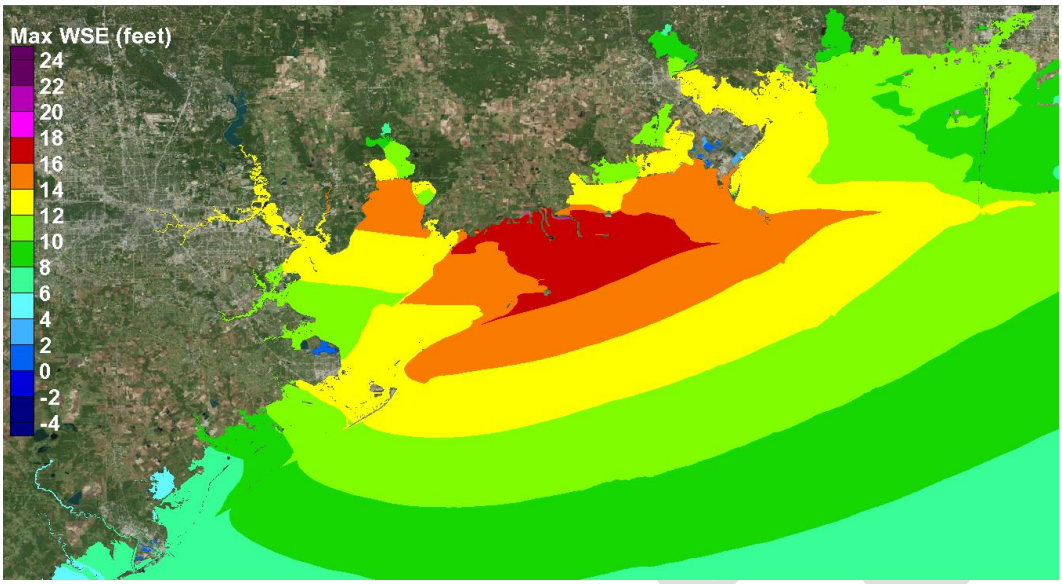

Figure 2-1. Map of computed maximum water surface elevations for Hurricane Ike

(WSE) field for the entire model domain. The maximum WSE computed using ADCIRC is directly comparable to those high water marks that reflect a still water level.

The zone of maximum computed peak storm surge occurs to the northeast of Galveston Bay, between the Bay and Port Arthur, with peak surges slightly exceeding 17 ft. Computed peak surges near the City of Galveston were 13 to 14 ft. From the City of Galveston moving north, peak surge values decrease along the western shoreline of Galveston Bay to values of 11 to 13 ft along Texas City, and 11 to 12 ft in the vicinity of Clear Lake. Peak surges then increase along the western shoreline to values of 13 to 14 ft in the upper reaches of the Houston Ship Channel. Peak surge along Galveston Island decreases from 13 to 14 ft at its northern end to 8 to 9 ft at the southern end. Peak surge along Bolivar Peninsula is 14 to 16 ft. All elevations are relative to NAVD88, the vertical datum used in the storm surge modeling.

Comparison with High Water Marks

A set of measured high water marks were derived from the same data sources that were considered in the original Risk MAP study: 1) high water marks extracted from recorded water surface elevation hydrographs that were measured with pressure gages deployed by the USGS, and reported by East et al (2009), 2) high water marks extracted from recorded hydrographs that were measured with permanent pressure gages which

are maintained by TCOON and NOAA, and reported on the NOAA Tides and Currents web site, 3) high water marks estimated from graphical plots of water surface elevation hydrographs that were measured with gages deployed by Kennedy et al (2011) ; and 4) a set of visually identified high water marks taken from FEMA's Texas Hurricane Ike Rapid Response Coastal High Water Mark Collection (2008) effort. Even though these same data sets were included in the original Risk Map model validation work, the exact data set which was adopted for each of the various data sources might be slightly different than the data set used here due, for example, to different decisions on which data were included/excluded from the analysis for various reasons.

An additional set of high water marks that were acquired within Galveston Bay by the Harris County Flood Control District (HCFCD), immediately following Hurricane Ike, that were not considered in the original Risk Map study, were considered in this re-evaluation. These data were acquired via personal communication with Mr. Steven Fitzgerald, Chief Engineer with HCFCD.

Only visually identified high water marks that reflect still-water elevations were considered in the analysis. These are the only types of high water marks that are appropriate for direct comparison with water surface elevations computed with ADCIRC. Only high water marks that were rated by the collectors as being of good or excellent quality were retained in the analysis. High water marks that were acquired at locations which did not fall within the computational grid mesh or were located a significant distance away from the inundated parts of the model domain were excluded from the analysis.

High Water Marks from Gage Measurements of Water Surface Elevation

High water marks from NOAA/TCOON maintained pressure gages were extracted by first displaying the water surface elevation hydrograph within the NOAA tides and currents web site (http://tidesandcurrents.noaa.gov/stations.html?type=Water+Levels), scrolling the cursor over the water surface elevation hydrograph to the time of maximum elevation and reading the maximum value directly from the screen.

The high water marks from gages deployed by the USGS were derived from hydrographs comprised of measured pressures every minute that

were subsequently converted to water surface elevation. See East et al (2009) for details of the data processing. Time series at perhaps a third of the locations showed data-point-to-data-point variability in water surface elevation due to the influence of short-period wind waves that were reflected in the pressure measurements. The degree of wave-induced variability varied for different gages.

The type of modeling being done here to simulate storm surge does not compute water surface elevation changes on time scales of seconds and fractions of a second, which occur for short-period wind waves. Instead a "mean", in the time sense, or much more slowly varying water surface elevation (often called the still water level) is computed by the ADCIRC model.

In an attempt to filter out these higher-frequency fluctuations, or "noise," from the measured data and develop an estimate of the still water level that is consistent with the water surface elevation, or storm surge, being computed with the models, a 20-min average was computed at approximately the time of maximum water level. The 20-min average value was used as the measured high water mark for that location.

The quality of the measured hydrographs was good, and high water marks derived from the measured hydrographs are considered to be the most accurate data which are available, more so than high water marks that are not based on measured data but rather reflect some other type of marking left behind by the elevated surge and waves such as the FEMA and HCFCD high water marks.

USGS/NOAA/TCOON gage-based high water marks from Matagorda, Brazoria, Galveston, Harris, Chambers, and Jefferson counties in Texas, and Cameron parish in Louisiana, were considered in the analysis. All high water marks that were located within the model domain were retained in the analysis; whereas, other marks that fell outside the model domain or fell outside the region of simulated inundation were not considered in the analysis.

The locations of 41 USGS gages, whose data were retained in the analysis, are shown as yellow dots in Figure 2-2. Locations of the 6 NOAA-TCOON gages are shown as magenta dots, and locations of the 5 Kennedy et al

Figure 2-2. Locations of USGS (yellow), NOAA/TCOON (magenta) and Kennedy (purple) gages.

gages are shown with purple dots. The Kennedy et al gages were deployed along the open coast, in relatively shallow water, at fairly regular alongshore spacing; although, data from the gage located closest to the City of Galveston were not available.. The NOAA/TCOON gages were mostly deployed within the bay systems, except for a single gage along the open coast at Galveston Pleasure Pier.

This set of gage-derived high water marks reflects a broad regional coverage, centered about the Houston-Galveston area which is of prime interest. Comparisons between surge model maximum water surface elevations and this measured data set best illustrates model accuracy for the entire region, with gages distributed rather uniformly throughout the region.

A scatter plot of the comparison between maximum water surface elevations computed with the ADCIRC model and gage-derived high water marks for each of the 52 gages is shown in Figure 2-3. A 45-degree dashed line also is shown in the figure. If there is perfect agreement between measurements and model results, then all points would fall on the dashed line. The distance away from the dashed line indicates the magnitude of error reflected in the model results.

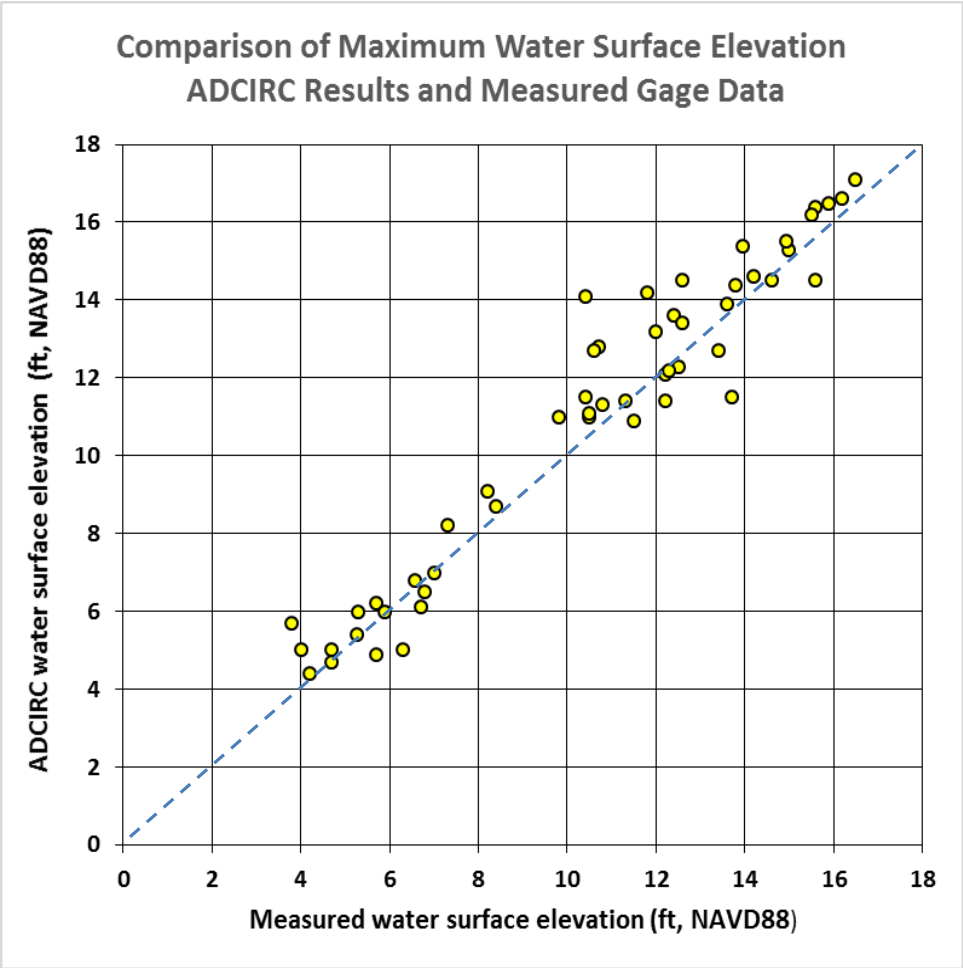

Figure 2-3. Scatter plot of measured and modeled maximum water surface elevations for all hydrograph-derived high water marks.

Average error and average absolute error were computed for all pairs of modeled and measured values, for each gage location. Average error was computed by subtracting the measured water surface elevation from the modeled elevation, and then taking an average. An average error of 0.47 ft was computed using model-measurement data pairs for the 52 gage locations. The positive average value indicates a slight positive bias, i.e., the model results are slightly higher than the measured values. Average absolute error provides a measure of the average magnitude of the difference between measured and modeled values, without regard for whether the modeled value is greater than or less than the measured value. The average absolute error for the entire data set was 0.81 ft. This error measure provides an overall estimate of model skill and accuracy in making peak storm surge estimates as part of the feasibility study, using the current model setup.

The scatter plot also reveals the slight high bias in the modeled high water marks, i.e. on average, modeled high water marks slightly exceed measured values. The modeled/measured high water mark differences and the bias evident in Figure 2-3 for the Houston-Galveston region are quite similar to the results for Hurricane Ike shown in the original FEMA Risk MAP study.

Visually Estimated High Water Marks

The locations of 69 high water marks acquired by FEMA following Hurricane Ike are shown as light blue dots in Figure 2-4. These data also are reasonably well distributed, regionally, to both the northeast and southwest of the Houston-Galveston region. Marks acquired to the northeast of Galveston Bay appear to have been mostly acquired along the inland edge of inundation caused by the hurricane. Coverage is not as uniformly distributed as was coverage of the gage-derived high water marks.

A scatter plot of the comparison between ADCIRC results and 69 FEMA high water marks is shown in Figure 2-5. The plot shows trends that are similar to those seen for the gage-derived high water marks. The average error for this data set was 0.44, and average absolute error was 0.98 ft; both results were similar to results for the previous data set.

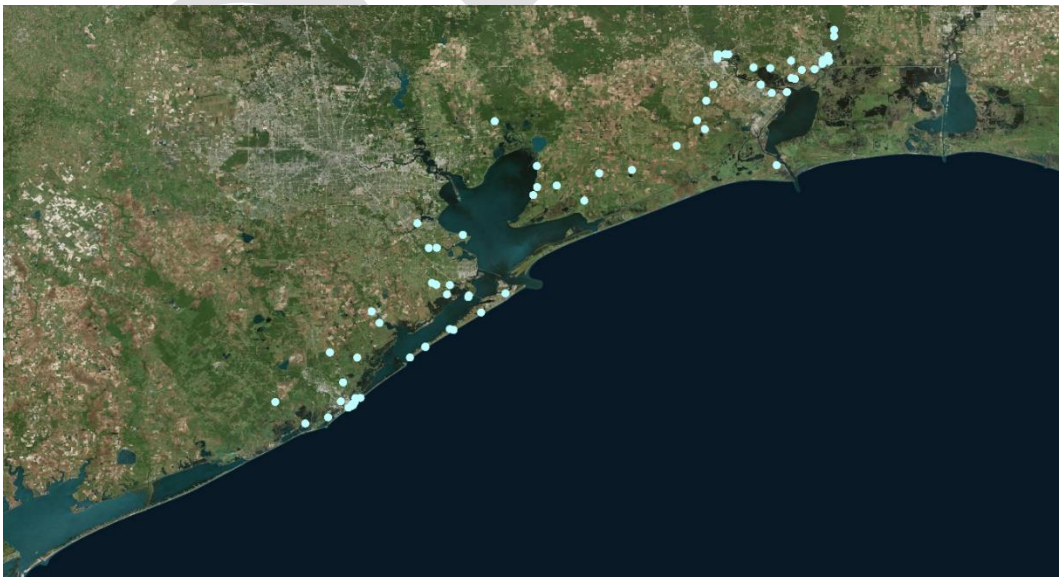

Figure 2-4. Locations of FEMA high water marks.

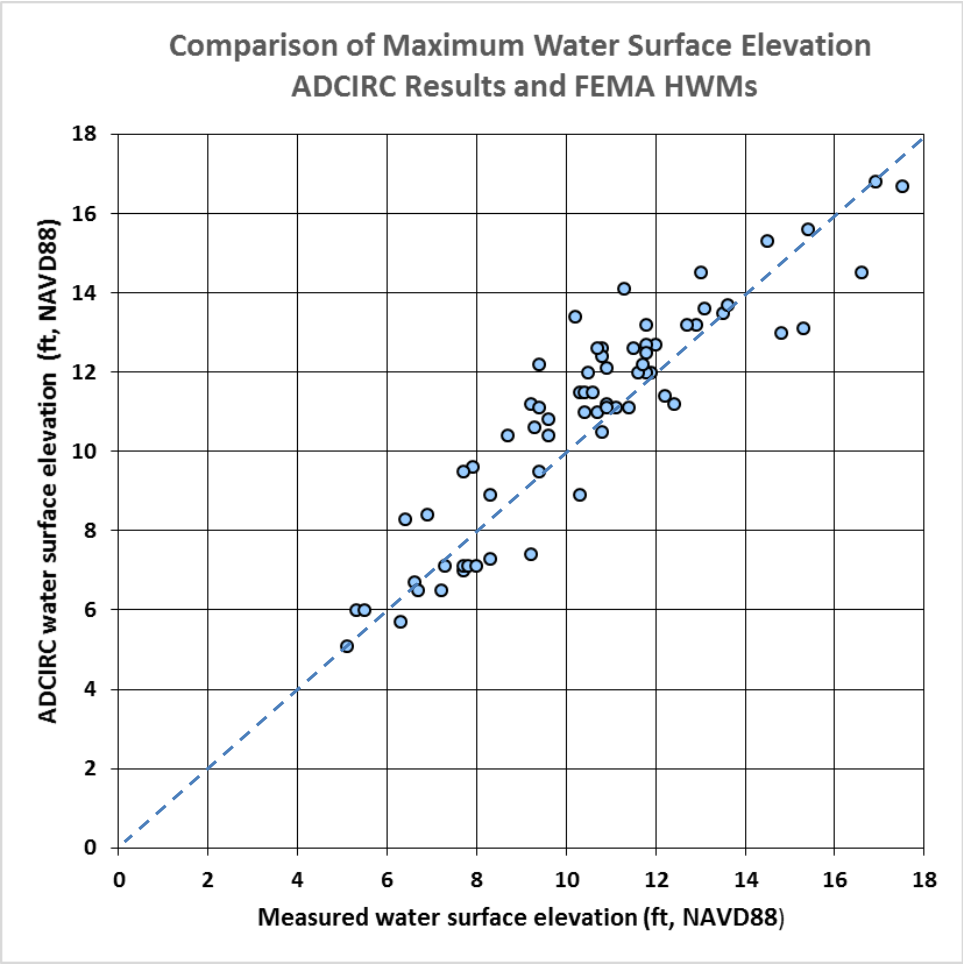

Figure 2-5. Scatter plot of measured and modeled maximum water surface elevations for the FEMA high water marks.

The set of HCFCD high water marks were not included in the validation done as part of the original Risk MAP study. They are included in the analysis reported here because they were all acquired within Galveston Bay, particularly in areas along the western side of the bay and in the upper reaches of the Houston Ship Channel that are of great interest in the economic analysis facet of the feasibility study.

The locations of 69 high water marks acquired by HCFCD are shown as green dots in Figure 2-6. These data were nearly exclusively acquired in the northwest portion of Galveston Bay and the vicinity of the upper reach of the Houston Ship Channel, i.e., in a much smaller area relative to that reflected in the other data sets.

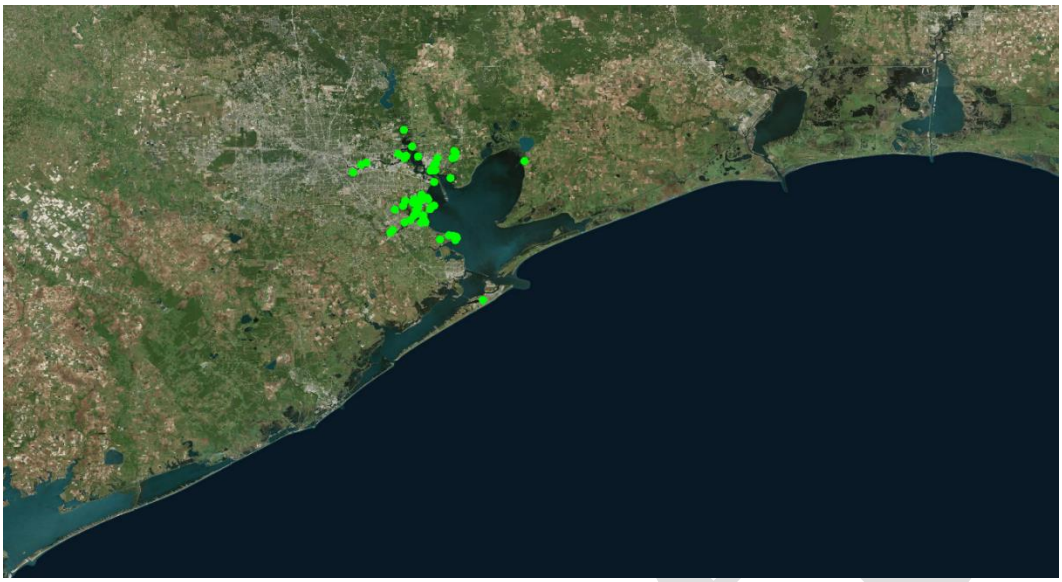

Figure 2-6. Locations of HCFCD high water marks.

A scatter plot of the comparison between ADCIRC results and the 69 HCFCD high water marks is shown in Figure 2-7. The plot shows trends that are similar to those seen for the gage-derived and FEMA high water marks. The average and average absolute errors computed for this data set are 0.42 ft and 1.00 ft, very similar to the values obtained for the other two data sets. The small positive bias of the model results seen in the gage-derived data comparisons and in the FEMA high water mark comparisons also are evident for the HCFCD data set.

Figure 2-8 shows a scatter plot for all the high water mark data sets, combined in a single plot. Not surprisingly, the same consistent trends that are evident for the individual data sets also are evident for the composite data set. The average and average absolute error computed for this entire set of 179 model-measurement data pairs is 0.44 ft and 0.98 ft, respectively.

The slight high bias of the model results is clearly seen in the figure as well. Results shown in Figure 2-8 indicate that the current modeling approach yields maximum water surface elevation results for Hurricane Ike that are very similar to those produced in the Risk MAP study. As a percentage of the peak storm surge of 11-14 feet that was generated by Ike along the western side of Galveston Bay and into the upper reaches of the Houston Ship Channel, the average absolute error reflects an error of 7 to 9%.

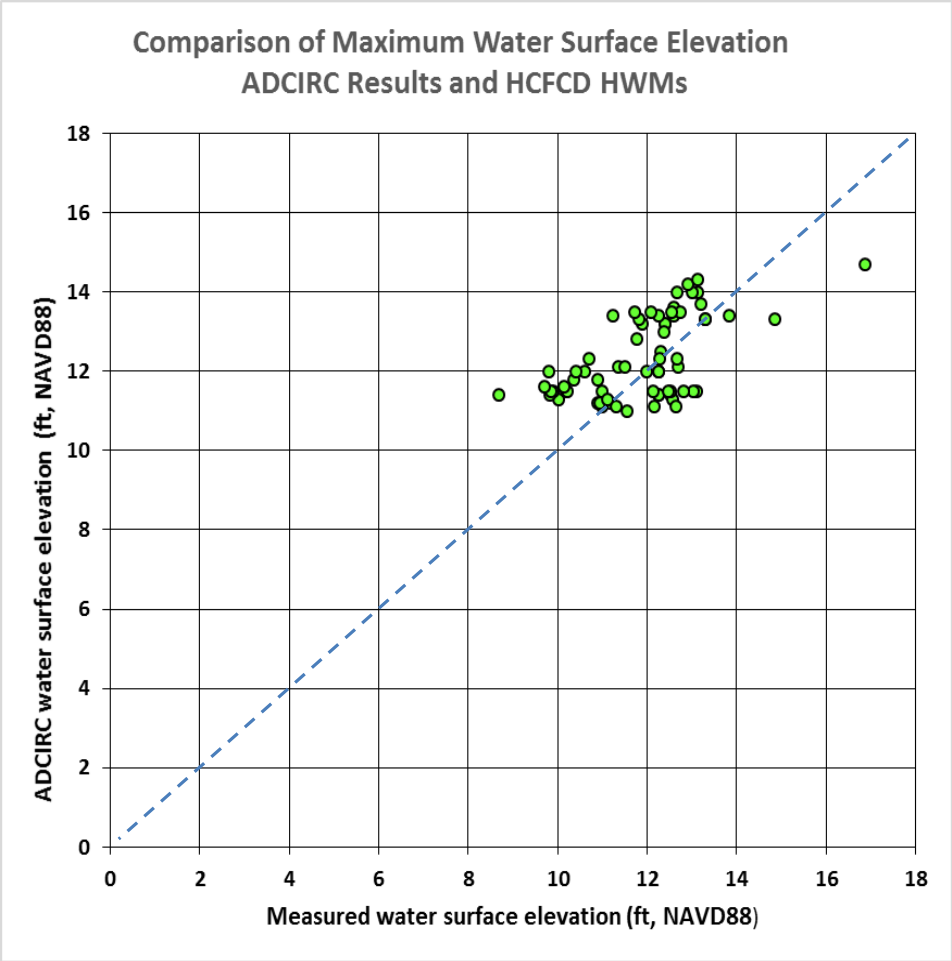

Figure 2-6. Scatter plot of measured and modeled maximum water surface elevations for the HCFCD high water marks.

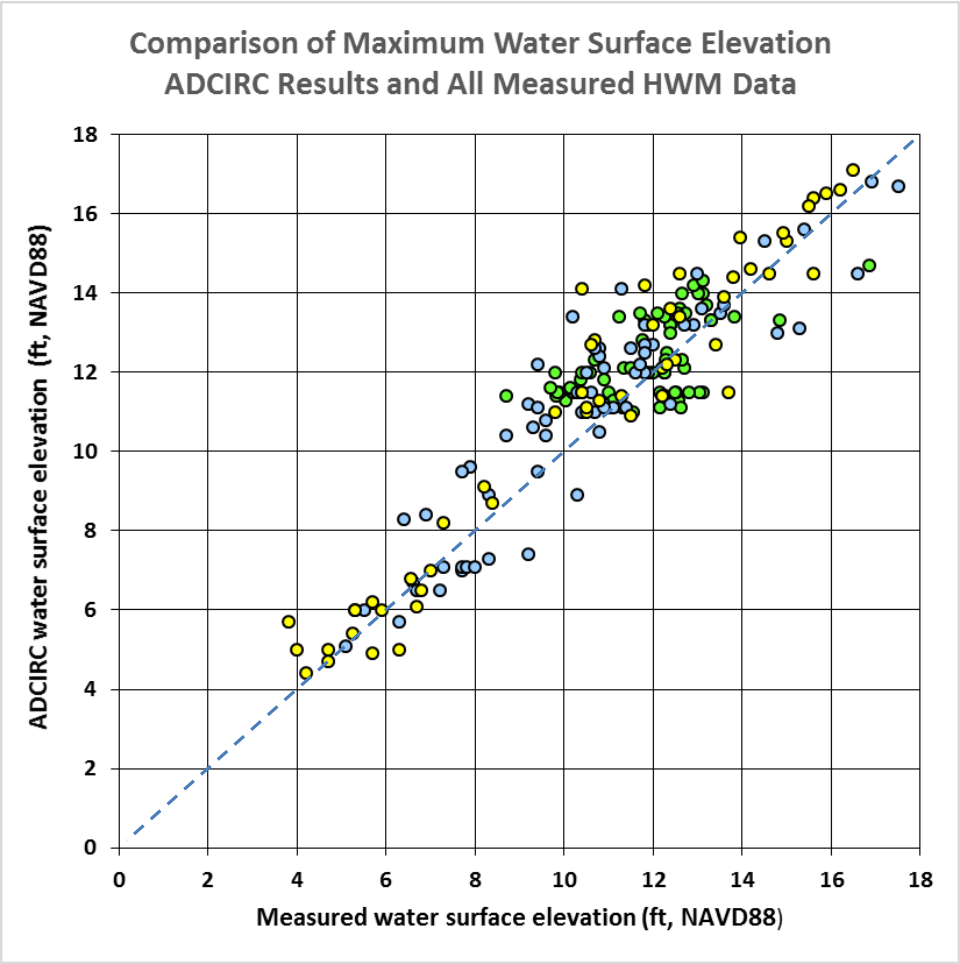

Figure 2-8. Comparison of ADCIRC maximum water surface elevations with high water marks measured by the USGS-NOAA-TCOON-Kennedy (yellow), FEMA (blue), and HCFCD (green).

3 Texas Coast Historic Hurricanes

Intensity of Historic Hurricanes

The National Weather Service (Roth) documented historic hurricanes that have impacted the Texas coast. Based on this work, Figure 1 shows the occurrence of Category 3, 4 and 5 hurricanes (the most severe hurricanes) from 1870 through 2010, as indicated by their central pressures (in mb). The National Weather Service defines hurricane categories based on maximum wind speed. However, central pressure is highly correlated to maximum wind speed, so central pressure also is a reasonably good indicator of hurricane intensity. The lower the central pressure the more intense is the hurricane, generally speaking. Hurricane central pressure is used here as the measure of hurricane intensity, for illustrative purposes and to compare the intensity of different historic and synthetic storms.

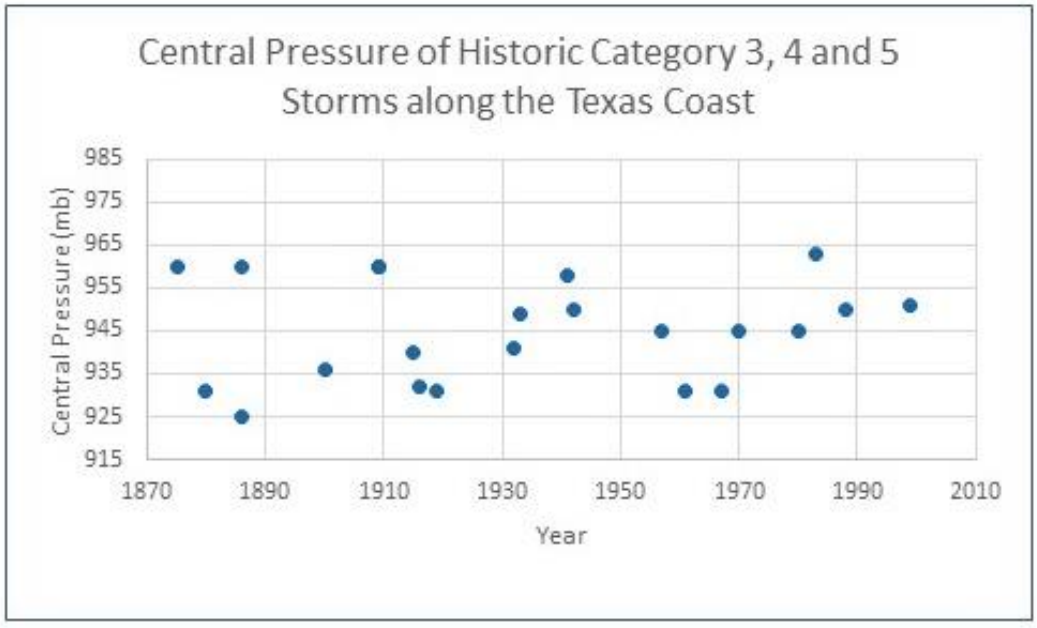

Figure 3-1. Occurrence of severe hurricanes along the Texas coast from the historic record.

Twenty-one hurricanes having intensities of Category 3, 4 or 5 occurred during this 140-year span, roughly once every 7 years on average. These storms generally have central pressures of 960 mb or less. Roth's work indicates that central pressure information for the hurricanes first became available in the 1870's. For three of the of Category 3 storms, central pressure information was not available. So, to still include these storms in

the figure a central pressure of 960 mb was assumed for illustrative purposes.

The historical record shows 7 storms having a central pressure of 935 mb or less during this time span. The occurrence of a storm of this intensity was not uniformly distributed during the 140 years.

The September 1900 Galveston Hurricane

The track and intensity characteristics for the 1900 Galveston Hurricane, based on information contained in the NOAA Hurdat2 data base, are shown in Table 3-1. Column 1 of the table shows the year, date and time (referenced to GMT) of each set of observations; columns 2 and 3 show the position of the eye of the hurricane, in latitude and longitude, along its path, or track; column 4 shows the maximum sustained 1-minute wind speed; column 5 shows a conversion of this 1-min wind speed to metric units; column 6 shows a conversion of the metric 1-min wind speed to a 10-min wind speed; and column 7 shows the observed central pressure in the eye. Few pressure observations were available for this storm.

The Galveston Hurricane of 1900 had a central pressure of 936 mb at landfall; the minimum central pressure is unknown. So in terms of intensity, the Texas coast has experienced a storm of this, or greater, intensity on a number of occasions during this 140-year period. Because of its notoriety, and fact that its intensity, while extreme, is not rare, the Galveston Hurricane of 1900 was thought to be a reasonable severe hurricane with which to examine the feasibility of the Ike Dike. The NOAA Digital Coast site reports the maximum wind speed for this hurricane to be 125 kts, a Category 4 hurricane.

Figure 3-2, generated using the NOAA Digital Coast web site, shows the track of the 1900 Galveston Hurricane among the tracks of 15 other severe historic hurricanes of Categories 3, 4 and 5. The storm tracked to the southwest of Galveston and landfall occurred to the southwest of Galveston, but this track caused the maximum wind band on the right hand side of the storm to directly impact Galveston. A number of severe historical hurricanes have tracked to the southwest of Galveston Bay.

Table 3-1. Galveston Hurricane of 1900, Track and Intensity Characteristics

Mo/Day/Yr/Hr (GMT)	Lat (deg)	Lon (deg)	Wmax (kt) Max sust.	Wmax (m/sec) Max sust.	Wmax[1] (m/sec) 10-min	Cp (mb) obs
1900/09/05/0:00	22N	79.5W	35	18.0	16.0	X
1900/09/05/6:00	22.4N	80.1W	35	18.0	16.0	X
1900/09/05/12:00	23N	80.7W	45	23.1	20.6	X
1900/09/05/18:00	23.5N	81.5W	55	28.2	25.2	X
1900/09/06/0:00	24.1N	82.3W	60	30.8	27.5	X
1900/09/06/6:00	24.8N	83.2W	65	33.3	29.8	X
1900/09/06/12:00	25.5N	84.1W	75	38.5	34.4	X
1900/09/06/18:00	26.1N	85.2W	85	43.6	38.9	974
1900/09/07/0:00	26.5N	86.2W	95	48.7	43.5	X
1900/09/07/6:00	26.8N	87.4W	105	53.9	48.1	X
1900/09/07/12:00	27N	88.7W	115	59.0	52.7	X
1900/09/07/18:00	27.2N	89.7W	125	64.1	57.3	X
1900/09/08/ 0:00	27.4N	90.6W	125	64.1	57.3	X
1900/09/08/6:00	27.6N	91.5W	125	64.1	57.3	X
1900/09/08/12:00	27.8N	92.4W	125	64.1	57.3	X
1900/09/08/18:00	28.2N	93.5W	120	61.6	55.0	X
1900/09/09/0:00	28.9N	94.7W	120	61.6	55.0	936
1900/09/09/2:00[2]	29.1N	95.1W	120	61.6	55.0	936
1900/09/09/6:00	29.8N	95.9W	90	46.2	41.2	X
1900/09/09/12:00	31N	96.9W	65	33.3	29.8	X
1900/09/09/18:00	32.2N	97.6W	50	25.7	22.9	X
1900/09/10/0:00	33.4N	97.8W	45	23.1	20.6	X

[1] factor of 0.88 used to convert max sustained wind speed to 10-min wind speed

[2] time of landfall

For the present study, the original plan was to simulate the 1900 Galveston Hurricane on its original track. A Planetary Boundary Layer (PBL) model representation of the storm winds and pressures, with best available information on hurricane parameters and track, was to be used to develop the wind and pressure fields required as input to the storm surge modeling.

However, in light of the lack of available central pressure data prior to landfall, through time, uncertainty in the radius to maximum winds value that was identified in a search for information, and relative lack of any other information for characterizing the spatial structure of the wind fields as the storm approached and crossed the continental shelf, the primary

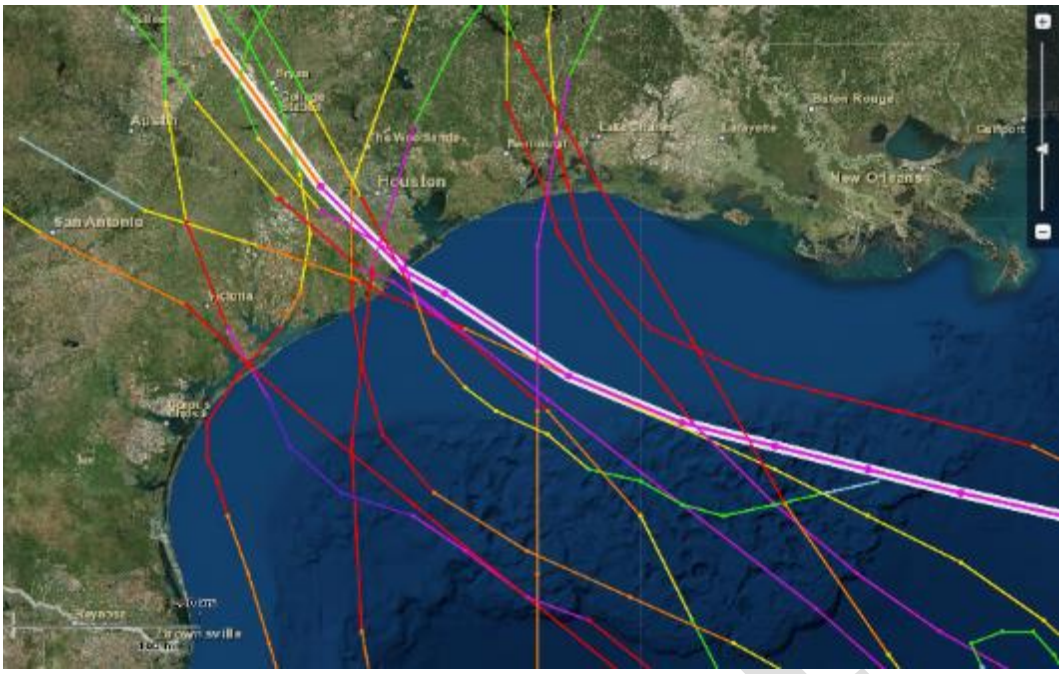

Figure 3-2. Track Galveston Hurricane, among other Category 3, 4 and 5 storms.

storm surge generation zone, a decision was made not to simulate this storm, and instead, compare it to other storms in the FEMA storm set.

Figure 3-3 compares the track for the 1900 Galveston Hurricane and the storm track considered in the FEMA Risk Map study that most closely matches the original the track. The FEMA storm track that is shown is named TXN SE Track 3b. The tracks are similar over the continental shelf, the primary storm surge generation zone. The track general track orientation and landfall location are quite similar; with landfall near San Luis Pass.

Table 3-3 compares various storm characteristics for the 1900 Galveston Hurricane with those for three FEMA Risk Map study storms, Storm 128, Storm 147, and Storm 158, which were all simulated for track TXN SE Track 3b. Column 2 shows that Storm 128 was a 900-mb storm, in terms of minimum central pressure, and Storms 158 and 147 were 930-mb storms. Based on minimum central pressure alone, Storm 128 would be expected to produce grater storm surge than the others, including the 1900 Galveston Hurricane. The first column compares the peak maximum wind speed (10-min wind speed), at any position along the track, and column 3 compares the maximum wind speed (10-min speed) at landfall.

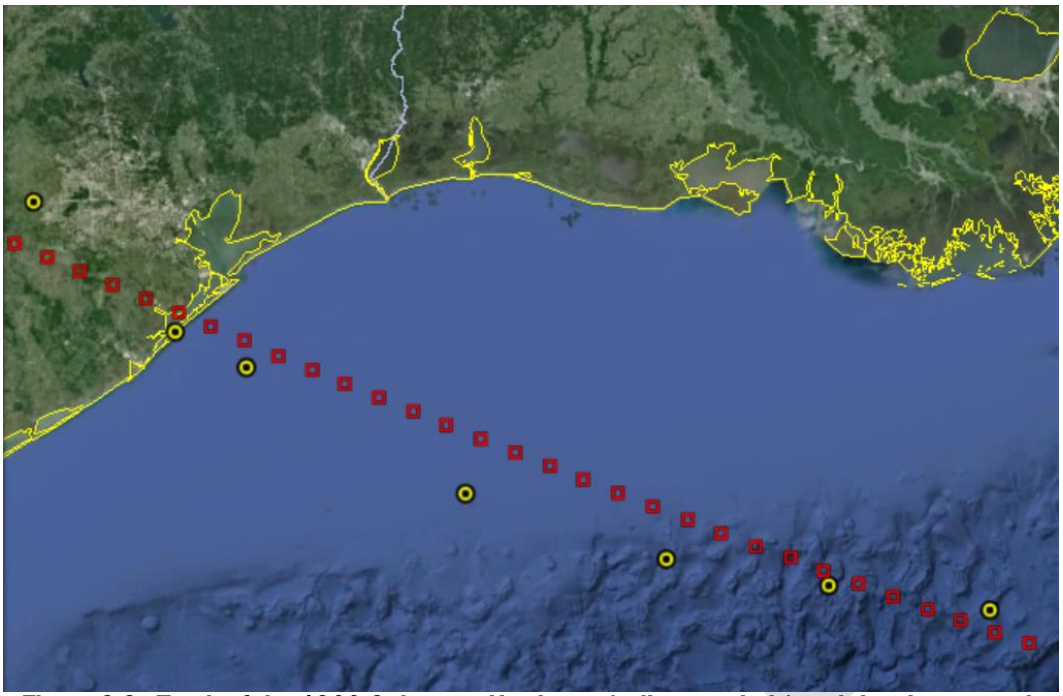

Figure 3-3. Track of the 1900 Galveston Hurricane (yellow symbols) and the closest track from the FEMA storm set (red symbols).

Table 3-2. Comparison of Storm Characteristics, 1900 Galveston Hurricane and Similar storms from the FEMA storm set.

Storm	Peak Wmax (m/sec) 10-min	Minimum Cp (mb)	Wmax at landfall (m/sec) 10-min	Cp at landfall (mb)	Rmax (nm)	Forward speed (kts)
1900 Galveston Hurricane	56.4	?	54.2	936	14	10 to 13
FEMA Storm 128	62.9	900	53.2	912	17.7-25.7	11
FEMA Storm 158	60.6	930	51.0	942	17.7-25.7	17
FEMA Storm 147	52.9	930	42.4	942	17.7-25.7	6

In terms of maximum wind speeds, Storms 128 and 158 are higher the 1900 Galveston Hurricane; the maximum wind speeds for Storm 147 are less than those for the 1900 Galveston Hurricane. The greater maximum wind speeds for Storms 128 and 158 would tend to produce larger storm surge than for the 1900 Galveston Hurricane. The maximum wind speed

at landfall is also is an important factor in defining the open coast storm surge, because winds are most effective in generating storm surge in shallower water. At landfall, the maximum wind speeds for Storms 128 and 158 are both slightly less than the value for the 1900 Galveston Hurricanes; the maximum wind speed for Storm 147 is much less than that for the 1900 Galveston Hurricane. In terms of maximum wind speed, storm 158 seems like it would produce open coast storm surge that is most similar to the 1900 Hurricane compared to the other two storms. The central pressure at landfall for Storm 158 is slightly higher (i.e. less intense) than that for the 1900 Hurricane; the central pressure for Storm 128 is much lower (i.e., more intense) than that for the 1900 Hurricane. In terms of the intensity parameters, central pressure and maximum wind speed; Storm 128 is expected to produce a greater storm surge than the 1900 Galveston Hurricane; Storm 158 is expected to produce a surge that is similar to the 1900 Hurricane; and Storm 147 is expected to produce less storm surge than the 1900 Hurricane.

The single radius-to-maximum–winds value for the 1900 Hurricane (14 n mi) is less than the values for Storms 128, 158 and 147 (17.7 to 25.7 n mi). Also, the track for the three FEMA storms was displaced a few miles to the northeast compared to the 1900 Hurricane track. Both the larger radius-to-maximum winds and the displacement in track would suggest that the zone of maximum surge will be displaced further to the north for the three FEMA storms, compared to the location of maximum surge for the 1900 Galveston Hurricane. In general, larger Rmax values also tend to produce larger open coast storms surges than smaller Rmax values.

The forward speed for the 1900 Galveston Hurricane is similar to that for Storm 128; but quite different from the forward speeds for Storms 158 and 147. In light of the work by Bunpapong and Reid (1985) for the Galveston area, the higher forward speed of Storm 158 is expected to increase the storm surge relative to the storm surge for a slower moving storm like Storm 147.

The peak storm surge at Galveston during the 1900 Galveston Hurricane was reported to be 15.2 ft (U.S. Weather Bureau, 1900), referenced to an unknown datum. The peak storm surge maps for the three FEMA storms, Storm 128, Storm 158 and Storm 147 are shown in Figure 3-4.

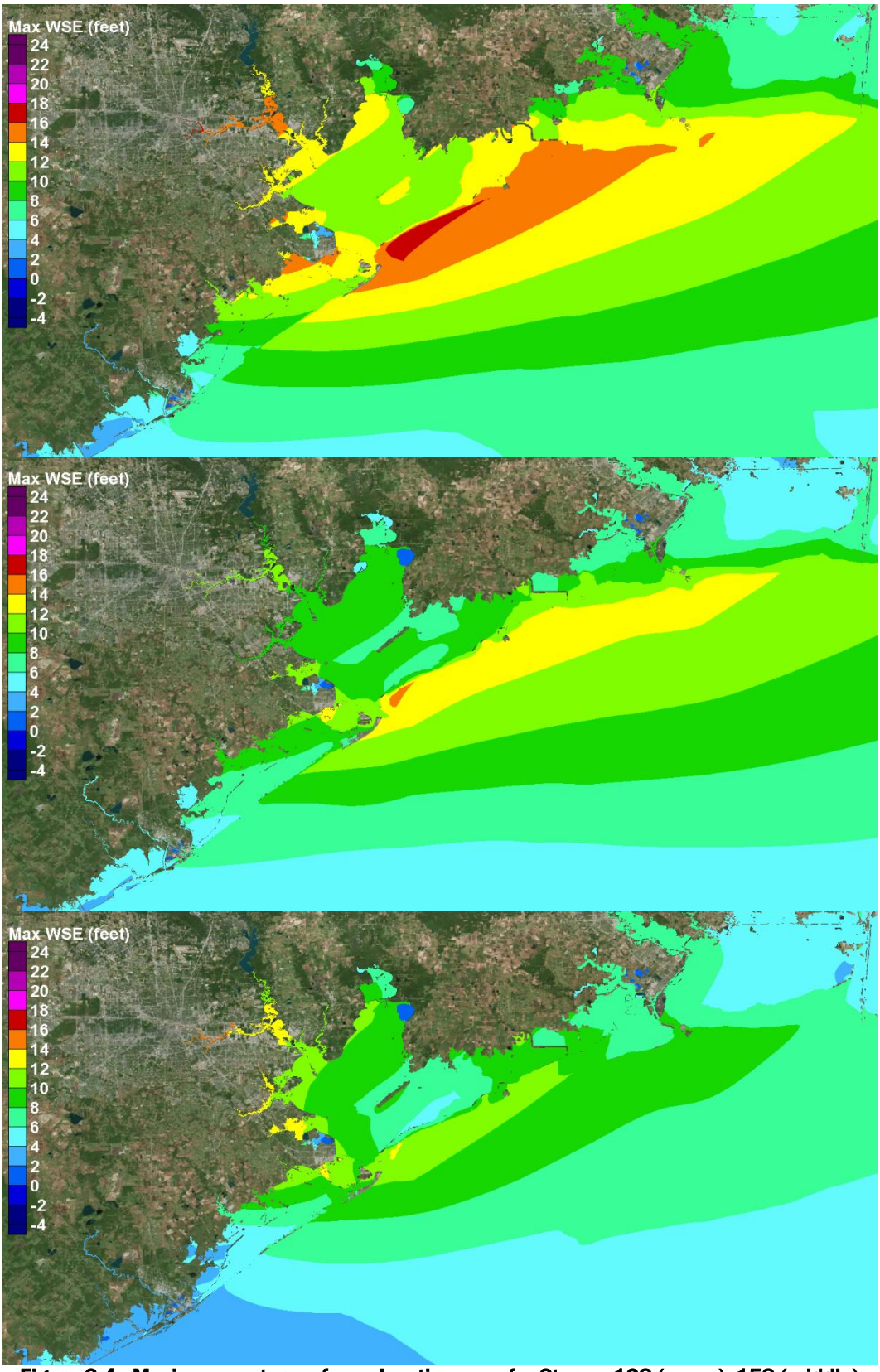

Figure 3-4. Maximum water surface elevation map for Storms 128 (upper), 158 (middle) and 147 (lower).

The zone of maximum storm surge for Storm 128 lies along Bolivar Peninsula, reaching a maximum value of 16 to 17 ft NAVD88. For Storm 158, the zone of peak surge also lies along the southern end of Bolivar Peninsula, with a maximum of just over 14 ft NAVD88. For Storm 147, the zone of peak surge also lies along the southern end of Bolivar Peninsula, with a maximum of just over 12 ft NAVD88. For reasons discussed earlier, the zone of maximum surge for the three FEMA storms is displaced further to the northeast than what would have been expected for the 1900 Galveston Hurricane. For the 1900 Hurricane, the zone of maximum surge would probably have been closer to the City of Galveston.

These peak storm surge results are consistent with the earlier discussion comparing intensity and the other parameters. The peak storm surge for Storm 128 (16 to 17 ft) was expected to be greater than the maximum observed during the 1900 Galveston Hurricane (approximately 15 ft), primarily because of its greater intensity offshore, similar intensity at landfall, and larger Rmax. The peak surge for Storm 158 (14 ft) was expected to be most similar to the 1900 Hurricane (15 ft) because of its slightly higher intensity offshore and slightly lower intensity at landfall. The maximum for Storm 147 (12 ft) was expected to be less than the observed value for the 1900 Hurricane (15ft) because of its lower intensity offshore and much lower intensity at landfall.

These results suggest that the modeling is producing results consistent with those that were observed during the 1900 Galveston Hurricane, for storms having similar tracks and intensity characteristics.

Hurricane Carla

Another more recent severe hurricane from the historic record is Hurricane Carla, in 1961. Figure 3-5 shows the track of Hurricane Carla. Hurricane Carla had a minimum central pressure of 931 mb and maximum wind speed of 155 kts. Hurricane Carla was a Category 5 storm offshore, with Category 5 strength winds occurring over the continental shelf, the zone where coastal storm surge and waves are effectively generated by the wind. The time during which Hurricane Carla reached Category 5 intensity is shown as the blue portion of the track in Figure 3-5. As it approached landfall, its intensity decreased to Category 4 strength. Storm parameters, as a function of time, for Hurricane Carla are shown in Table 3-3.

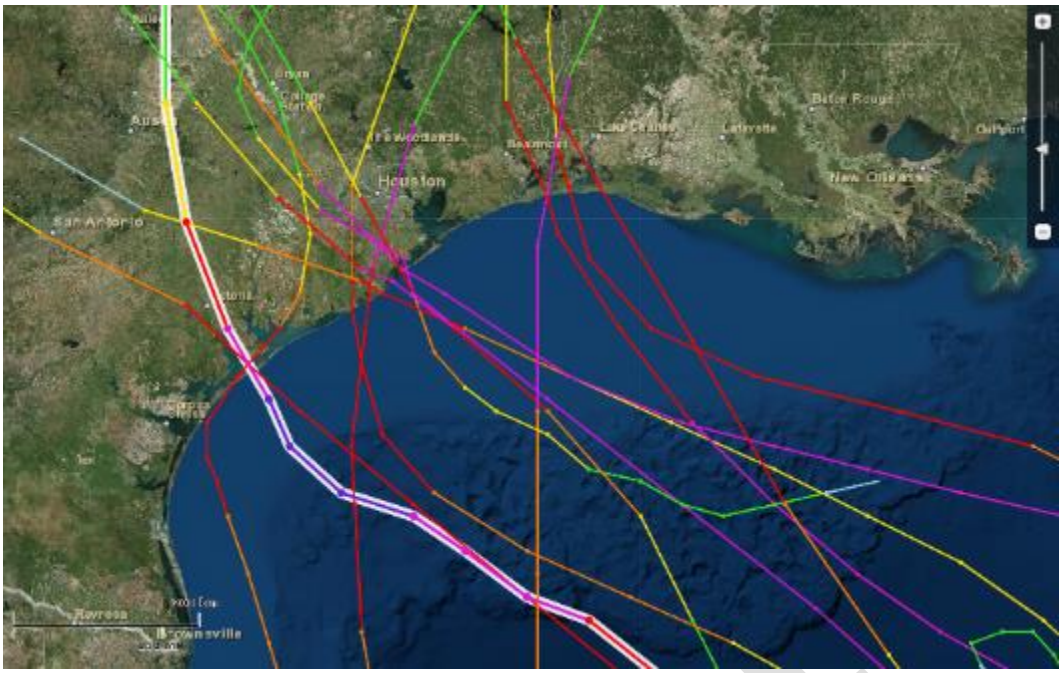

Figure 3-5. Track of the Hurricane Carla in 1961, among other Category 3, 4 and 5 storms.

The track of Hurricane Alicia (1983) is shown in Figure 3-6, along with the track of Carla. The track of Alicia is nearly parallel to the track of Carla, at least over the continental shelf where storm surge is created. A re-tracked Hurricane Carla, with the track displaced to the northeast so that the maximum wind bands directly impact Galveston and western Galveston Bay, was considered in the feasibility study to examine the storm surge that would be generated in the Houston-Galveston area due to a Category 5 intensity storm. The landfall location of the re-tracked Hurricane Carla was selected to be nearly the same as the landfall location of Hurricane Alicia, at San Luis Pass. The Category 5 strength of this storm, with landfall at San Luis Pass, was expected to produce significantly greater storm surge along the open coast and in Galveston Bay compared to the 1900 Galveston Hurricane or Hurricane Ike (2008).

Hurricane Carla was considered in the storm surge model validation conducted as part of the FEMA Risk MAP study of flood risk remapping for the Texas coast (FEMA 2011), so the highest quality wind fields were available for this storm. For the re-tracked Hurricane Carla simulation, the wind and pressure fields used in FEMA (2011) were simply modified by shifting them in latitude and longitude such that landfall at San Luis Pass was achieved. No other changes were made to the wind and pressure fields.

Table 3-3. Hurricane Carla (1961) Track and Intensity Characteristics

Mo/Day/Yr/Hr (GMT)	Lat (deg)	Lon (deg)	Wmax (kt) Max sust.	Wmax (m/sec) Max sust.	Wmax[1] (m/sec) 10-min	Cp (mb) obs
1961/09/05/12:00	16.3N	82.7W	40	20.5	18.1	997
1961/09/05/18:00	16.9N	83.1W	45	23.1	20.3	993
1961/09/06/0:00	17.4N	83.6W	50	25.7	22.6	990
1961/09/06/6:00	18.1N	84.3W	55	28.2	24.8	987
1961/09/06/12:00	18.8N	85.1W	65	33.3	29.3	984
1961/09/06/18:00	19.1N	85.6W	70	35.9	31.6	981
1961/09/07/0:00	19.5N	85.9W	75	38.5	33.9	978
1961/09/07/6:00	20.2N	86.0W	80	41.0	36.1	975
1961/09/07/12:00	20.9N	86.0W	85	43.6	38.4	973
1961/09/07/18:00	21.7N	86.3W	95	48.7	42.9	970
1961/09/08/0:00	22.3N	87.3W	100	51.3	45.1	968
1961/09/08/6:00	22.8N	87.8W	105	53.9	47.4	966
1961/09/08/12:00	23.1N	88.3W	110	56.4	49.7	965
1961/09/08/18:00	23.4N	89.2W	110	56.4	49.7	962
1961/09/09/0:00	23.7N	89.8W	110	56.4	49.7	959
1961/09/09/6:00	24.0N	90.2W	110	56.4	49.7	956
1961/09/09/12:00	24.6N	91.0W	110	56.4	49.7	953
1961/09/09/18:00	24.9N	91.8W	110	56.4	49.7	948
1961/09/10/0:00	25.6N	92.6W	110	56.4	49.7	944
1961/09/10/6:00	26.1N	93.3W	115	59.0	51.9	940
1961/09/10/12:00	26.3N	93.9W	120	61.6	54.2	937
1961/09/10/18:00	26.7N	94.5W	130	66.7	58.7	936
1961/09/11/0:00	27.0N	95.0W	140	71.8	63.2	936
1961/09/11/6:00	27.2N	95.7W	150	77.0	67.7	936
1961/09/11/12:00	27.6N	96.2W	145	74.4	65.5	935
1961/09/11/18:00[2]	28.0N	96.4W	125	64.1	56.4	931
1961/09/12/0:00	28.6N	96.8W	100	51.3	45.1	940
1961/09/12/6:00	29.5N	97.2W	80	41.0	36.1	955
1961/09/12/12:00[2]	30.5N	97.4W	60	30.8	27.1	975
1961/09/12/18:00	31.8N	97.4W	45	23.1	20.3	979
1961/09/13/0:00	32.8N	97.2W	40	20.5	18.1	980
1961/09/13/6:00	33.5N	97.0W	35	18.0	15.8	X

[1] factor of 0.88 used to convert max sustained wind speed to 10-min wind speed

[2] time of landfall occurred at approximately 20:00 GMT on 09/11/1900

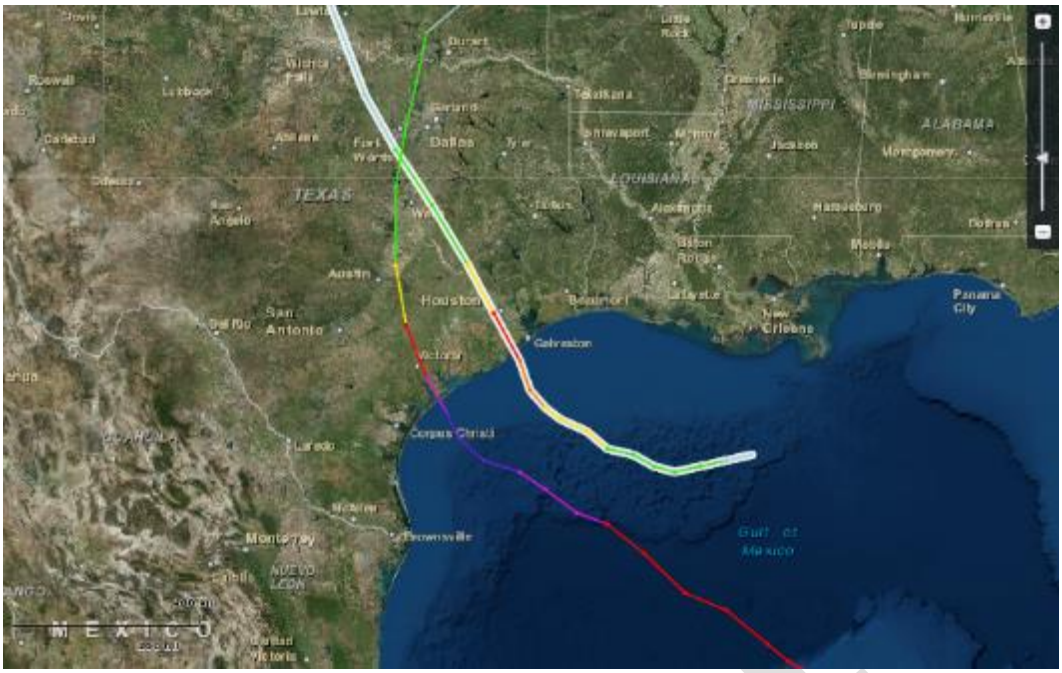

Figure 3-6. Tracks of Hurricanes Carla (1961) and Alicia (1983). Alicia is highlighted.

The final historic hurricane to be considered in the feasibility study will be a re-tracked Hurricane Ike (2008). Since Hurricane Ike is the most recent major hurricane to strike the Texas coast, most people remember it and relate to it. The track for Hurricane Ike is shown in Figure 5, among other Category 2 storms in the NOAA Digital Coast data base. The storm will be modified by shifting its track to the southwest so that its impact on Galveston and western Galveston Bay is increased. The landfall location of the re-tracked Ike will be at San Luis Pass, the same position as the re-tracked Carla storm.

Hurricane Ike was only a Category 2 intensity hurricane (central pressure of 950 mb and a maximum wind speed of 95 kts) as it made landfall and tracked up the center of Galveston Bay. Its maximum winds were around 95 kts for the entire transit across the continental shelf. However its large size was a strong contributor to the high coastal storm surge that was generated. Storm size and intensity are the two most important factors in dictating the magnitude of the open coast storm surge. Hurricane Ike was considered in the storm surge model validation conducted as part of the

FEMA flood risk remapping study, so the highest quality wind fields available for the storm will be used.

Hereafter in this document, the 1900 Galveston Hurricane, the re-tracked Hurricane Carla, and the re-tracked Hurricane Ike will be referred to as the “historic” storms or hurricanes.

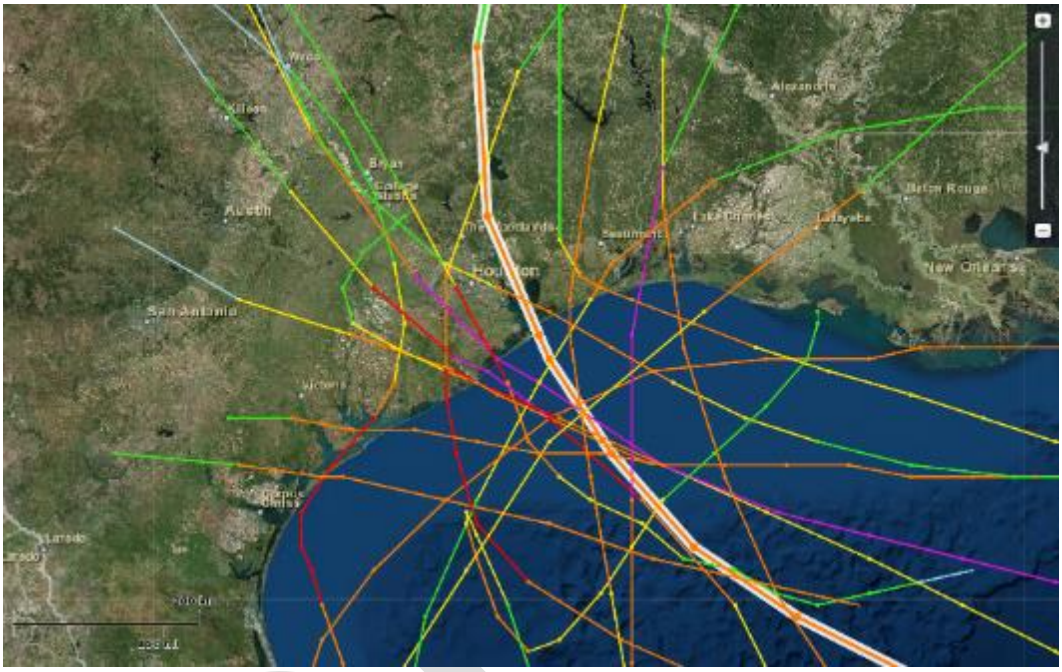

Figure 5. Track of the Hurricane Ike in 2008, among other Category 2 storms.

4 The "Bracketing" Set of Hypothetical Synthetic Storms

A set of 25 hypothetical synthetic hurricanes was simulated. The set includes 21 storms, each on a unique storm track, or trajectory, selected from among those tracks that were considered in the original FEMA Risk MAP studies (FEMA 2011) to update flood insurance rate maps for the Texas and Louisiana coasts. The trajectories at which these storms approach the coast can be divided into three categories.

The first category is the "direct-hit" category. These storms follow the same path and have the same landfall angle of approach, but are of differing central pressures and forward speeds. The radius-to-maximum winds is the same for all four storms. The direct-hit track, shown in Figure 6, runs along the western shoreline of Galveston Bay. The direct-hit set was selected to examine the storm surge within the region as a function of primarily intensity, for existing and with-dike conditions. Characteristics of the direct-hit storm set are given in Table 1.

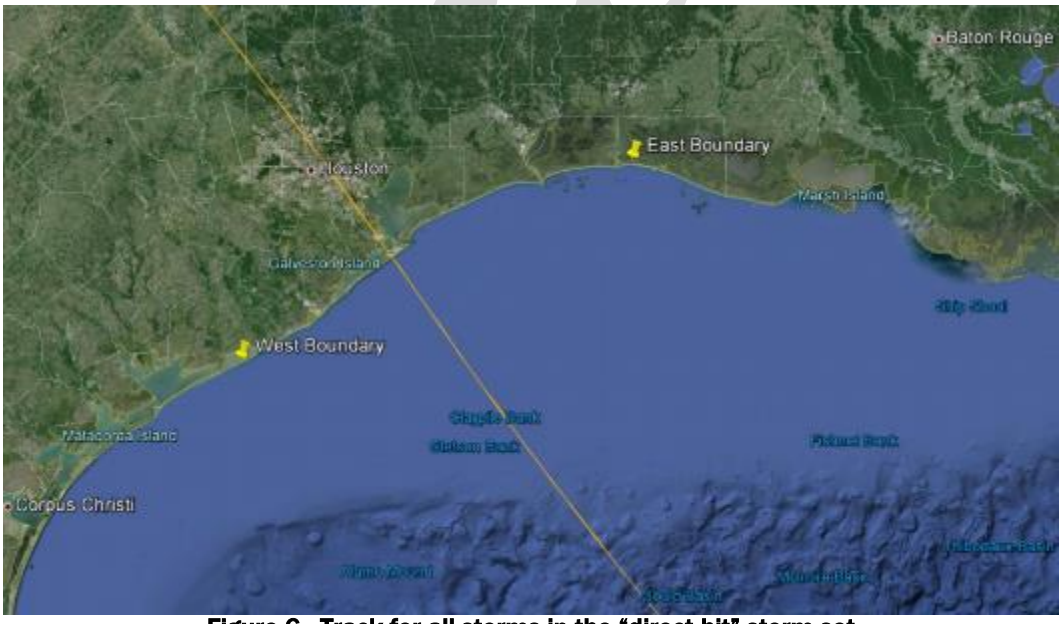

Figure 6. Track for all storms in the "direct-hit" storm set

Table 1. Characteristics of the direct-hit set.

Storm ID	Landfall		Heading	CP	Vf	Rmax
	Lat	Lon	(deg)	(mb)	(kn)	(nmi)
TEX_FEMA_RUN122.TROP	29.27	-94.84	-35	900	11	17.7
TEX_FEMA_RUN155.TROP	29.27	-94.84	-35	930	17	17.7
TEX_FEMA_RUN121.TROP	29.27	-94.84	-35	960	11	17.7
TEX_FEMA_RUN561.TROP*	29.27	-94.84	-35	975	11	17.7

The second category consists of 12 synthetic storms making landfall at varying locations on Texas' northeastern coast, shown in Figure 7. Known as the North Texas set or the TX-12, three originate in the northern Gulf of Mexico off the western coast of Florida, five originate outside the Gulf of Mexico and enter the Gulf of Mexico through the Yucatan Straits between Mexico and Cuba, and the final four originate in the southwestern Gulf of Mexico. The storms all have an identical central pressure of 900 mb, but differ in other parameters, such as the forward speed, radius-to-maximum-winds, and angle (heading) at which the storm makes landfall varying from -41° to 11°. Characteristics of the 12 storms in the North Texas set are given in Table 2.

The third and final category of synthetic hurricanes consists of 9 storms making landfall in the vicinity of the north Texas and western Louisiana coast (shown in Figure 8). Known as the West Louisiana set or the LA-9, three originate off the coast of southern Florida near the Florida Strait, four originate outside the Gulf and enter the Gulf through the Yucatan Straits between Mexico and Cuba, and two originate in the south central Gulf of Mexico and head west, then take a sharp turn in the northern direction. Like the second category, the North Texas set, these storms all have the same central pressure of 900 mb with other parameters, such as the angle at which the storm makes landfall, varying from -57° to 11°. Characteristics of the 9 storms in the West Louisiana set are given in Table 3.

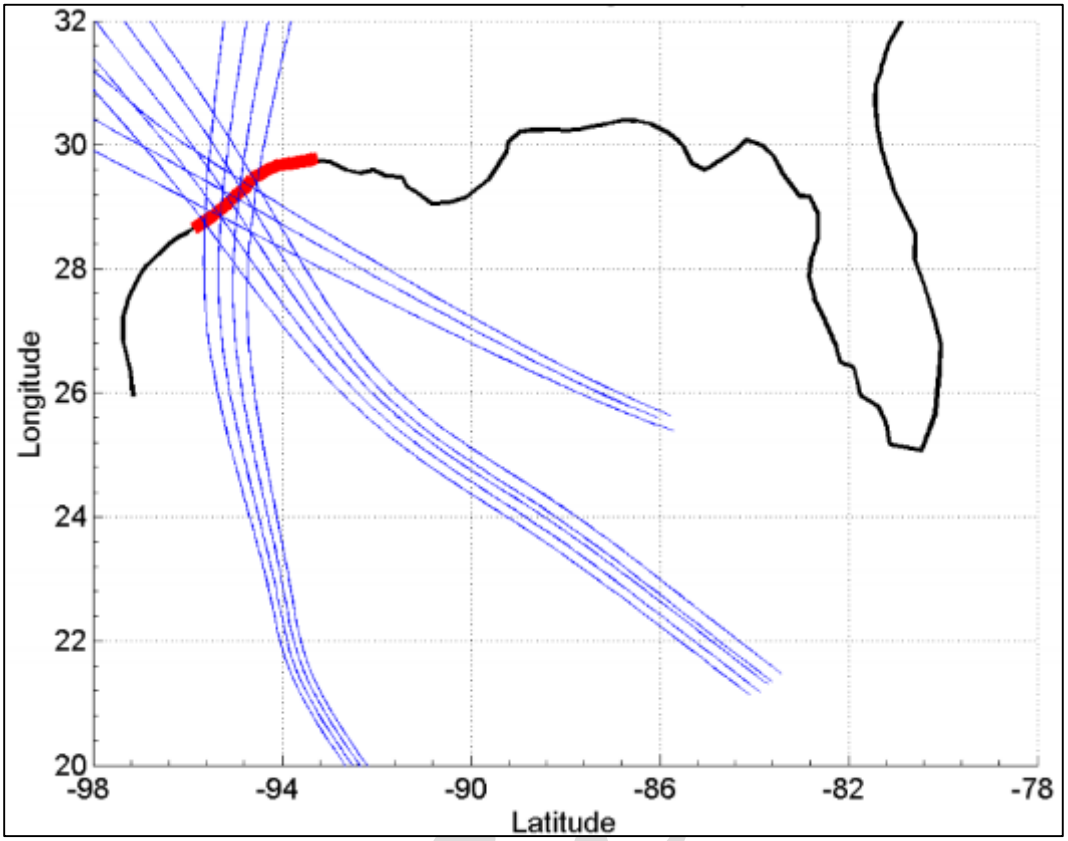

Figure 7. Tracks for the 12 storms from the North Texas set

Table 2. Characteristics of the 12-storm North Texas set.

Storm ID	Landfall		Heading	CP	Vf	Rmax
	Lat	Lon	(deg)	(mb)	(kn)	(nmi)
TEX_FEMA_RUN027.TROP	28.75	-95.65	-41	900	11	21.8
TEX_FEMA_RUN036.TROP	29.09	-95.09	-37	900	11	21.8
TEX_FEMA_RUN045.TROP	29.46	-94.61	-35	900	11	21.8
TEX_FEMA_RUN057.TROP	28.89	-95.40	-64	900	11	18.4
TEX_FEMA_RUN061.TROP	29.35	-94.72	-64	900	11	18.4
TEX_FEMA_RUN077.TROP	28.96	-95.28	6	900	11	18.4
TEX_FEMA_RUN081.TROP	29.51	-94.50	11	900	11	18.4
TEX_FEMA_RUN128.TROP	29.16	-95.01	-63	900	11	17.7
TEX_FEMA_RUN134.TROP	28.76	-95.64	3	900	11	17.7
TEX_FEMA_RUN136.TROP	29.23	-94.90	8	900	17	17.7
TEX_FEMA_RUN142.TROP	28.91	-95.36	-37	900	6	17.7
TEX_FEMA_RUN144.TROP	29.27	-94.84	-37	900	6	17.7

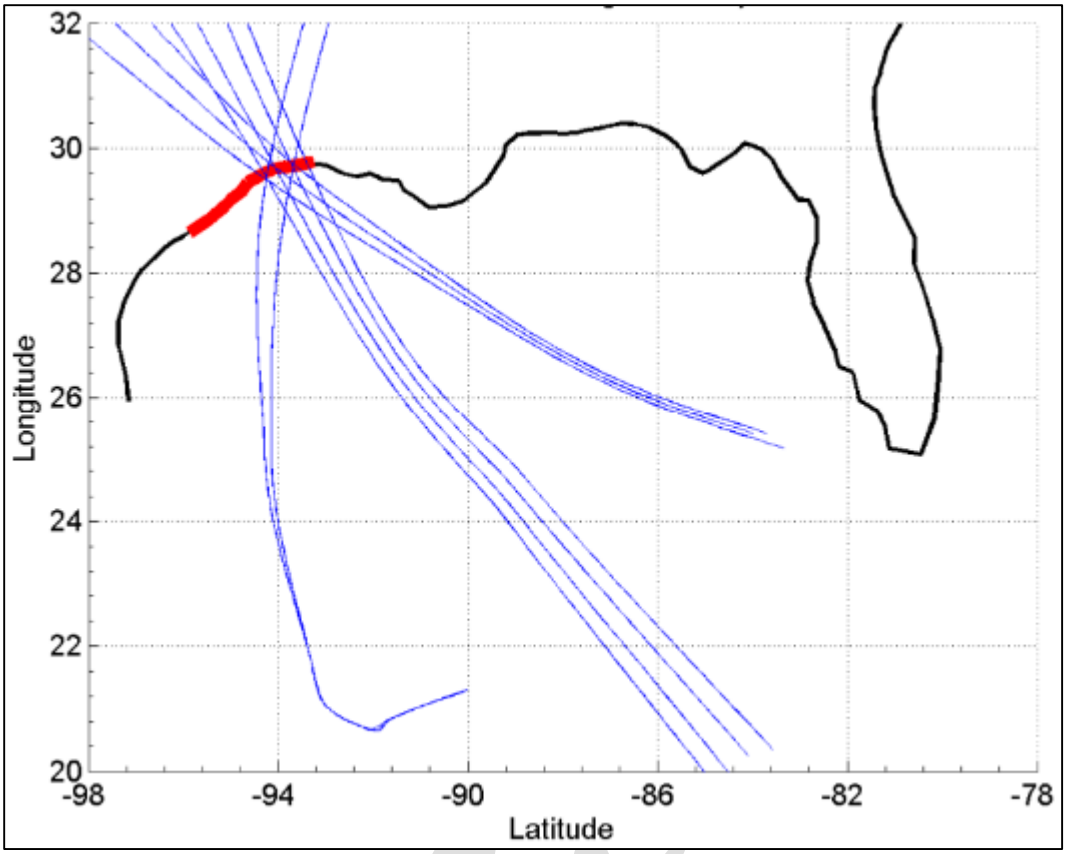

Figure 8. Tracks for the 9 storms from the West Louisiana set

Table 3. Characteristics of the 9-storm West Louisiana set.

Storm ID	Landfall		Heading	CP	Vf	Rmax
	Lat	Lon	(deg)	(mb)	(kn)	(nmi)
JPM_FEMA_RUN209.TROP	29.59	-94.29	-35	900	11	21.8
JPM_FEMA_RUN218.TROP	29.71	-93.69	-28	900	11	21.8
JPM_FEMA_RUN249.TROP	29.56	-94.37	-57	900	11	18.4
JPM_FEMA_RUN253.TROP	29.72	-93.63	-53	900	11	18.4
JPM_FEMA_RUN269.TROP	29.61	-94.22	11	900	11	18.4
JPM_FEMA_RUN326.TROP	29.68	-94.04	-57	900	11	17.7
JPM_FEMA_RUN332.TROP	29.72	-93.67	11	900	11	17.7
JPM_FEMA_RUN338.TROP	29.67	-94.05	-30	900	6	17.7
JPM_FEMA_RUN340.TROP	29.76	-93.39	-26	900	6	17.7

The twelve storms comprising the North Texas set are shown with pink tracks in Figure 4; the nine storms comprising the West Louisiana set are shown with green tracks in Figure 9. The spacing between tracks, at landfall, is approximately 20 miles. Figure 4 shows the storm numbering scheme that is used throughout this report. The storm numbers are also indicated in the storm ID, which is the first column of Tables 1, 2 and 3.

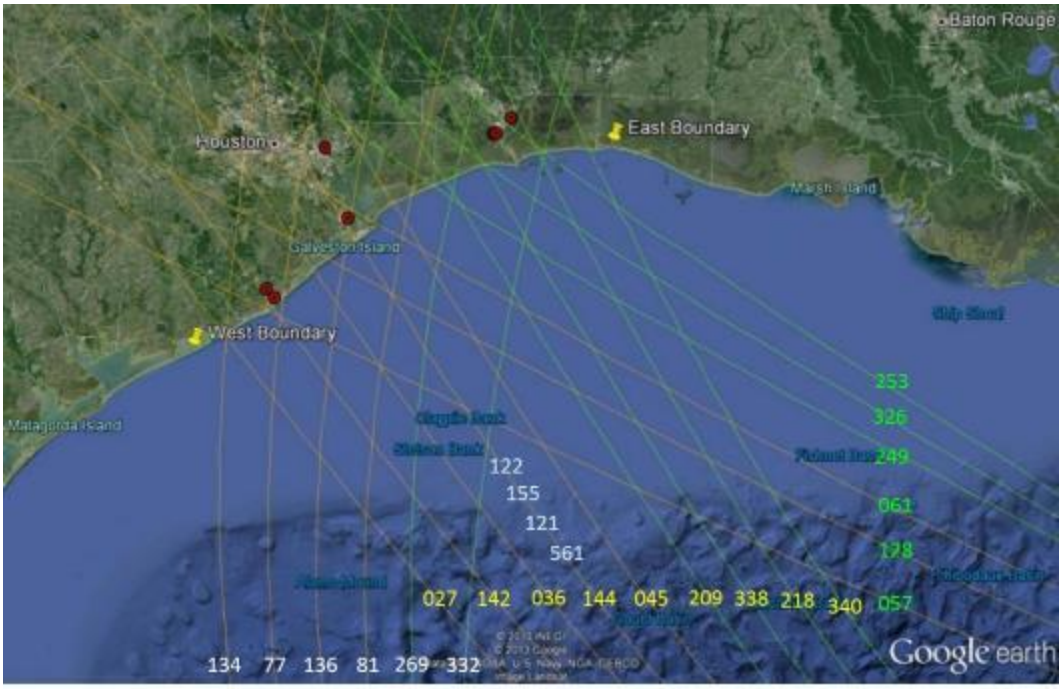

Figure 9. Storm tracks for the Texas set (in pink) and the Louisiana set (in green).

Most of the storms in the bracketing set have central pressures of 900 mb. The hurricane wind and pressure model using in this feasibility study simulates a decrease in storm intensity and an increase in the radius to maximum winds just before landfall (a process call storm filling). This filling process has been observed for severe storms. As a result of storm filling, the central pressure at landfall for these 900-mb storms rages from approximately 910 mb to 920 mb. These are severe hurricanes, all having maximum wind speeds of about 125 kts, or of Category 4 intensity on the Saffir-Simpson wind intensity scale. Central pressure is highly correlated to maximum wind speed. In terms of intensity, these storms are generally more severe than those that have occurred along the Texas coast over the past 140 years (see Figure 1), with the notable exception of Hurricane Carla in 1961, which reached Category 5 as it moved across the continental shelf then weakened to Category 4 intensity at landfall.

5 Hurricane Surge Generation on the Open Coast – Causative Factors

What Causes a Storm Surge?

Hurricanes are intense storms that originate in tropical waters and derive their energy from warm water. They weaken in intensity when the heat source is diminished or removed, which occurs when the storm passes over cooler water or when winds are blowing over land. Hurricanes also can be weakened by vertical wind shear. Hurricanes are low-pressure systems, in which winds spin counterclockwise (in the northern hemisphere) around the storm's center, or eye. A hurricane's intensity is measured by its maximum wind speed and central pressure; the two are strongly correlated. Hurricane intensity, size, path, and speed of movement all change with time during any particular event. Hurricane characteristics can vary widely from storm to storm.

Storm surge is defined here as an anomalous increase in the water level associated with a coastal storm. Storm surge is a long wave that is primarily forced by wind and to a lesser degree by spatial gradients in atmospheric pressure and momentum fluxes associated with waves, particularly in the surf zone.

The modeling being used in this feasibility study to simulate the development of storm surge treats each of these contributions to storm surge, as described below.

Wind

Wind exerts a shear stress on the water surface, which acts to push water in the direction of the wind. Shear stress is a nonlinear function of the wind speed, i.e., it is related to wind speed raised to the second or third power, depending on the formulation of wind drag coefficient used to calculate surface stress for different wind speeds. For example, an increase in wind speed by a factor of 2 will increase the surface shear stress by a factor of 4 to 8. The contribution to storm surge caused by wind stress is called wind set-up.

Wind is most effective in creating a set-up (increase) in the water level when it blows over shallow water because, in the balance of momentum, the effective wind stress is inversely proportional to water depth. Therefore storm surge is mostly generated on the continental shelf, in the shallow nearshore coastal region and in shallow bays and estuaries. Wind is much less effective in creating wind set-up in deep water. The magnitude of wind set-up depends on the fetch, or the distance over which a wind blows, in addition to the duration or persistence of winds.

Atmospheric Pressure

An elevated water surface dome is created under the center of a low pressure storm system, which contributes to the storm surge. Atmospheric pressure is the weight of air above the water. In regions of high pressure (at the storm periphery), the force pushing down on the water is greater than the force over regions of low pressure (storm center). This horizontal gradient in atmospheric pressure forces water to move from regions of higher pressure toward regions of lower pressure. Water is forced toward the eye of the hurricane, which creates the dome of water. The amplitude of this contribution to storm surge is dependent upon the magnitude of the difference between the peripheral and central pressures; but it can be as much as several feet for a major hurricane. This pattern of water movement is not static; instead, it moves with the translating hurricane.

Waves

Storm winds also result in the generation of energetic short-period waves, which at elevated water levels can pose a significant coastal flood hazard and cause structural damage. Similar to the generation of wind set-up, storm wave characteristics (height, period, and direction) are strongly influenced by wind speed and direction, fetch, and the persistence of wind from a particular direction. Higher wind speed, greater fetch distance and longer duration generally lead to greater wave energy (higher wave height) and longer wave periods. However, unlike storm surge, waves are very effectively generated in deep water and the most energetic waves are usually found in deeper water. Waves generated by a hurricane propagate outward away from the storm in all directions. Along the open coast, severe hurricanes typically generate significant wave heights of 15 to 30 ft, with typical peak wave periods of 10 to 15 sec. In more sheltered areas, storm wave heights and wave periods are generally smaller.

As obliquely incident wind waves propagate into shallow water their propagation speed slows, they begin to "feel" the bottom, turn and seek to align themselves in such a way that wave crests approach in a direction increasingly more parallel to the shoreline. In the absence of wind energy input this refraction process generally causes a decrease in wave height, although complex irregular bathymetry can create patterns of locally increased and decreased wave height. Some wave energy is dissipated due to bottom friction and white-capping. But generally during hurricanes, strong onshore winds continue to act as an energy source offsetting energy losses associated with these other processes.

As waves propagate into even more shallow water, they shoal, steepen and eventually break, dissipating energy much more strongly. In response to this depth-induced dissipation, significant wave height decreases. In the inner surf zone, despite the presence of high winds, wave energy becomes saturated and the local significant wave height is generally limited to values of 0.4 to 0.6 times the local water depth. Wave height can be smaller if wind input is reduced and energy is dissipated by vegetation or diminished in some other way due to sheltering or disruption of wave propagation by buildings, other landscape features, or by debris.

Wave transformation and breaking is strongly dependent upon the local water depth. If the storm surge significantly changes the local water depth, wave transformation and breaking processes will be altered accordingly. Increases in water depth associated with increases in storm surge generally enable greater wave energy (height) to be present locally.

As waves break on a beach in very shallow water, wave heights decrease and the flux of wave momentum in the onshore direction is reduced. This change in wave momentum is balanced by an increase in the mean water level, a contribution to the storm surge called wave setup. Wave setup is usually treated in engineering analysis as a "mean" (in time) quantity that varies every half hour or hour as the incident wave conditions change.

The magnitude of wave setup is greatest right at the shoreline, and the maximum value is roughly 10 to 20% of the incident significant wave height at the seaward edge of the surf zone, i.e., the breaking wave height. For example, incident waves having a significant height of 20 ft can force a maximum wave setup at the shoreline of 2 to 4 ft. Wave setup produces an additional increase in the storm surge elevation, which in turn exacerbates

wave runup on beaches and structures and increases the potential for inundation and subsequent propagation of waves over inundated terrain.

Storm Surge along the Texas Coast

In addition to atmospheric pressure and wave effects, storm surge along the north Texas coast is strongly influenced by two wind-forced contributors. One is the development of a wind-driven surge forerunner, an Ekman wave that develops as along-shore moving water on the continental shelf forced by the hurricane's peripheral winds which is then directed onshore by the Coriolis force even while the storm is well offshore. The second contributor is the direct effect of the highest winds in the core of the hurricane as it crosses the continental shelf and approaches landfall, pushing the shelf waters toward the coast and into the bay.

Within Galveston Bay, storm surge is highly dependent upon infilling that occurs due to surge propagation over the low barrier islands and through the passes linking the Gulf of Mexico to Galveston Bay and West Bay, and by local wind-set up. For the bracketing set of 25 storms, the maximum simulated water surface elevation was 25 ft NAVD88 in the upper reaches of the Houston Ship Channel. Peak surge can vary significantly within Galveston Bay, depending on storm track and location.

Surge Forerunner

In a broad sense, a hurricane forerunner is a rise in the water surface elevation at the coast when the eye of the hurricane is far offshore in very deep water, and which is not directly attributable to the strong core winds closer to the eye of the storm. Several contributors to the forerunner have been identified, including the hurricane's far-field winds as well as other wave dynamics associated with the fact the Gulf of Mexico is a nearly enclosed basin, but forced by the flux of water through the Florida Straits and the Yucatan Straits. The Coriolis force, which acts on moving water and is associated with the rotation of the earth, is a critical factor in development of the forerunner.

Ekman Wave Formation

Kennedy et al (2011) described and documented well what appears to be the most significant contribution to the forerunner, or mechanism driving the forerunner, along the northwest Texas Gulf coast. They identified the forerunner during Hurricane Ike through measurements, and verified it using modeling and analysis. This mechanism is the development of a

wind-driven surge forerunner, an Ekman wave, that develops as along-shore moving water on the continental shelf forced by the hurricane's peripheral winds, then directed onshore by the Coriolis force (to the right in the northern hemisphere) even while the storm is well offshore. Kennedy et al (2011) found that this contribution to the water surface elevation steadily increased over a period of several days before Ike's landfall and reached approximately 6 feet in amplitude.

Figure 10, from Kennedy et al (2011), shows the measured water surface elevation during Hurricane Ike which was recorded at a gage located on the open coast, in shallow water, just east of Bolivar Peninsula. Measured water surface elevations are shown in black, results of a storm surge model simulation with the Coriolis force turned on are shown in red, and results from a model simulation without Coriolis forcing are shown in blue. Measured data show a steady rise in water level beginning 2 days prior to landfall, when the storm was located in the deep water region of the Gulf. The forerunner gradually increased to an elevation of approximately 6 ft (2 meters) at a time 12 hours prior to landfall, after which the core winds of the storm began to dominate the surge response along the coast. Without Coriolis forcing included in the model, the forerunner could not be simulated at all.

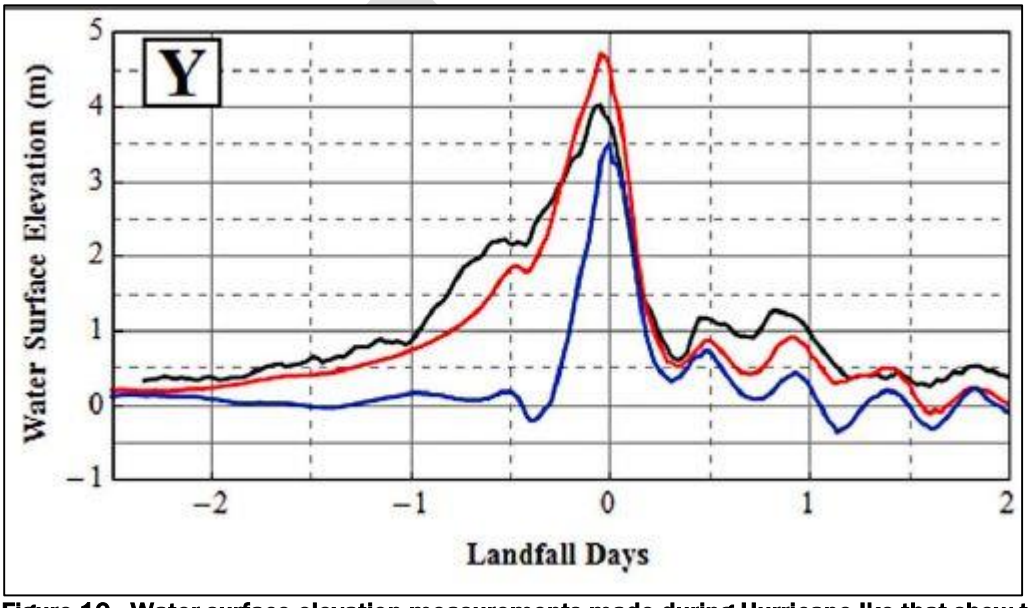

Figure 10. Water surface elevation measurements made during Hurricane Ike that show the wind-driven forerunner, from Kennedy et al (2011)

The work of Kennedy et al (2011) showed the importance of the wide continental shelf off the Louisiana-Texas coast in development of the Ekman wave, forced initially by the wind, which then propagates along the shelf to the south as a free wave once the wind forcing subsides. Because of the generation mechanism involved, the counterclockwise rotation of winds about the hurricane eye, and the wide continental shelf along the Louisiana and north Texas coasts, conditions are generally favorable to force a significant forerunner for all major hurricanes that approach the coast along the northwest Gulf of Mexico.

Figure 11 shows the Gulf of Mexico bathymetry, where the shallower depths on the shelf are shown as the color-shaded contours. The shallow areas with colored contours reflect the location and varying width of the continental shelf around the periphery of the Gulf. The very deep portion of the Gulf, beyond the continental shelf, is indicated by the monochrome maroon colored area. As stated previously, winds are only important in generating a storm surge on the shelf and in adjacent shallow coastal and bay waters. The extensive shelf situated along the northwestern Gulf coast is a critical factor in the development of the forerunner, and storm surge in general, in the Houston-Galveston region.

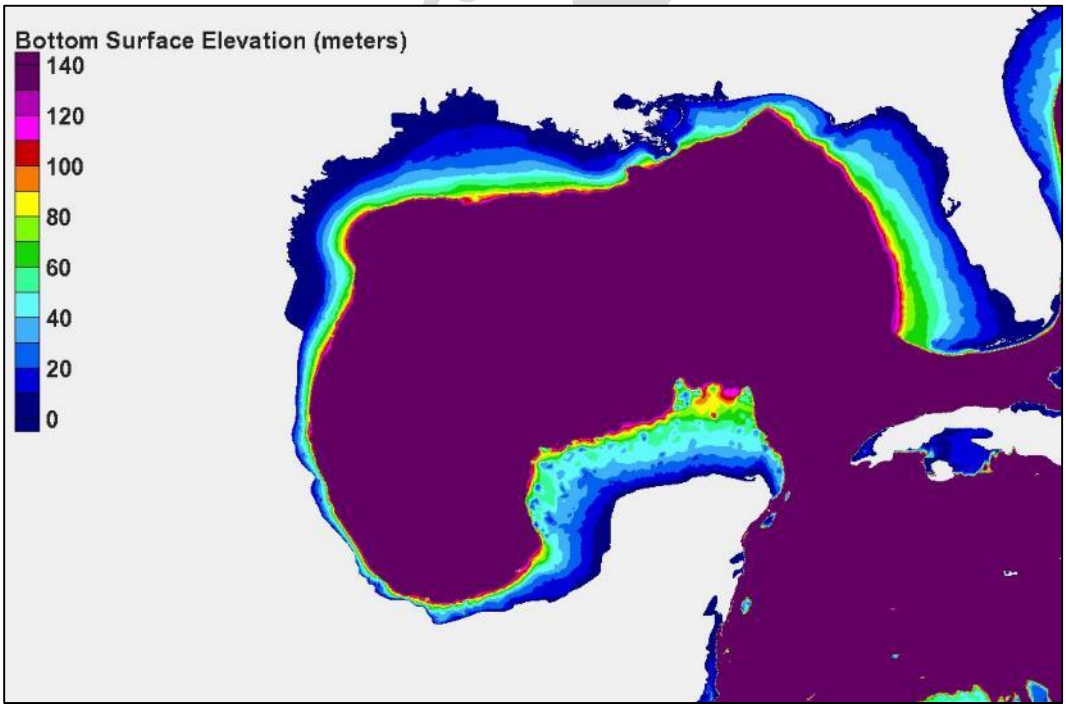

Figure 11. Bottom surface elevation in the Gulf of Mexico

Volume Mode Oscillation

In a study funded by the U.S. Army Corps of Engineers, Bunpapong et al (1985) identified other contributors to the forerunner in the Gulf of Mexico, arising from physical processes other than far-field winds blowing along the shelf. For the Texas coast near Galveston, they found one mechanism in particular to be more significant than several others they identified.

Using model simulations and measured water surface elevation data from tide measurement stations located around the periphery of the Gulf, for Hurricanes Carla (1961) and Allen (1980), they showed that as a hurricane enters the Gulf of Mexico, an in-phase difference in the magnitude of the volume of water entering/leaving the Florida and Yucatan Straits (both in or both out), a volume mode or Helmholtz type of oscillation is excited throughout the entire Gulf. For this mode of oscillation, the water surface of the entire Gulf rises and falls in phase, with a nearly uniform amplitude throughout the Gulf. The flux of water through the Straits is driven by both wind and the atmospheric pressure gradient associated with the storm, with the latter forcing water from regions of high atmospheric pressure toward the low-pressure center of the hurricane. They found that the effect of wind-driven transport was the most important.

Bunpapong et al (1985) found that for hurricanes, having a central pressure deficit of 80 mb and a radius to maximum winds of 16 n mi, which entered the Gulf through the Yucatan Straits on a straight track resulting in landfall on the Texas coast, a forerunner was generated at Galveston that had an amplitude of approximately 0.7 ft. A hurricane with an 80-mb pressure deficit is akin to a hurricane having a central pressure of approximately 930 mb and a far-field pressure of 1010 mb. They found that for larger storms, having the same pressure drop of 80 mb but radius to maximum winds of 32 n mi, the amplitude of the volume mode oscillation doubled to 1.3 ft. For pressure drops of 40 mb and 120 mb, and the larger radius to maximum winds of 32 n mi, they found amplitudes of 0.7 and 2 ft, respectively. They found that the hurricane path and evolution play important roles in dictating the amplitude of the forerunner.

A significant forerunner was not always generated; the amplitude depended on storm track, intensity and size. They showed that for hurricanes of lesser intensity when entering the Gulf through the Florida

Straits, and for hurricanes originating within the Gulf, the amplitude of this volume mode along the Texas coast was less than when an intense storm enters through the Yucatan Straits.

For this particular contribution to the forerunner, the timing between this volume mode oscillation and the primary wind induced surge generated at the coast determines whether or not this mode oscillation contributes to the peak surge or detracts from it. This will depend upon the relative timing of the two contributors, which is strongly influenced by the hurricane's forward speed. Bunpapong et al (1985) found that increasing forward speed produced a significant increase in peak open coast surge along the Texas coast, but that different forward speeds had little effect on the amplitude of the volume model oscillation.

The follow-on work plan proposes to further examine the effect of this forerunner mechanism on peak surge in the Houston-Galveston region, confirming the maximum amplitude of this mechanism for intense storms that enter the Gulf, examining sensitivity of the amplitude to location of entry into the Gulf (which influences the Strait fluxes driven by the wind), the prevalence of this phenomenon, the likelihood that it can be an additive effect to the open coast surge, and the influence of forward speed on peak surge.

An Example of Forerunner Development: Direct-hit Storm 122

The model simulation for Storm 122, a direct-hit storm having central pressure of 900 mb at its most intense stage, a forward speed of 11 kts, and a radius to maximum winds of 17.7 n mi, is used to illustrate development of the hurricane surge forerunner. This storm originated outside the Gulf and entered through the Yucatan Straits, at its northernmost point. However, its central pressure as it entered the Gulf through the Yucatan Straits was not very intense, only 980 mb with a far field pressure of 1013 mb; i.e., a pressure deficit of only 33 mb.

The modeling of surge being done in this feasibility study should be able to simulate the volume mode oscillation identified by Bunpapong et al (1985). Both the wind and atmospheric pressure gradient forcing are being simulated in the storm surge modeling and water flux through both Straits is being well simulated since the surge model's open water boundaries are located in the middle of the Atlantic Ocean. Because Storm 122 is not very intense as it enters the Gulf, and because the wind-driven water flux is directed out of one Strait and into the other as a result of its

entry location, the amplitude of the volume mode contribution to the forerunner is expected to be small for this storm, on the order of a few tenths of a foot at most, based on the results of Bunpapong et al (1985).

Figure 12 shows the simulated Gulf-wide field of water surface elevation and wind vectors for Storm 122 just before its entry into the Gulf, almost 3 days before making landfall at Galveston. At this point in time the central pressure of the storm is 980 mb. The initial water surface elevation for this simulation is about 0.9 ft NAVD88, or approximately 0.4 ft above mean sea level to account for steric increases in Gulf water levels during the summertime hurricane season. The very small circular light blue area just south of Cuba reflects a small dome of water beneath the eye of the hurricane that is forced by atmospheric pressure gradients which push water toward the storm center.

Figure 13 shows the water surface elevation and wind vectors for Storm 122, about a day later, 2 days prior to landfall. At this point in time the storm's central pressure is 942 mb. The counterclockwise rotation of wind vectors about the eye of the storm is quite evident. The dome of water under the eye of the storm has grown, having a maximum water surface elevation of more than 3 ft NAVD88, 2 to 2.5 feet above mean sea level. The dome is following the eye of the storm as it transits across the Gulf toward the Texas coast.

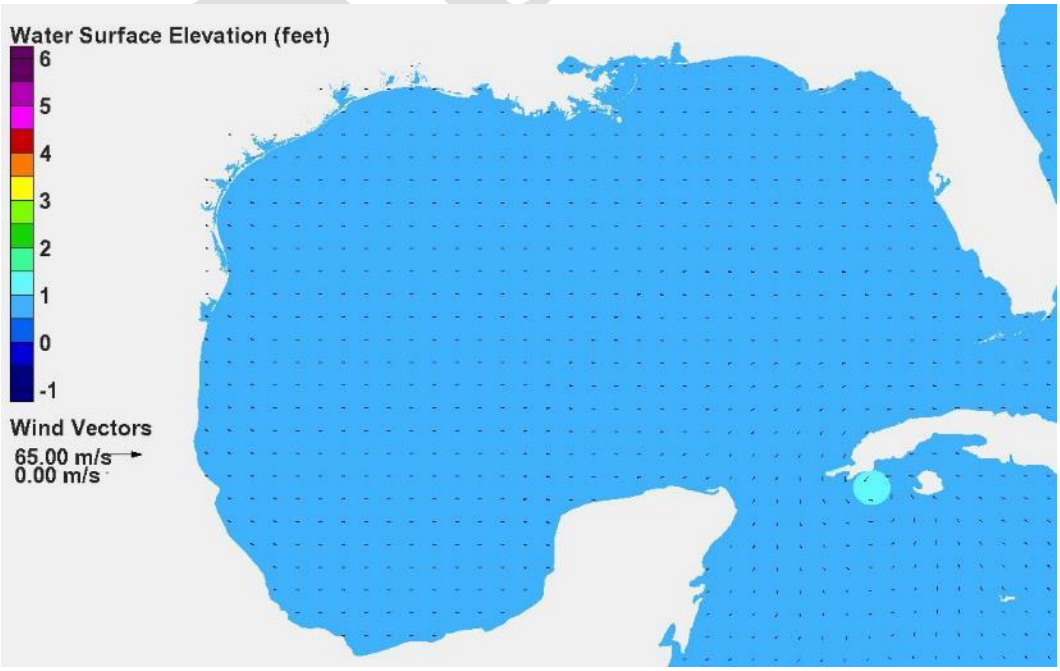

Figure 12. Water surface elevation and wind vectors in the Gulf of Mexico nearly 3 days before landfall for Storm 122 (direct-hit track, 900 mb)

Also evident are increasing water surface elevation along sections of the Gulf coast where the winds are blowing along the continental shelf, the shelf is widest, and a Kelvin wave is being forced. The figure clearly shows the development of this wind driven contribution to the forerunner, along the Louisiana-Texas coast; it's also evident along other regions of the Gulf having a wider continental shelf where winds blow along the coast. Along the north Texas coast, the increase in water surface elevation is approximately 1 ft. Also note the near uniform increase in water surface elevation through the Gulf, compared with the elevation in the previous figure. This appears to be associated with the volume model of oscillation, forced by entry of the storm into the Gulf about a day earlier.

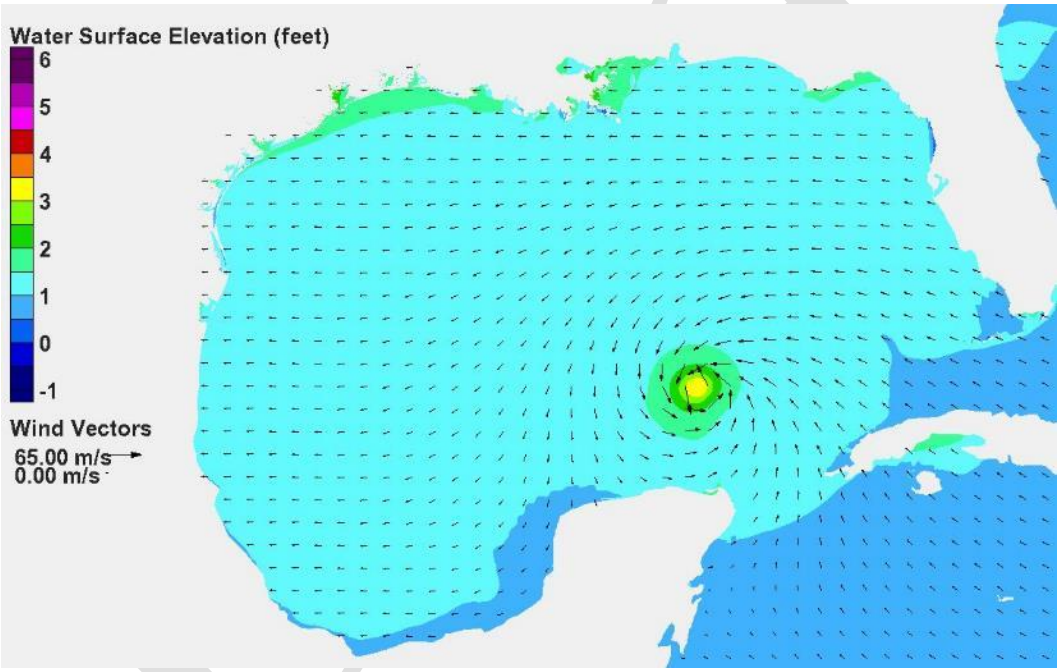

Figure 13. Water surface elevation and wind vectors in the Gulf of Mexico 2 days before landfall for Storm 122 (direct-hit track, 900 mb)

It should be noted that in these idealized synthetic hurricane simulations the hurricane is the only meteorological system in the Gulf; there are no other weather systems. So winds throughout the Gulf are only influenced by the hurricane and its forward speed as calculated by the planetary boundary layer wind model being used in the simulations. Along the northern Gulf coastline, winds blow along the coast from the east due to the counterclockwise wind circulation about the eye and its forward speed.

Figure 14 shows the water surface elevation and wind vectors for Storm 122, one day prior to landfall. The dome of water under the eye of the storm has grown as the storm intensifies to its minimum central pressure

of 900 mb. The maximum water surface elevation within this dome is greater than 4 ft NAVD88, 3 to 3.5 feet above mean sea level. Along the north Texas coast, due to the wind-driven forerunner, the increase in water surface elevation is approximately 1.5 to 2 ft above mean sea level.

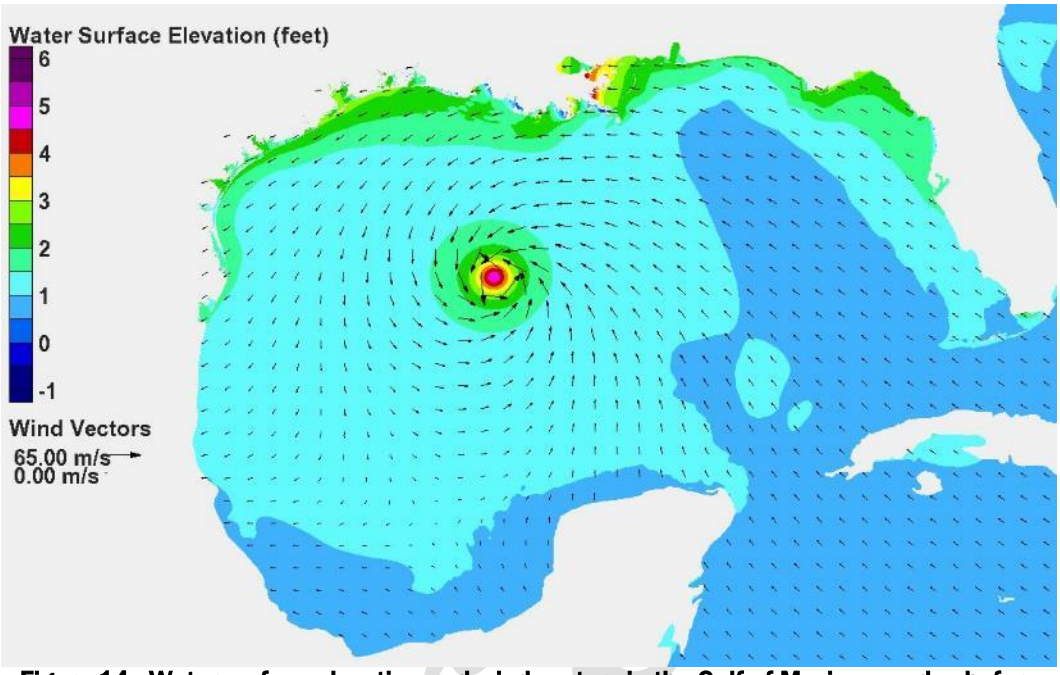

Figure 14. Water surface elevation and wind vectors in the Gulf of Mexico one day before landfall for Storm 122 (direct-hit track, 900 mb)

Figure 15 shows the water surface elevation and wind vectors for Storm 122, 12 hours after landfall. The hurricane has moved inland, the wind forcing is diminished and changed in direction, yet the water surface remains elevated along many coastal areas where the shelf is wide. This observation is consistent with the finding of Kennedy et al (2011) that the Kelvin wave becomes a free wave, moving along the shelf, after the wind forcing diminishes.

Figure 16 shows the water surface elevation and wind vectors for Storm 122, one day after landfall. The hurricane has moved well inland, and the wind forcing has decreased further. Evidence of the forerunner along the coast where the shelf is widest persists.

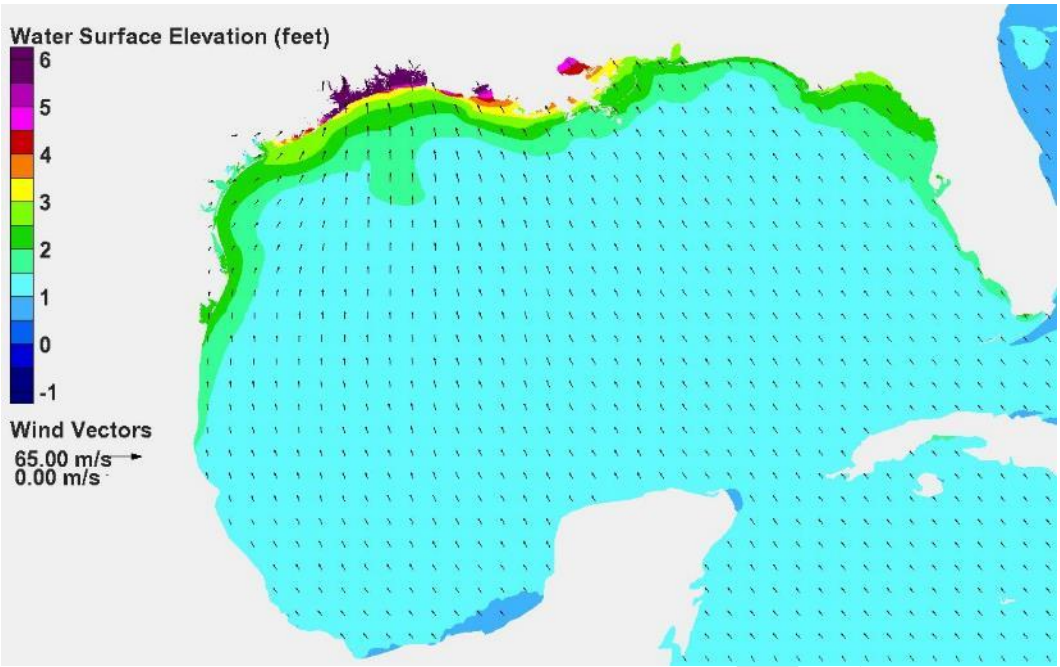

Figure 15. Water surface elevation and wind vectors in the Gulf of Mexico 12 hours after landfall for Storm 122 (direct-hit track, 900 mb)

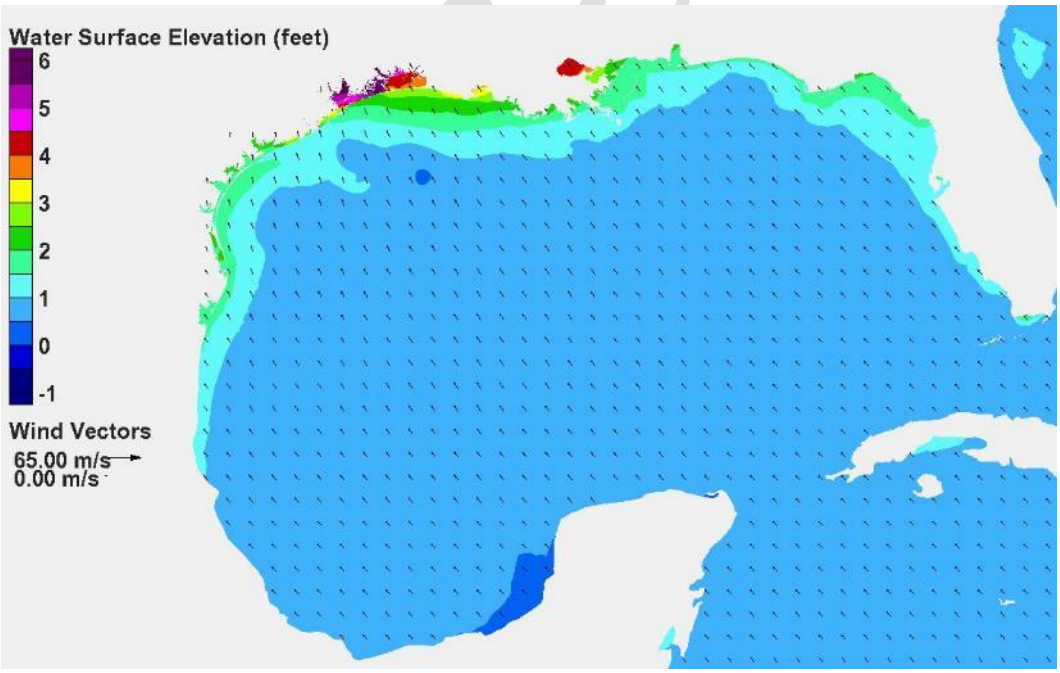

Figure 16. Water surface elevation and wind vectors in the Gulf of Mexico one day after landfall for Storm 122 (direct-hit track, 900 mb)

Comparing Figure 16 with Figure 15, snap-shots in time separated by 12 hours, a nearly uniform change in water surface elevation throughout the entire Gulf is evident. The entire Gulf water surface has decreased during this 12-hour period of time. Comparing Figure 12 prior to the hurricane entering the Gulf, with Figure 13 reflecting conditions a day later, a uniform increase in water surface elevation Gulf-wide also is evident. The color changes suggest an increase and decrease of about the same magnitude. This type of change is consistent with the volume mode, or Helmholtz, type of oscillation identified by Bunpapong et al (1985).

To further illustrate the development of the forerunner, Figure 17 shows the temporal variation of water surface elevation through time, during the first 60 hours of the simulation, at three locations: the open coast at Galveston (Pleasure Pier), inside Galveston Bay near the Clear Lake area along the western shoreline, and well into the Houston Ship Channel. The figure shows a slow steady increase in water surface elevation associated with the wind-driven Ekman wave, an increase of about 2 ft during the first 2 days, then nearly another foot of rise over the next 10 hours. The rate at which the surge builds noticeably increases at hour 50 as the storm winds over the continental shelf increase. Landfall occurs at hour 70. Also evident is the penetration of the forerunner into Galveston Bay for this storm. Elevations are higher inside the Bay due to an additional contribution of wind setup, where winds from the northeast set up the western side of the Bay by an additional 0.5 ft.

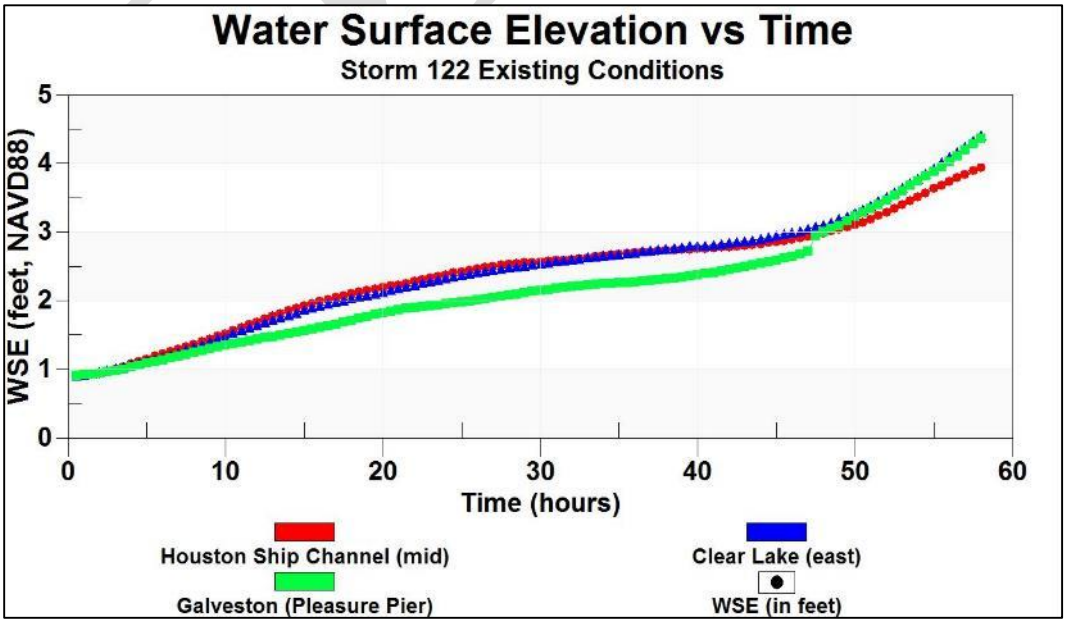

Figure 17. Temporal variation of water surface elevation showing forerunner development.

Surge Generation by the Core Winds

As the eye of the storm approaches the continental shelf, the stronger winds in the core of the storm, closest to the eye, begin to dominate the generation of the surge on the shelf. Winds are most effective in pushing water in the relatively shallow depths on the shelf, and, since the relationship between wind speed and surface wind stress is highly nonlinear, they become increasingly more effective as the hurricane moves toward shore into shallower and shallower water. . The increasing wind speed and resulting surface stress, and the presence of increasingly more shallow water causes the effect of the wind stress on the shelf and near the coast to increase dramatically as the hurricane moves towards the coastline. These processes are illustrated via the series of water surface elevation-wind snapshots for Storm 122 in Figures 18 through 22, which show the developing storm surge for the 12-hour period prior to landfall.

Figure 18 shows conditions 12 hours prior to landfall. The forerunner effect on the shelf and at the coastline are evident. The forerunner has increased the water surface elevation to nearly 4 ft NAVD88 along the coastline. Also evident is the effect of wind in the very shallow Galveston and West Bays, setting up the water surface on the downwind side (southwest side) of each bay due to winds blowing from the northeast.

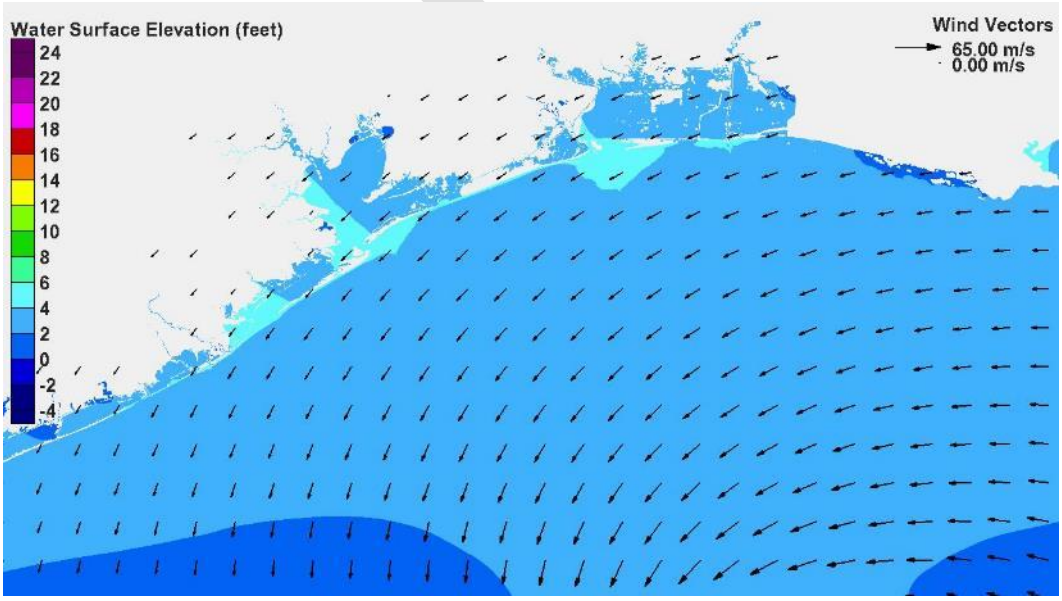

Figure 18. Water surface elevation and wind vectors 12 hours before landfall for Storm 122 (direct-hit track, 900 mb)

Figure 19 shows conditions 3 hours later, at a time 9 hours prior to landfall at Galveston. The eye of the hurricane is clearly visible, as evidenced by the counterclockwise wind circulation around the eye. The dome of water beneath the eye which is forced by the atmospheric pressure gradients is visible. Also evident is the increase in surge in the right front quadrant of the storm (viewed relative to the direction of storm advance). This is the zone where the surface winds have their maximum speed and greatest surge building capacity. Surge is building farther out on the shelf due to the higher core winds and decreasing water depth. The wind-driven surge on the shelf associated with the core winds is beginning to merge with the surge that has been forced as a forerunner closer to the shore.

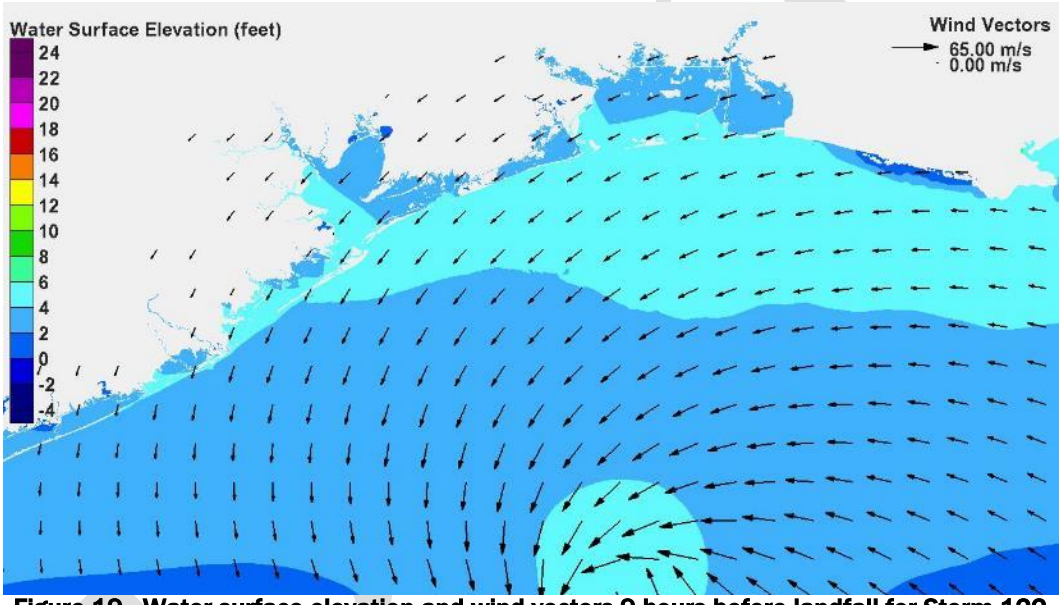

Figure 19. Water surface elevation and wind vectors 9 hours before landfall for Storm 122 (direct-hit track, 900 mb)

Figure 20 shows conditions 3 hours later at a time 6 hours before landfall. As the core winds move into increasingly more shallow water, surge on the shelf is increasing. The surge generated by the core winds is merging with the forerunner surge.

The same pattern of surge evolution is shown in Figure 21, three hours later, at a time 3 hours prior to landfall. The surge associated with the core winds and the forerunner have now merged. The core winds are producing waves, and have been even when the storm center was in deep water. The wave setup created by breaking waves is also contributing to the storm surge, but the storm surge is now primarily being forced by the core winds.

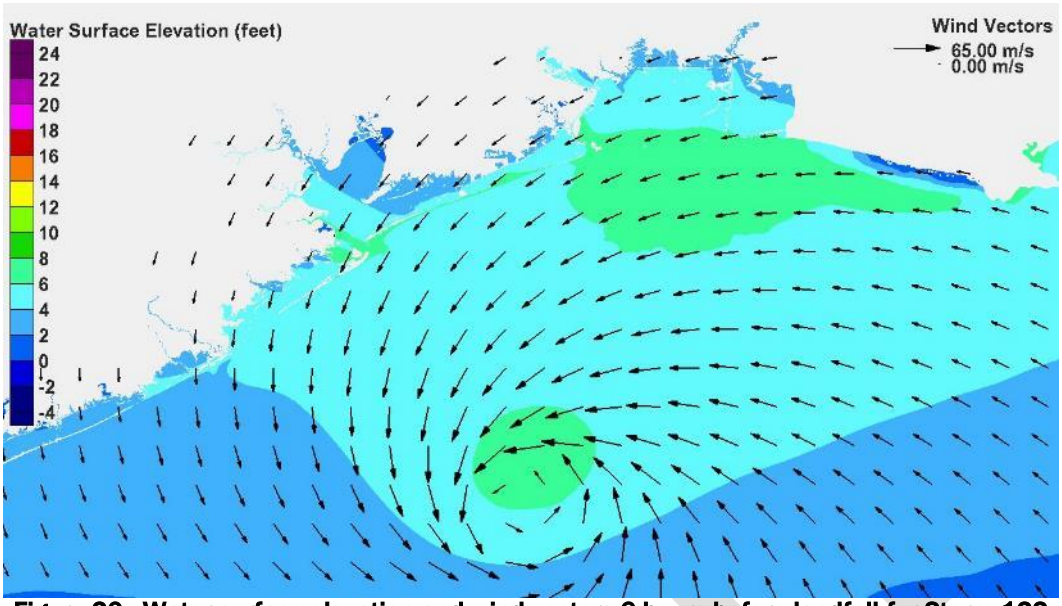

Figure 20. Water surface elevation and wind vectors 6 hours before landfall for Storm 122 (direct-hit track, 900 mb)

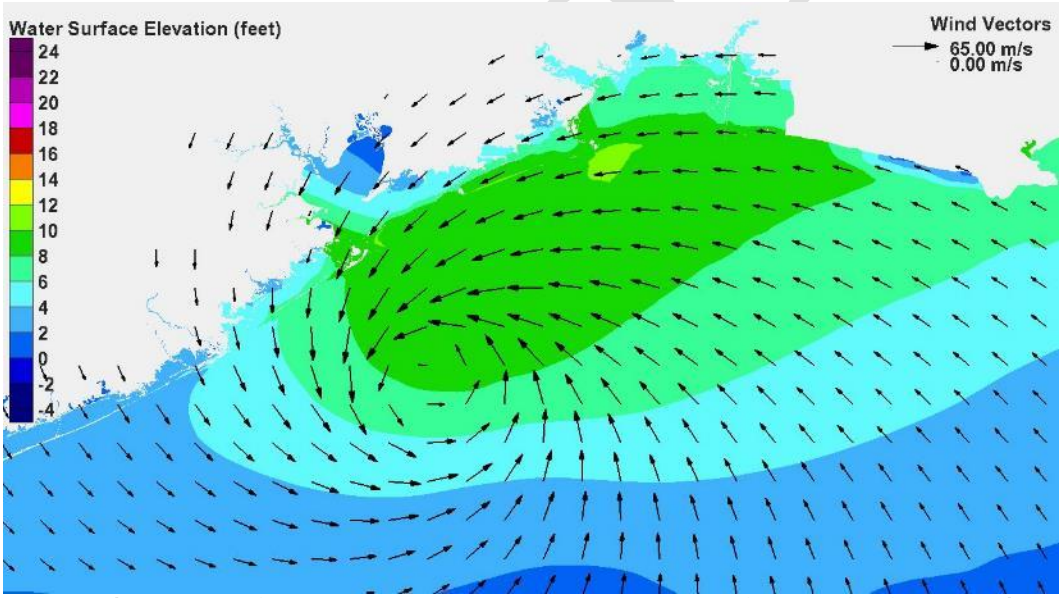

Figure 21. Water surface elevation and wind vectors 3 hours before landfall for Storm 122 (direct-hit track, 900 mb)

Figure 22 shows conditions at landfall. The surge at the coast has rapidly increased to levels in excess of 18 ft along Bolivar Peninsula. The onshore-directed winds have pushed the water that was accumulating on the shelf up against the coastline, with even greater force and effectiveness because of the very shallow water depths.

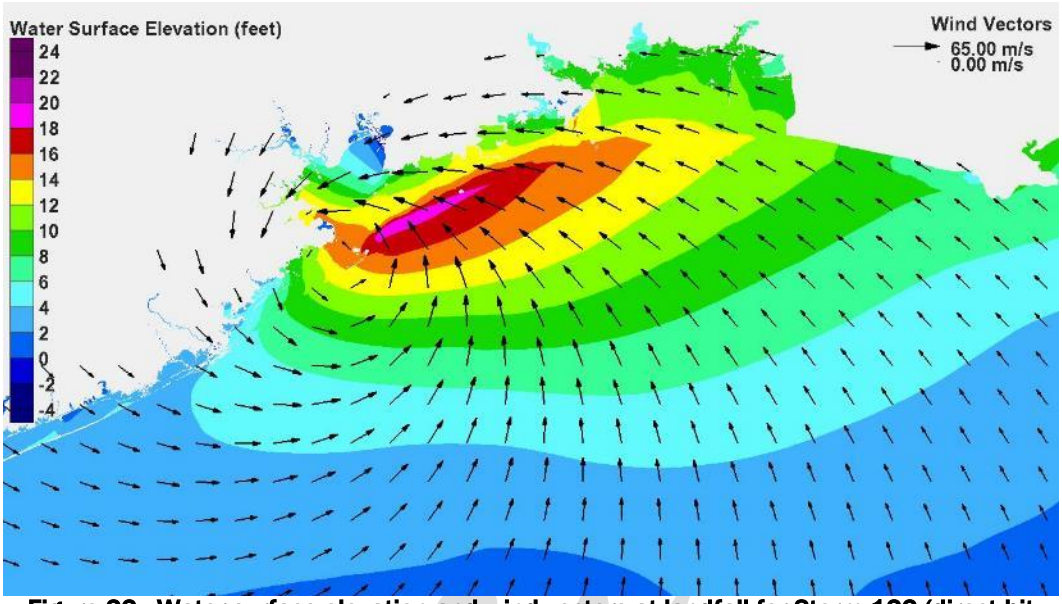

Figure 22. Water surface elevation and wind vectors at landfall for Storm 122 (direct-hit track, 900 mb)

The focus of this chapter was the development of storm surge on the open coast. The following chapter will focus on surge development within Galveston Bay.

6 Hurricane Surge Generation within Galveston Bay – Causative Factors

Introduction

In a semi-enclosed shallow water body like Galveston Bay (having an average water depth of approximately 10 ft), water levels will respond to both a filling action and a tilting of the water surface. Lake Pontchartrain near New Orleans, which also is semi-enclosed and has a water depth similar to Galveston Bay, responded to Hurricane Katrina with both filling and tilting of the water surface as the storm's eye moved through the region.

Filling arises from several sources. Filling occurs in response to water surface elevation differences (or head differences) between the ocean and bay at each of the passes that connect the two water bodies. Filling also occurs in response to overflow of adjacent barrier islands during extreme surge levels. Head differences are primarily caused by the surge forerunner and increased ocean surge associated with arrival of the storm's core winds. The tilting of the water surface within the bay occurs in response to local wind speed and direction, with a setup in water surface on the downwind side of the bay and possibly a set-down in water surface on the upwind side.

There is feedback between filling and tilting of the water surface, and the interactions are complex. Set-down is reduced within the bay if the filling rate is large enough to fill the area where wind is acting to set down the water surface. Also, the wind-induced tilting of the water surface within the bay can influence the head difference between ocean and bay, thereby affecting flow through the inlets, which in turn influences the filling rate. The greater the head difference, the faster the rate of filling. The magnitude of the water surface slope within the bay, i.e. the degree of tilting, is dependent upon the amount of filling. The greater the water depth in the bay, the less is the water surface slope induced by a certain wind speed. Filling acts to increase water surface elevations throughout the bay system, which reduces the degree of tilting of the water surface. The tilting of the water surface within the bay responds rather quickly to

changes in wind direction and therefore the tilting can be quite sensitive to storm track and position of the storm center relative to the bay. The modeling done in this feasibility study simulates well this complex interaction between filling and tilting of the water surface slope within Galveston Bay.

Surge generation within the Bay will be discussed for both the existing and with-dike conditions. In general the dike eliminates or dramatically reduces the filling action, which is substantial for existing conditions. The dike does not eliminate local tilting of the water surface within the bay. But by eliminating or reducing filling, the dike has a substantial beneficial effect on surge conditions within the Bay.

Existing Conditions

Previous sections of the report covered storm surge development during the several days prior to landfall, and development of the open coast surge. The focus here is on surge development within Galveston Bay. Surge development is once again illustrated via a series of water surface elevation-wind vector snapshots in time, one hour apart, spanning the time period from 6 hours before landfall to 10 hours after landfall. These are shown in Figures 23 through 37.

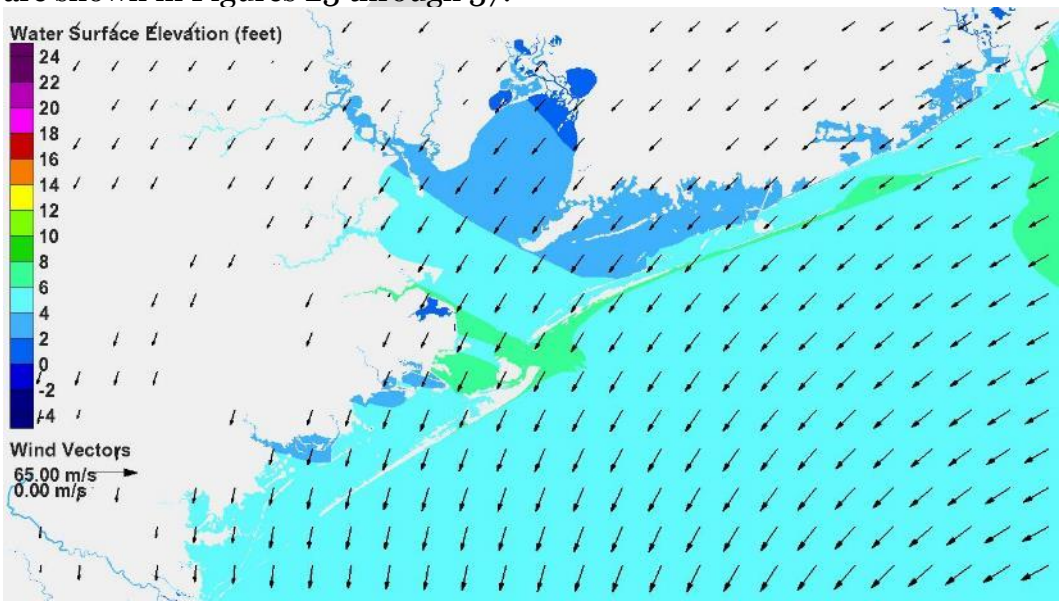

Figure 23. Water surface elevation and wind vectors 6 hours before landfall for Storm 122 (direct-hit track, 900 mb)

Figures 23 through 25 show the water surface slope within the bay, or tilt, increasing as the storm moves closer and wind speeds increase. Wind sets

up the water surface in the southwest corner of the bay. Filling of the bay through the passes by the forerunner has raised the water surface throughout the entire bay. Flow over the low barrier islands has begun.

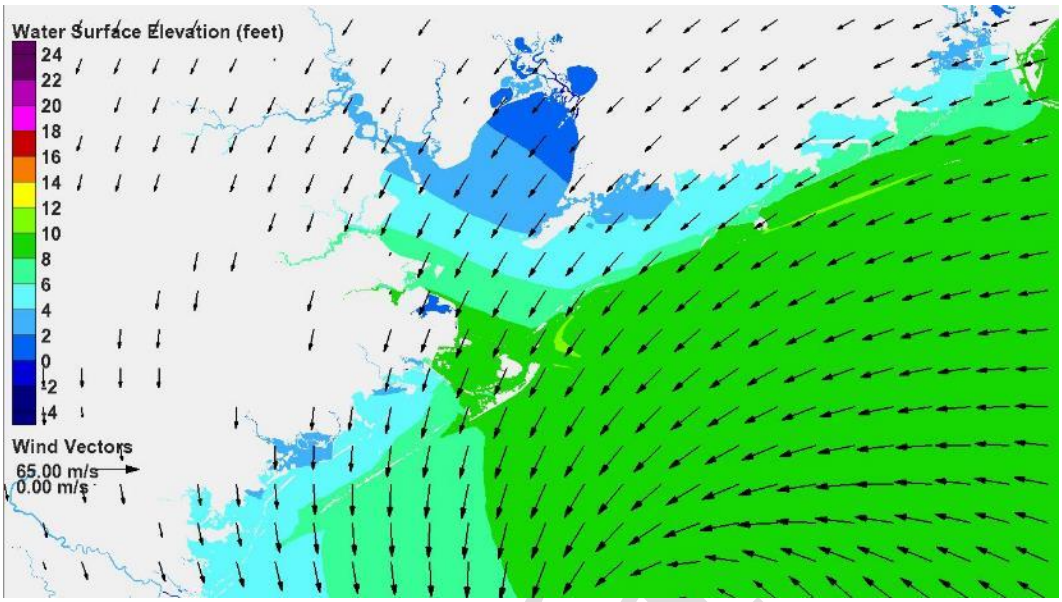

Figure 24. Water surface elevation and wind vectors 3 hours before landfall for Storm 122 (direct-hit track, 900 mb)

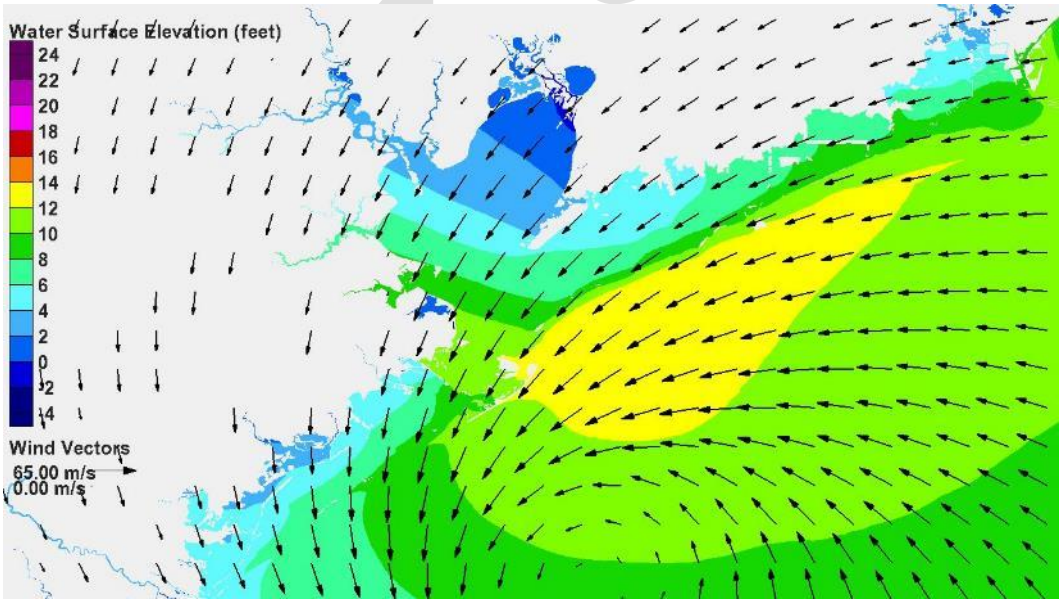

Figure 25. Water surface elevation and wind 2 hours before landfall for Storm 122 (direct-hit track, 900 mb)

In Figures 26 and 27, near landfall, filling due to barrier island overflow continues. The open coast surge of 18 ft has overwhelmed Bolivar

Peninsula; surge of 8 to 14 ft has overwhelmed most of Galveston Island. Once overtopped, barrier island overflow is the predominant source of bay filling. Local wind setup continues, building surge at Texas City and Galveston.

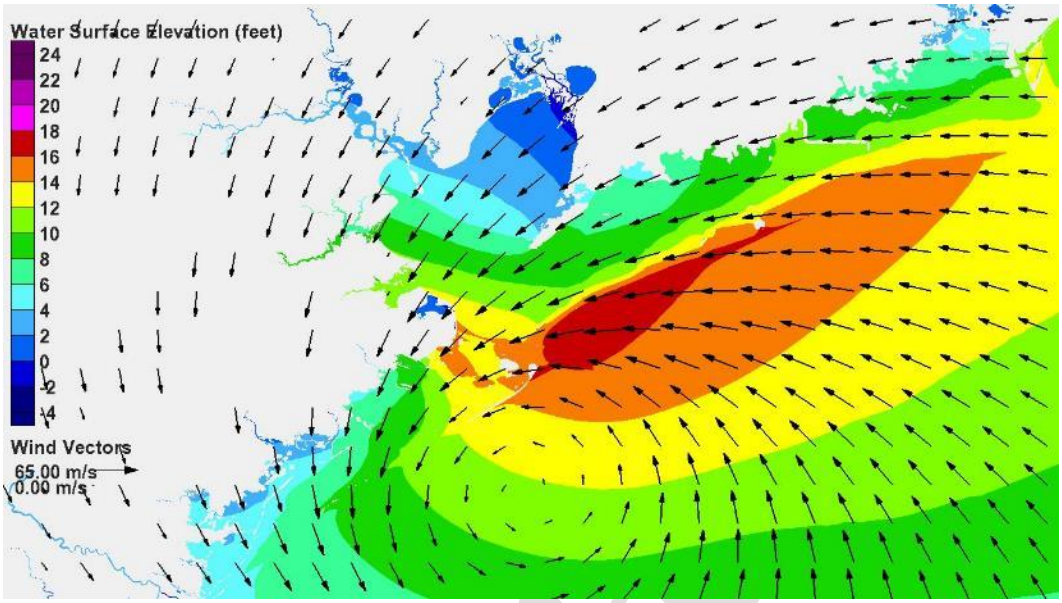

Figure 26. Water surface elevation and wind vectors 1 hour before landfall for Storm 122 (direct-hit track, 900 mb)

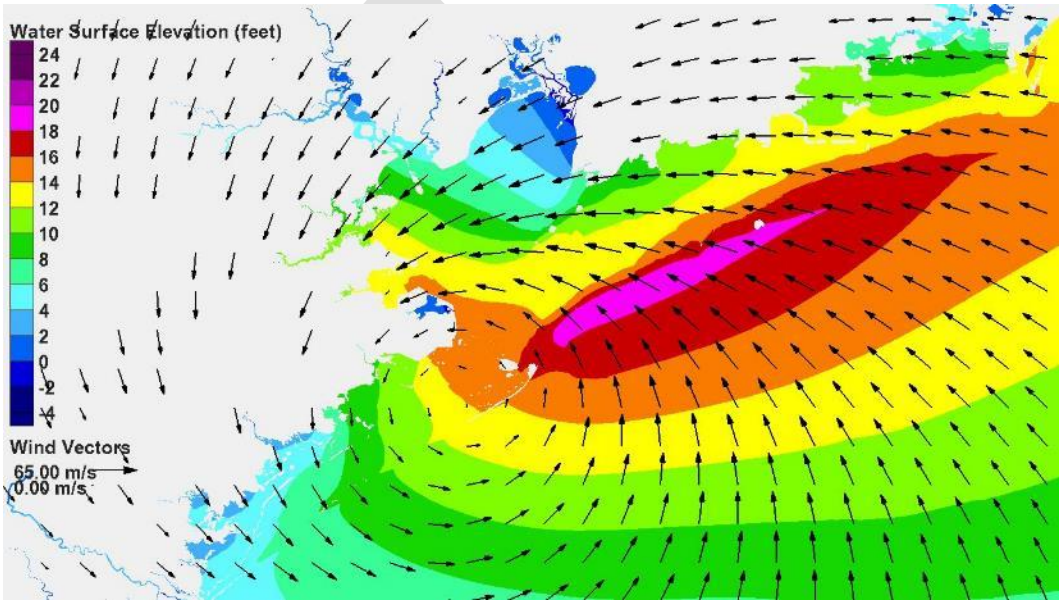

Figure 27. Water surface elevation and wind vectors at landfall for Storm 122 (direct-hit track, 900 mb)

The water surface slope within the Bay is changing. Figures 26 through 29 show the shifting wind pattern. In a matter of hours, winds have quickly shifted from the northeast, then from the east, then the southeast, then from the south. Winds are blowing onshore, strongly driving the water farther inland, toward the northwest inside the bay. Surge is 13 to 15 feet along the western shoreline of the Bay and at Galveston.

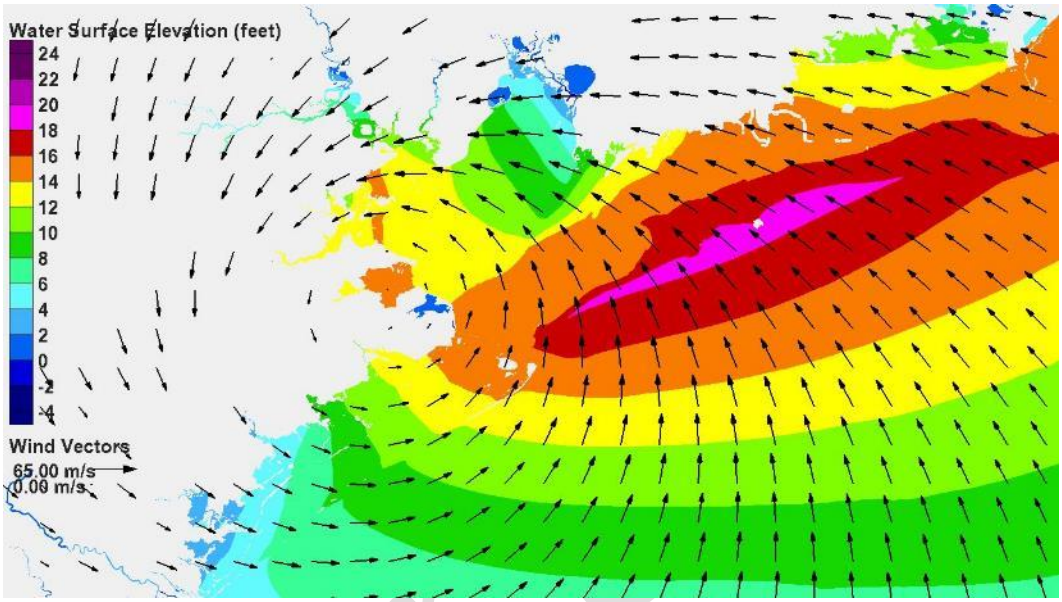

Figure 28. Water surface elevation and wind vectors 1 hour after landfall for Storm 122 (direct-hit track, 900 mb)

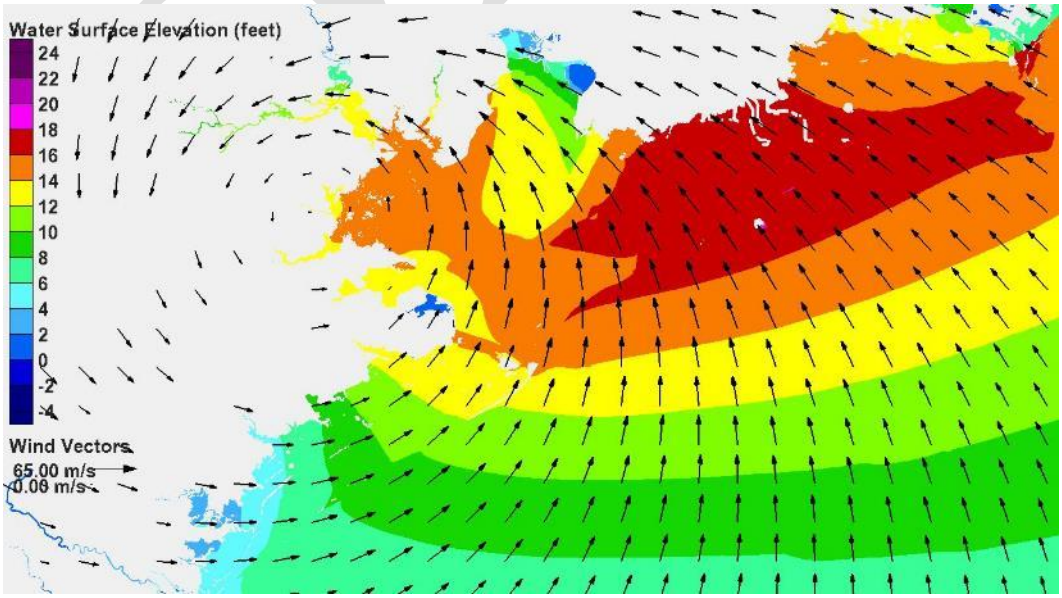

Figure 29. Water surface elevation and wind vectors 2 hours after landfall for Storm 122 (direct-hit track, 900 mb)

Figures 30 and 31 show the surge 3 to 4 hours after landfall. The eye is moving through the Houston area. Winds from the south persist, pushing water that has accumulated within the Bay to the north. Surge is building in the upper reaches of Galveston Bay and the Houston Ship Channel. Surge is already subsiding at the coast and lower parts of the Bay.

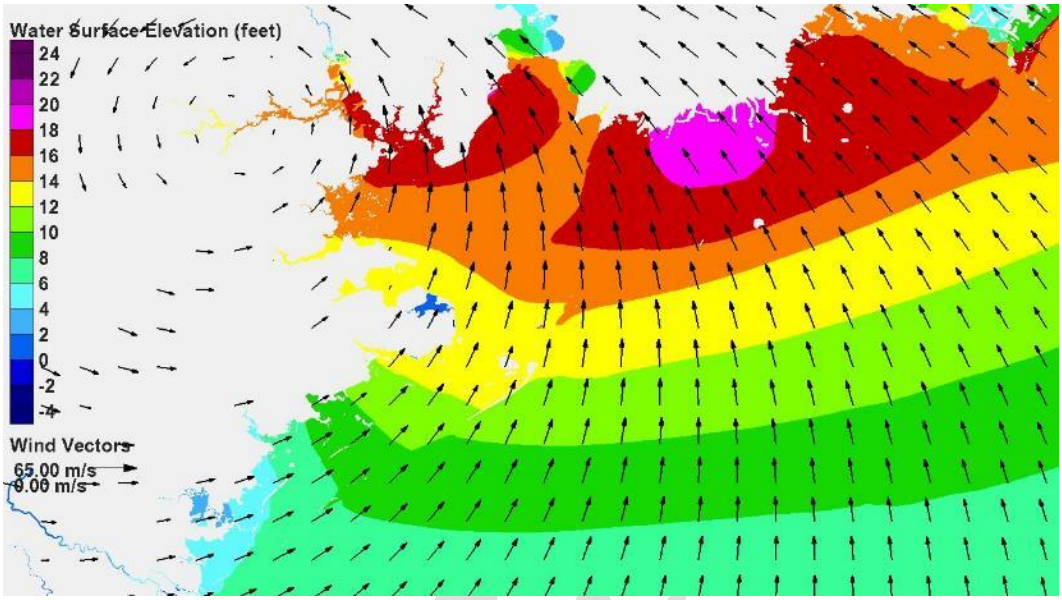

Figure 30. Water surface elevation and wind vectors 3 hours after landfall for Storm 122 (direct-hit track, 900 mb)

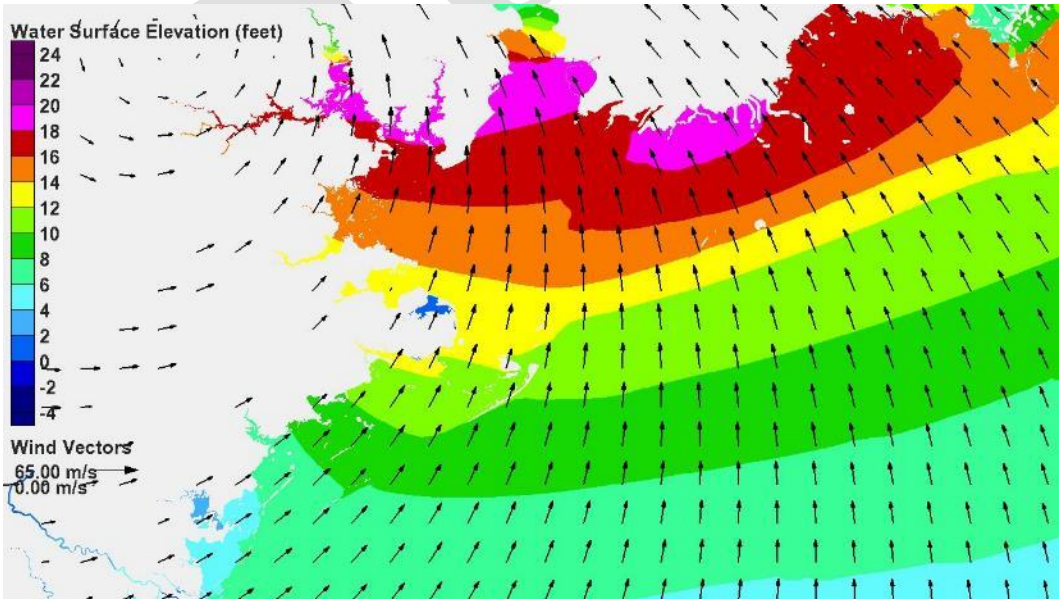

Figure 31. Water surface elevation and wind vectors 4 hours after landfall for Storm 122 (direct-hit track, 900 mb)

In Figures 32 and 33, the pattern of winds from the south continues, increasing the surge in the upper reaches of Galveston Bay. While surge levels at Galveston continue to decrease to 10 ft, surge in upper reaches of the Houston Ship Channel is approaching its maximum value of 19 ft. Surge levels in the middle of the Bay remain steady, at 13 to 17 ft.

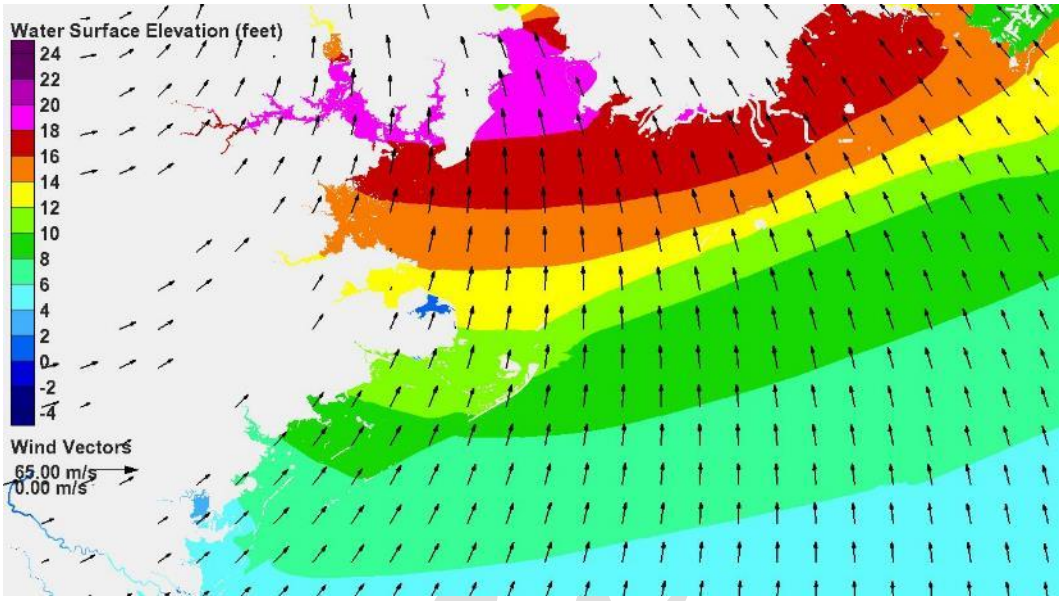

Figure 32. Water surface elevation and wind vectors 5 hours after landfall for Storm 122 (direct-hit track, 900 mb)

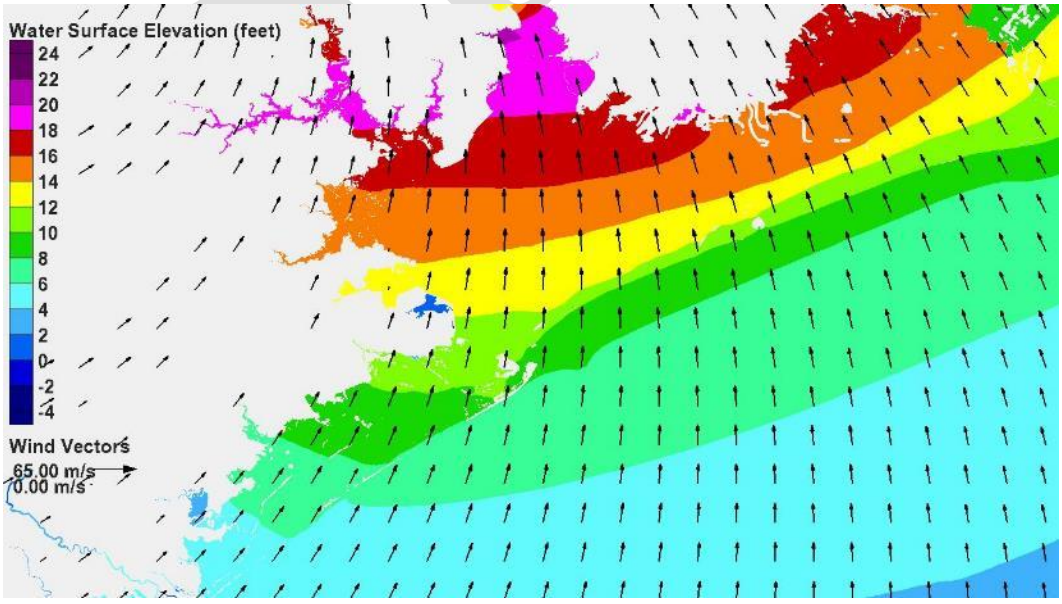

Figure 33. Water surface elevation and wind vectors 6 hours after landfall for Storm 122 (direct-hit track, 900 mb)

Figures 34 and 35 show the storm surge field 7 and 8 hours after landfall, respectively. Surges in the upper reaches of the Houston Ship Channel have reached their peak and are beginning to subside. Winds remain from the south but they are diminishing in strength. Surge within the whole Houston-Galveston area is beginning to recede back over the barrier islands and through the passes. Surge along the western bay is 11 to 15 ft.

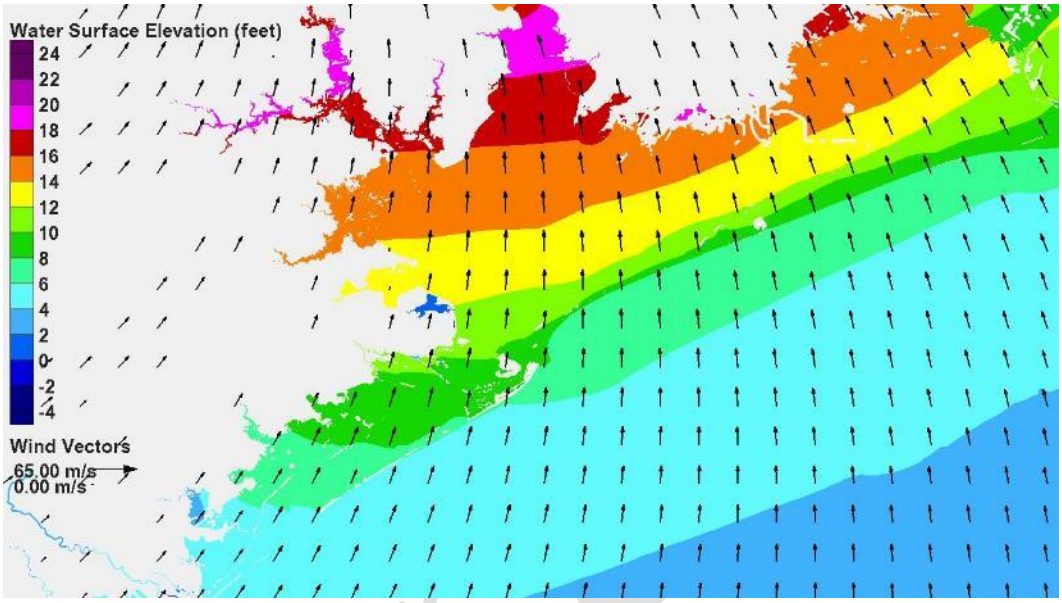

Figure 34. Water surface elevation and wind vectors 7 hours after landfall for Storm 122 (direct-hit track, 900 mb)

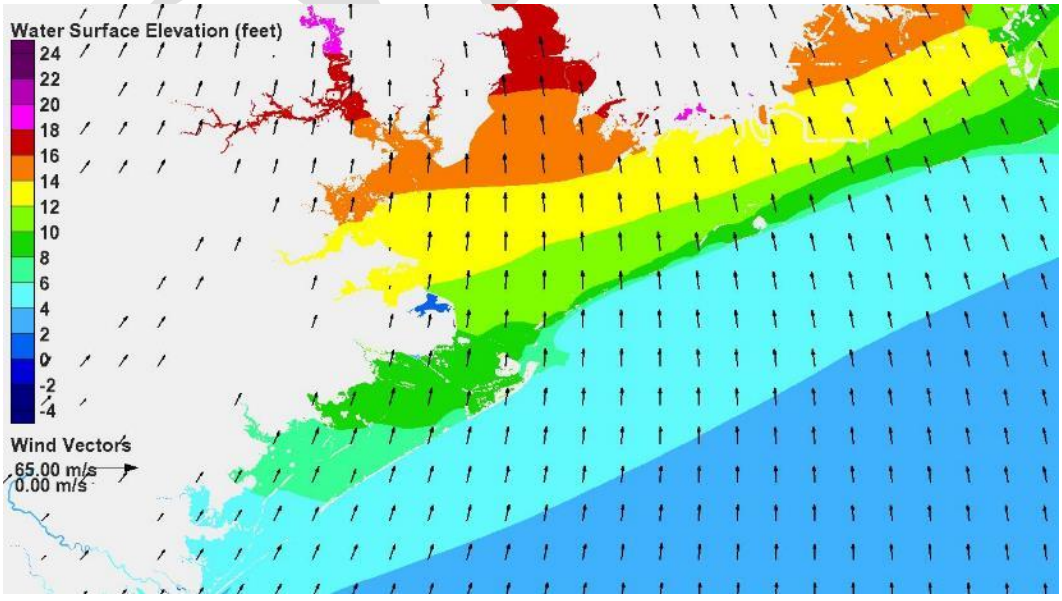

Figure 35. Water surface elevation and wind vectors 8 hours after landfall for Storm 122 (direct-hit track, 900 mb)

Continued recession of the surge is shown in Figures 36 and 37, 9 and 10 hours after landfall, respectively. Surges in the upper Bay and Houston Ship Channel still exceed 14 ft. Surge along the west shoreline of the Bay are 9 to 14 ft. Surge levels along the open coast have receded to 5 ft, facilitating flow of water from the Bay back to the Gulf.

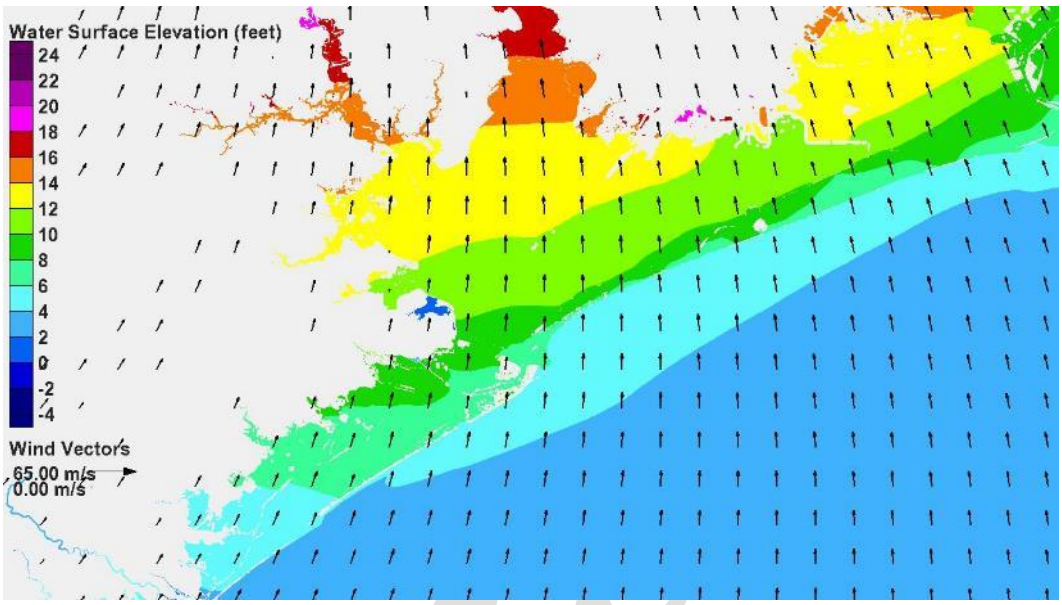

Figure 36. Water surface elevation and wind vectors 9 hours after landfall for Storm 122 (direct-hit track, 900 mb)

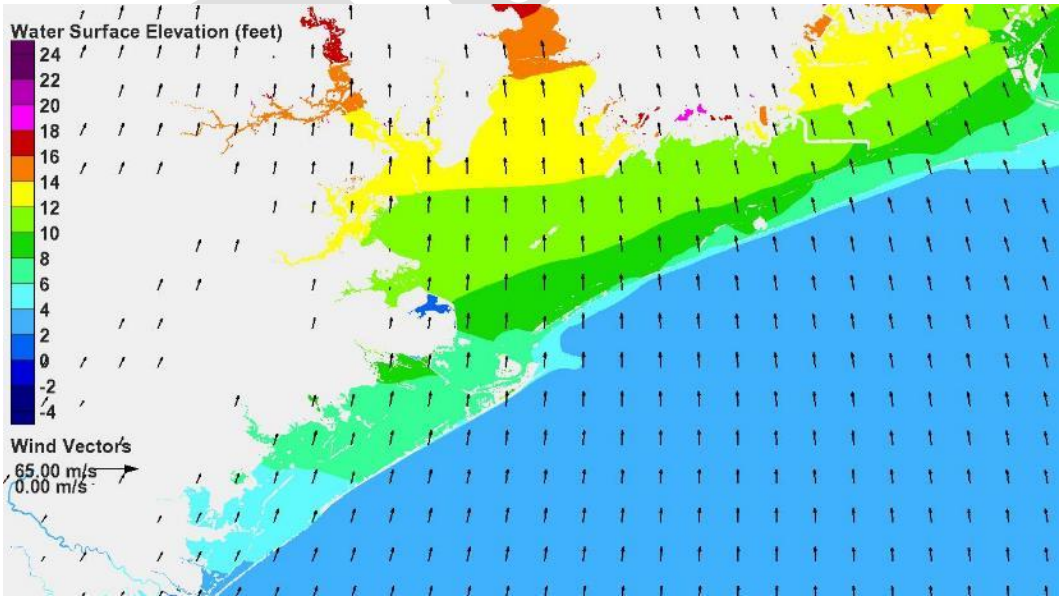

Figure 37. Water surface elevation and wind vectors 10 hours after landfall for Storm 122 (direct-hit track, 900 mb)

Figure 38 shows the temporal variation of storm surge at five locations: Galveston (Pleasure Pier) on the open coast, the Bay side of the City of Galveston, just north of Texas City along the western Bay shoreline, the Clear Lake area along the Bay shoreline, and in the upper reach of the Houston Ship Channel. Storm surge at the Pleasure Pier and the Bay side of Galveston rose rapidly, from 7 ft to a peak of about 15 feet, in 3 to 4 hours. A similar rate of rise is seen at other locations along the western Bay shoreline. The hydrographs at Texas City and Clear Lake show persistent surge levels of 13 to 15 ft for about 7 hours, following slightly higher peak surges, after the eye moves through and winds blow steadily from the south. At Galveston, surge decreases relatively quickly after the time of peak surge. The hydrograph shape in the Houston Ship Channel is quite different. There is actually a decrease from 4 ft to 3 ft when other locations are experiencing a rapid increase in surge. This occurs as strong local winds set up the southwest part of the Bay, drawing water from the upper parts, as landfall is nearing. But as the eye moves through and wind direction changes rapidly, storm surge in the upper reaches of the Houston Ship Channel changes dramatically, increasing from 3 ft to 19 ft in the span of only 6 hours. Peak surge occurs about 7 hours after landfall, much later than at the other locations. The rates at which surge falls following passage of the hurricane through the region are much less than the rates of rise as the surge was building. Even 20 hours after landfall, surge levels in the Bay vary from 3 ft (lower Bay) to 10 ft (upper Bay).

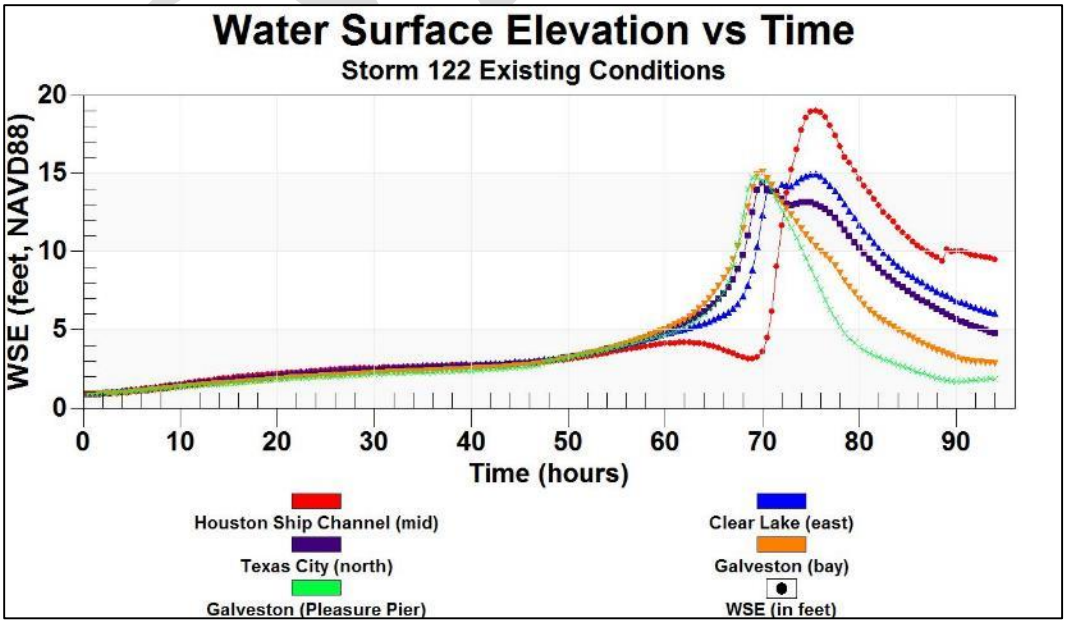

Figure 38. Temporal variation of water surface elevations within Galveston Bay for Storm 122 , existing conditions

Surge Generation in Galveston Bay - With the Ike-Dike Concept

Figures 39 to 53 show snapshots of water surface elevation and wind vectors for with-dike conditions. Snapshots in time are shown for the same times prior to, at, and after landfall as were shown in the previous section. In general, the dike greatly reduces or eliminates flow over the barrier islands, resulting in a significant reduction in storm surge within the Bay. Barrier island overflow is the dominant contributor to filling within the Bay for the existing condition. Some major storms overtop the dike that is being considered at present, but that volume is considerably less than the volume that can flow over the low barrier islands. The dike does not alter wind fields within the Bay, however, so tilting of the water surface by the wind within the Bay is not affected very much by the presence of the dike.

Figure 29 shows conditions within the Bay 6 hours before landfall. Persistent winds from the northeast set up the southwest corners of Galveston and West Bays, as they have been doing prior to this time. In the absence of a source of water to raise the Bay's water level, the northeast corner is being set down by the wind, i.e., negative water surface elevations. Water is being pushed from Galveston Bay into West Bay, subject to constrictions that impede the water from doing so.

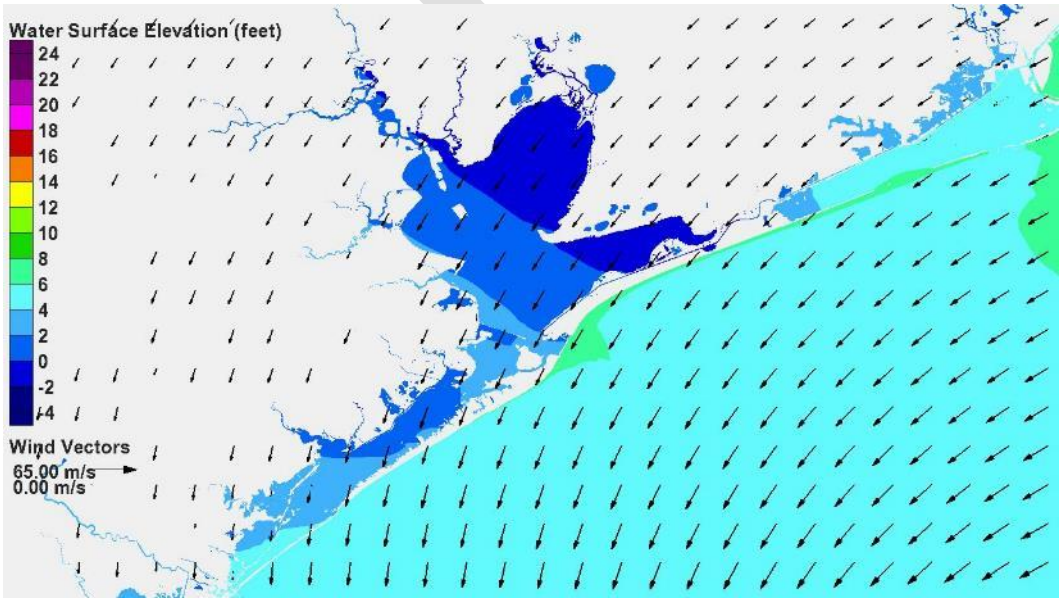

Figure 39. Water surface elevation and wind vectors 6 hours before landfall for Storm 122 (direct-hit track, 900 mb)

Figures 40 and 41 show the storm approaching and wind speeds within the Bay increasing. The increase in speed increases the water surface slope, or tilt, within the Bays forcing water from the northeast parts of Galveston Bay to the southwest part and then into West Bay. The tilting action is drawing water out of the upper reaches of the Houston Ship Channel.

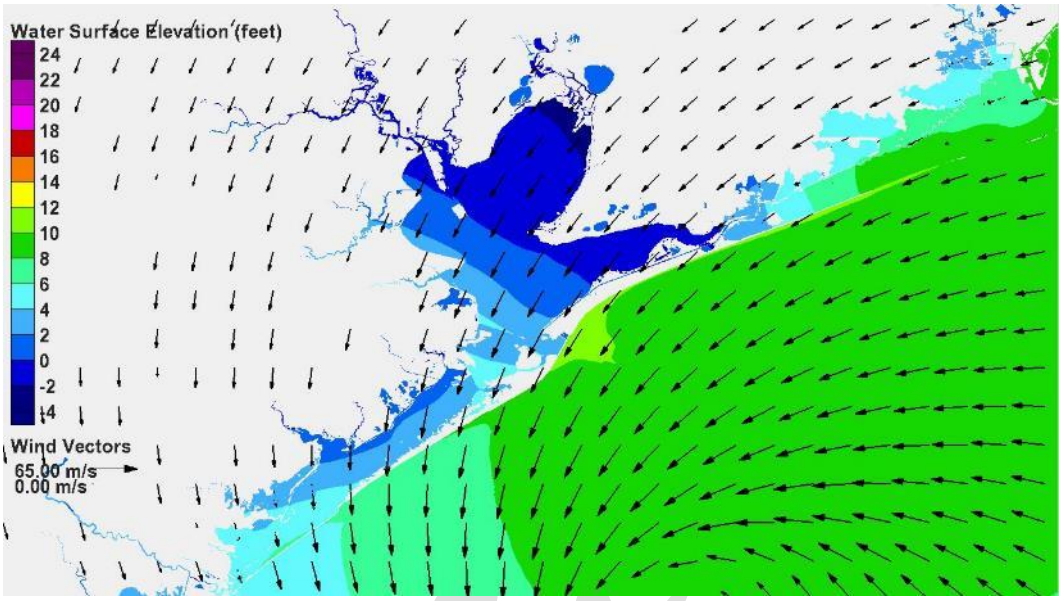

Figure 40. Water surface elevation and wind vectors 3 hours before landfall for Storm 122 (direct-hit track, 900 mb)

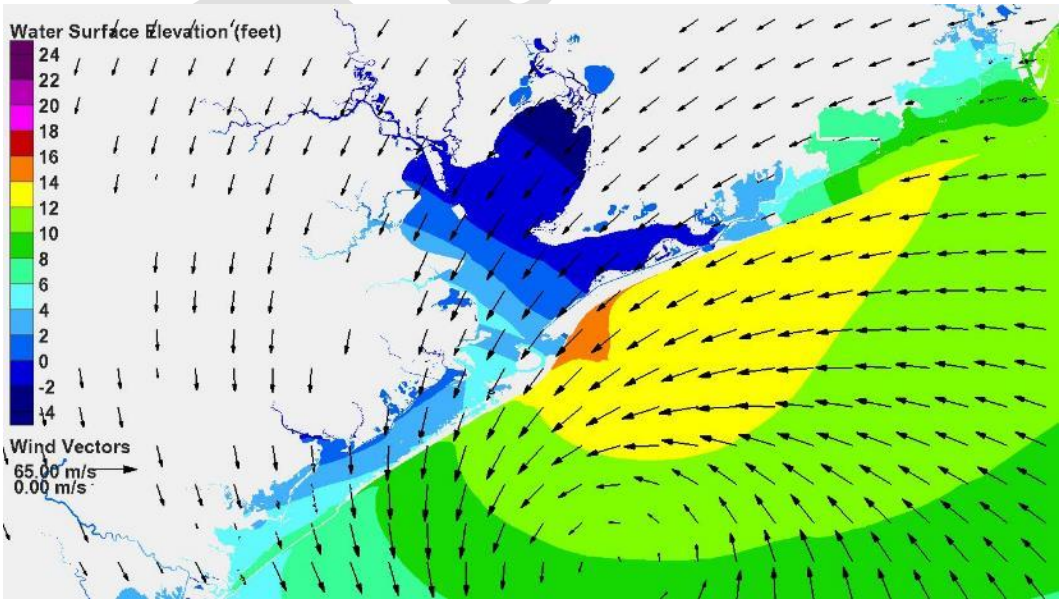

Figure 41. Water surface elevation and wind vectors 2 hours before landfall for Storm 122 (direct-hit track, 900 mb)

Figures 42 and 43 show conditions near landfall. The tilting action is exacerbated by the higher wind speeds in the Bay. The surge at the southwest corner of Galveston Bay reaches 8 to 9 ft, some 7 ft less than for existing conditions. The dike is being overtopped along Galveston Bay.

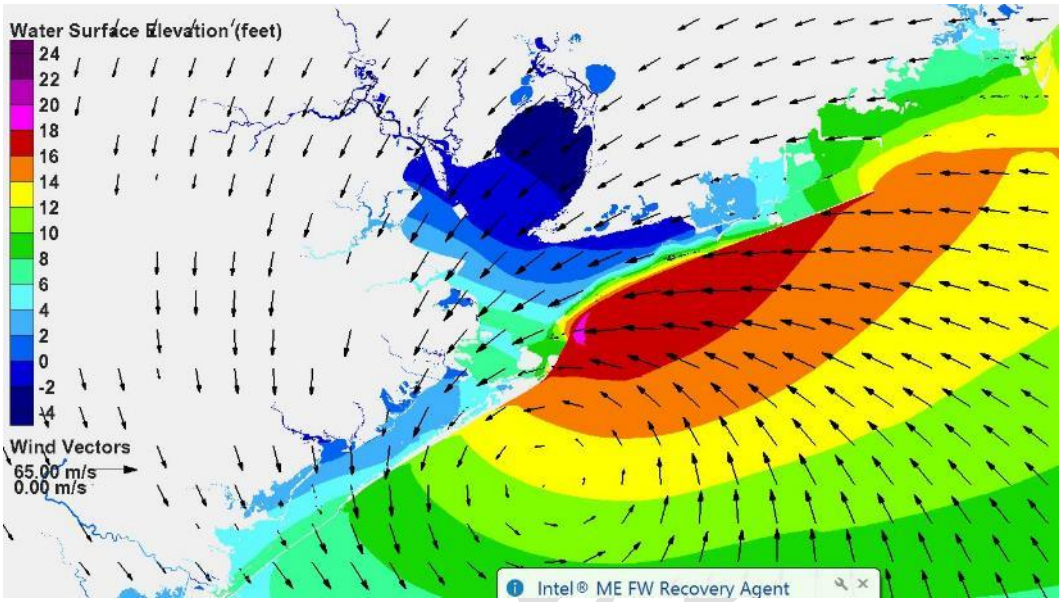

Figure 42. Water surface elevation and wind vectors 1 hour before landfall for Storm 122 (direct-hit track, 900 mb)

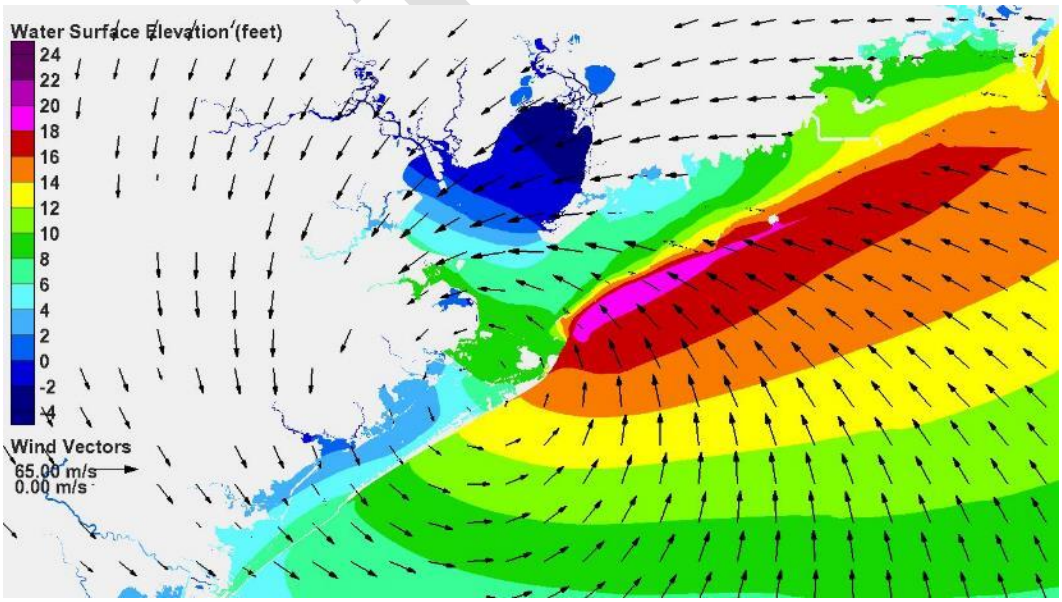

Figure 43. Water surface elevation and wind vectors at landfall for Storm 122 (direct-hit track, 900 mb)

Figures 44 and 45 show conditions just after landfall. Overflow continues along Bolivar Peninsula; no overflow is occurring along Galveston Island. Winds are shifting rapidly, and water is being driven to the northern parts of the Bay and into the upper reaches of the Houston Ship Channel. Surge on the Bay side of Galveston has reached its peak of 8 to 10 ft.

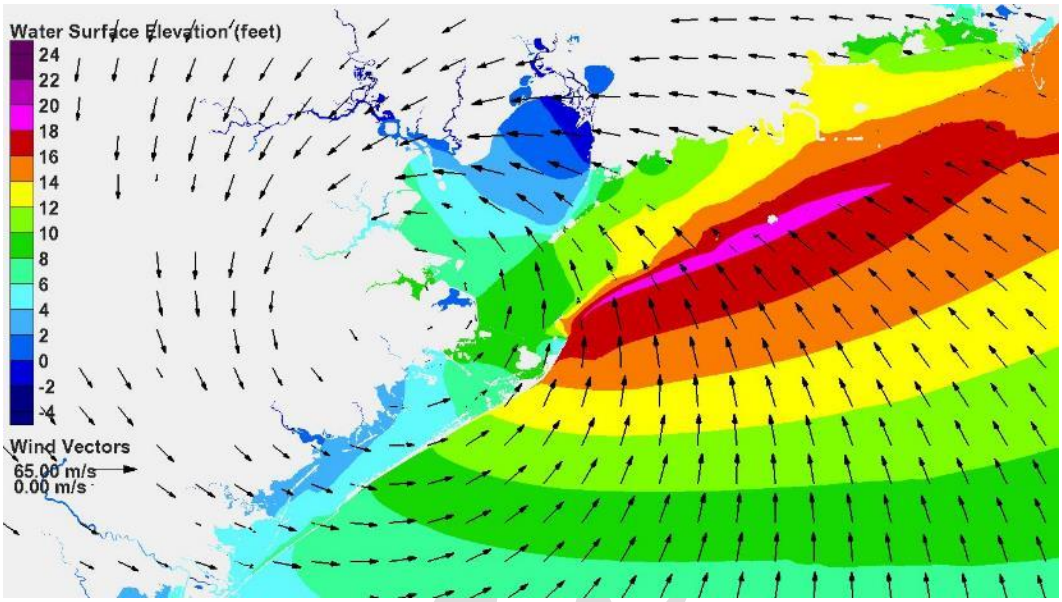

Figure 44. Water surface elevation and wind vectors 1 hour after landfall for Storm 122 (direct-hit track, 900 mb)

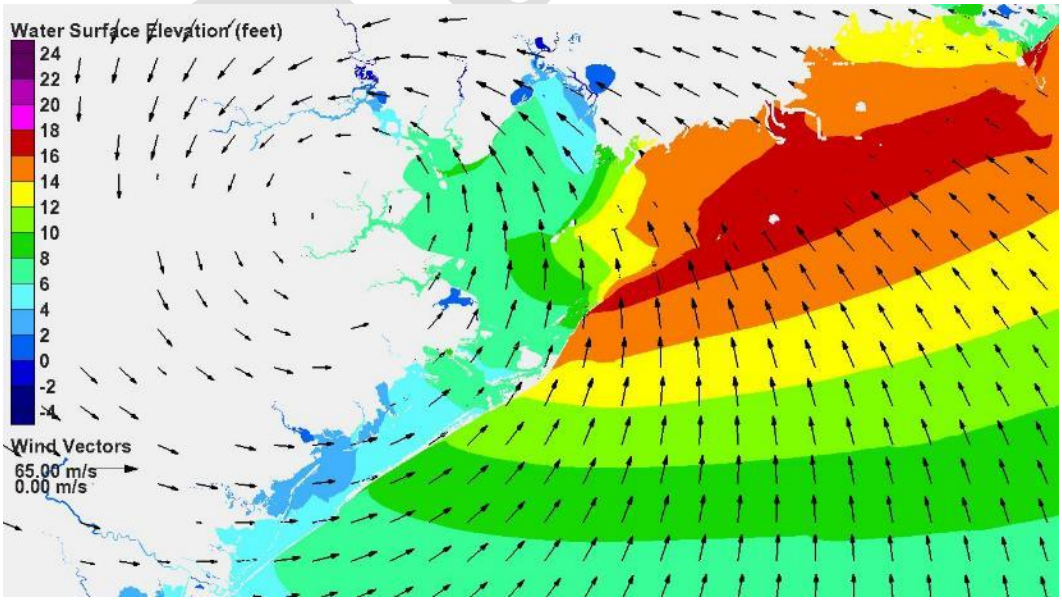

Figure 45. Water surface elevation and wind vectors 2 hours after landfall for Storm 122 (direct-hit track, 900 mb)

Figures 46 and 47 show conditions as the hurricane eye moves though the City of Houston. Water is being driven by southerly winds from West Bay into Galveston Bay and into the upper parts of the Galveston Bay system including the upper reaches of the Houston Ship Channel. Surge along the western shoreline of the Bay is 6 to 10 feet, some 5 to 6 feet less than for existing conditions. Surge along the back side of Galveston Island is less than 6 ft. Flow over the dike along Bolivar Peninsula has ceased, since the ocean surge is already beginning to subside following landfall.

Water is moving around the north extent of the dike and toward the bay. The Ike Dike concept was represented in the initial modeling as a finite length barrier with no tie-ins to higher ground. Decisions on where to terminate the dike and how to transition the dike to higher natural elevation will be made in the future. But to reduce the amount of encroachment around the structure, the dike will be extended in the next phase of the feasibility study. By not having tie-ins, the present simulations are likely overstating the amount of water entering the Bay.

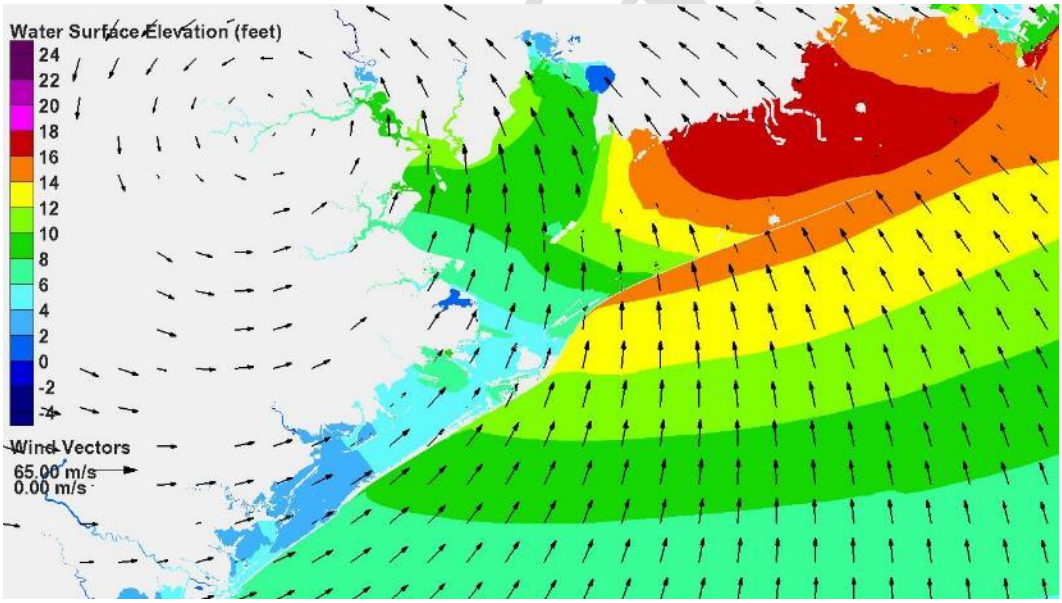

Figure 46. Water surface elevation and wind vectors 3 hours after landfall for Storm 122 (direct-hit track, 900 mb)

Figures 47 and 48, 4 and 5 hours after landfall, respectively, show persistent winds from the south as the hurricane moves out of the region. Surge has reached its maximum in the upper Houston Ship Channel, nearly 13 ft, some 6 feet less than for existing conditions. Surges along the western shoreline of Galveston Bay also have peaked but are stationary.

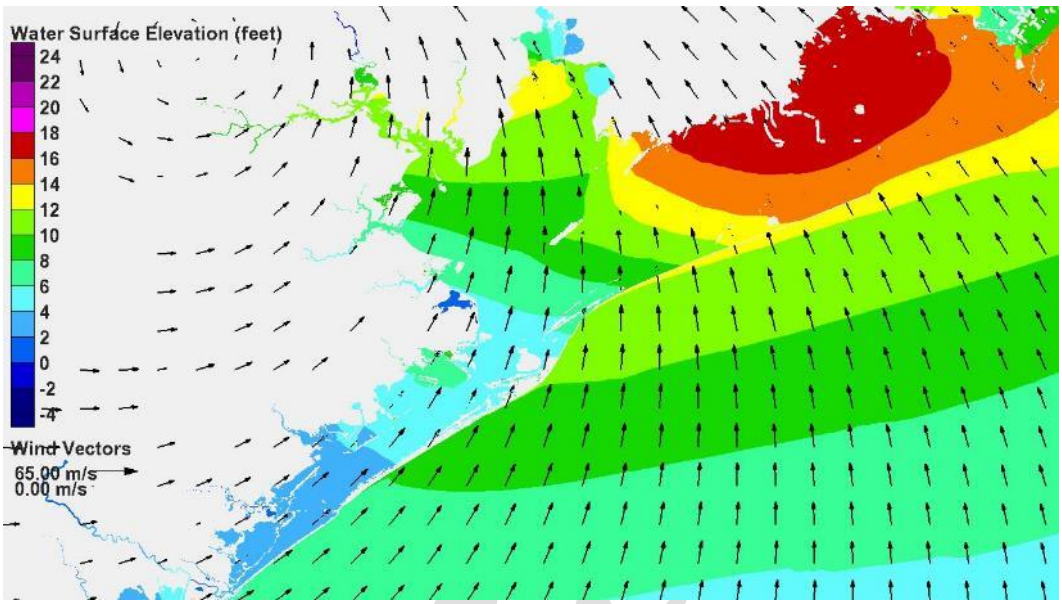

Figure 47. Water surface elevation and wind vectors 4 hours after landfall for Storm 122 (direct-hit track, 900 mb)

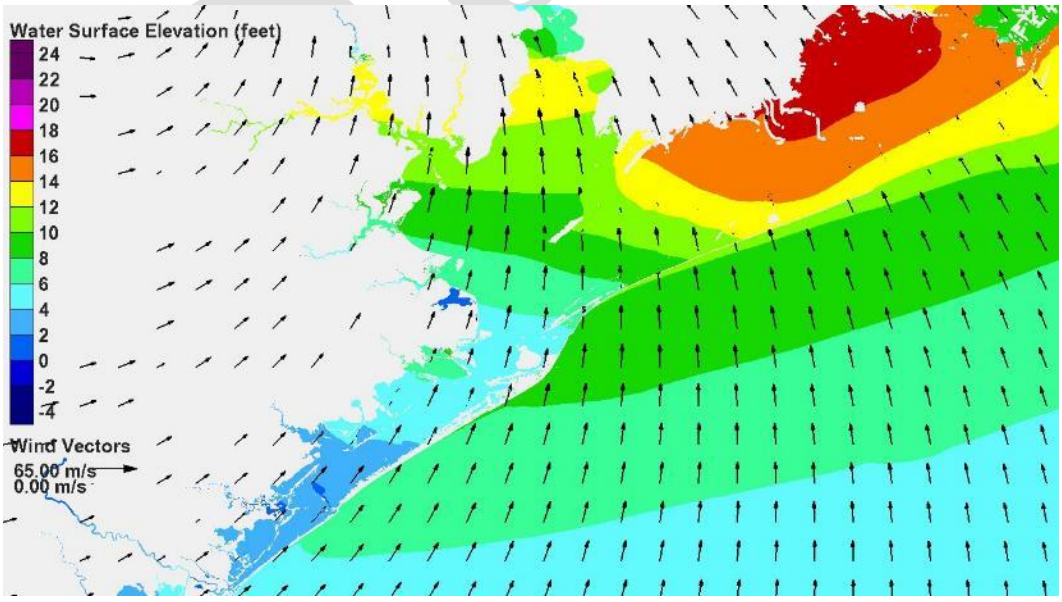

Figure 48. Water surface elevation and wind vectors 5 hours after landfall for Storm 122 (direct-hit track, 900 mb)

Figures 49 through 53 show persistent surge levels along the western shoreline of the Bay, and decreasing surge in the upper Houston Ship Channel. Water that encroached around the northern extent of the dike is moving into the Bay and acting to fill it. This is an artifact of not having tie-ins of the dike to higher ground.

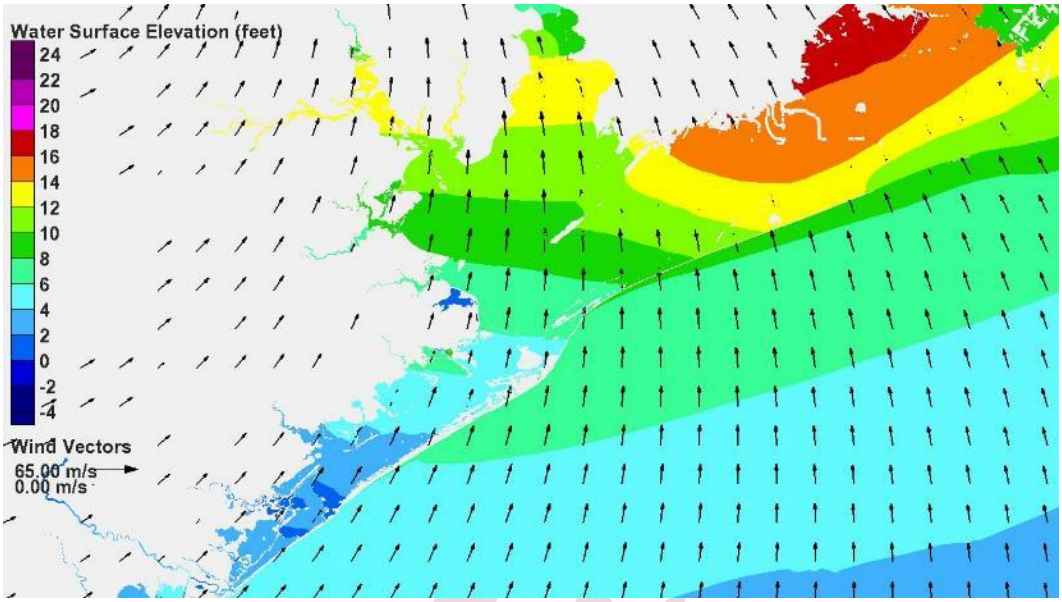

Figure 49. Water surface elevation and wind vectors 6 hours after landfall for Storm 122 (direct-hit track, 900 mb)

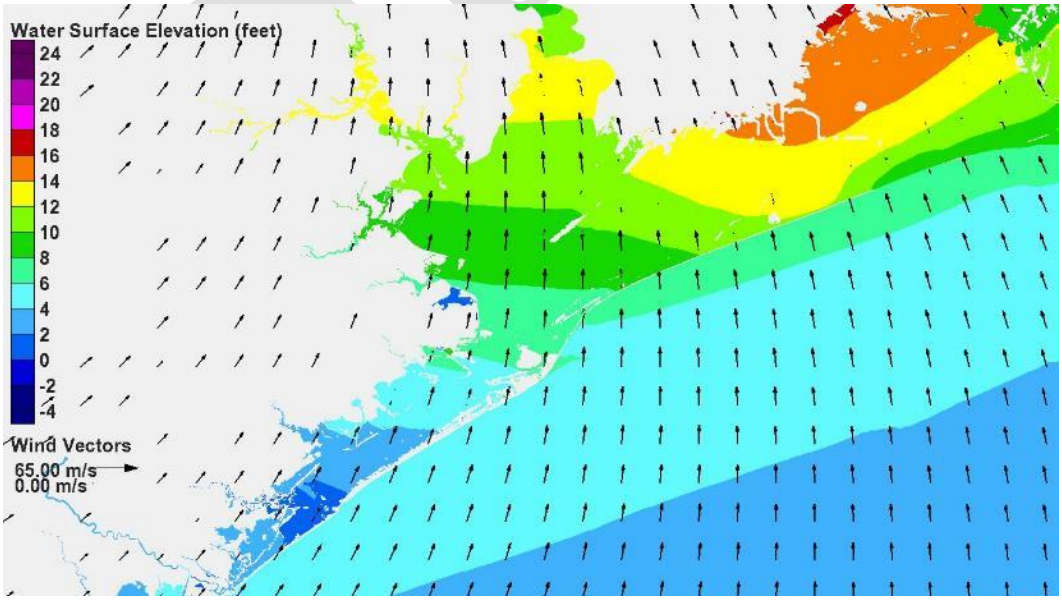

Figure 50. Water surface elevation and wind vectors 7 hours after landfall for Storm 122 (direct-hit track, 900 mb)

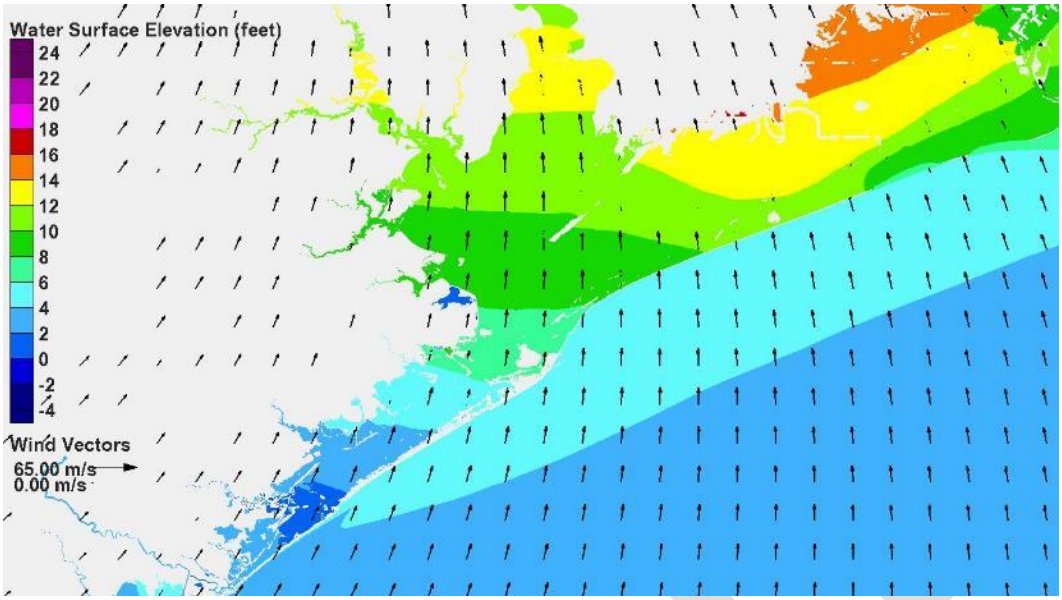

Figure 51. Water surface elevation and wind vectors 8 hours after landfall for Storm 122 (direct-hit track, 900 mb)

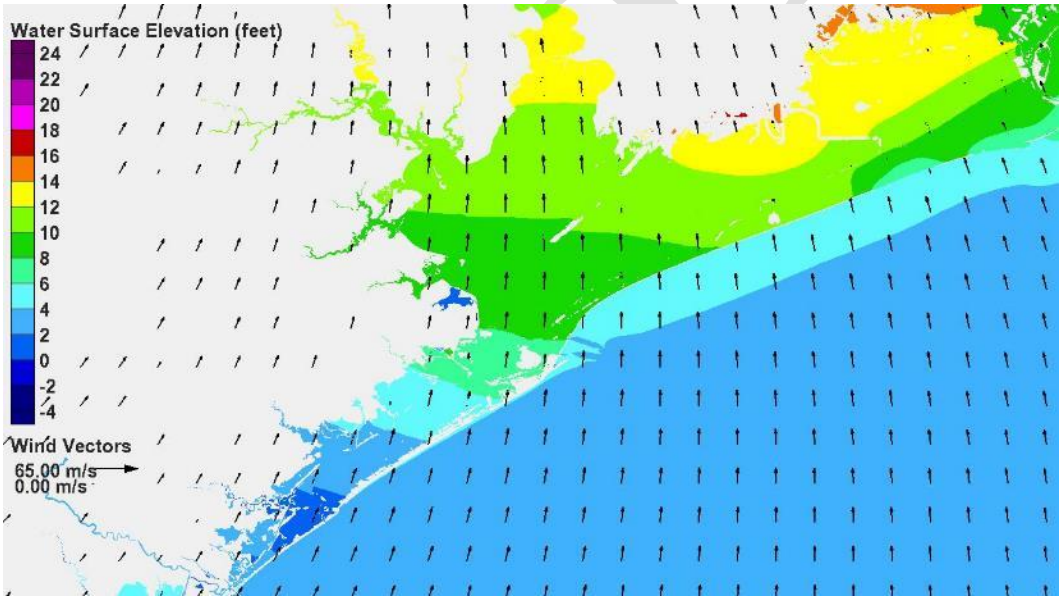

Figure 52. Water surface elevation and wind vectors 9 hours after landfall for Storm 122 (direct-hit track, 900 mb)

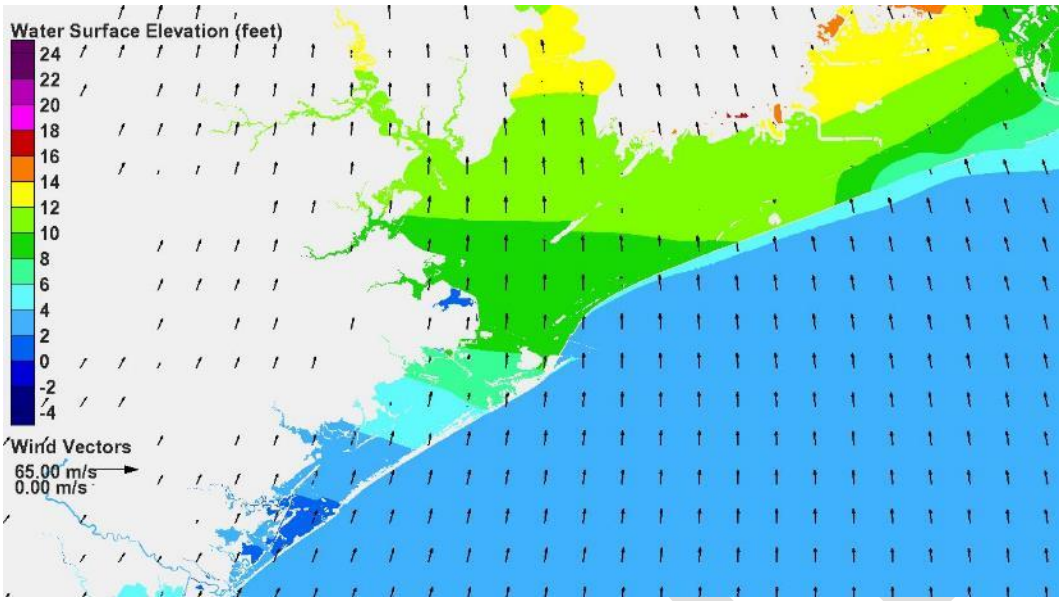

Figure 53. Water surface elevation and wind vectors 10 hours after landfall for Storm 122 (direct-hit track, 900 mb)

Figure 54 shows computed water surface elevation as a function of time for the with-dike condition for Storm 122. Results are shown for the same 5 locations that were shown in Figure 38 for existing conditions.

At Galveston Pleasure Pier, the hydrograph shape is nearly identical to the shape for existing conditions. The surge forerunner on the open coast is unchanged by the dike. With a dike in place, peak surge on the ocean side of Galveston is about 15.5 ft, 0.5 feet more than for existing conditions. This small increase is expected. A substantial dike, levee or floodwall will allow surge to be stacked against it by the wind instead of overtopping a lower barrier island. This increase must be accounted for in any final design of the Ike dike concept.

Inside the Bay, at Galveston, the timing of the peak surge is the same as for existing conditions, but the peak surge is reduced from 15 ft to 9 ft, a decrease of 6 ft. At Texas City, the timing of peak surge is the same as for existing conditions, but the peak surge is reduced from 14 ft to 8 ft, also a 6 ft decrease. At Clear Lake the timing of peak surge is the same, but the peak surge is reduced from 14 to 7 feet, a decrease of 7 feet. In the upper reach of the Houston Ship Channel the initial drawdown of water is greater for the with-dike condition, compared to the existing condition. The peak surge is reduced from 19 ft to 12.5 ft, a decrease of 6.5 ft. As with the existing condition, the rate of rise in surge in the upper Houston Ship

Channel is rapid, increasing from -2 ft to +13 ft, a change of 15 ft, in only 2 to 3 hours. The timing of peak surge is the same.

The elevated water levels evident late in the hydrograph are primarily an artifact due to encroachment of the surge around the north end of the dike, allowing a large amount of water to enter the bay. The dike, as it's initially represented and implemented in the modeling, holds the water inside the Bay. In actuality the dike would be built with lateral terminations, or tie-ins to higher ground, that would prevent or substantially reduce surge encroachment around the end of the dike. Gates would be built in the passes and opened following passage of the storm to allow water to leave the Bay and return to the ocean.

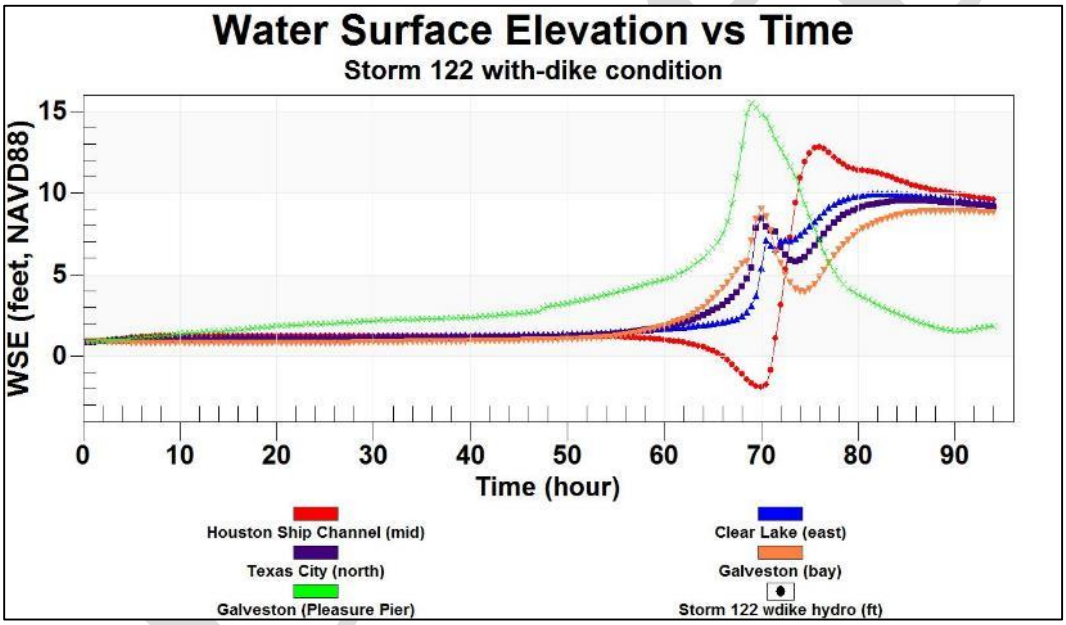

Figure 54. Temporal variation of water surface elevations within Galveston Bay for Storm 122, with-dike condition

7 Influence of Storm Track on Surge Development

Introduction

The influence of hurricane track on storm surge development was examined by comparing surge generation for a single severe hurricane approaching from each of three different approach directions: from the south, from the south-southeast, and from the southeast. First, the development of the surge forerunner was examined as a function of track, then development of the surge associated with arrival of the storm's stronger core winds was examined.

For the forerunner analysis, three storms were selected from the bracketing set that had the same values of minimum central pressure, forward speed, and radius to maximum winds. Central pressure and radius to maximum winds are generally considered to be the two most important parameters that determine open coast surge amplitude and peak surge for a particular coastal setting like the north Texas coast. Bunpapong et al (1985) found that forward speed was important for this region. One storm was selected from each of the three track groups represented in the bracketing set; the three were chosen to have as similar a landfall location as possible, subject to the constraint of having the same hurricane parameters. The three storms selected were Storms 134, 122 (extensively described previously in this report) and 128. The forerunner analysis considered the time period when the hurricane was well offshore and the forerunner surge was building, up until a time that is 12 hours before landfall.

Development of the storm surge associated with arrival of the core winds, as a function of storm track, also was examined for each of the three approach directions. For this analysis, three storms were selected that had approximately the same landfall location, the same minimum central pressure and the same radius to maximum winds. The storms selected for this analysis were Storms 136, 122 and 128. Storm 136 has a different forward speed compared to the others; however, the landfall location for storm 136 is approximately 50 miles north of the landfall location for Storm 134 and closer to the landfall location of the other two. The three chosen storms make landfall along the upper half of Galveston Island.

Forerunner Surge Development as a Function of Storm Track

Storms 134 (south), 122 (south-southeast) and 128 (southeast) were compared to examine forerunner development. Each has a minimum central pressure of 900 mb, a radius-to-maximum-winds of 17.7 n mi, and a forward speed of 11 kts, and the same value of the Holland B parameter, 1.27, which controls the radial distribution of wind speed. The paths through the Gulf for storms in each of the three directional groupings were shown in Figure 7, and their individual paths in the Houston-Galveston Region were shown in Figure 9.

Storm 128 originates within the Gulf, in deep water, west of the Florida peninsula. From its time of origin, the storm immediately begins to move across the Gulf until it makes landfall just south of Bolivar Roads 45 hrs after its initiation. The storm had an initial central pressure of 980 mb, and it begins to intensify immediately after its origin. Its central pressure decreases rapidly to 960 mb after 3 hours, decreases to 930 mb during the next 9 hrs, and then decreases to its minimum of 900 mb during the following 9 hours. The storm maintains its minimum central pressure until just before landfall, 24 hours later, when storm filling occurs the storm weakens and central pressure increases.

Storm 122 originates just outside the Gulf, south of Cuba, and it enters the Gulf near the northern limit of the Yucatan Straits. Its central pressure at the time of origin is 980 mb. It starts moving on its track for 8 hrs while maintaining the initial central pressure of 980 mb, before it begins to intensify. Once intensification begins, the central pressure decreases to 960 mb over the next 7 hours, decreases to 930 mb over the ensuing 12 hrs, and decreases to its minimum pressure of 900 mb during the following 12 hrs. The storm maintains its minimum central pressure until just before landfall, 31 hours later.

Storm 134 originates on land near the Yucatan peninsula, with an initial central pressure of 980 mb. For 28 hrs the hurricane remains stationary with a central pressure of 980 mb. For the next 18 hours, while the storm moves to the north, the central pressure remains at 980 mb. Then the storm begins to intensify over the next 5 hours, with the central pressure decreasing to 960 mb. During the next 6 hours the central pressure decreases to 930 mb, and then 7 hours later decreases to its minimum central pressure of 900 mb. The storm maintains its minimum pressure until just before landfall, 31 hours later.

From the time all three storms commence movement along their respective tracks, Storm 122 is in motion for 70 hours and it has the longest path to landfall. Storm 134 has a slightly shorter path, compared to Storm 122, and it is in motion for 67 hours. Storm 128 takes the shortest path to landfall, and it is in motion for 45 hours. Prior to landfall, the durations for which each storm has a central pressure of 900 mb are: 31 hours for Storm 122, 31 hours for Storm 134, and 24 hours for Storm 128.

Figures 7-1 through 7-5 show snap-shots in time of water surface elevation and wind vectors at different times prior to landfall. The snap-shots are used to illustrate position of the storm and the evolution of the surge forerunner. Forerunner amplitudes cited in the following discussion are estimated visually from the graphical images. Computed time series of water surface elevation, which characterize the forerunner amplitude more accurately, are presented and discussed later.

Figure 7-1 shows results for Storms 134 and 122 60 hrs prior to each storm's landfall. Results are not shown for Storm 128, since its time of origin was later and there is no snap-shot for this storm 60 hrs before landfall. Storm 134 is just beginning its movement into the Gulf, and it is undergoing intensification. Storm 128 has recently entered the Gulf and also is experiencing intensification.

For both storms, the wind-induced surge forerunner has already started to develop along the Louisiana and north Texas coasts. The magnitude of the forerunner surge along the Louisiana and north Texas coasts is similar. Near Galveston, the water surface elevation is approaching between 1 and 1.5 ft NAVD88 for both storms. The NAVD88 datum is the vertical datum used for all references to water surface elevation; for the rest of this chapter, the datum will be omitted from water surface elevation references. Since the initial water surface elevation for all the hypothetical storm simulations is 0.9 ft (about 0.4 ft above mean sea level), the amplitude of the forerunner, relative to mean sea level, is between 0.1 and 0.6 ft.

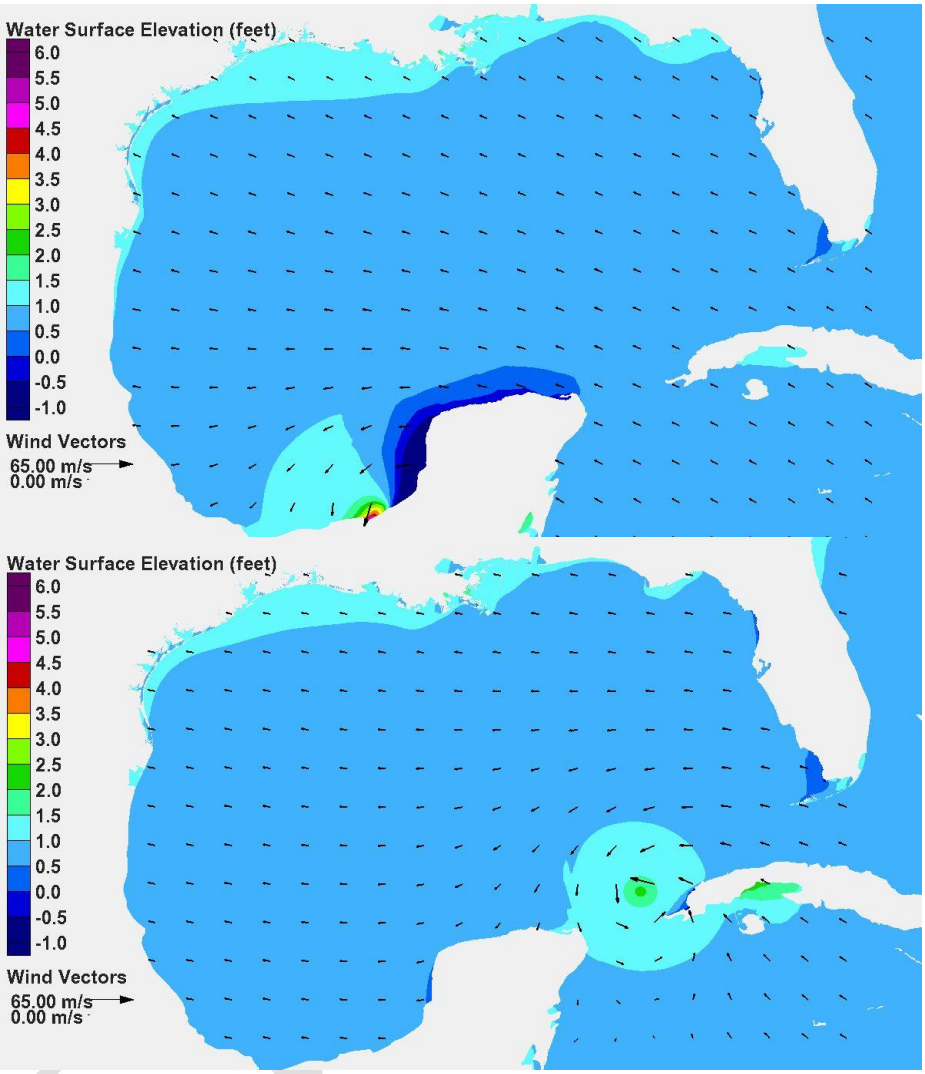

Figure 7-1. Water surface elevation and wind vectors 60 hours before landfall, Storm 134 (upper panel), Storm 122 (lower panel).

Along both the Louisiana and Texas coasts, the area reflecting the presence of the surge forerunner correlates well with the location of the continental shelf, which indicates the importance of wind forcing on the shelf in forerunner development.

In some places along the Texas shelf the wind has a significant onshore component. Along the north Texas shelf, winds are directed primarily onshore for both storms, but slightly more onshore for Storm 134. Along the Louisiana shelf the wind is directed more along the shelf. For Storm 122, along the Louisiana coast, wind sets in motion a current that is moving to the west along the continental shelf which is then directed to the right, or toward shore, by the Coriolis force, forming the forerunner. Along the Louisiana coast the winds for Storm 134 are directed slightly

more onshore than they are for Storm 122, but they also have an alongshore component. Onshore-directed winds of the same speed are more effective in building the surge at the coast than are along-shore directed winds of the same speed. However, the alongshore blowing winds also set in motion a movement of water along the shelf from Louisiana toward Texas which eventually increases the amount of water on the Texas shelf that can be blown toward shore by the core winds of the hurricane. Far-field winds that blow directly onshore would not tend to produce this alongshore moving water. The amplitude of the surge forerunner along the Texas coast is slightly larger for Storm 134 compared to Storm 122 because the winds are directed more onshore and because the alongshore moving water on the shelf has not yet moved from Louisiana toward Texas.

It is worth noting that in these simulations there is only one contributor to winds in the Gulf, the hurricane itself, as simulated by the PBL model which is an idealized wind model. In real situations, other weather systems would be present and influence winds in the Gulf and on the shelf as the hurricane either forms within the Gulf or enters the Gulf. These other weather systems, and how they interact with an approaching hurricane, will influence winds over the shelf (both speed and direction); and therefore, they can influence development of the forerunner. Generation of the forerunner by wind along the Louisiana and Texas continental shelves will be strongly influenced by the local wind conditions on these two shelves.

Figure 7-2 shows snap-shots for all three storms 48 hrs prior to landfall for Storms 134 and 122. The snap shot for Storm 128 is actually taken slightly later, 45 hours prior to landfall; it has just originated in the Gulf. All three storms are intensifying at this stage in time. Storm 122 is the most intense of the three, so its far field winds along the Texas and Louisiana coasts are slightly greater. Winds along the Louisiana and Texas coasts are directed more onshore for storm 134 compared to Storm 122. Wind is pushing water along the coast, from Louisiana toward Texas, for both storms. The amplitude of the surge forerunner along the north Texas coast, above the initial mean water surface elevation used in the modeling, is similar for Storm 122 compared to Storm 134, approximately 1 ft, but seemingly slightly larger for storm 122. For Storm 128, which is the least intense storm of the three at this time, the forerunner surge along the Louisiana and Texas coasts is quite small.

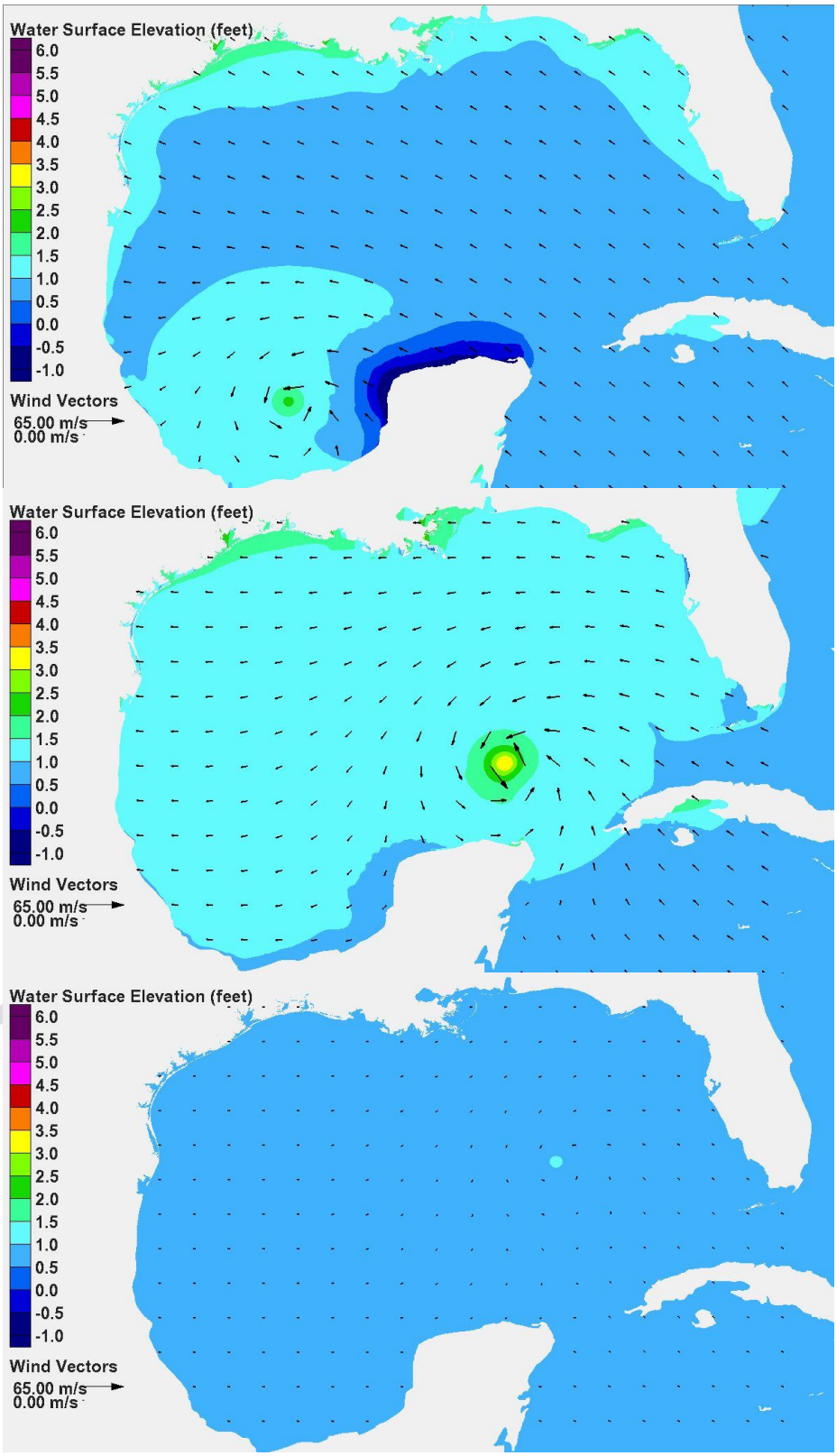

Figure 7-2. Water surface elevation and wind vectors 48/45 hours before landfall, Storm 134 (upper panel), Storm 122 (middle panel), Storm 128 (lower panel).

The snap-shot for Storm 122 shows evidence of the volume-mode contribution to the forerunner investigated by Bunpapong et al (1985); the entire water surface within the Gulf is elevated for this storm, which was not evident in results for the other two storms. Because they do not pass through the ports leading to the Gulf, the volume mode contribution to the forerunner for Storms 134 and 128 is expected to be less than the volume model oscillation for Storm 122. Because Storm 122 is relatively weak when it enters the Gulf, its volume model oscillation is expected to be small.

Figure 7-3 shows snap-shots for all three storms 36 hrs prior to landfall for each storm. Storm 122 is the most intense of the three at this stage as well; Storm 128 is the least intense. The amount of water building beneath the eye of the storm is a measure of storm intensity. The bulge of water under the eye develops because of atmospheric pressure gradients. The lower the central pressure in the eye the larger the spatial pressure gradients that act to pus water toward the eye from all directions. Of the three storms the bulge for Storm 122 is greatest, indicating its greater intensity (i.e., its lower central pressure). None of the storms has yet reached its minimum central pressure (or strongest winds).

Intensity affects the magnitude of the simulated far field winds as well as the core winds. Winds for Storms 122 and 128 continue to be directed more parallel to shore along the north Texas and Louisiana coasts, pushing water along the shelf and toward the coastline by the Coriolis force. Winds for Storm 134 are directed much more onshore, directly pushing water up against the coastline. Both alongshore winds/water movement (because of the Coriolis force) and onshore winds/water movement act to increase the water surface elevation at the coast

At the time shown in Figure 7-3, Storm 122 has the largest surge forerunner. The forerunner amplitude for Storm 134 is only slightly less and the forerunner for Storm 128 is the smallest but is developing. The forerunner amplitude near the Galveston region is between 1 and 1.5 ft for Storms 122 and 134. Even though Storm 122 is more intense and has been since its inception, creating stronger winds along the shelves, the onshore directed far field winds of Storm 134 still produces a significant forerunner.

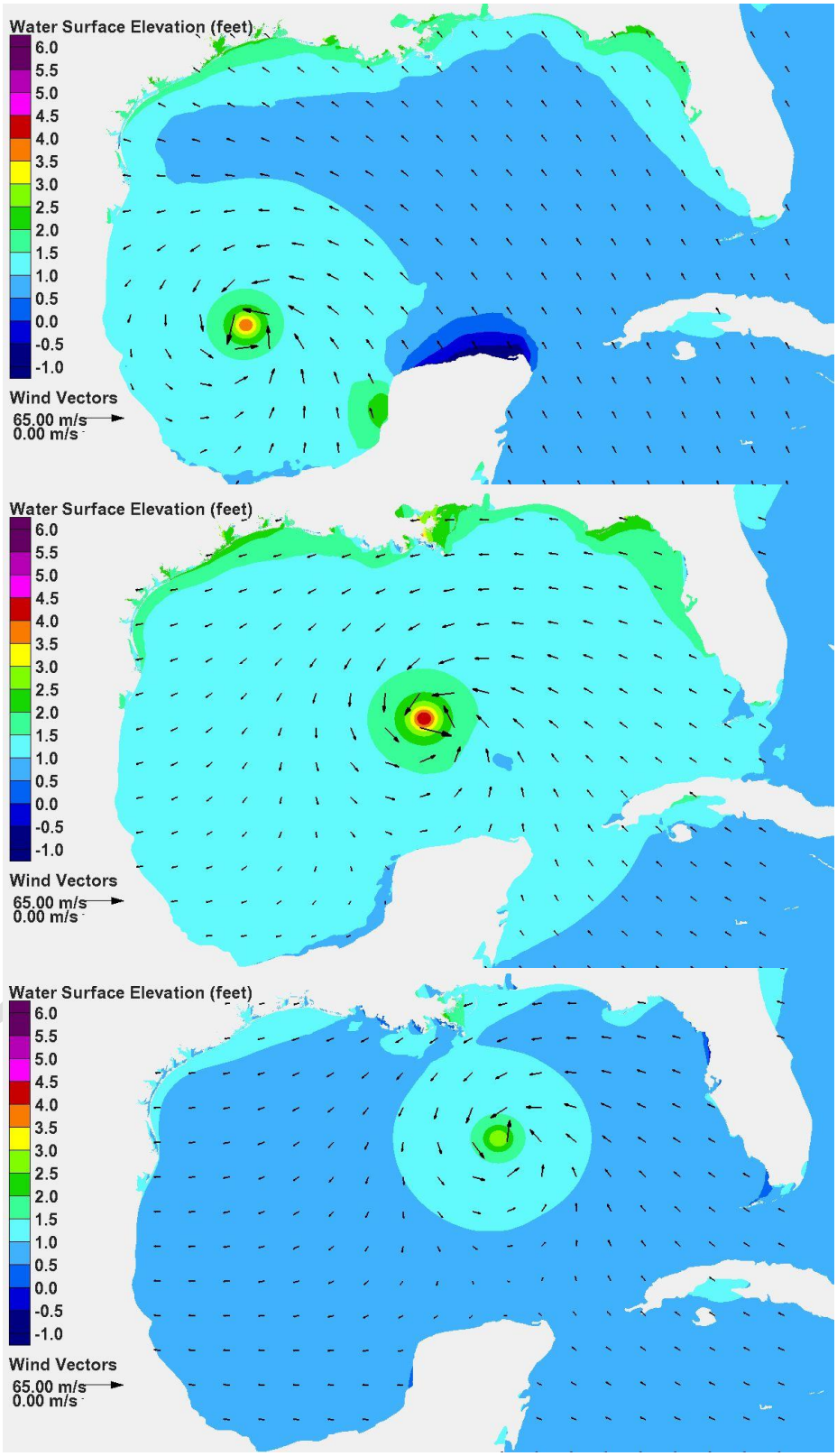

Figure 7-3. Water surface elevation and wind vectors 36 hours before landfall, Storm 134 (upper panel), Storm 122 (middle panel), Storm 128 (lower panel).

For Storm 128, a change is taking place along the Louisiana coast. Winds there are becoming increasingly directed more toward the offshore as the eye of the hurricane moves to the west and closer to landfall. The offshore directed winds are reducing the water surface elevation along the Louisiana coast and the along-shelf movement of water from the Louisiana shelf toward the north Texas shelf. The smaller surge forerunner for Storm 128 at this point in time is attributed to its lower intensity, its lag in time of intensification relative to the other two storms, and offshore directed winds.

For all three storms the wind-driven forerunner is present along the entire Texas shelf, and the width of the zone of highest forerunner surge is strongly correlated to the width of the shelf.

This snapshot for Storm 122, again, also reflects a uniform increase in water surface elevation, throughout the Gulf, indicative of the volume mode oscillation.

Figure 7-4 shows snap-shots for all three storms 24 hrs prior to landfall for each storm. At this point, all three storms have reached their most intense stage, a minimum central pressure of 900 mb. The water surface elevation increase under the eye of each storm is similar because the central pressure is the same. The amplitude of this bulge in the water surface is approximately 4 ft for each storm.

Wind speeds on the Texas and Louisiana shelves are now increasing as a result of the intensification and increasing proximity of the eye to the shelf. Winds for Storms 122 and 128 continue to have greater along-shelf components along the entire Texas coast, which are acting to build the forerunner. For Storm 134 winds are still directed somewhat onshore along the Texas coast, which is quite effective in developing the forerunner. It is noteworthy that the south Texas shelf is not nearly as wide as the north Texas and Louisiana shelves. Therefore, wind forcing along the south Texas shelf is not expected to develop as much of a forerunner. For Storms 122 and 134, winds along the Louisiana shelf have a significant alongshore component, pushing water to the west and onto the north Texas shelf.

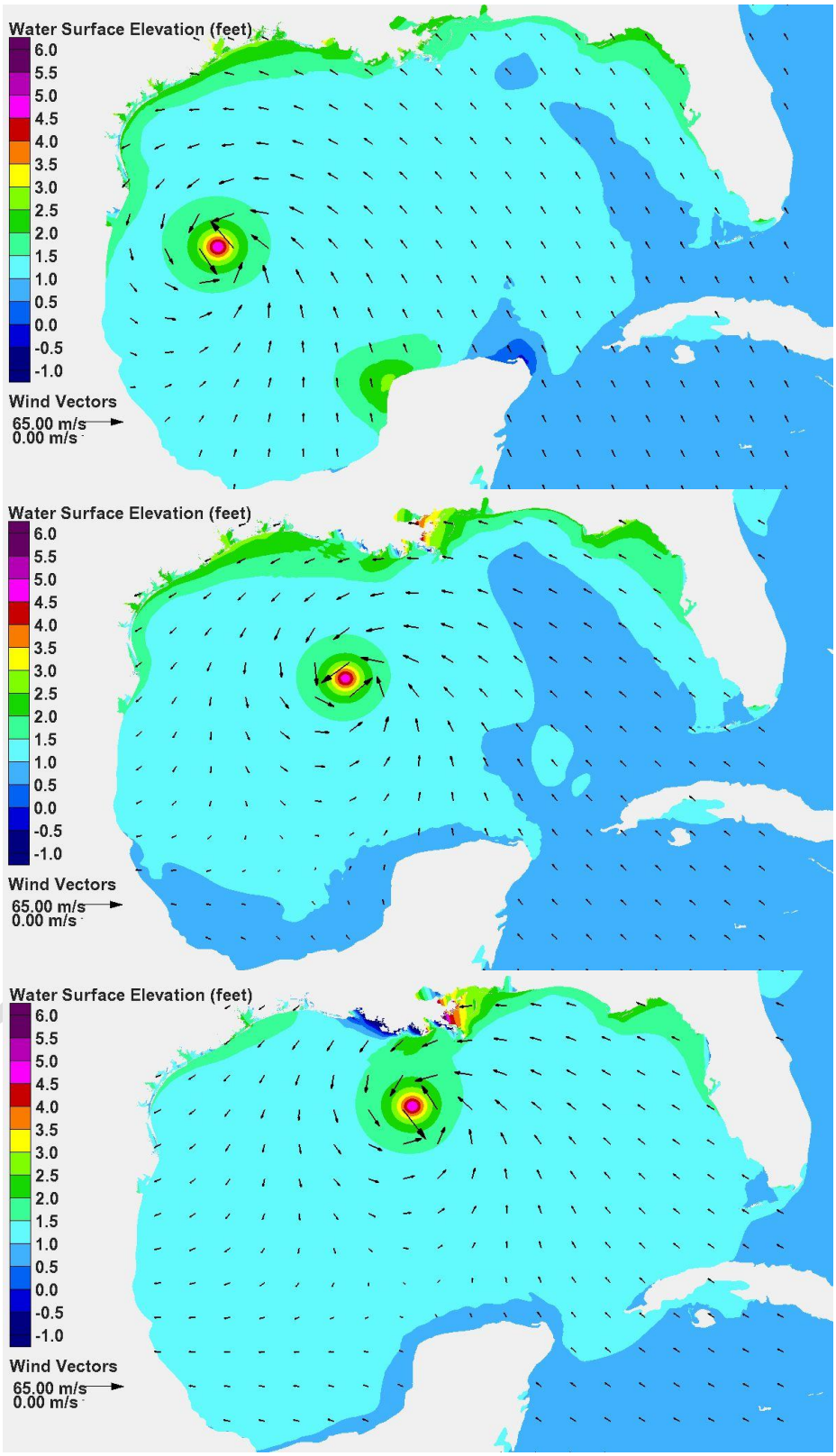

Figure 7-4. Water surface elevation and wind vectors 24 hours before landfall, Storm 134 (upper panel), Storm 122 (middle panel), Storm 128 (lower panel).

For Storm 128, winds are becoming stronger over the Louisiana shelf and continue to be directed toward the offshore as the eye of the hurricane moves to the west. Storm 128 winds are directed along the Texas shelf. Since both onshore and alongshore winds act to develop the forerunner on the Texas coast, all three storms are having this effect.

The closer proximity of Storm 134 to the south Texas coast, and the higher winds over the Texas shelf, is resulting in a larger forerunner there compared to the other storms. Storm 122 has the largest surge forerunner along the Louisiana coast. Both Storms 122 and 134 have generated a forerunner having a similar amplitude along the north Texas coast. The forerunner for Storm 134 is only slightly less in these areas. The forerunner amplitude near Galveston is between 1.5 and 2.0 ft for Storms 122 and 134.

The forerunner amplitude at the north Texas coast is smallest for Storm 128, approaching 1 ft. The offshore directed winds for Storm 128 are setting down the water surface (negative water surface elevations) in places along the Louisiana coast. Compared to Storms 122 and 134, the wind pattern for Storm 128 significantly reduces the amount of water that moves along the Louisiana and Texas shelves, which in turn reduces the amplitude of the surge forerunner along the north Texas coast by reducing the along-shelf movement of water from the Louisiana shelf toward the Texas shelf.

For all three storms the wind-driven forerunner is present along the entire Texas shelf, and the width of the zone of highest forerunner surge continues to be strongly correlated to the width of the shelf. The close proximity of Storm 134 to the south Texas coast means the surge forerunner is most pronounced there due to the higher alongshore and onshore winds.

Figure 7-5 shows snap-shots for all three storms 12 hrs prior to landfall for each storm. All three storms are at their most intense state in terms of central pressure and wind speeds.

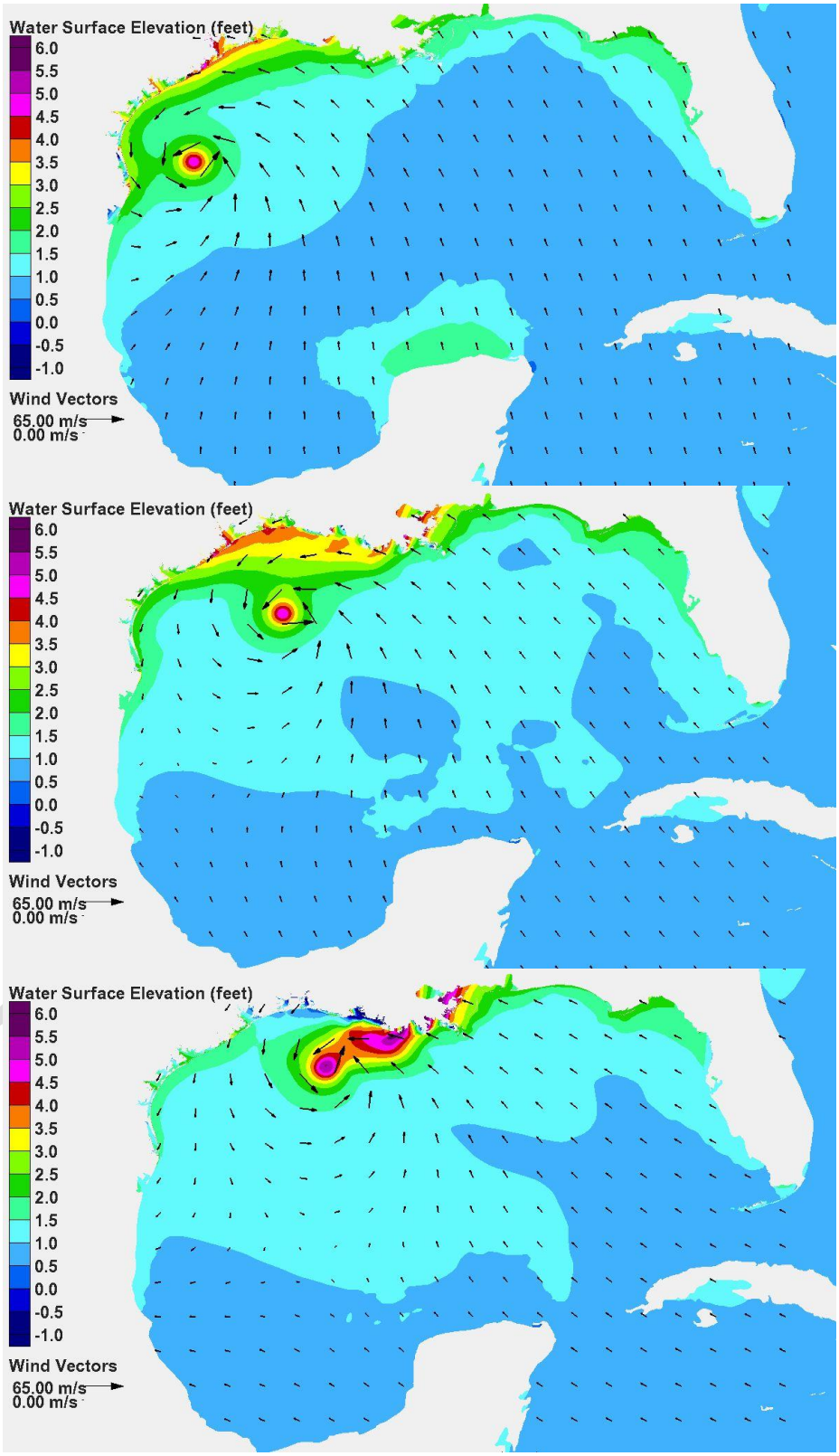

Figure 7-5. Water surface elevation and wind vectors 12 hours before landfall, Storm 134 (upper panel), Storm 122 (middle panel), Storm 128 (lower panel).

At this point, with the eyes closer to landfall, wind directions along the north Texas coast are becoming different for each storm. For Storm 134, winds are directed more onshore, winds for Storm 122 are directed more alongshore, and winds for Storm 128 are directed more offshore.

Forerunner amplitude is increasing for Storms 134 and 122 along the Louisiana and Texas coasts. Storm 122 has the largest surge forerunner along the open coast, with considerable water being pushed from the Louisiana shelf onto the Texas shelf. The forerunner amplitude near Galveston is between 2.5 and 3.0 ft for Storms 122 and 134. For Storm 122, the along-shelf movement of water from Louisiana to Texas is greatest and contributes to the higher forerunner surge along the north Texas coast. Storms 122 and 134, and to a lesser degree Storm 128, are creating a forerunner surge along the south Texas coast driven by the alongshore movement of water and the Coriolis force. Again, because of the close proximity of Storm 134 to the south Texas coast and the resulting higher wind speeds, the surge forerunner there is most pronounced.

The forerunner amplitude for Storm 128 has reached its maximum near Galveston and is beginning to decrease due to the pattern of offshore-directed winds as the eye approaches. As Storm 128 moves closer to the Houston-Galveston region, the offshore-directed winds begin to decrease the forerunner surge along the north Texas coast. That trend will continue until the core winds arrive on the shelf and increase the storm surge.

The surge response along the open north Texas coast is beginning to change from forerunner dominance (caused by far field winds) to dominance of the hurricane's core winds. The close proximity of the eye of Storm 122 to the shelf is beginning to force a much greater surge response on the Louisiana shelf, pushing a considerable amount of water toward the north Texas shelf. The eye from Storm 134 is farther from the wider Louisiana and north Texas shelves, but the onshore directed winds continue to build the forerunner. For Storm 128, winds along the north Texas shelf are directed offshore, decreasing forerunner development.

At 12 hours prior to landfall, the eyes of the three hurricanes are still in deep water but about to enter onto the continental shelf. Storm 128 is closest, and strong winds are beginning to force a much greater surge response on the Louisiana shelf.

Development of Surge within the Bays Due to Forerunner Propagation and Winds

Discussion now shifts to forerunner propagation through the passes that connect the Gulf with the bays, and how surge response within the bays develops as a function of bay filling associated with forerunner penetration and local wind conditions. As was the case for the open coast, bay surge response is strongly influenced by storm track because of the dependence of wind direction on track. Figures 7-6 through 7-9 show the surge forerunner response and wind conditions in the immediate Houston-Galveston region for the same three storms (Storms 134, 122 and 128), zooming in on the bays and nearshore coastal region. The figures show snap-shots of water surface elevation (as color-filled contours) and wind (as vectors) at times 48/45, 36, 24 and 12 hrs prior to landfall (45 for Storm 128 which originated later than the others).

The snap-shots in Figure 7-6 are 48/45 hrs prior to landfall. Water surface elevation along the open coast at the entrance to Galveston Bay is between 1.5 and 2 ft for Storms 134 and 122, and a negligible amount for Storm 128. Elevations inside both Galveston and West Bays are similar to those in the Gulf, suggesting effective penetration of the forerunner into both bays at this time. For Storm 134, winds are blowing approximately onshore from the southeast, and for Storm 122 winds are blowing from slightly south of east. Inside the bay, local winds are setting up the water surface from southeast to northwest for Storm 134 and from east to west for Storm 122, creating a tilt to the water surface in both cases. In response to the local wind, water moves within the bays such that water surface elevation contours are generally perpendicular to the wind direction. A sloping water surface is evident having an increase from one side of the bay to the other in the wind direction of approximately 1 ft.

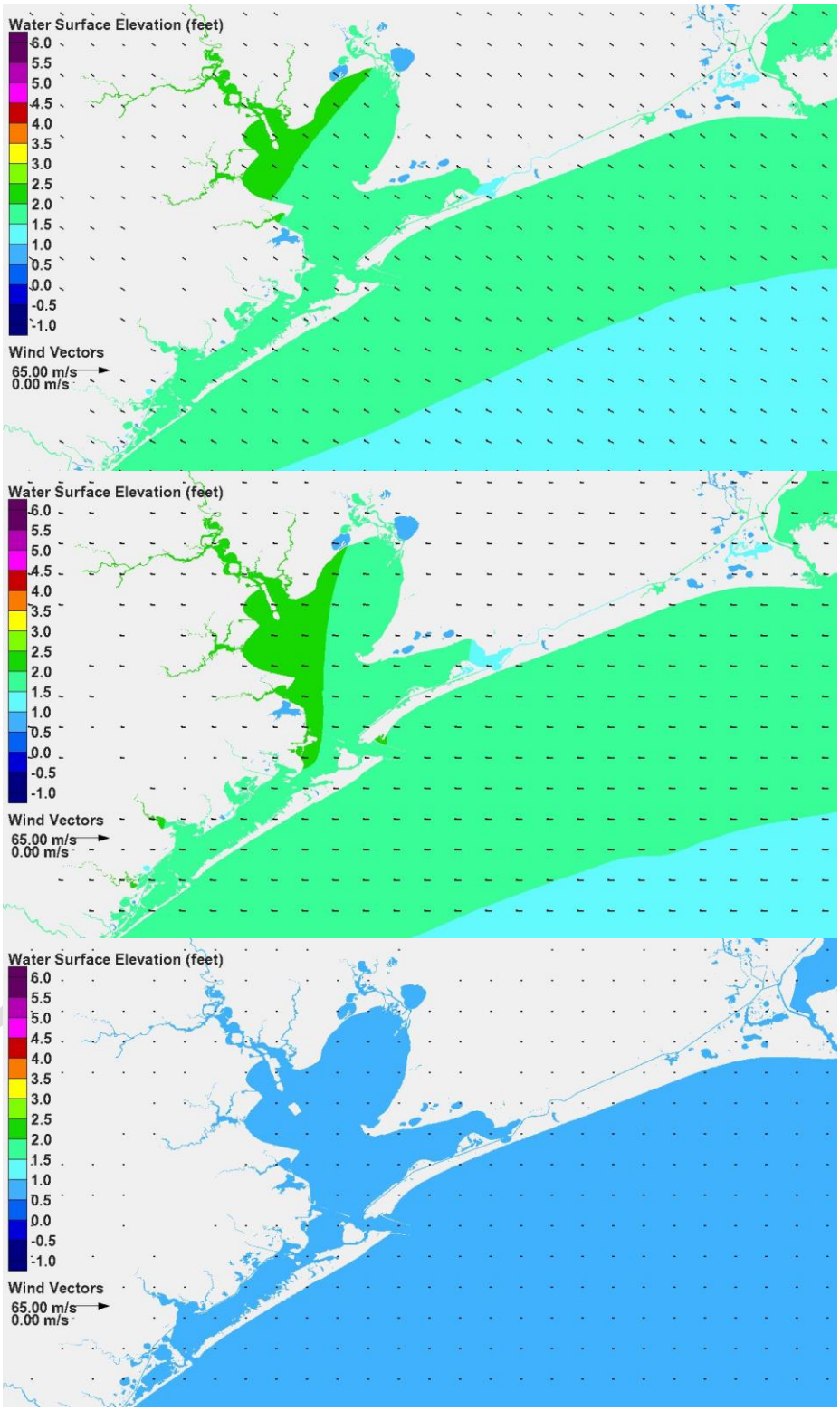

Figure 7-6. Water surface elevation and wind vectors 48/45 hours before landfall, Storm 134 (upper panel), Storm 122 (middle panel), Storm 128 (lower panel).

A point at the center of Galveston Bay is reasonably indicative of the Bay's overall water surface elevation in that it removes the effect of the tilting water surface. The water surface elevation in the middle of the bay is between 1.5 and 2 ft for Storm 134 and nearly 2 ft for Storm 122, indicating that the surge forerunner has effectively propagated into the bay and raised the entire water level through this filling action. The forerunner amplitude within the Bay is slightly greater for Storm 122, compared to Storm 134. The local wind imposes a tilt to the water surface (setting it up on downwind side and setting it down on the upwind side) that is superimposed on the raised water level.

For Storm 134 in particular, winds blowing from the southeast tend to set up the water surface along the open coast and the northwest part of Galveston Bay and set down the water surface along the southeast side of the Bay. This pattern of water surface elevation, for this wind direction, will create a water surface elevation gradient, or head difference, across the entrance pass at Bolivar Roads which will enhance propagation of the forerunner into the Bay, i.e., it will enhance filling of the Bay. The same process can occur at San Luis Pass.

For Storm 128, winds are still quite small within the Bay, so tilting of the water surface is evident in Figure 7-6. The degree of tilting is a function of the local wind speed within the Bay.

Figure 7-7 shows results for all three storms 36 hrs prior to landfall. Within the Bay, winds for Storms 134 and 122 are still from different directions. Wind direction for each storm is similar to what it was 12 hours earlier, so the general patterns of water surface tilting remain the same as the previous snap-shot, although the magnitude is slightly greater.

For Storm 134, the open coast water surface elevation is a slightly greater than 2 ft. The elevation in the middle of the bay appears to be about the same or slightly higher. As discussed for the previous snap-shots, southeasterly winds which are directed onshore give a "boost" to filling by setting down the lower part of the Bay, which increases the head difference across the pass.

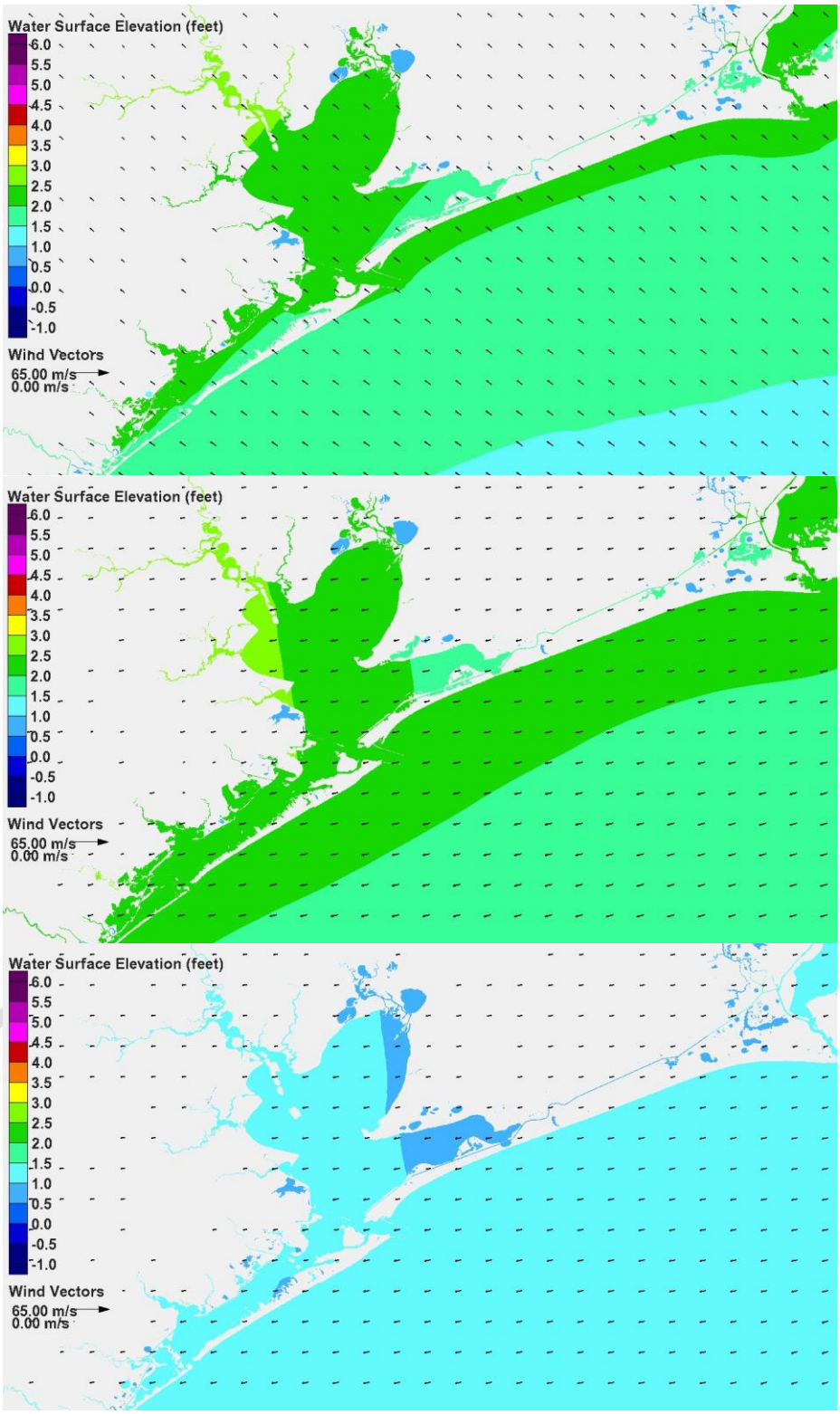

Figure 7-7. Water surface elevation and wind vectors 36 hours before landfall, Storm 134 (upper panel), Storm 122 (middle panel), Storm 128 (lower panel).

For Storm 122, the open coast water surface elevation at the entrance to the Bay is greater than for Storm 134, closer to 2.5 ft. The water surface in the middle of the Bay appears to be about the same for Storm 122, about 2.5 ft. The wind direction for Storm 122, winds from the east, does not produce the same degree of enhanced filling as Storm 134. Winds from the east tend to set up the western side of the Bay. Since Bolivar Roads is situated closer to the west side of Galveston Bay, a higher wind setup there reduces the head difference across Bolivar Roads pass, which in turn reduces the filling rate. If the wind were blowing from the north the wind setup on the south side of the Bay would be maximized, the head difference across the pass would be minimized, and the filling rate through the pass would be minimized.

For Storm 128, winds are also from the east, similar to Storm 122, and the pattern of water surface tilt is similar. The higher winds for Storm 122 create a greater degree of tilt within the Bay. At this time before landfall, Storms 122 and 134 have a greater intensity, i.e., higher wind speeds, than Storm 128. The forerunner amplitude on the open coast is lower for Storm 128, so the degree of filling within the Bay is expected to be less.

Figure 7-8 shows results for each of the three storms 24 hrs prior to landfall. The storms are closer to the coast so winds within the Bay are stronger. Storm 128 has just reached its minimum central pressure of 900 mb, while the other two storms have been at their minimum central pressure for 7 hours. Wind speeds in the Bay for the three storms are similar and are shifting in the counterclockwise direction. For Storm 134, winds are now blowing from the east-southeast; winds for Storm 122 are blowing from the east-northeast; and winds for Storm 128 are blowing from the northeast.

For all three storms, in response to the change in wind direction, the pattern of water surface tilt has also changed. In each case, the contours of constant water surface elevation within the Bay remain nearly perpendicular to the wind direction. Water is moving within the bay in response to the wind to create the water surface elevation gradient, or tilt.

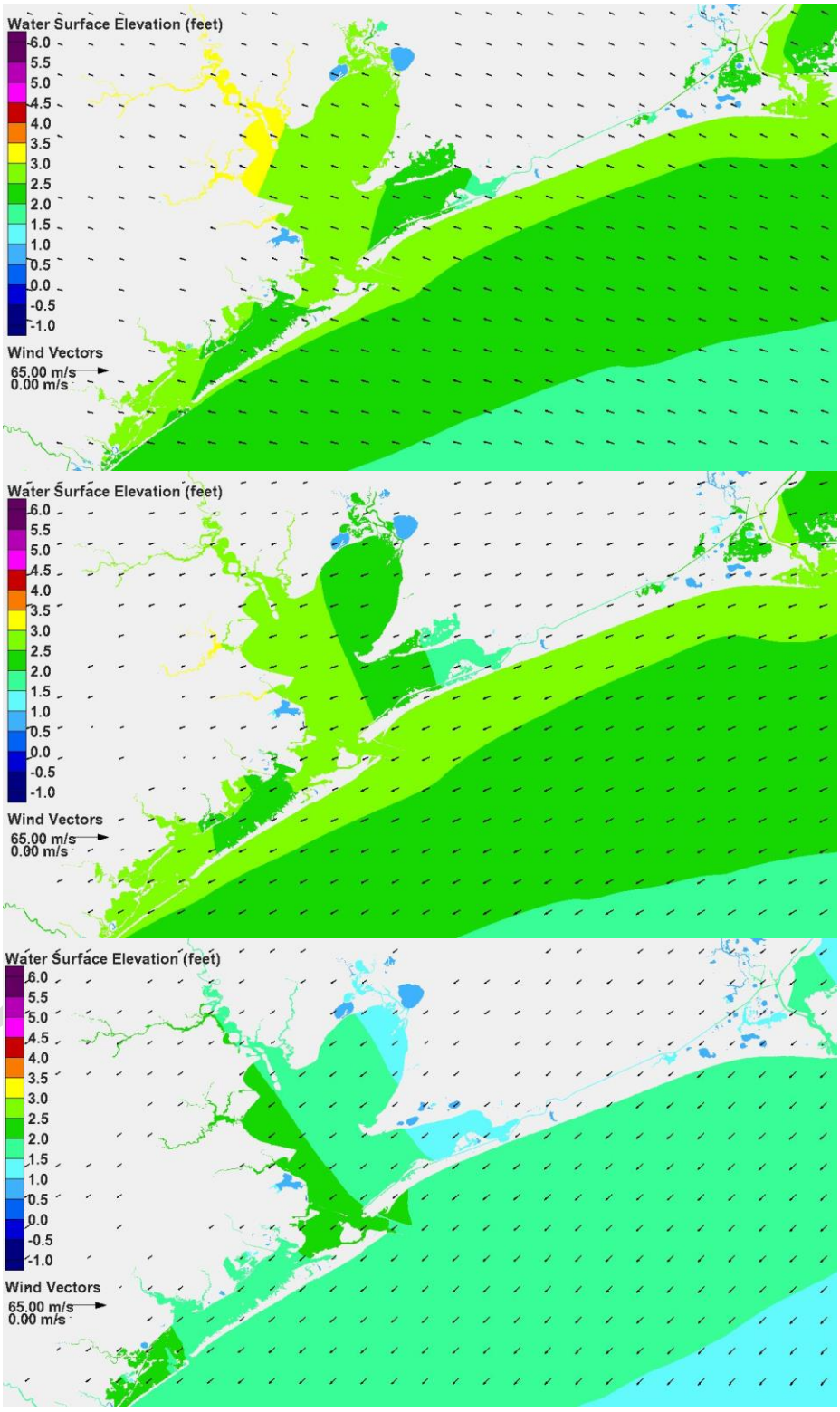

Figure 7-8. Water surface elevation and wind vectors 24 hours before landfall, Storm 134 (upper panel), Storm 122 (middle panel), Storm 128 (lower panel).

It is important to note that wind effectively establishes the water surface tilt throughout Galveston Bay, projecting the same tilting pattern into the upper reaches of the Houston Ship Channel and into other estuaries. This is the case for all three storms, and is seen in the water surface elevation fields for all three.

The amplitude of the forerunner on the open coast is slightly greater for Storm 122 than for Storm 134. The amplitude of the forerunner at the coast for Storm 128 is 0.5 to 0.75 ft lower than for the other storms. The water surface elevation in the middle of the Bay is still greatest for Storm 134, slightly more than the elevation for Storm 122. Storms approaching from the south tend to increase propagation of the forerunner surge into the Bay compared to tracks from the south-southeast and southeast.

The magnitude of the water surface tilt (the difference between water surface elevations on opposite sides of the bay in the direction of the wind) is similar for Storms 122 and 134, approximately 1.5 ft. However, the water surface elevations are higher for Storm 134, compared to Storm 122, because of the higher degree of Bay filling. The magnitude of the tilt for Storm 128 is about 1 ft across the Bay, which is larger than the previous snap-shot.

These snap-shots also illustrate a feature in the water surface slope within West Bay that is worth noting. West Bay has been filling, just as Galveston Bay has been filling, due to the open coast forerunner surge driving the filling action. At this point, winds in West Bay have a significant easterly component, more so for Storms 122 and 128, and less so but still present for Storm 134. This easterly wind component is acting to set up the west end of West Bay. It is also acting to enhance water movement from Galveston Bay into West Bay, particularly for Storms 122 and 128, where winds are blowing in the direction of the long axis. For all three storms, there is some indication that the water surface elevation on the Bay side of San Luis Pass is nearly the same or greater than the water surface elevation on the Gulf side. Once the water surface elevation is greater on the Bay side, water will actually start to flow back toward the Gulf through San Luis Pass. This flow reversal might have implications for design and operation of any gate at San Luis pass that is a structural component of the Ike Dike concept.

Figure 7-9 shows snapshots 12 hrs prior to landfall. At this point all three storms have been at their most intense stage for 12 hrs for Storm 128 and approximately 18 hrs for the other two storms. Winds are continuing to shift direction with a counterclockwise rotation; winds are now blowing from the east, northeast, and north-northeast for Storms 134, 122 and 128, respectively.

The water surface in Galveston Bay responds predictably to the shift in winds, moving quickly to establish contours of constant water surface perpendicular to the wind direction. Wind speed is increasing as is the magnitude of water surface slope in response to the higher winds.

The magnitude of the water surface tilt from one side of the bay to the other, in the direction of the wind, is approximately 2 ft for Storms 134 and 122. The tilt for Storm 128 is now nearly the same as it is for the other two storms, approximately 2 ft, because winds within the Bay are quite similar for all three storms. For Storm 128, the northeast-most portion of Galveston Bay (in Trinity Bay) is set down by the wind. The water surface elevation here is approaching 0 ft NAVD88 which is about 0.5 ft below mean tide level.

The degree of Bay filling, as estimated by the water surface elevation in the middle of the Bay, is between 3.5 and 4 ft for Storm 134, approximately 3.5 for Storm 122, and between 1 and 1.5 ft for Storm 128. For Storm 128, winds were blowing from the northeast 12 hrs earlier and are now blowing from the north-northeast. Recall from the previous report section that this wind direction is decreasing the amplitude of the surge forerunner along the open coast. This trend is seen in the lower panel of Figure 7-9. Winds from northerly directions set up the lower, or southern, portion of Galveston Bay. The decreased open coast water surface elevation and the higher elevation on the Bay side at Bolivar Roads due to wind setup both act together to reduce filling of the Bay by reducing the head difference across Bolivar Roads. These processes are key factors in reducing forerunner penetration into Galveston Bay for storms that approach from the southeast or from more easterly directions.

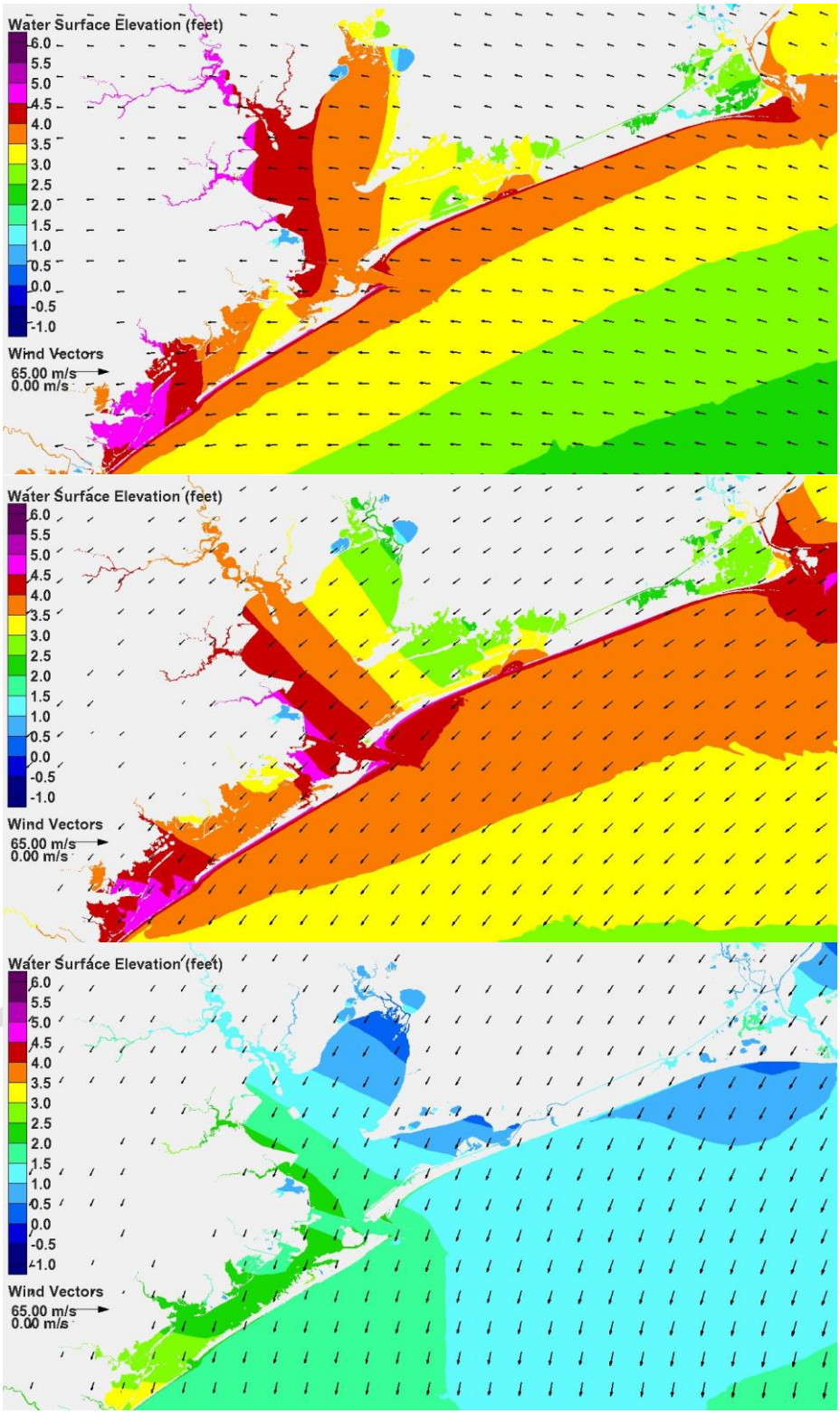

Figure 7-9. Water surface elevation and wind vectors 12 hours before landfall, Storm 134 (upper panel), Storm 122 (middle panel), Storm 128 (lower panel).

For all three storms, in response to the wind direction, the pattern of water surface tilt in the coupled system is forcing water from Galveston Bay into West Bay, and wind is setting up the west end of West Bay. The mean water surface in West Bay is as high, or higher, than it is in Galveston Bay, particularly for Storm 128. For all three storms, the water surface elevation on the Bay side of San Luis Pass is higher than the elevation on the Gulf side, causing water to flow toward the Gulf through the Pass.

To further support this surge forerunner analysis and to provide more quantitative information on water surface elevations and forerunner amplitude, water surface elevation time series were generated for all three storms at the six locations shown in Figure 7-10. The six locations are: 1) the open Gulf coast at Galveston Pleasure Pier, 2) the bay side of the City of Galveston where West Bay meets Galveston Bay, which is also indicative of the bay side of Bolivar Roads, 3) Texas City, 4) the entrance of the tidal channel that leads to the Clear Lake area, 5) the upper Houston Ship Channel, and 6) a point in the middle of Galveston Bay called Trinity Bay (central). Trinity Bay is the large embayment on the northeast side of Galveston Bay.

Figure 7-10. Locations of hydrographs considered in the analysis of forerunner development as a function of storm track.

Figures 7-11 through 7-13 show times series at the six locations for Storms 134, 122 and 128, respectively. The vertical axis for each graph is water surface elevation, in feet, NAVD88. The horizontal axis is time, in hours, from the beginning of the simulation. The last point in time shown in each graph is 12 hours prior to landfall for that particular storm. For example, in Figure 7-11, hour 83 on the horizontal axis corresponds to a time 12 hours prior to landfall. Hour 71 on the horizontal axis is 24 hours before landfall, and so on.

Figure 7-11, for Storm 134, shows that the water surface elevation time series at all five locations inside the bay equal or exceed the open coast time series at Galveston Pleasure Pier. This indicates that the open coast surge forerunner effectively propagates into the Bay through the passes, i.e. fills the Bay, for this general storm track. At the Trinity Bay (central) location, which approximates the average water surface elevation within the Bay, the time series lies consistently above the open coast time series for most of the time shown. This reflects the "boost" to the filling rate described previously that arises because the far field winds are primarily directed onshore as the storm approaches.

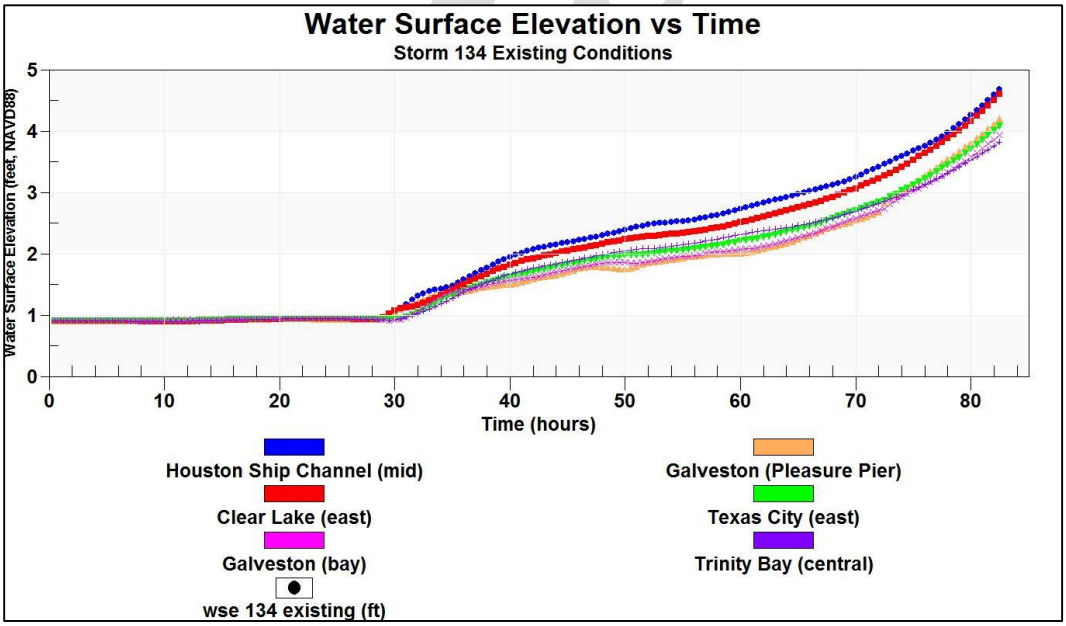

Figure 7-11. Temporal variation of storm surge for Storm 134.

Twelve hours prior to landfall, the open coast surge forerunner at Galveston Pleasure Pier has an amplitude of nearly 3.5 ft relative to mean sea level, which corresponds to the water surface elevation of nearly 4 ft NAVD88 seen at the end of the time series. This amplitude is nearly identical to that in the middle of the bay at Trinity Bay (central). At 24 hours prior to landfall, the open coast forerunner has a smaller amplitude of 2.1 ft, while the amplitude in the middle of the bay is about 0.2 ft higher, 2.3 ft.

Within the Bay, both the filling action and tilting action caused by local wind contribute to the water surface elevations. Higher water surface elevations are evident for locations in the upper parts of the Bay (including the upper Houston Ship Channel and Clear Lake), with the highest being in the upper reaches of the Channel. Lower water surface elevations are seen for locations in the lower parts of the Bay (bay side of Galveston and Texas City). This pattern is consistent with winds blowing from the southeast, which occurred during much of the forerunner development period of time.

Figure 7-12, for Storm 122, shows similar trends. The water surface elevation time series at all five locations inside the Bay equal or exceed the open coast time series at Galveston Pleasure Pier. For Storm 122 the open coast surge forerunner also effectively propagates into the Bay through the passes. For this and other storms on this general track, effective propagation of the forerunner into the Bay is expected.

Within the Bay, both the filling action and tilting action caused by local wind contribute to the water surface elevations. Higher water surface elevations are evident for locations in the northwestern parts of the Bay (including the upper Houston Ship Channel and Clear Lake), with those two locations having nearly the same water surface elevations for much of the forerunner development period. Compared to Storm 134, there is less variation in the time series along the western side of the Bay. This tendency is due to the prevalence of easterly winds, which tend to set up the western side of the Bay where most of the monitoring locations are situated.

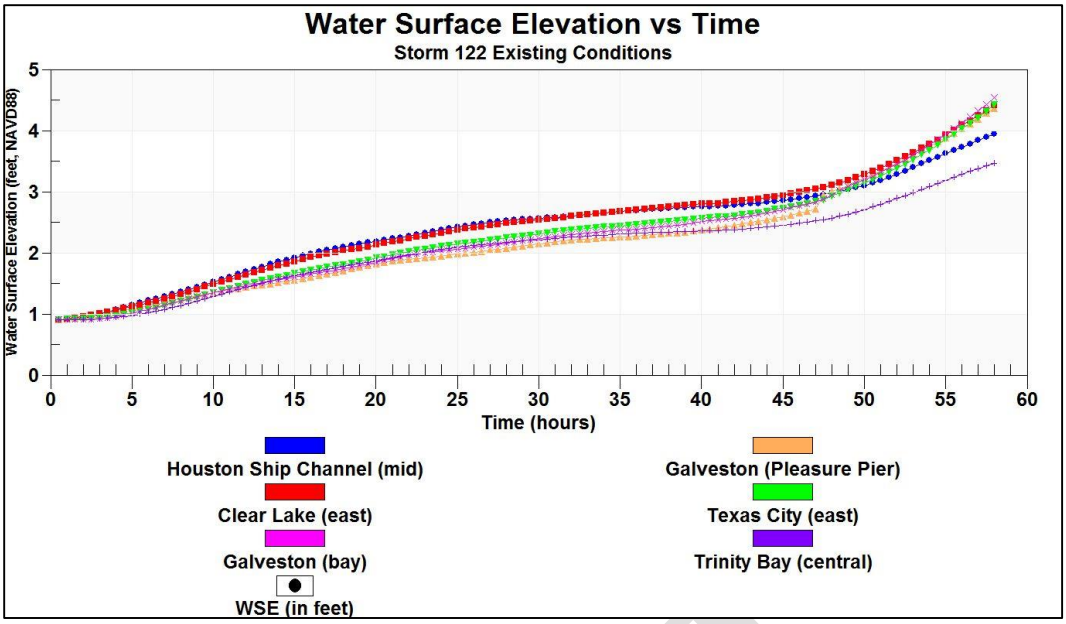

Figure 7-12. Temporal variation of storm surge for Storm 122.

In the middle of the Bay, the Trinity Bay (central) time series is very similar to the open coast time series at Galveston Pleasure Pier. Storms on this track do not appear to produce the "boost" in forerunner propagation into the Bay that was observed for Storm 134.

For Storm 122, twelve hours prior to landfall, the open coast surge forerunner at Galveston Pleasure Pier has an amplitude of 3.9 ft relative to mean sea level (elevation of 4.4 ft NAVD88). This amplitude is approximately 0.9 ft higher than the forerunner amplitude at Trinity Bay (central). At 24 hours prior to landfall, the open coast forerunner has a smaller amplitude of 2.1 ft, while the amplitude in the middle of the bay is about 0.1 ft lower, 2 ft.

Figure 7-13, for Storm 128, shows very different trends in forerunner propagation into the bay and evolution compared to Storms 134 and 122. All the time series for Storm 128 show an initial build-up of the surge forerunner, as did the other two storms. However, the trend of increasing forerunner amplitude changes to a trend of decreasing amplitude about 20 hours prior to landfall. The exact time of change is a function of the storm's forward speed. As the storm on this track moves closer to shore, winds begin to shift to northerly directions, diminishing the surge forerunner amplitude and pushing water way from the coast.

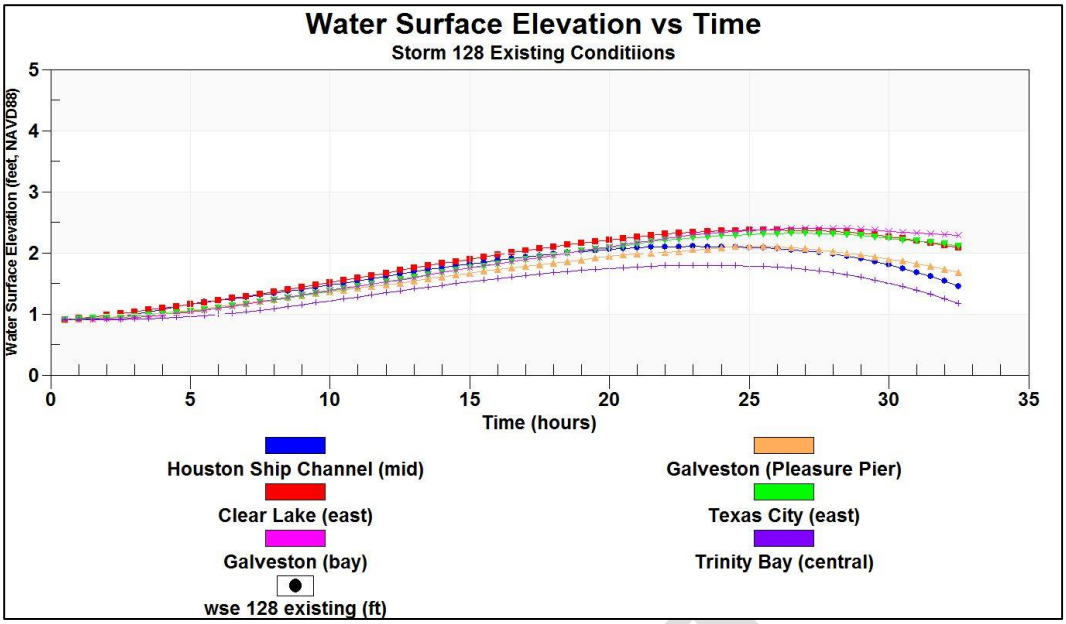

Figure 7-13. Temporal variation of storm surge for Storm 128.

For Storm 128 the forerunner amplitude on the open coast is greater than the amplitude in the middle of the Bay for the entire duration of the storm. This indicates a reduced capacity of the forerunner to penetrate into the Bay through the passes. This behavior is caused by the easterly winds (early) and northeasterly winds (later) which tend to set up the western side of the Bay (early) and southwesterly side (later), where most of the monitoring locations are situated. For this storm there is also much less variation in the time series along the western side of the Bay, due to the same prevailing wind directions. In the latter stages of forerunner development, when winds are blowing more out of the north, water is pulled from the upper reaches of that part of the Bay system.

Twelve hours prior to landfall, the open coast surge forerunner at Galveston Pleasure Pier has an amplitude of 1.2 ft relative to mean sea level. This amplitude is approximately 0.6 ft higher than the forerunner amplitude at Trinity Bay (central) at the same time. At 24 hours prior to landfall, the open coast forerunner has a higher amplitude of 1.4 ft, while the amplitude in the middle of the bay is about a 0.2 ft lower, 1.2 ft.

Galveston Bay Storm Surge Response to the Hurricane's Core Winds

For these three storms, until 12 hours prior to landfall, the surge forerunner dictates surge development along both the open coast and within Galveston and West Bays. As the storms move onto the continental shelf the storm's core winds, i.e., those winds closer to the eye particularly on the right hand side where wind speeds are generally highest, begin to dominate the surge development process. The temporal rate of change in water surface elevation begins to increase; because, as the eye moves into shallower water, winds become increasingly more effective in pushing water. The effective surface wind stress in the water momentum balance is inversely related to water depth. Therefore, for the same wind speed, the effective wind stress is less in deeper water and greater in shallower water; and it is greatest in the very shallow water of the nearshore coastal zone and in the shallow bays.

Figures 7-14 through 7-22 show snap-shots in time for three storms from the bracketing set. Storm 136 approaches from the south, Storm 122 approaches from the south-southeast, and Storm 128 approaches from the southeast. Storm 136 was selected to represent storms approaching from the south, instead of Storm 134 which was selected previously, because the landfall location for storm 136 is closer to the landfall locations of the other two storms. All three storms have the same minimum central pressure (900 mb) and the same radius to maximum winds (17.7 n mi). Storm 136 has a faster forward speed, 17 kts. Forward speeds for the other two storms are 11 kts.

The snaps-shots show the water surface elevation field as filled color contours and the wind field as black vectors, for the immediate Houston-Galveston region. Note the change in water surface elevation scale for this series of figures, compared to that used in the previous discussion of the forerunner. A color bar scale that ranges from -4 to +24 ft is used in this report section. Each figure contains three images. The top panels show results for Storm 136, results for Storm 122 are shown in the middle panel, and results for Storm 128 are shown in the bottom panel. Each figure reflects a different point in time as the hurricane approaches the coast, makes landfall, and then moves out of the Houston-Galveston region. This analysis advances the progression in time from the point where it ended in the previous report section, 12 hours before landfall. The first figure shows results 6 hours prior to landfall and the last figure shows results 9 hours

after landfall. The time increments between snap-shots are variable; they are concentrated on times around landfall.

Figure 7-14 shows results 6 hrs prior to landfall. Wind speeds are increasing as the eye moves closer to shore. For each of the storms, wind directions are similar to what they were 6 hrs earlier; but they continue to shift, rotating in the counterclockwise direction. At this point, in Galveston Bay, winds for Storm 136 are blowing from the east-northeast, winds for Storm 122 are blowing from the northeast, and winds for Storm 128 are blowing from the north-northeast.

For all three storms the higher wind speeds are creating a larger gradient, or tilting, in the water surface. For Storm 136 the region of highest surge within Galveston Bay is along the western shoreline, and the zone of highest surge extends into the upper reaches of the Houston Ship Channel. In West Bay the east-northeasterly winds set up the western side of the bay and push water from Galveston Bay into West Bay. For the other two storms, the zone of highest surge is at the southwest corner along the bay side of the City of Galveston. This water surface pattern also acts to push water from Galveston Bay into West Bay. For Storms 136 and 122, local winds having a significant northerly component and they set down the water surface in the upper reaches of the Channel. For all three storms, the northeast part of Galveston Bay is being set down by the wind.

Figure 7-15 shows snap shots 3 hrs prior to landfall. The eye of the hurricane is beginning to enter the image for all three storms. The curvature of the wind field about the eye, associated with the counterclockwise wind circulation in a hurricane, is evident for all three storms. For Storm 136 (upper panel), winds in Galveston Bay are still blowing from the east-northeast, which is producing the highest surges within Galveston Bay along its western shoreline. Along this side of the Bay, easterly winds are forcing a higher surge into the western reaches of the Clear Lake and Dickinson areas, where wind is pushing water up into the channels and estuaries, establishing the same water surface gradient that is evident throughout the rest of the Bay. Increasing wind speeds within the Bay are increasing the magnitude of the water surface elevation gradient.

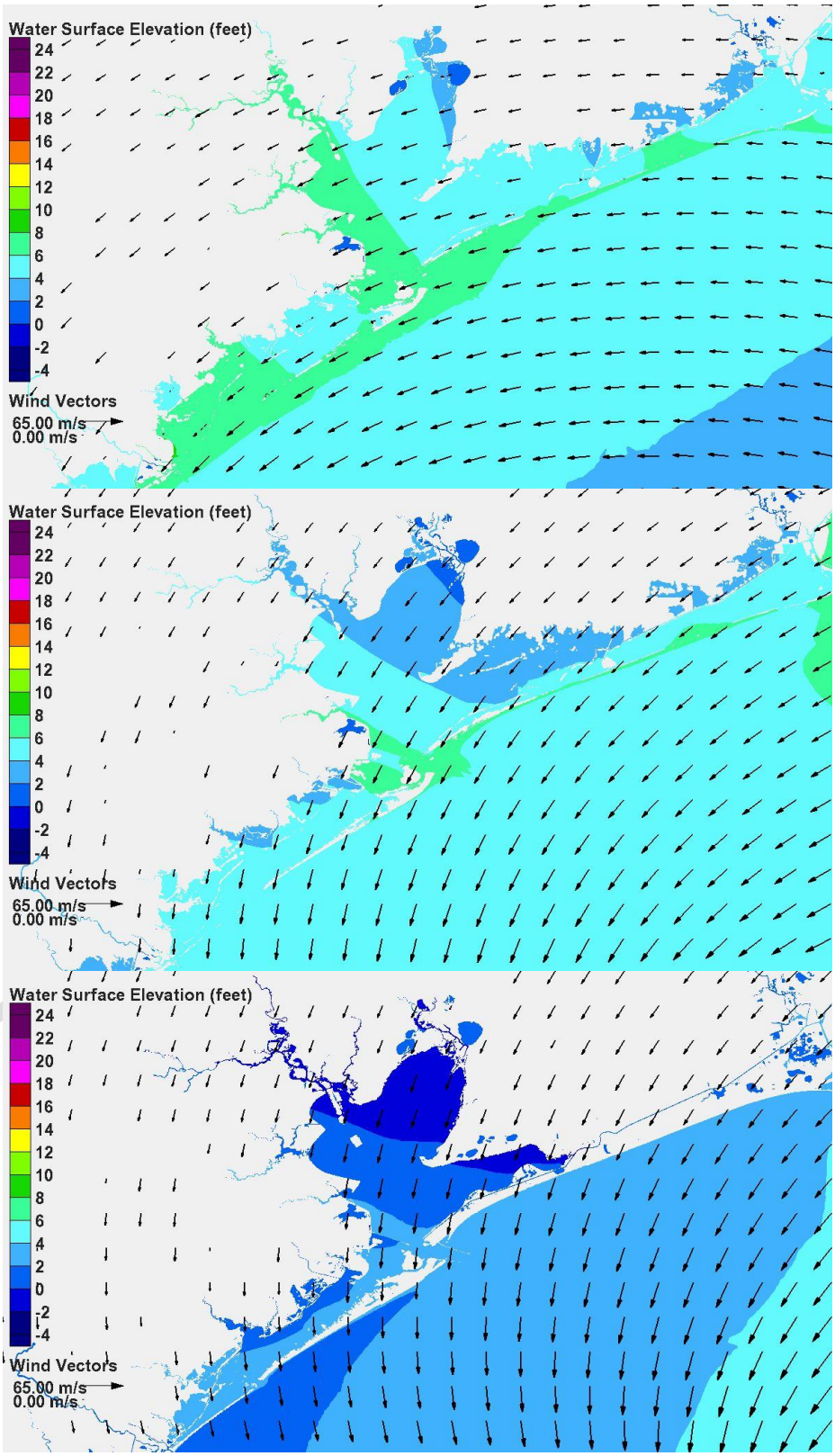

Figure 7-14. Water surface elevation and wind vectors 6 hours before landfall, Storm 136 (upper panel), Storm 122 (middle panel), Storm 128 (lower panel).

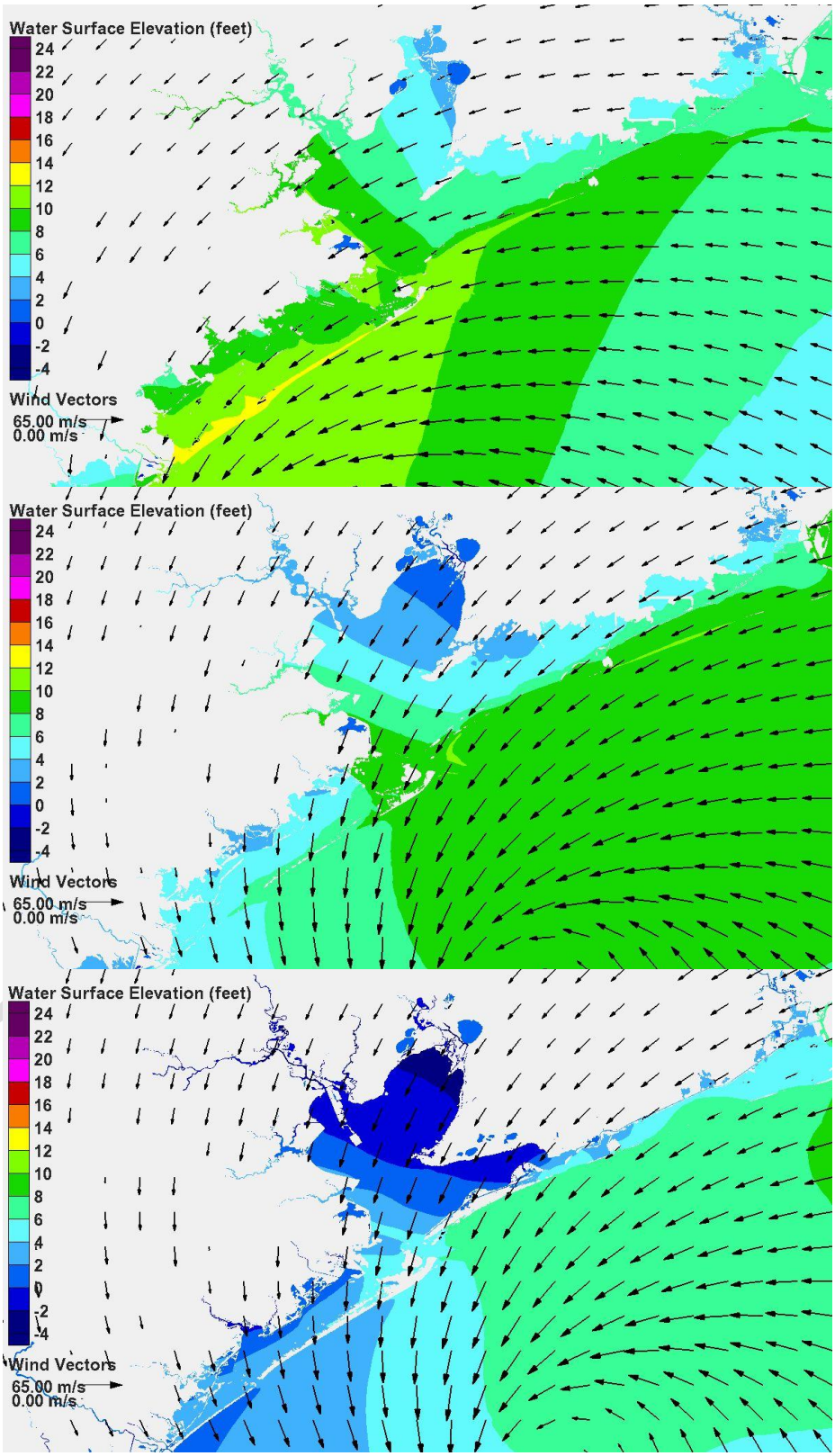

Figure 7-15. Water surface elevation and wind vectors 3 hours before landfall, Storm 136 (upper panel), Storm 122 (middle panel), Storm 128 (lower panel).

Along the open coast, the zone of highest surge for Storm 136 is near San Luis Pass, and it is moving to the northeast as the storm advances toward the northeast. This is a different direction of peak surge migration compared to the other two storms, which are moving into the region from the east and northeast.

In West Bay for Storm 136, winds are blowing from the northeast in the direction of the long axis of the Bay, due to the curvature in the core hurricane winds. This wind direction acts to set up the western side of the Bay, which continues to force water from Galveston Bay into West Bay. The highest surge in West Bay at this point in time is at its western end. Along the open coast, winds also are pushing water into the region from the east. Considerable flow over Galveston Island and Bolivar Peninsula is taking place.

For Storm 122, along the coast, surge is growing and developing from the east and northeast, and moving into the Houston-Galveston region from that direction. In response, the largest surges are along the Gulf side of Bolivar Peninsula. Within Galveston Bay winds are blowing from the northeast to north-northeast directions, setting up the southwest corner of the Bay. The largest surge at his point within Galveston Bay is at this corner, near the bay side of the City of Galveston. Within West Bay, due to curvature of the hurricane wind field, winds are blowing from the north-northeast and setting up the water surface on the bay side of Galveston Island. Water is moving from Galveston Bay into West Bay due to the gradient in water surface elevation between the two bays. Surge on the Gulf and bay sides of Galveston Island are nearly the same. Considerable flow over the barrier islands is taking place.

The pattern of storm surge development for Storm 128 is similar to that for Storm 122. The coastal surge is building and moving into the region from the east and northeast. Winds within Galveston Bay are nearly the same as for Storm 122. In response, a similar water surface elevation gradient is established within the Bay, although absolute elevations are greater for Storm 122 because of the greater forerunner penetration. The maximum surge within the Bay at this time is also on the bay side of the City of Galveston. Some flow over Bolivar Island is occurring; little flow is apparent over Galveston Island at this point because of lower water surface elevations.

Figure 7-16 shows conditions approximately 1 hr before landfall. The wind fields are fairly similar for all three storms because the eyes have similar positions, and the counterclockwise wind circulation about the eye is similar for all three storms. In the previous set of snap-shots (see Figure 7-15) 3 hrs before landfall, because of the counterclockwise wind circulation, winds were blowing more or less along the coast for Storms 122 and 128, pushing water into the nearshore coastal region from the east. As these storms approach landfall winds will become directed more onshore, like Storm 136 shows for this time. In response to onshore winds, surge that has been building from the east is driven toward shore. As the storms move into shallower water the highest core winds to the right hand side of the eye become increasingly more effective in pushing the water in the direction of the wind and building the storm surge against the coastline.

Along the open coast, the zone of peak surge for Storm 136 continues to move to the northeast and is now situated at the City of Galveston. For both Storms 122 and 128, surge continues to build from the east and the zone of peak surge is positioned along Bolivar Peninsula. For all three storms, Galveston Bay is filling because of the large volume of water that is flowing over Bolivar Peninsula into the bay, which is then pushed by the wind toward the Bay. The high open coast surge also is propagating into the bay through Bolivar Roads.

Flow over Galveston Island is occurring for all three storms. Winds in West Bay are directed offshore along the western portion of Galveston Island, on onshore along the eastern portion, for all three storms. Offshore-directed winds act to push water against the back side of Galveston Island and drive flow over the inundated barrier island.

Within Galveston Bay, winds are from the east-northeast for Storm 136 and from the northeast for the other two storms. These wind directions continue to set up the water surface along the western shoreline of the Bay for Storm 136, and along the southwestern shoreline of the Bay for Storms 122 and 128. The higher wind speeds are increasing the degree of tilt, or the gradient, in the water surface. The highest surge remains along the bay side of the City of Galveston and the Texas City area at this point for all three storms. The surge at this location also is influenced by the propagation of coastal surge through the pass at Bolivar Roads.

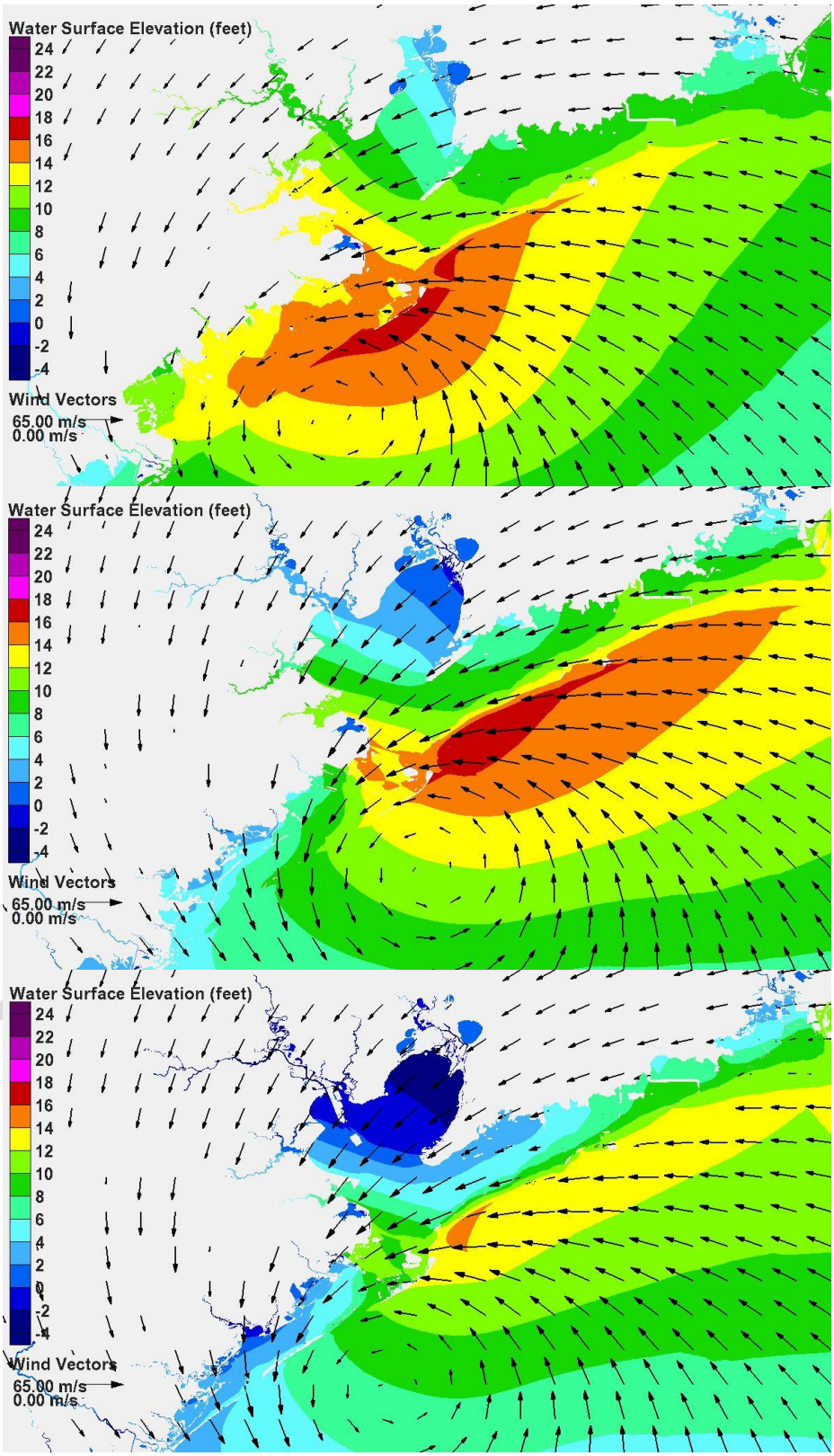

Figure 7-16. Water surface elevation and wind vectors 1 hour before landfall, Storm 136 (upper panel), Storm 122 (middle panel), Storm 128 (lower panel).

Figure 7-17 shows the storm surge and wind fields at landfall. Winds are directed onshore to the east of the eye for all three storms. For Storm 136, the zone of peak surge continues to move toward the northeast and is now situated at the western end of Bolivar Peninsula. For Storms 122 and 128, the zones of peak surge persist along Bolivar Peninsula. Winds to the east of the eye continue to push surge over Bolivar Peninsula and into the Bay. Winds in West Bay are directed offshore along those parts of the island to the left, or west, of the eye. The offshore-directed winds continue to stack water against the Bay side of Galveston Island and push water over the inundated island.

At this time, wind conditions within the Bay are quite similar for all three storms, blowing from the east, and forcing a similar water surface tilt. Differences in absolute elevation between storms are due to different forerunner penetration and differing amounts of filling by flow over the barrier islands. Winds in the Bay are shifting rapidly, and the water surface elevation field responds quickly to the wind shift. Water is moving rapidly to establish the primary momentum balance between wind shear stress and water surface slope.

Figure 7-18 shows conditions 1 hr after landfall. The eyes of the storms are moving inland; as they do so, winds are rapidly shifting within Galveston and West Bays. The curvature in wind fields produces considerable variation in wind direction for all the storms, but less so for Storm 128 since its eye is the farthest away from the Bay. With the eye being farther away, the curvature of the wind fields in the Bay is less. For all three storms, water that has been pushed into Galveston Bay is now starting to be driven to the north and northwest sides. Water also is filling the northeast parts of the Bay that previously had been p set down by the wind. In West Bay the winds are shifting rapidly, blowing from the northwest for Storms 136 and 122. For Storm 128, winds are now blowing from the south in the eastern portion of the Bay, setting up the north side. The water surface is responding quickly to the shifts in wind conditions in these shallow bays.

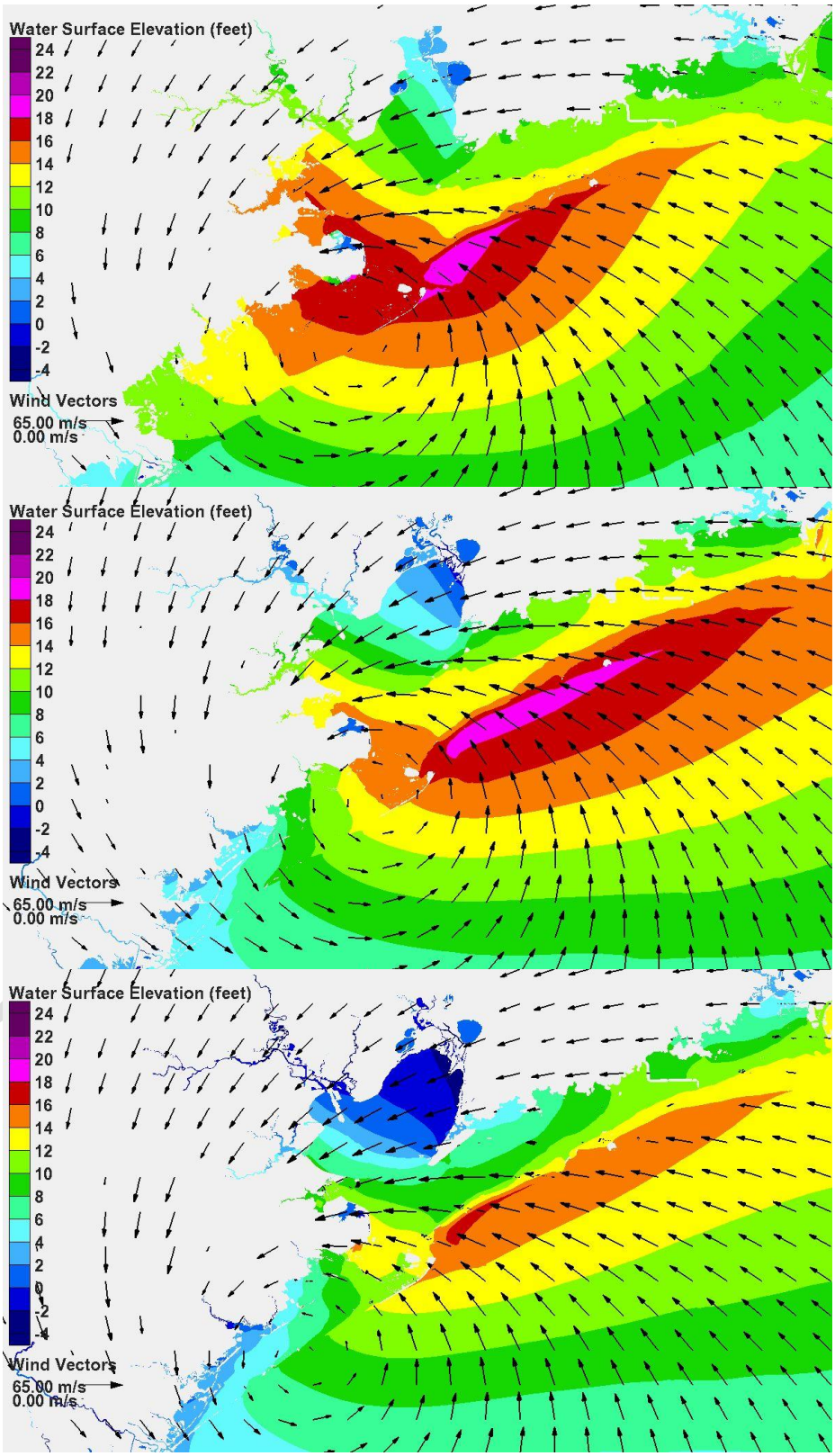

Figure 7-17. Water surface elevation and wind vectors at landfall, Storm 136 (upper panel), Storm 122 (middle panel), Storm 128 (lower panel).

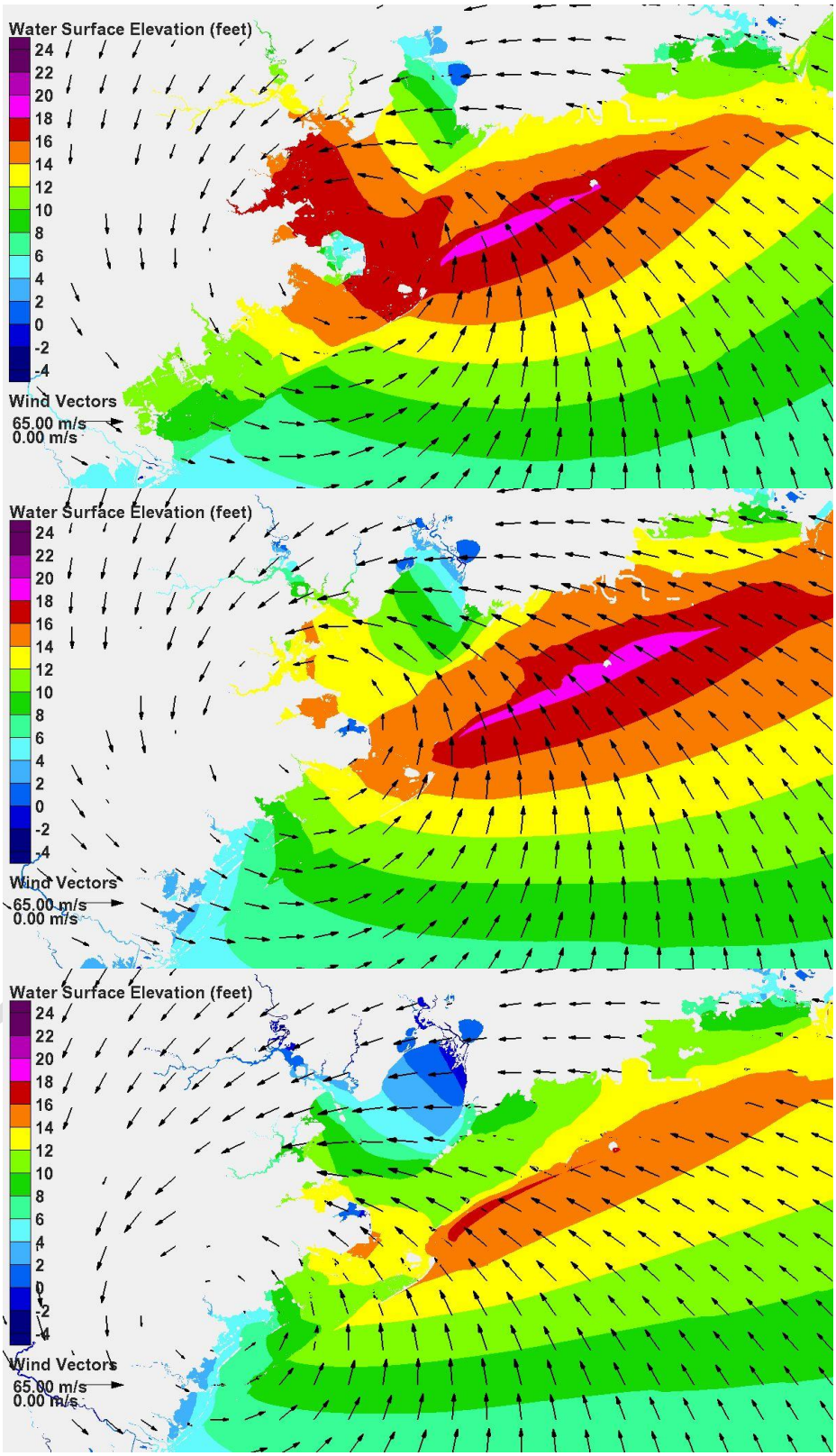

Figure 7-18. Water surface elevation and wind vectors 1 hour after landfall, Storm 136 (upper panel), Storm 122 (middle panel), Storm 128 (lower panel).

Along the open coast, the zone of highest surge for Storm 136 continues to move to the northeast and is situated along the middle and eastern portions of Bolivar Peninsula. For Storms 122 and 128, the zone of highest surge persists along Bolivar Peninsula. The onshore winds along Bolivar Peninsula, for all three storms, continue to build surge against the coastline and push water across the inundated barrier island.

Figure 7-19 shows water surface elevation and wind fields 2 hrs after landfall. Along the open coast, persistent onshore winds for all three storms push water against the coast, across the inundated Bolivar Peninsula, and then into Galveston Bay.

For Storm 136, the eye of the storm is positioned directly over Galveston Bay and moving toward the north. Winds throughout the Bay are quite variable in direction, with no persistent direction, and are characterized by relatively lower wind speeds because of the presence of the eye. In response, water surface elevations throughout much of the Bay are somewhat uniform at this time. The northeast part of the Bay continues to fill. In West Bay winds are blowing from the west and west- northwest, setting up the eastern side.

The eye for Storm 122 is moving along the western shoreline of Galveston Bay toward the north-northwest, and is positioned near the northwest corner at this time. Winds in Galveston Bay are generally blowing to the north, pushing water toward the north. Winds in West Bay are blowing from west and southwest, depending on location within the Bay, and are setting up the eastern.

The eye of Storm 128 made landfall farthest to the west of the three storms. It is moving toward the northwest, and this movement is increasing its distance from the Bay. Winds within Galveston Bay are all directed to the northwest, pushing water in that direction and setting up the northwest corner. The northeast corner also is filling due to water surface elevation gradients that force water from areas of high surge to areas of lower surge. Winds in West Bay are blowing from the south, setting up the north side and pushing water inland. Water is being pushed across the inundated Galveston Island toward the north.

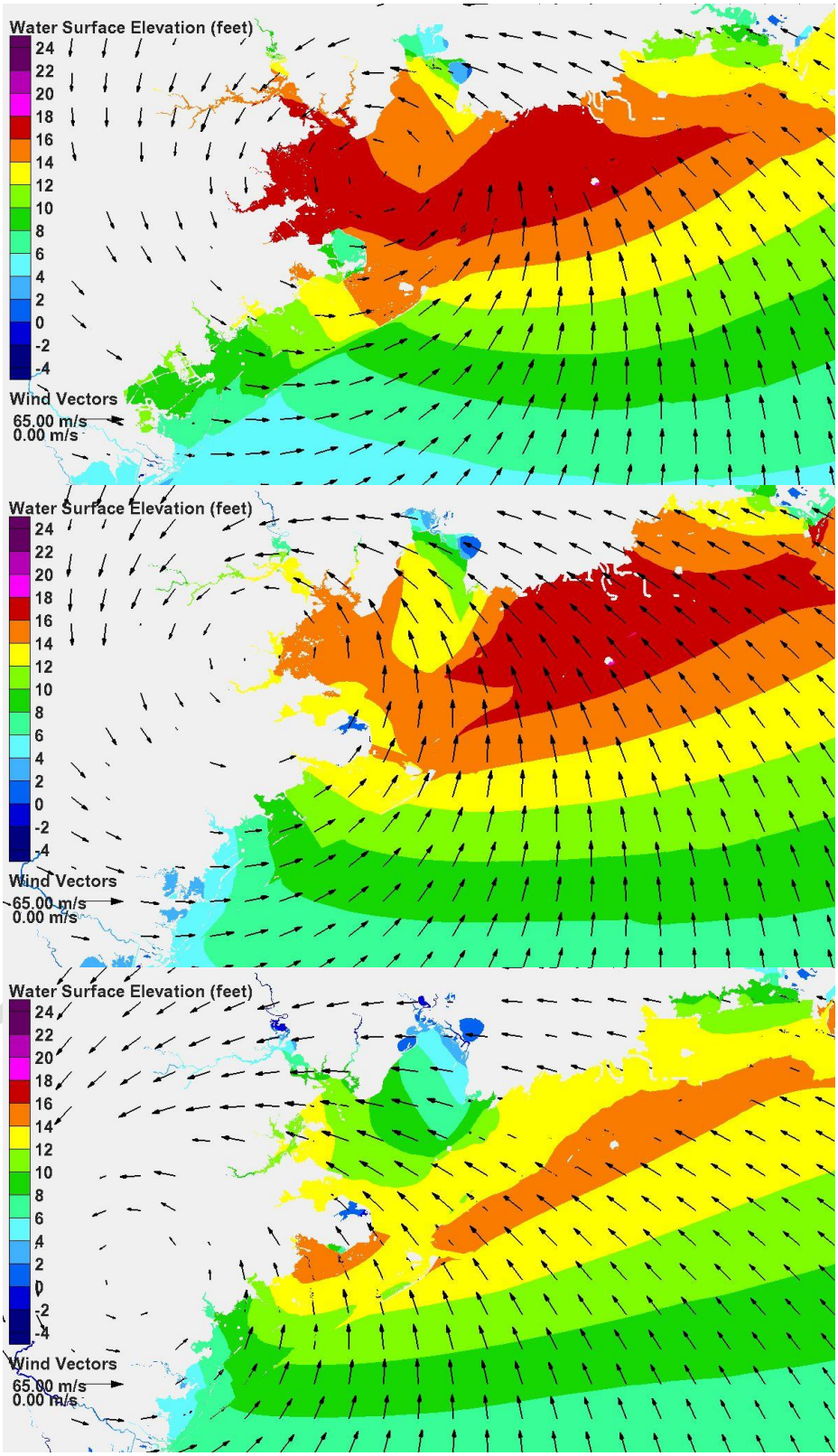

Figure 7-19. Water surface elevation and wind vectors 2 hours after landfall, Storm 136 (upper panel), Storm 122 (middle panel), Storm 128 (lower panel).

Figure 7-20 shows conditions 3 hrs after landfall. Along the open coast, persistent onshore winds for all three storms continue to push water against the coast and across the inundated Bolivar Peninsula. For Storms 122 and 128, the water being pushed across Bolivar Peninsula continues to flow into Galveston Bay, toward the north for Storm 122 and toward the northwest for Storm 128. However, the eye of Storm 136 has moved north of Galveston Bay, and strong winds on the back side of the eye are now directed toward the east. Those winds push water toward the east side of Galveston Bay.

Figure 7-21 shows winds and water surface elevation fields 6 hours after landfall. Along the open coast winds have an onshore component for all three storms, but more so for Storms 122 and 128 than for Storm 136. Winds for Storm 136 are blowing more from the southwest. Within Galveston Bay, winds for Storm 136 are from the west-southwest throughout the region. Winds for Storms 122 and 128 are from the south and south-southeast, respectively, throughout the region. As the eye of the storm moves farther away, the winds become more uniform in direction because the degree of curvature of the wind fields lessens with distance away from the eye.

The open coast storm surge is subsiding for all three storms, most rapidly for Storm 136. For this storm and at this time, the water surface elevation is higher in Galveston Bay than along the open coast; and in response, water is flowing from the Bay back to the Gulf. This same process is occurring in West Bay, where water is flowing back over Galveston Island toward the Gulf. For Storms 122 and 128, the response along the barrier islands is quite different. Southerly winds continue to push water toward the coast, across the inundated Bolivar Peninsula and Galveston Island, and into Galveston Bay and West Bay, respectively.

Different water surface responses also are occurring within the Bays. For Storm 136 winds in Galveston Bay are directed toward the east. In response, the water surface is set up on the east side of the Bay and set down along the western shoreline. Westerly winds in West Bay set up the east end and set down the west end. For Storm 122, persistent southerly winds continue to push water that has accumulated in Galveston Bay to the north, setting up the water surface in the northern parts of the system and pushing water into the channels and estuaries. The persistent southerly wind is establishing a large south-to- north water surface

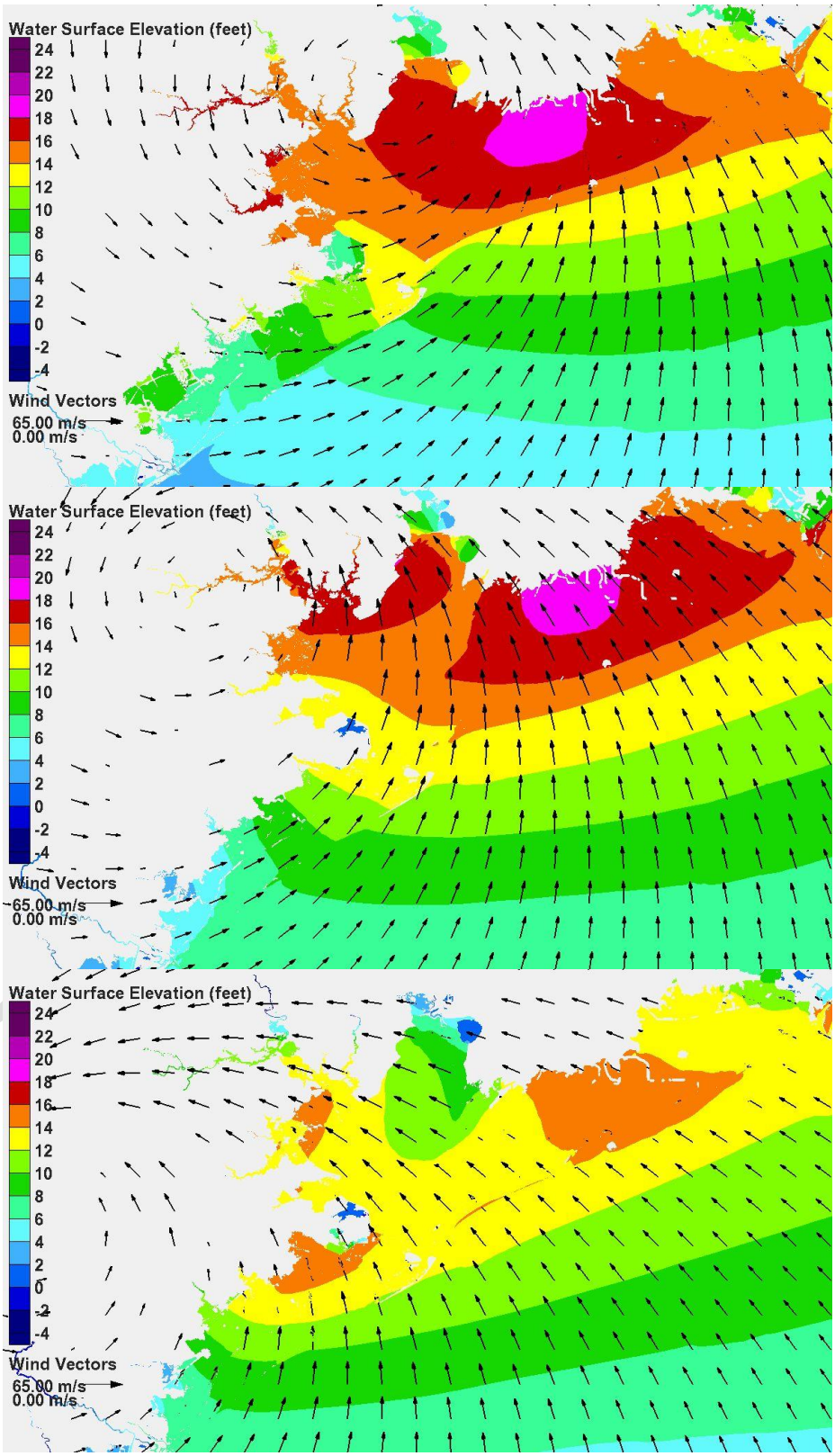

Figure 7-20. Water surface elevation and wind vectors 3 hours after landfall, Storm 136 (upper panel), Storm 122 (middle panel), Storm 128 (lower panel).

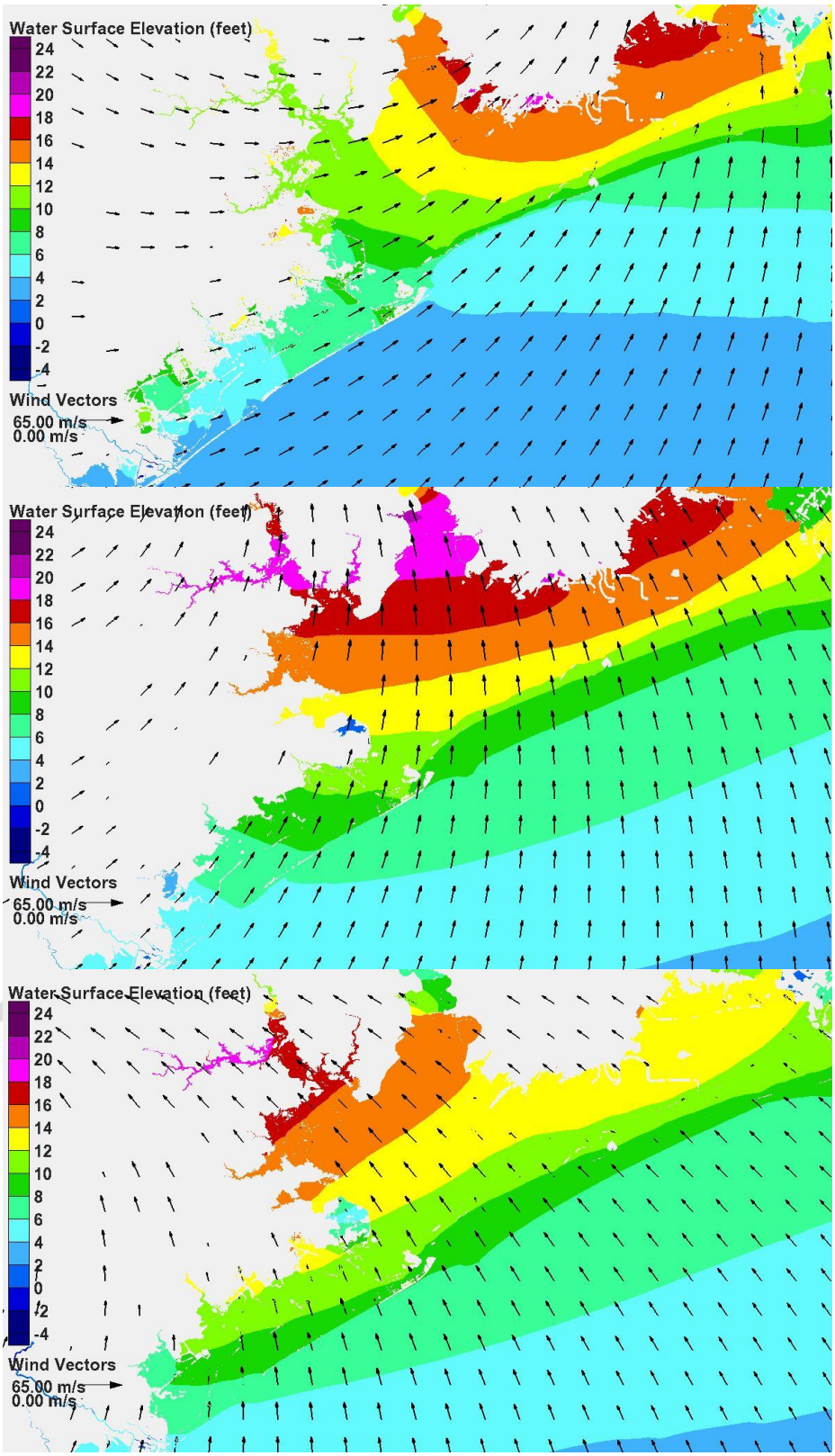

Figure 7-21. Water surface elevation and wind vectors 6 hours after landfall, Storm 136 (upper panel), Storm 122 (middle panel), Storm 128 (lower panel).

gradient throughout the Bay. In West Bay, southeasterly winds set up the northeast corner.

The surge development process within the Bay at this time is similar for Storm 128, compared to Storm 122. Uniform winds from the south-southeast set up the north-northwest parts of the Bay, pushing water in that direction and into channels and estuaries, and establishing a persistent water surface gradient throughout the Bay. In West Bay southerly winds set up the north side and push water inland.

Figure 7-22 shows conditions 9 hours after landfall. At this time the storm eyes have moved well away from the Houston-Galveston region and winds are rather uniform in direction throughout the region for each storm. Wind directions for each storm are quite similar to what they were 3 hrs earlier. Wind speeds are decreasing for each storm as the eye moves farther away from the region.

Within the Bays, surges have reached their maximum values and are decreasing. However, even 9 hours after landfall, high surges persist throughout the system and in particular the northern parts of the system.

For all three storms, the open coast storm surge is subsiding, water is draining from the Bays and flowing back to the Gulf. This draining takes place much more slowly than the filling did. As water surface elevations decrease to values lower than crest elevations of the degraded barrier islands, draining will be restricted to flow through passes and any breach channels that formed on the eroded barrier islands during the storm.

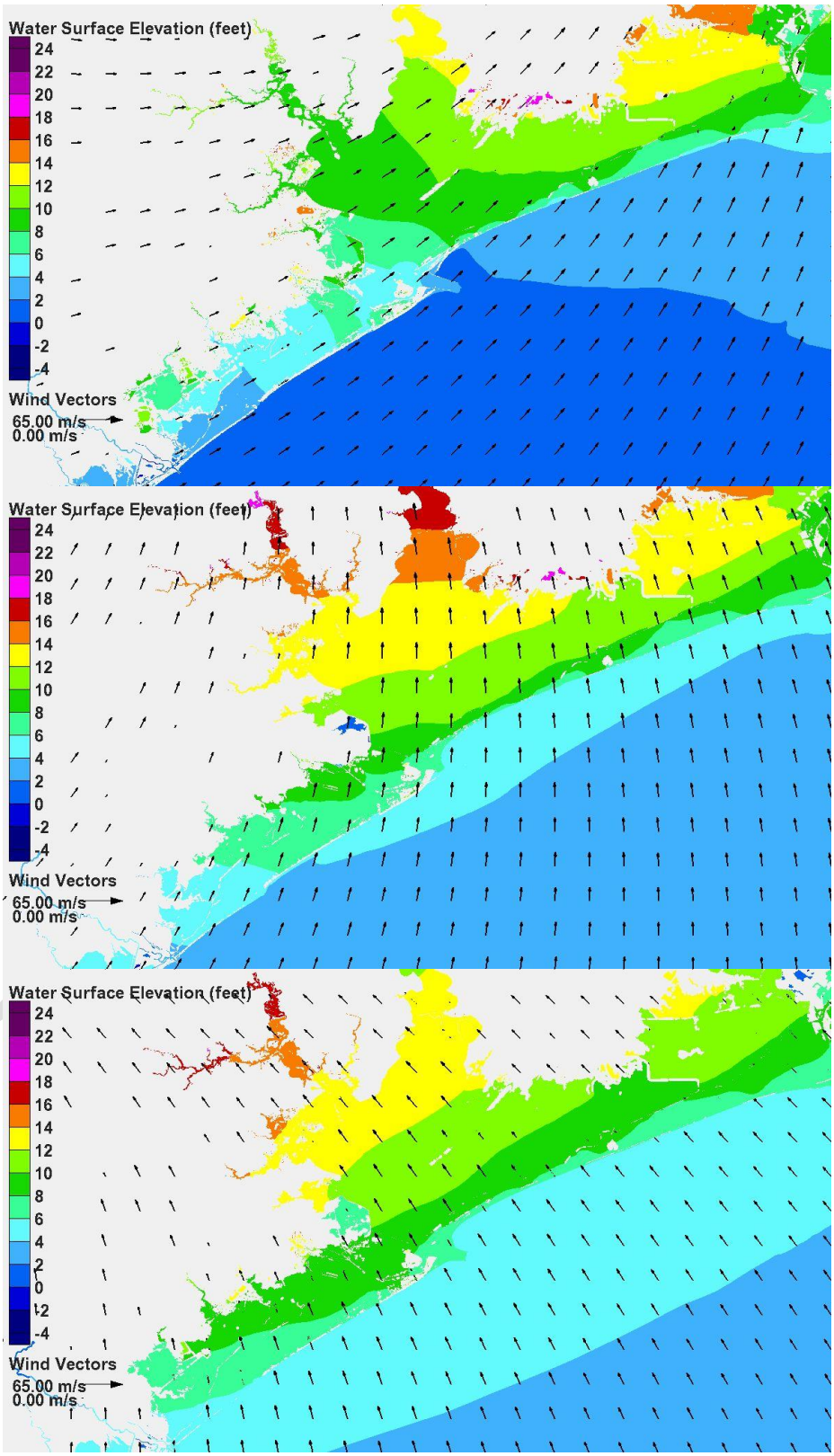

Figure 7-22. Water surface elevation and wind vectors 9 hours after landfall, Storm 136 (upper panel), Storm 122 (middle panel), Storm 128 (lower panel).

8 Reduction in Flooding Achieved with the Ike Dike

Introduction

Reduction in flooding achieved by the Ike Dike concept was examined by comparing maximum water surface elevation maps for existing conditions with maximum water surface elevation maps for with-dike conditions. The maximum water surface elevation maps were computed for each storm in the following way: at every grid node of the computational mesh used in the storm surge modeling, the maximum water surface elevation is recorded, regardless of when it occurred during the hurricane simulation. The water surface elevation maxima at every grid mesh node are then used to develop the maximum water surface elevation map. A difference map was computed by subtracting the with-dike map from the existing condition map for each storm. All water surface elevations are relative to the NAVD88 vertical datum, which is about 0.5 ft below the mean sea level tidal datum.

For each storm a figure is provided which shows three maps, one for existing conditions (top panel), one for with-dike conditions (middle panel), and the difference map (bottom panel). The water surface elevation color bar scale used for each map is shown in each panel. The same scale is used throughout this chapter. Following the figure showing the maps, storm surge information for existing conditions, with-dike conditions, and the difference, is shown in tabular and descriptive form for each of 9 locations in the Houston-Galveston region: Galveston (Gulf side), Galveston (Bay side), rest of Galveston Island west of the City of Galveston, Bolivar Peninsula, the Texas City area, Clear Lake area, Bayport Area, and the upper reaches of the Houston Ship Channel. The tables help quantify reduction in surge achieved with the dike. The reduction is generally not uniform throughout the Houston-Galveston region for a particular storm, and the reductions at each location vary from storm to storm.

Storms are divided into four groupings, and results provided below are grouped in the same way. The first group is the direct-hit set of four storms, all on the same track, with varying intensity (900 mb, 930 mb, 960 mb and 975 mb). The other groupings are based on storm track, one

group for each of the three main approach directions, south, south-southeast and southeast. All storms in the three track groups were 900 mb storms. The storms in each grouping have the same heading but they differ in their landfall location.

Landfall location has great influence on the storm surge that is experienced in the Houston-Galveston region. Storms that make landfall at a distance of one radius-to-maximum-winds to the west of Bolivar Roads tend to produce the largest storm surge in the most economically sensitive areas. For the storms simulated here, one radius-to-maximum-winds distance to the west of Bolivar Roads is approximately at San Luis Pass. So the storm(s) in each track grouping that make(s) landfall nearest San Luis Pass tends to produce the largest storm surge in the Houston-Galveston region for that group of storm tracks.

As the landfall location moves east of Bolivar Roads, the maximum surge will be located well to the east of Galveston Bay. For these storms, as the distance between landfall position and Bolivar Roads increases, the region of maximum surge will occur farther and farther way from the Houston–Galveston region and storm surge within the region will decrease. This trend is evident in the results shown below. Storms in the West Louisiana set tended to make landfall well to the east of Galveston Bay, and the surges they generated in the area of interest tended to be much less than surge generated by the storms in the North Texas set. Therefore this report will only show results for the North Texas set.

The Long Dike or Levee Effect

When a long coastal dike, seawall or levee is constructed to reduce the risk of storm flooding, it can result in a local increase of storm surge compared to surge that would have occurred at that same location had the dike or other structure not been present. The structure provides a barrier for the wind-driven water to stack up against, and it restricts the ability of the water to move elsewhere away from the structure. This increase in surge occurs for the Ike Dike concept and is seen in the results that follow. Surge is generally increased by amounts of up to 1.5 ft for the 900 mb storms that have been simulated. The maximum increase tends to occur where the storm surge is greatest. If flow over the dike commences, as it does for a number of the storms, this will tend to mask the amount of the increased surge had the dike been higher and prevented overflow from

occurring. This effect and the surge increase must be recognized and factored into the design of the risk reduction measure.

Hurricanes of Varying Intensity - The Direct-Hit Set

Results for the direct-hit set of four storms illustrate the benefits of the Ike Dike concept in reducing storm surge for hurricanes of varying intensity. The four storms have the same track, shown in Figure 68, but different central pressures: Storm 122 (900 mb), Storm 155 (930 mb), Storm 121 (960 mb) and Storm 561 (975 mb).

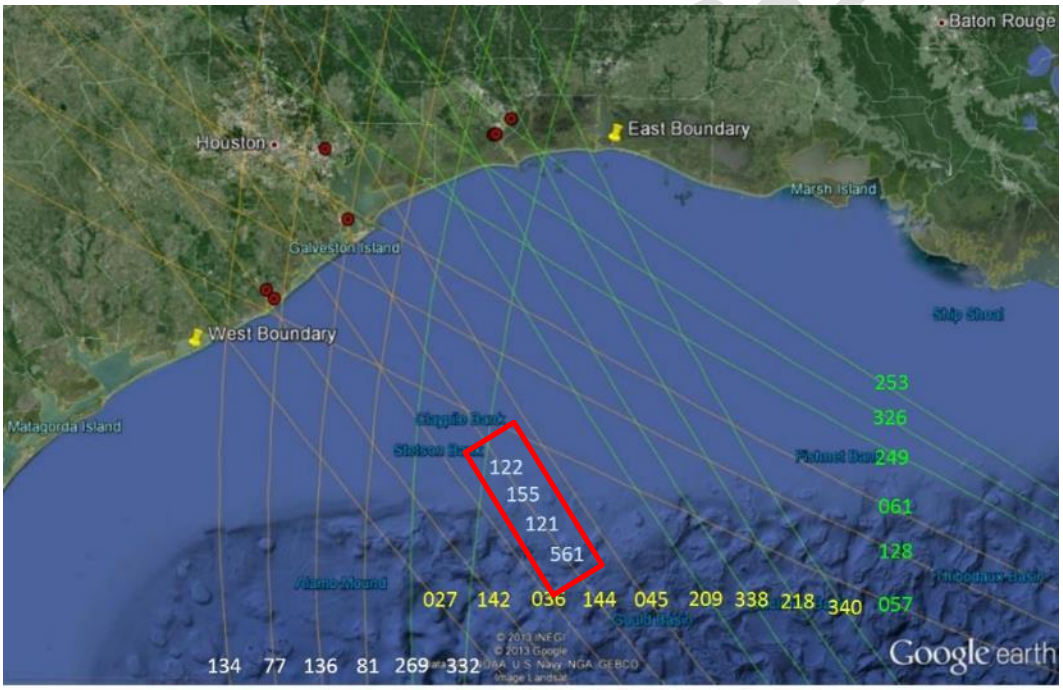

Figure 68. Direct-hit group of hurricanes approaching from the southeast (storms 122 (900 mb), 155 (930 mb), 121 (960 mb), 561 (975 mb))

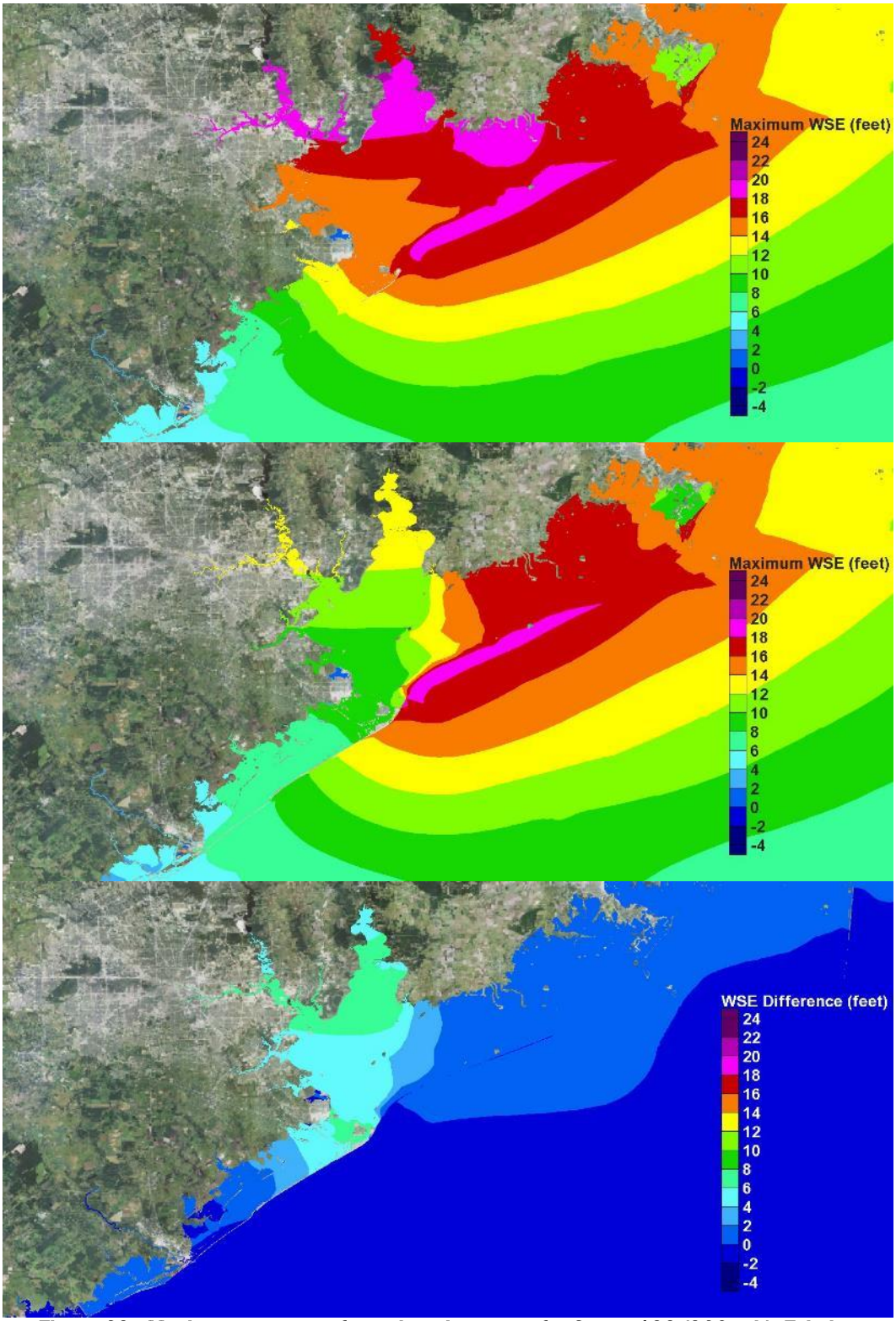

Figure 69. Maximum water surface elevation maps for Storm 122 (900 mb). Existing conditions (top); With-dike conditions (middle); Difference in maximum water surface elevation (bottom)

Table 4. Summary of Maximum Storm Surge Conditions for Storm 122.

Location	Existing Condition	With-Dike Condition	Changes
Galveston (Gulf side)	13.5 to 16.5 ft	14 to 17.5 ft	The dike causes surge by 0.5 to 1 ft in front of the seawall. Overtopping and overflow expected.
Galveston (Bay side)	14 to 16 ft	8.5 to 11 ft	Reduction of 5.5 ft to 6 ft
Rest of Galveston Island	7 to 14 ft, increasing from west to east	6.5 to 8.5 ft	Reductions of 0 ft in the west to 5.5 ft in the east.
Bolivar Peninsula	18 to 18.5 ft	14 to 17 ft	0 to 2 ft. Overflow and overtopping along most/all of the dike. No significant change
Texas City area	11 to 15 ft	8.5 to 9.5 ft	Reduction of 4.5 to 5.5 ft
Clear Lake Area	15 to 15.5 ft	9.5 to 10.5 ft	Reduction of 5 to 5.5 ft
Bayport Area	15.5 to 16.5 ft	10.5 to 11.5 ft	Reduction of 5.5 to 6 ft
Upper reaches of Houston Ship Channel	19 to 20 ft	13 to 14 ft	Reduction of 6 to 7 ft

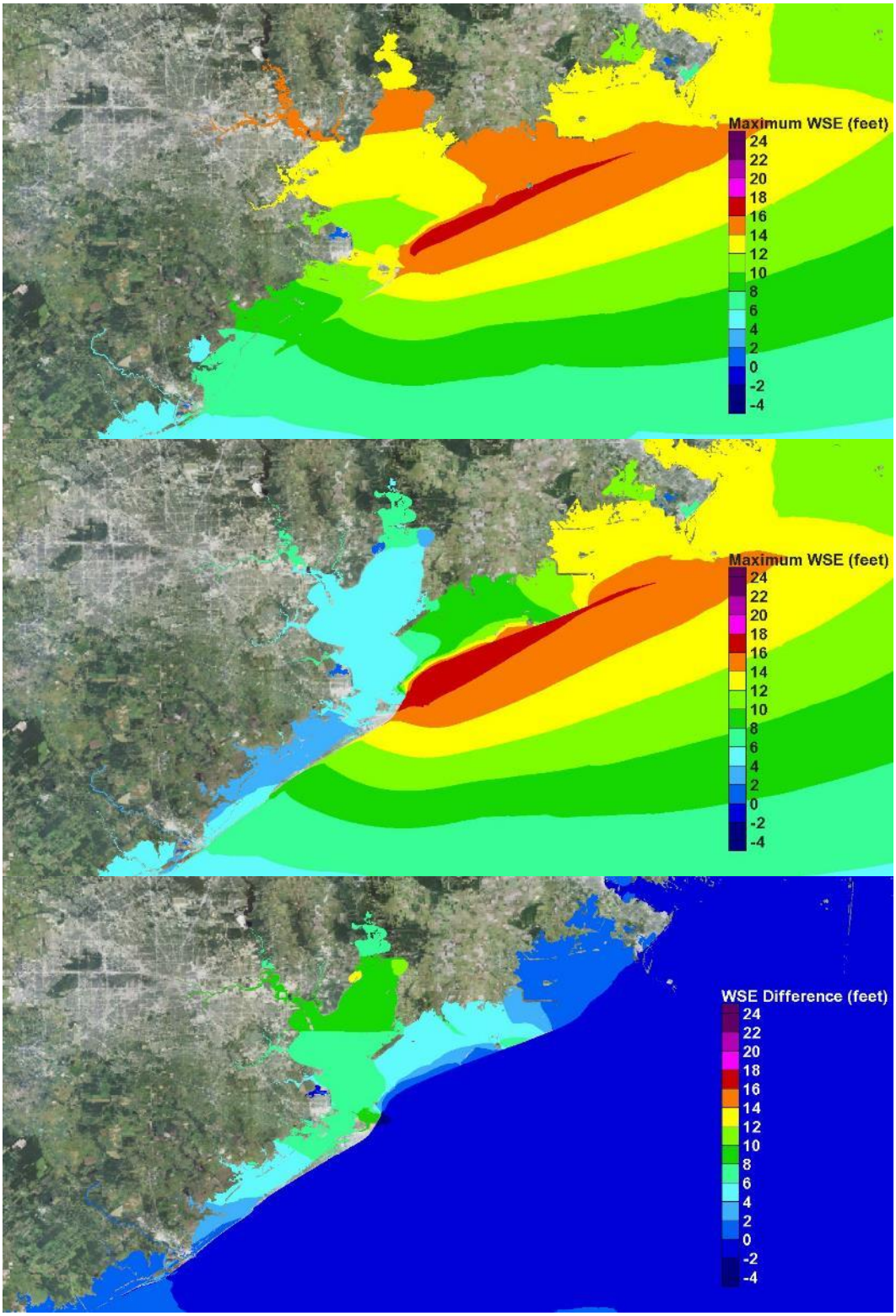

Figure 70. Maximum water surface elevation maps for storm 155 (930 mb). Existing conditions (top); With-dike conditions (middle); Difference in maximum water surface elevation (bottom)

Table 5. Summary of Maximum Storm Surge Conditions for Storm 155.

Location	Existing Condition	With-Dike Condition	Changes
Galveston (Gulf side)	11 to 15 ft increasing from west to east	12 to 16 ft	Increase of 1 ft. Increase in overtopping is expected.
Galveston (Bay side)	11 to 14 ft increasing from west to east	4 to 5.5 ft	Reduction of 7 to 10 ft
Rest of Galveston Island	7 to 11 ft, increasing from west to east	4 to 4.5 ft	Reductions of 2 ft in the west to 6 ft in the east.
Bolivar Peninsula	16 to 17 ft	10 to 16 ft	0 to 4 ft. Presence of the dike increases surge in front of dike by 1 ft. Overflow along most/all of the dike
Texas City area	11.5 to 12.5 ft	4 to 5 ft	Reduction of 7 to 8 ft
Clear Lake Area	13 ft	4 to 5 ft	Reduction of 7.5 to 8.5 ft
Bayport Area	13.5 ft	5 to 5.5 ft	Reduction of 8 to 8.5 ft
Upper reaches of Houston Ship Channel	15 ft	7 ft	Reduction of 8 ft

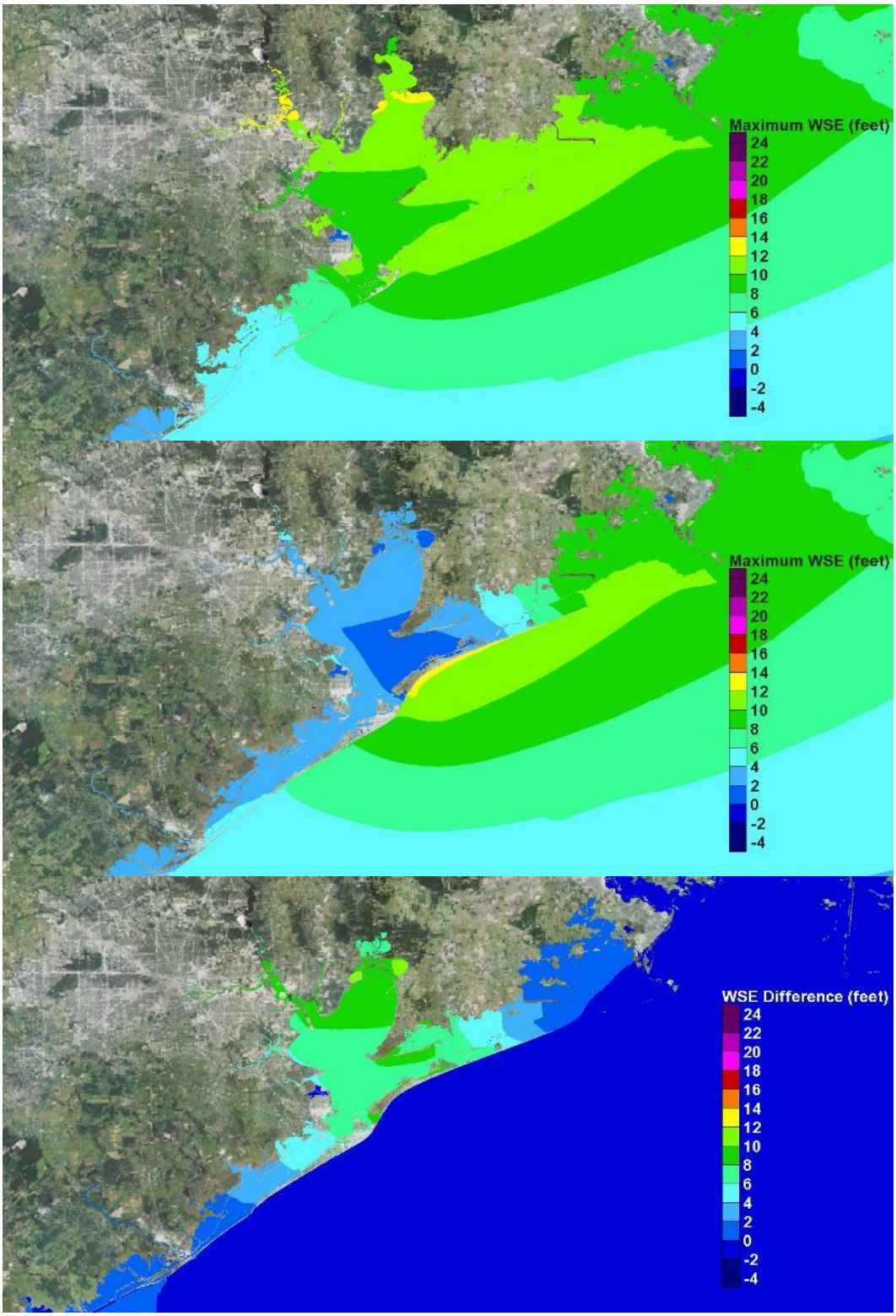

Figure 71. Maximum water surface elevation maps for storm 121 (960 mb). Existing conditions (top); With-dike conditions (middle); Difference in maximum water surface elevation (bottom)

Table 6. Summary of Maximum Storm Surge Conditions for Storm 121.

Location	Existing Condition	With-Dike Condition	Changes
Galveston (Gulf side)	7.5 to 10.5 ft	8 to 10.5 ft	Increase of 0 to 0.5 ft. No significant change.
Galveston (Bay side)	8.5 to 10.5 ft	2.5 to 3 ft	Reduction of 6 to 8 ft
Rest of Galveston Island	5 to 8 ft, increasing from west to east	3 to 4 ft	Reductions of 1 ft in the west to 5 ft in the east.
Bolivar Peninsula	11 to 11.5 ft	2 to 2.5 ft	Presence of the dike increases surge by 1 ft on ocean side. Reduction in bay of 9 ft
Texas City area	8.5 to 11 ft	2 to 4 ft	Reduction of 6 to 7 ft
Clear Lake Area	10 ft	3 to 4 ft	Reduction of 7 ft
Bayport Area	10 to 10.5 ft	3 to 4 ft	Reduction of 7 to 7.5 ft
Upper reaches of Houston Ship Channel	12 to 12.5 ft	3 to 4 ft	Reduction of 8 to 9 ft

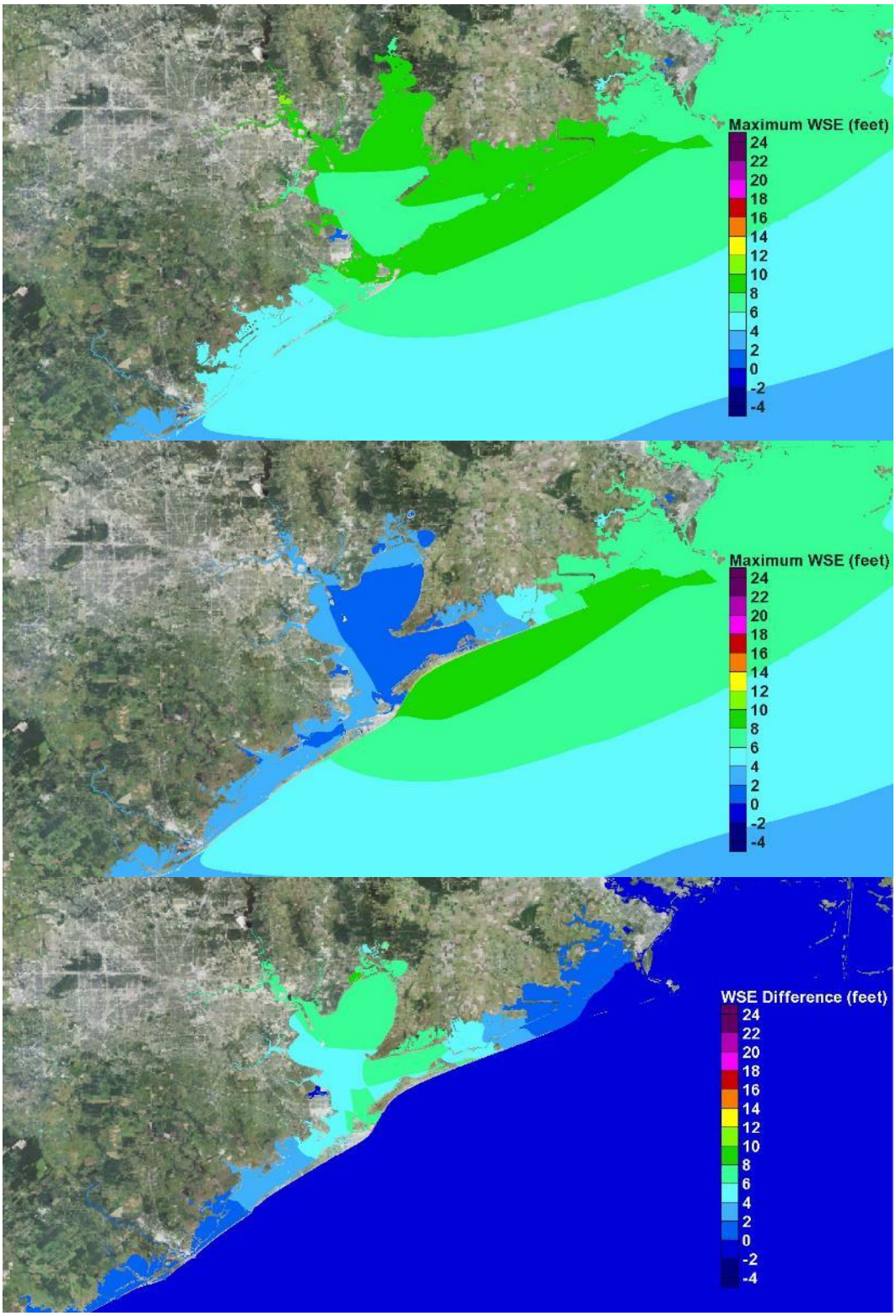

Figure 72. Maximum water surface elevation maps for storm 561 (975 mb). Existing conditions (top); With-dike conditions (middle); Difference in maximum water surface elevation (bottom)

Table 7. Summary of Maximum Storm Surge Conditions for Storm 561.

Location	Existing Condition	With-Dike Condition	Changes
Galveston (Gulf side)	7 to 8.5 ft	7 to 8.5 ft	No change
Galveston (Bay side)	7.5 to 8.5 ft	2 to 2.5 ft	Reduction of 5 to 6.5 ft
Rest of Galveston Island	4.5 ft in the west to 6.5 ft in the east	2 to 3 ft	Reductions of 1.5 ft in the west to 4 ft in the east.
Bolivar Peninsula	9 ft	2 to 3 ft	Reduction of 6 to 7 ft
Texas City area	8 to 8.5 ft	2.5 to 3 ft	Reduction of 5 to 6 ft
Clear Lake Area	8 ft	3 ft	Reduction of 5 ft
Bayport Area	8.5 ft	2 to 3 ft	Reduction of 6 ft
Upper reaches of Houston Ship Channel	9 to 10 ft	3 to 4 ft	Reduction of 6 to 7 ft

Major Hurricanes Approaching from the South

The following results are for the group of four North Texas storms that approached from the south. The influence of landfall position on maximum storm surge in Galveston Bay is evident. Storm 077 produces the maximum surge in the region, followed by Storm 134, Storm 136 and Storm 081, in order of deceasing maximum surge in the Houston-Galveston region.

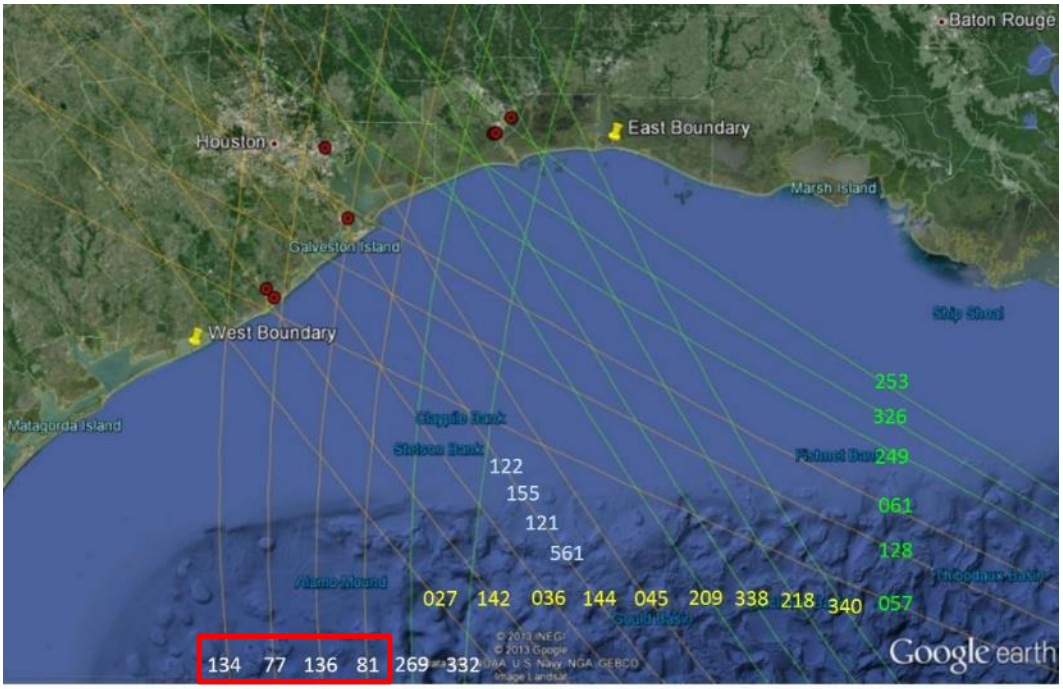

Figure 73. Group of hurricanes approaching from the south (storms 134, 77, 136, 81)

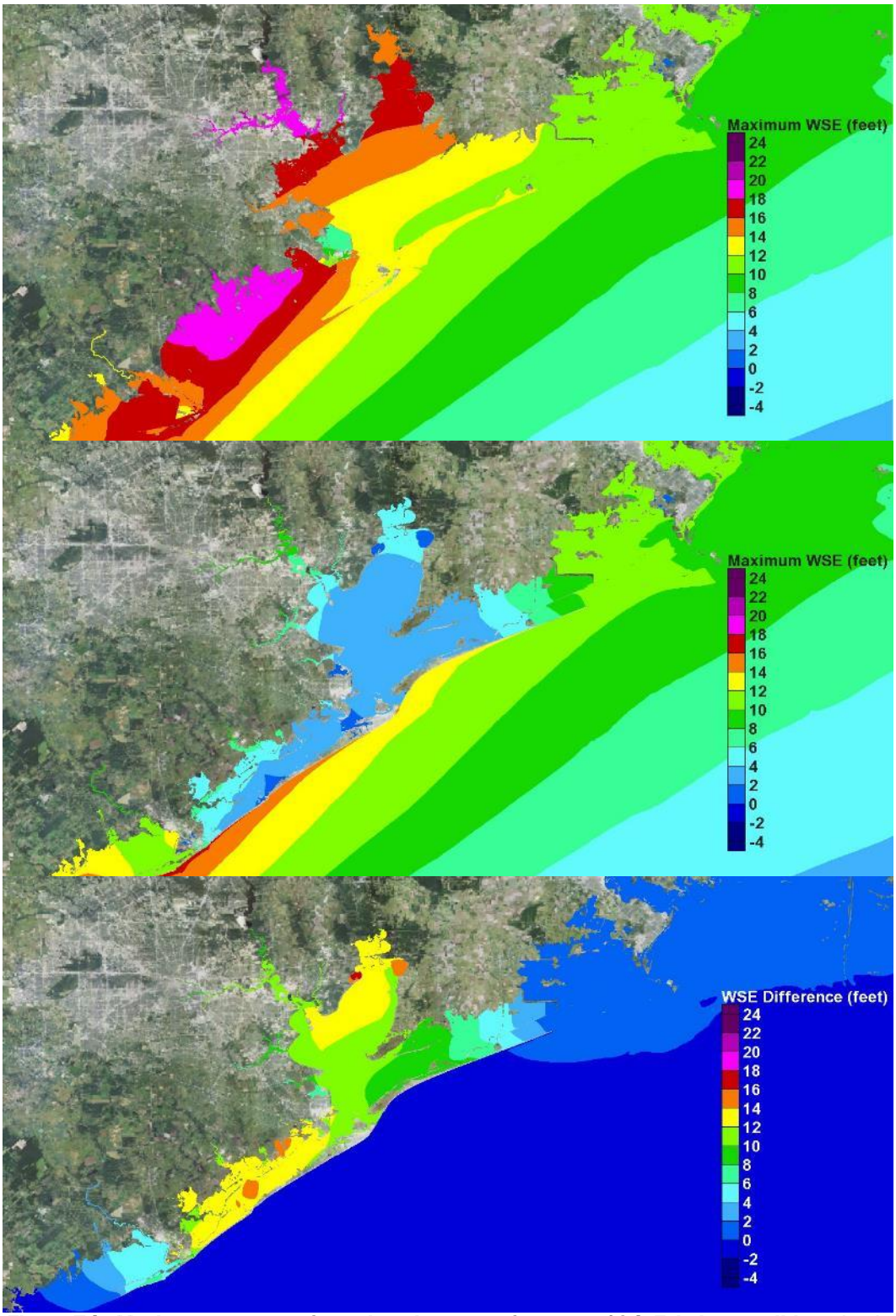

Figure 74. Maximum water surface elevation maps for storm 134. Existing conditions (top); With-dike conditions (middle); Difference in maximum water surface elevation (bottom)

Table 8. Summary of Maximum Storm Surge Conditions for Storm 134.

Location	Existing Condition	With-Dike Condition	Changes
Galveston (Gulf side)	13 to 14 ft	13 to 14 ft	No change
Galveston (Bay side)	13 ft	2 to 3 ft	Reduction of 11 ft
Rest of Galveston Island	14 to 16 ft	2 to 4.5ft	Reductions of 12 to 14 ft
Bolivar Peninsula	12 to 13 ft	3 to 4 ft	Reduction of 8 to 10 ft
Texas City area	13 to 16.5 ft	2.5 to 3 ft	Reduction of 12 ft. Prevented interior flooding.
Clear Lake Area	15 to 16.5 ft	4 to 5 ft	Reduction of 11 to 12 ft
Bayport Area	17 to 18 ft	4 to 5 ft	Reduction of 12 ft
Upper reaches of Houston Ship Channel	19 to 20 ft	8 to 9 ft	Reduction of 11 to 12 ft

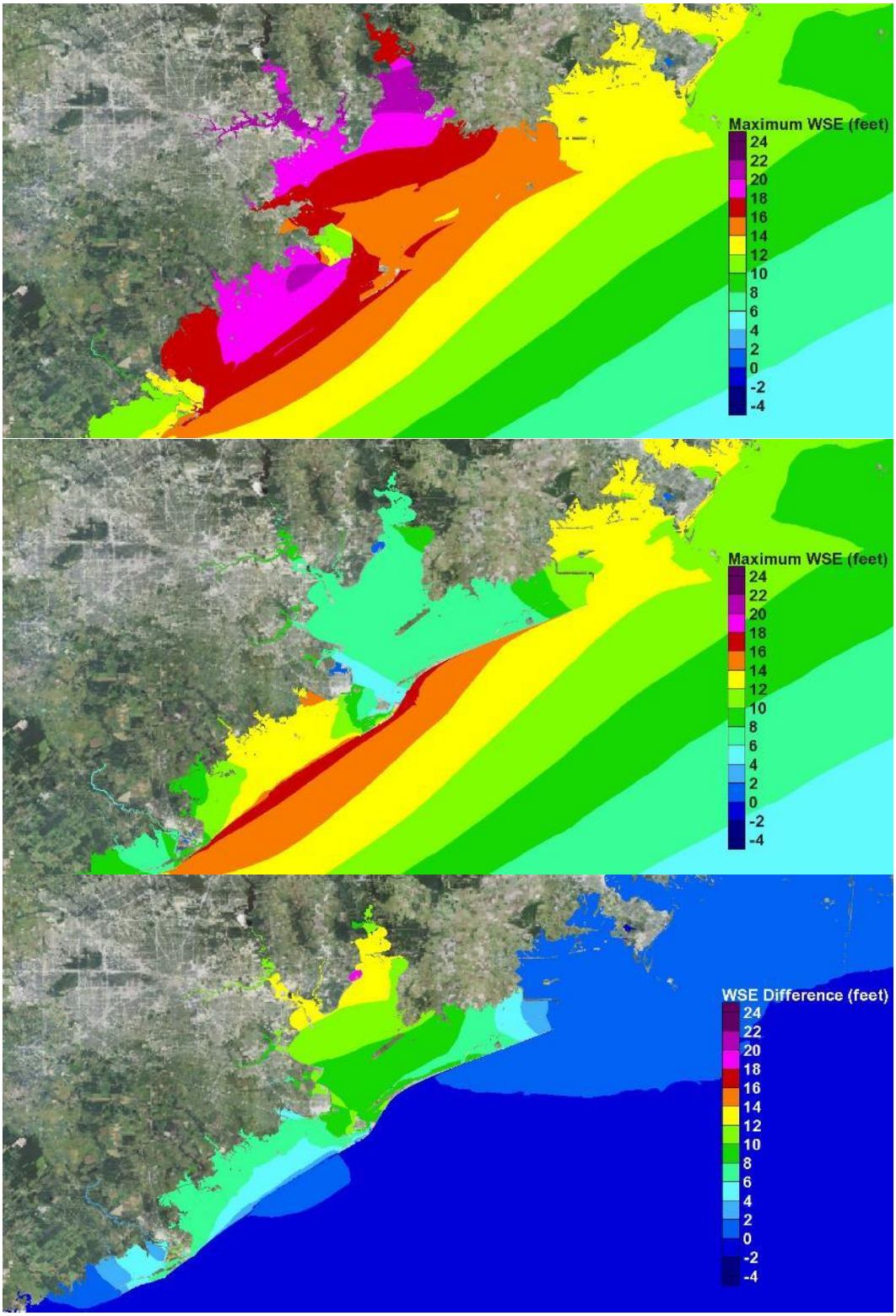

Figure 75. Maximum water surface elevation maps for storm 077. Existing conditions (top); With-dike conditions (middle); Difference in maximum water surface elevation (bottom)

Table 9. Summary of Maximum Storm Surge Conditions for Storm 077

Location	Existing Condition	With-Dike Condition	Changes
Galveston (Gulf side)	16 ft	16 to 16.5 ft	0 to 0.5 ft increase. Increase in overtopping expected.
Galveston (Bay side)	16 ft	6 to 10 ft	Reduction of 6 to 10 ft
Rest of Galveston Island	16.5 to 17 ft	10 to 16 ft	Overtopping/overflow of the dike. Reduction of 4 to 6 ft.
Bolivar Peninsula	13 to 16 ft	6 to 8 ft	Reduction of 6 to 9 ft
Texas City area	16 to 22 ft	7 to 13 ft	Reduction of 8 to 11 ft. Prevented interior flooding.
Clear Lake Area	17 to 19 ft	7 ft	Reduction of 10 to 12 ft
Bayport Area	19 ft	7 ft	Reduction of 12 to 12.5 ft
Upper reaches of Houston Ship Channel	21 to 22 ft	9 to 10 ft	Reduction of 11 to 12 ft

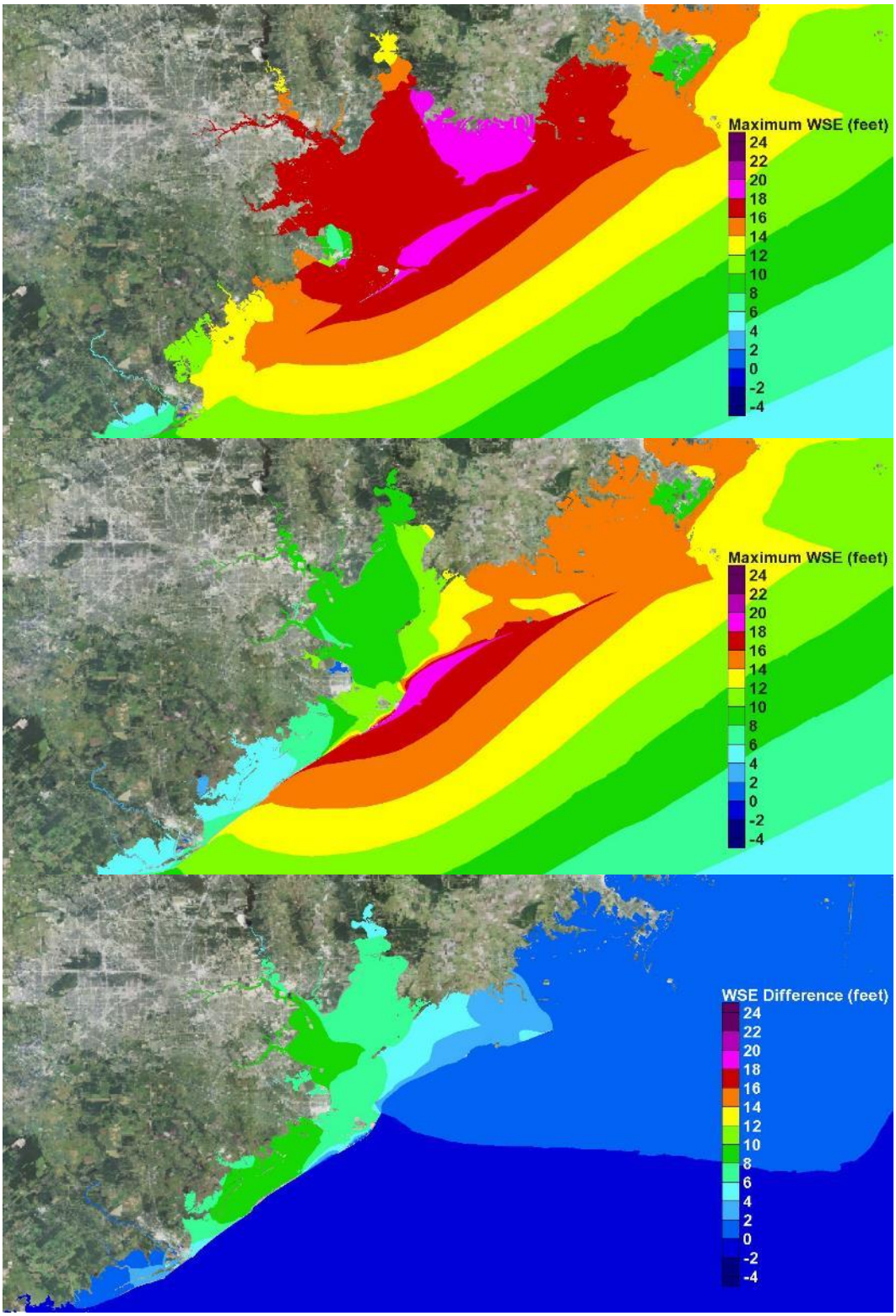

Figure 76. Maximum water surface elevation maps for storm 136. Existing conditions (top); With-dike conditions (middle); Difference in maximum water surface elevation (bottom)

Table 10. Summary of Maximum Storm Surge Conditions for Storm 136

Location	Existing Condition	With-Dike Condition	Changes
Galveston (Gulf side)	18 ft	18 to 19.5 ft	0 to 1.5 ft increase. Increase in overtopping and overflow is expected.
Galveston (Bay side)	18 ft	12 ft	Reduction of 6 ft
Rest of Galveston Island	12 to 17 ft, increasing from west to east	5 to 10 ft	Some overtopping and overflow of the dike. Reduction of 7 to10 ft.
Bolivar Peninsula	16 to 19 ft	12 to 17 ft	Overtopping/overflow of the dike. Reduction of 3 to 4 ft
Texas City area	18 to 19 ft	9 to 10 ft	Reduction of 8 to 9 ft. Significantly reduced interior flooding.
Clear Lake Area	17 ft	7.5 to 9 ft	Reduction of 8 to 9 ft
Bayport Area	18 ft	10 ft	Reduction of 8 to 9 ft
Upper reaches of Houston Ship Channel	17 to 18 ft	10 ft	Reduction of 7 to 8 ft

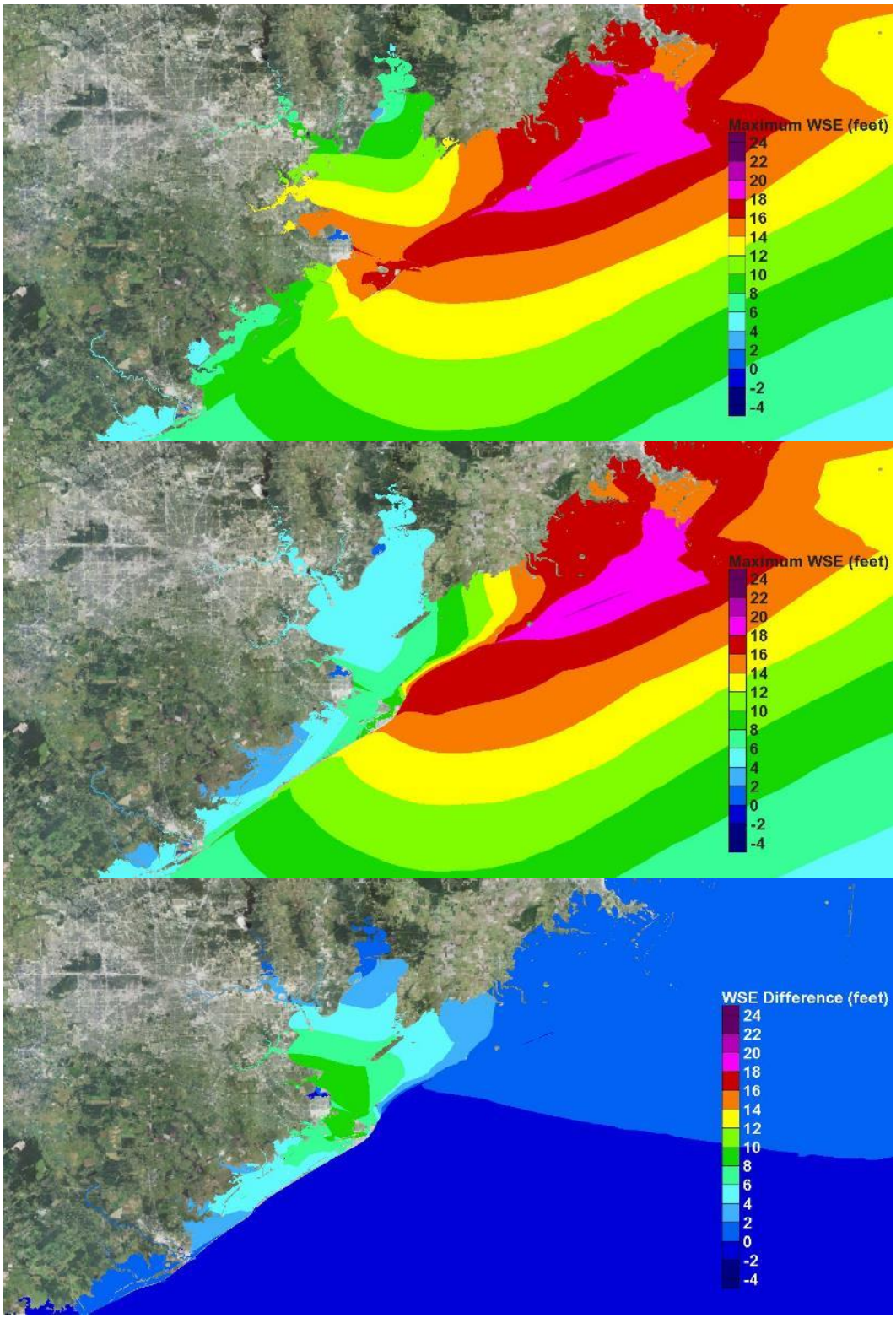

Figure 77. Maximum water surface elevation maps for storm 081. Existing conditions (top); With-dike conditions (middle); Difference in maximum water surface elevation (bottom)

Table 11. Summary of Maximum Storm Surge Conditions for Storm 081

Location	Existing Condition	With-Dike Condition	Changes
Galveston (Gulf side)	13 to 16 ft	13 to 16 ft	No change
Galveston (Bay side)	14 to 16 ft	8 ft	Reduction of 6 to 8 ft
Rest of Galveston Island	8 to 13 ft, increasing from west to east	5 to 6 ft	Reduction of 3 to 7 ft.
Bolivar Peninsula	17 to 19 ft	12 to 18 ft	Overtopping/overflow of the dike. Reduction of 1 to 4 ft
Texas City area	11 to 16 ft	6 to 8 ft	Reduction of 7 to 10 ft.
Clear Lake Area	12 to 14 ft	5 to 6 ft	Reduction of 6.5 to 8.5 ft
Bayport Area	11 ft	5 to 6 ft	Reduction of 5 to 6 ft
Upper reaches of Houston Ship Channel	7 to 8 ft	4 to 5 ft	Reduction of 3 ft

Major Hurricanes Approaching from the South-Southeast

The following results are for the group of five North Texas storms that approach from the south-southeast. The influence of landfall position on maximum storm surge in Galveston Bay is again evident. Storms making landfall to the west of Bolivar Roads tended to produce larger surges in the region than storms making landfall very close to, or to the east of, Bolivar Roads. Storm 036 produces the maximum surge in the region, followed by Storm 027, Storm 142, Storm 144 and Storm 045, in order of decreasing maximum surge. Based solely on track, with other storm parameters being the same, Storm 142 would be expected to produce a larger surge in the region compared to Storm 027. Storms 027 and 142 have different radii to maximum winds. The radius for Storm 027 is 21.8 n mi; the radius for Storm 142 is 17.7 n mi. The forward speed for Storm 027 is 11 kts, whereas for storm 142 it is slower, 6 kts. Intensity and storm size are the two factors that tend to influence peak surge the most. Bunpapong et al (1985) also found that forward speed is important along the Texas coast; the faster the forward speed the greater the peak surge. The larger radius to maximum winds and the faster forward speed combine to create the larger surge for Storm 027 compared to the surge for Storm 142 which makes landfall closer to Bolivar Roads.

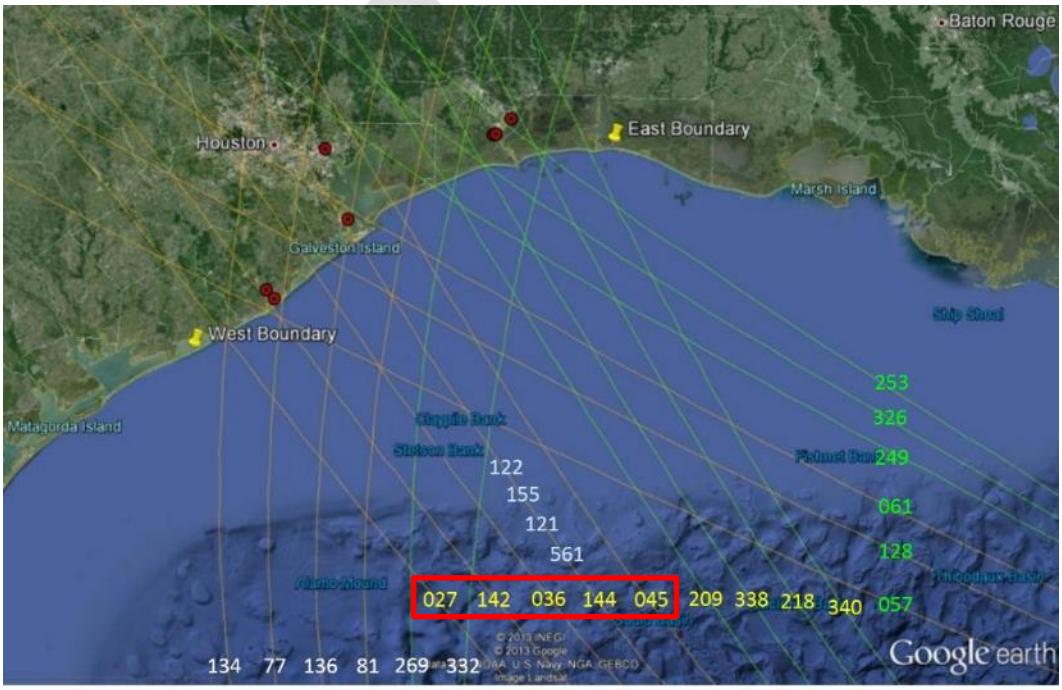

Figure 78. Group of hurricanes approaching from the south-southeast (storms 027, 142, 036, 144, 045)

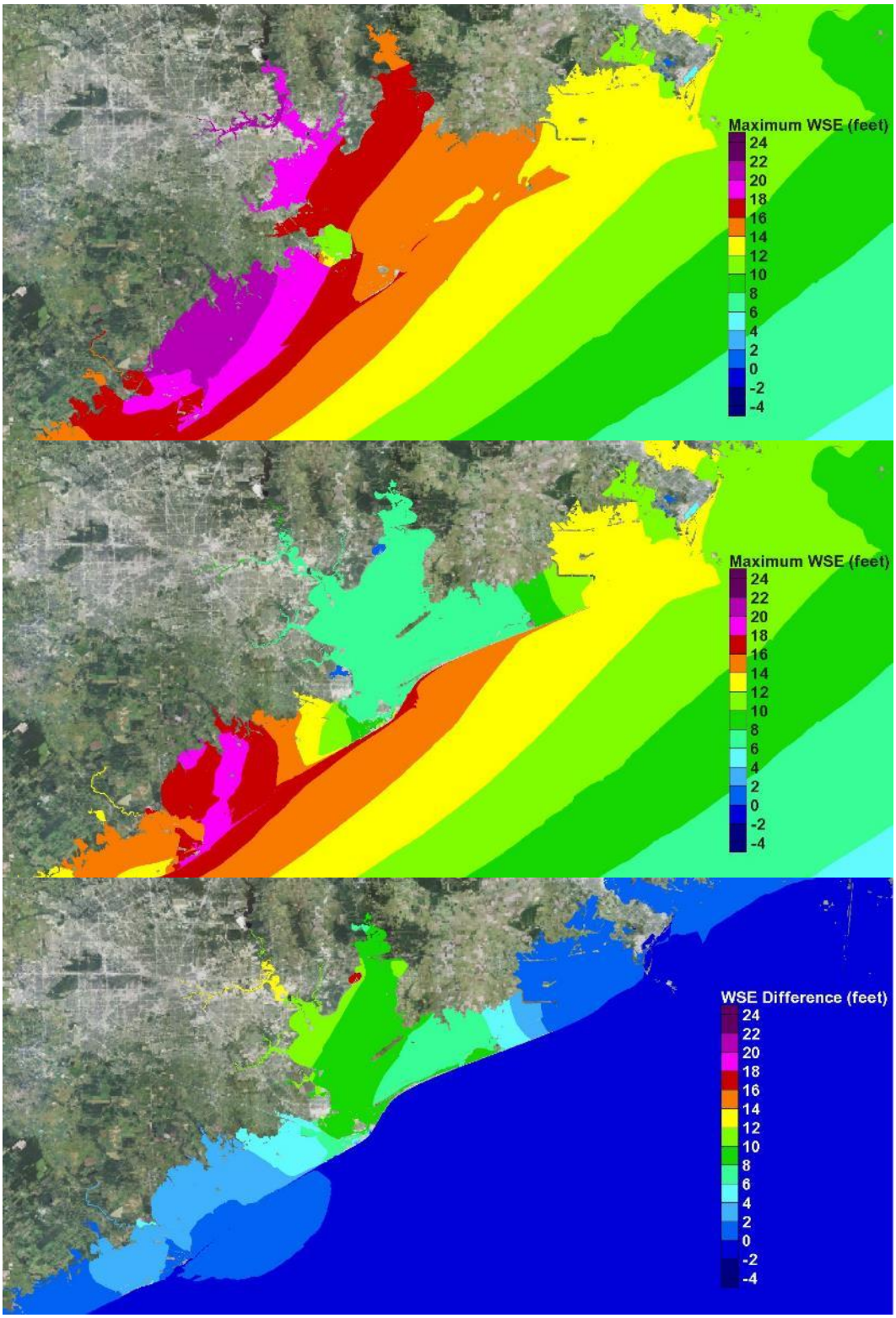

Figure 79. Maximum water surface elevation maps for storm 027. Existing conditions (top); With-dike conditions (middle); Difference in maximum water surface elevation (bottom)

Table 12. Summary of Maximum Storm Surge Conditions for Storm 027

Location	Existing Condition	With-Dike Condition	Changes
Galveston (Gulf side)	16 ft	16 ft	No change
Galveston (Bay side)	15 to 16 ft	8 to 10 ft	Reduction of 7 to 8 ft
Rest of Galveston Island	16 to 18.5 ft, decreasing from west to east	12 to 18.5 ft	Overtopping/overflow of the dike. Reduction of 1 to 6 ft.
Bolivar Peninsula	13 to 16 ft	7 to 10 ft	Reduction of 6 to 8 ft
Texas City area	15 to 19 ft	7 to 13 ft	Reduction of 5 to 10 ft. Eliminated interior flooding.
Clear Lake Area	18 to 19 ft	7 ft	Reduction of 11 to 12 ft
Bayport Area	19 ft	7 ft	Reduction of 12 ft
Upper reaches of Houston Ship Channel	21 ft	7 ft	Reduction of 13 to 14 ft

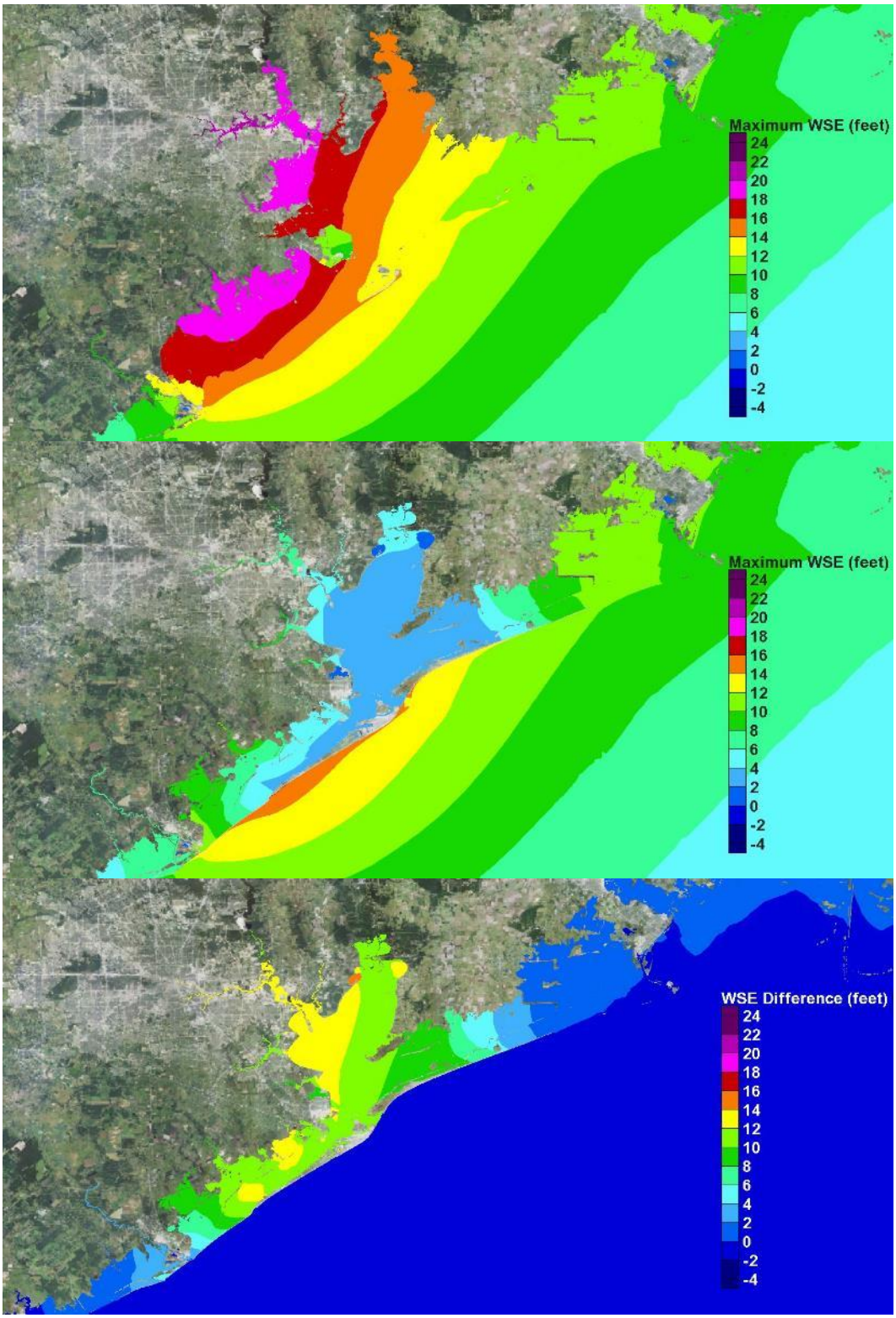

Figure 80. Maximum water surface elevation maps for storm 142. Existing conditions (top); With-dike conditions (middle); Difference in maximum water surface elevation (bottom)

Table 13. Summary of Maximum Storm Surge Conditions for Storm 142

Location	Existing Condition	With-Dike Condition	Changes
Galveston (Gulf side)	14 ft	14 ft	No change
Galveston (Bay side)	13 to 14 ft	3 ft	Reduction of 10 to 11 ft
Rest of Galveston Island	14 ft	3 to 6 ft	Reduction of 10 to 12 ft.
Bolivar Peninsula	11 to 13 ft	3 to 8 ft	Reduction of 5 to 10 ft
Texas City area	15.5 to 17.5 ft	4 to 5 ft	Reduction of 11 to 12 ft. Eliminated interior flooding.
Clear Lake Area	18 to 19 ft	6 ft	Reduction of 12 to 13 ft
Bayport Area	19 ft	5ft	Reduction of 13 to 14 ft
Upper reaches of Houston Ship Channel	20-21 ft	7 ft	Reduction of 13 to 14 ft

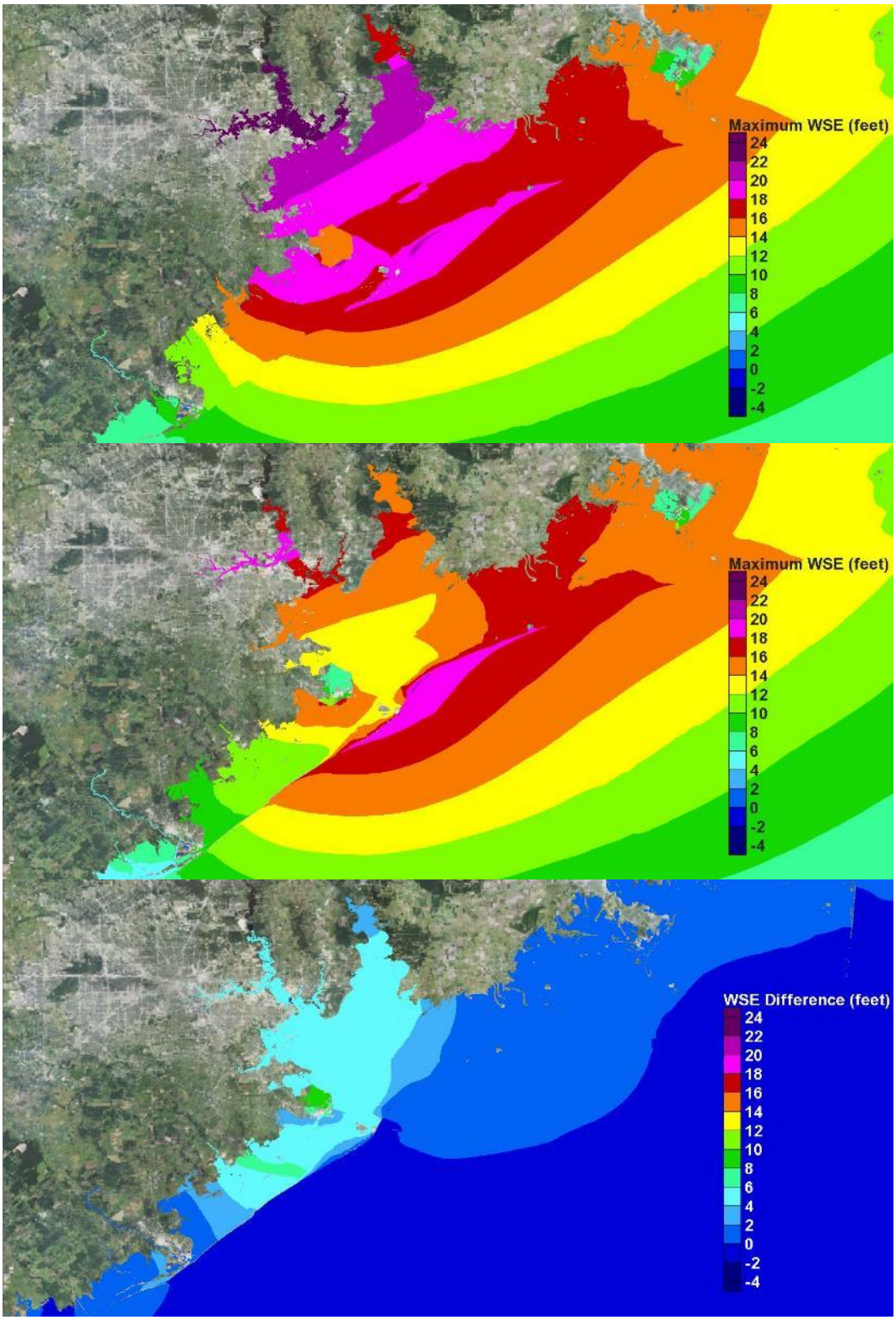

Figure 81. Maximum water surface elevation maps for storm 036. Existing conditions (top); With-dike conditions (middle); Difference in maximum water surface elevation (bottom)

Table 14. Summary of Maximum Storm Surge Conditions for Storm 036

Location	Existing Condition	With-Dike Condition	Changes
Galveston (Gulf side)	18 to 19 ft	18 to 19 ft	No change. Overflow and overtopping of the seawall
Galveston (Bay side)	18 ft	13 to 15 ft	Reduction of 3 to 5 ft
Rest of Galveston Island	12 to 18 ft increasing from west to east	10 to 17 ft	Some overflow and overtopping of the dike. Reduction of 2 to 6 ft.
Bolivar Peninsula	18 to 20 ft	14 to 17 ft	Overflow and overtopping of the dike. Reduction of 1 to 4 ft
Texas City area	18 to 20 ft	13 to 16 ft	Reduction of 4 to 5 ft. Reduced interior flooding.
Clear Lake Area	19 ft	14 to 15 ft	Reduction of 4 to 5 ft
Bayport Area	21 ft	15ft	Reduction of 4 to 5 ft
Upper reaches of Houston Ship Channel	24-25 ft	19 to 20 ft	Reduction of 5 ft

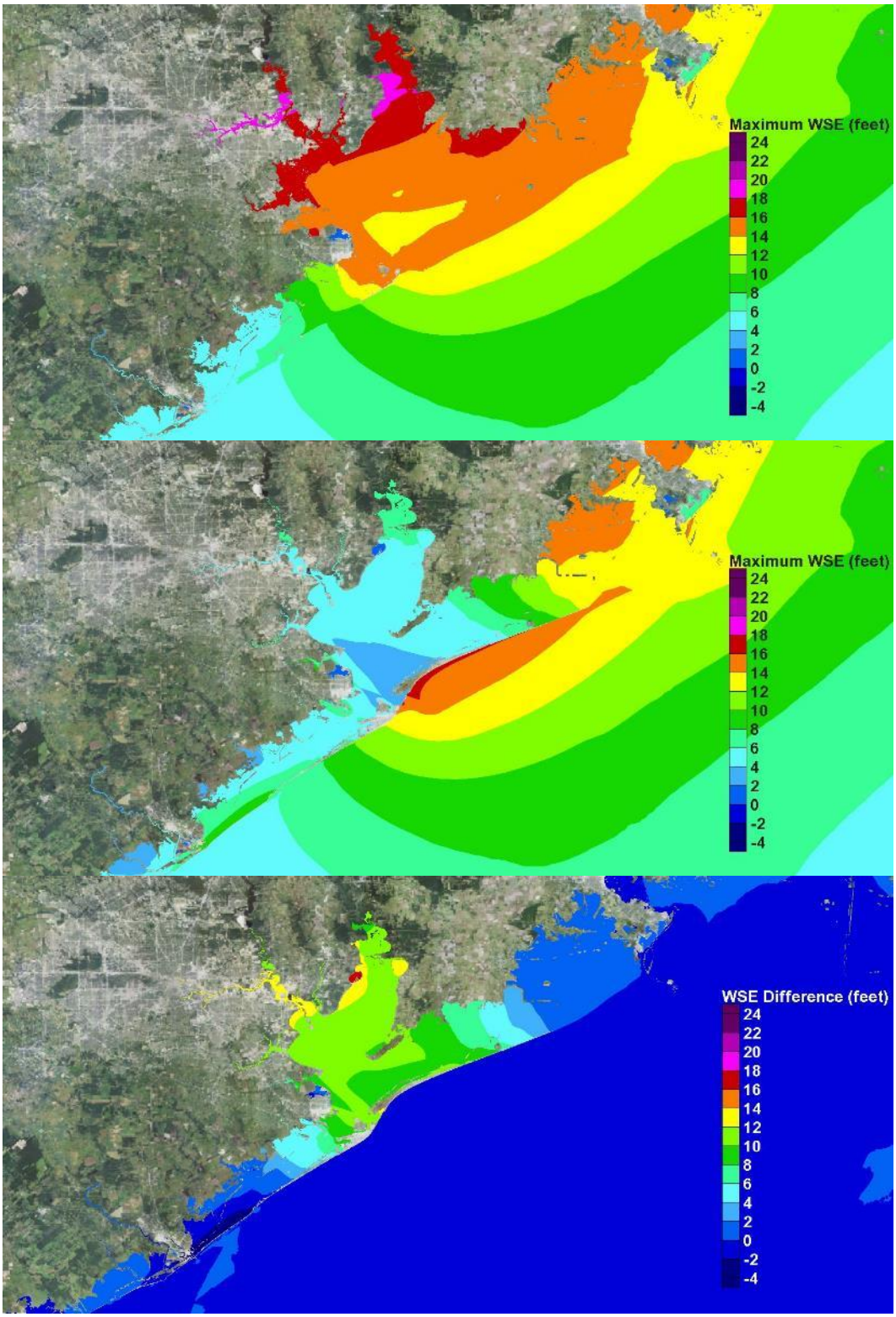

Figure 82. Maximum water surface elevation maps for storm 144. Existing conditions (top); With-dike conditions (middle); Difference in maximum water surface elevation (bottom)

Table 15. Summary of Maximum Storm Surge Conditions for Storm 144

Location	Existing Condition	With-Dike Condition	Changes
Galveston (Gulf side)	11 to 14 ft	11 to 14 ft	No change.
Galveston (Bay side)	13 to 14.5 ft	4 to 5 ft	Reduction of 8 to 11 ft
Rest of Galveston Island	5 to 11 ft increasing from west to east	5 to 8 ft	Reduction of 0 to 7 ft on the east; increase of 2 to 3 ft on the west.
Bolivar Peninsula	14 to 15.5 ft	3 to 12 ft	Increase of 0 to 0.5 ft at the dike. Reduction of 4 to 10 ft
Texas City area	11 to 15 ft	5 to 6.5 ft	Reduction of 6 to 9 ft
Clear Lake Area	16 to 16.5 ft	4 to 5 ft	Reduction of 11 ft
Bayport Area	16.5 to 17 ft	5ft	Reduction of 11.5 to 12 ft
Upper reaches of Houston Ship Channel	18 to 19 ft	6 ft	Reduction of 12 to 13 ft

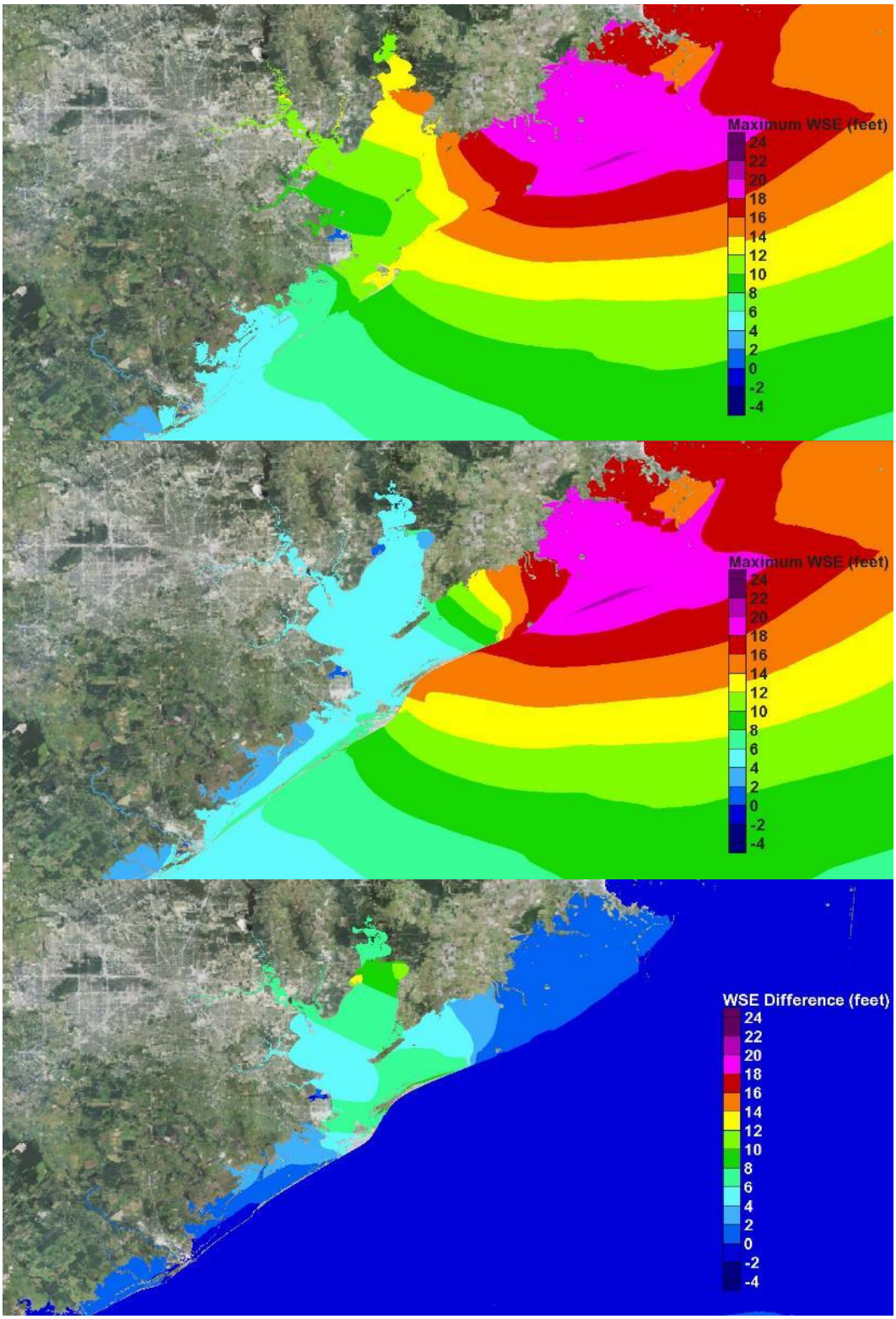

Figure 83. Maximum water surface elevation maps for storm 045. Existing conditions (top); With-dike conditions (middle); Difference in maximum water surface elevation (bottom)

Table 16. Summary of Maximum Storm Surge Conditions for Storm 045

Location	Existing Condition	With-Dike Condition	Changes
Galveston (Gulf side)	9 to 12 ft	9 to 12 ft	No change.
Galveston (Bay side)	11 to 12 ft	5 to 7 ft	Reduction of 5 to 6 ft
Rest of Galveston Island	5 to 8 ft increasing from west to east	5 to 6 ft	Reduction of 0 to 4 ft on the east. Increase of 0 to 1 ft on the west.
Bolivar Peninsula	13 to 18.5 ft	4 to 18.5 ft	Increase of 0.5 to 1 ft at the dike. Overflow and overtopping of the dike. Reduction of 0 to 7 ft
Texas City area	8 to 11 ft	4 ft	Reduction of 4 to 7 ft
Clear Lake Area	9 ft	4 ft	Reduction of 5.5 ft
Bayport Area	10.5 ft	4.5 ft	Reduction of 6 ft
Upper reaches of Houston Ship Channel	11 to 11.5 ft	5 ft	Reduction of 6 to 6.5 ft

Major Hurricanes Approaching from the Southeast

The following results are for the group of three North Texas storms that approach from the southeast. Storm 057 produces the greater surge in the region, followed closely by Storm 128 and Storm 061, in order of decreasing maximum surges. The peak surges for Storms 057 and 128 are similar. Storm 057 makes landfall to the west of San Luis Pass, Storm 128 to the east of San Luis Pass, both approximately equidistant from the pass. Storm 061 makes landfall at Bolivar Roads. Storm 057 has a radius to maximum winds that is lightly larger (18.4 n mi) than the radius for Storm 128 (17.7 n mi), which contribute to its slightly greater surge in the Bay.

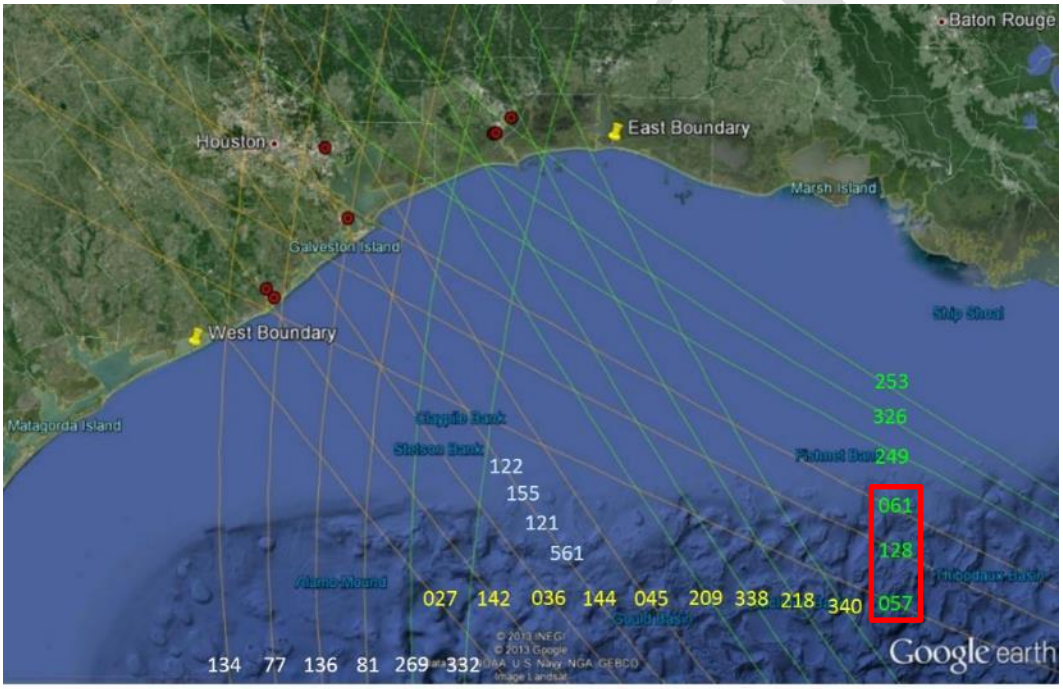

Figure 84. Group of hurricanes approaching from the southeast (storms 057, 128, 061)

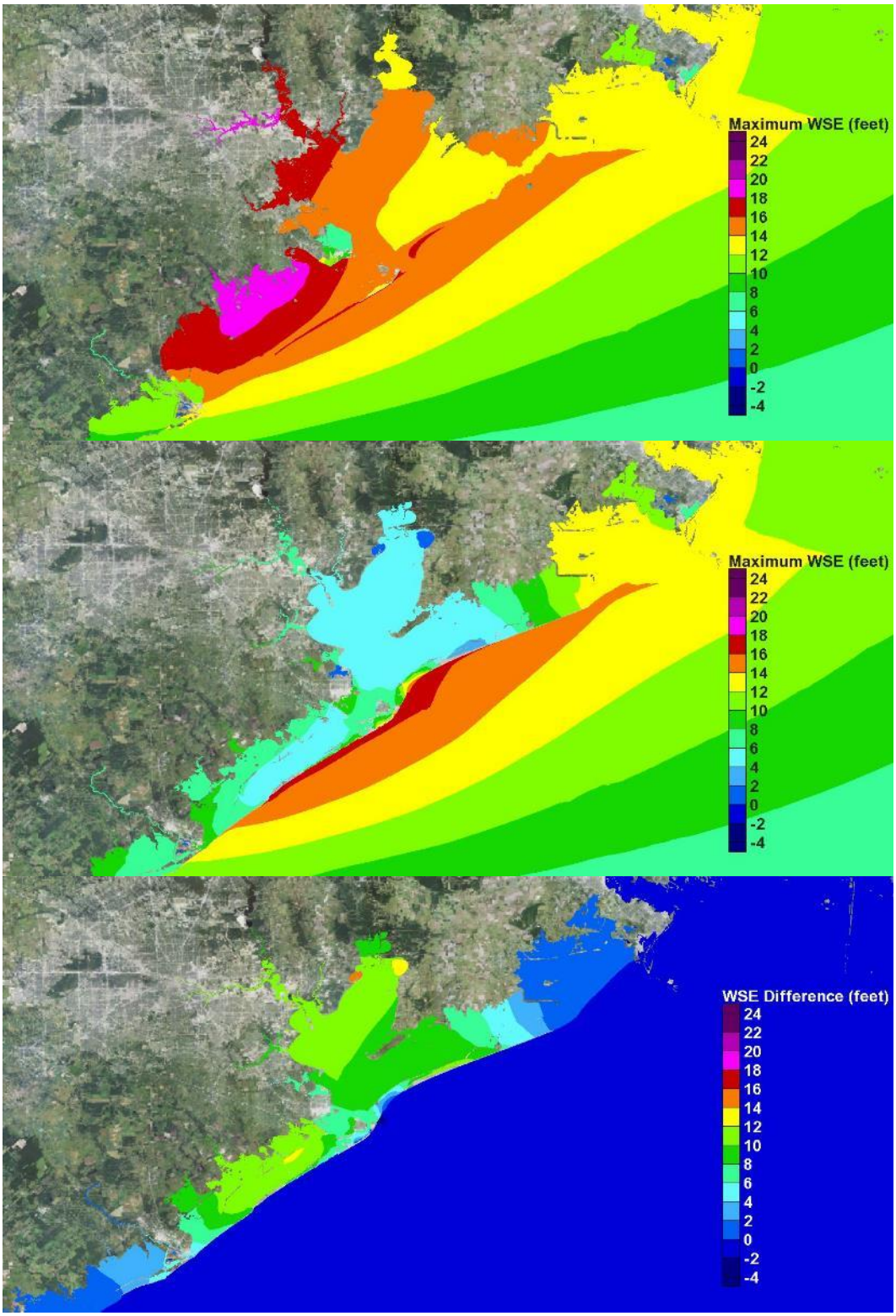

Figure 85. Maximum water surface elevation maps for storm 057. Existing conditions (top); With-dike conditions (middle); Difference in maximum water surface elevation (bottom)

Table 17. Summary of Maximum Storm Surge Conditions for Storm 057

Location	Existing Condition	With-Dike Condition	Changes
Galveston (Gulf side)	16 ft	16.5 ft	Increase of 0 to 0.5 ft. Increase in overtopping of the seawall expected.
Galveston (Bay side)	14 to 15 ft	6 to 7 ft	Reduction of 7 to 8 ft
Rest of Galveston Island	15.5 to 16 ft	5 to 6.5 ft	Reduction of 8 to 11 ft
Bolivar Peninsula	14.5 to 16 ft	6 to 13 ft	Increase of 0.5 to 1 ft at the dike on west end. Overflow and overtopping of the dike. Reduction of 2 to 8 ft
Texas City area	15 to 17.5 ft	7 to 8.5 ft	Reduction of 7 to 9 ft. Eliminates interior flooding.
Clear Lake Area	16.5 ft	6 ft	Reduction of 10.5 ft
Bayport Area	17 ft	6 ft	Reduction of 11 ft
Upper reaches of Houston Ship Channel	18 to 19 ft	6 to 7 ft	Reduction of 11.5 ft

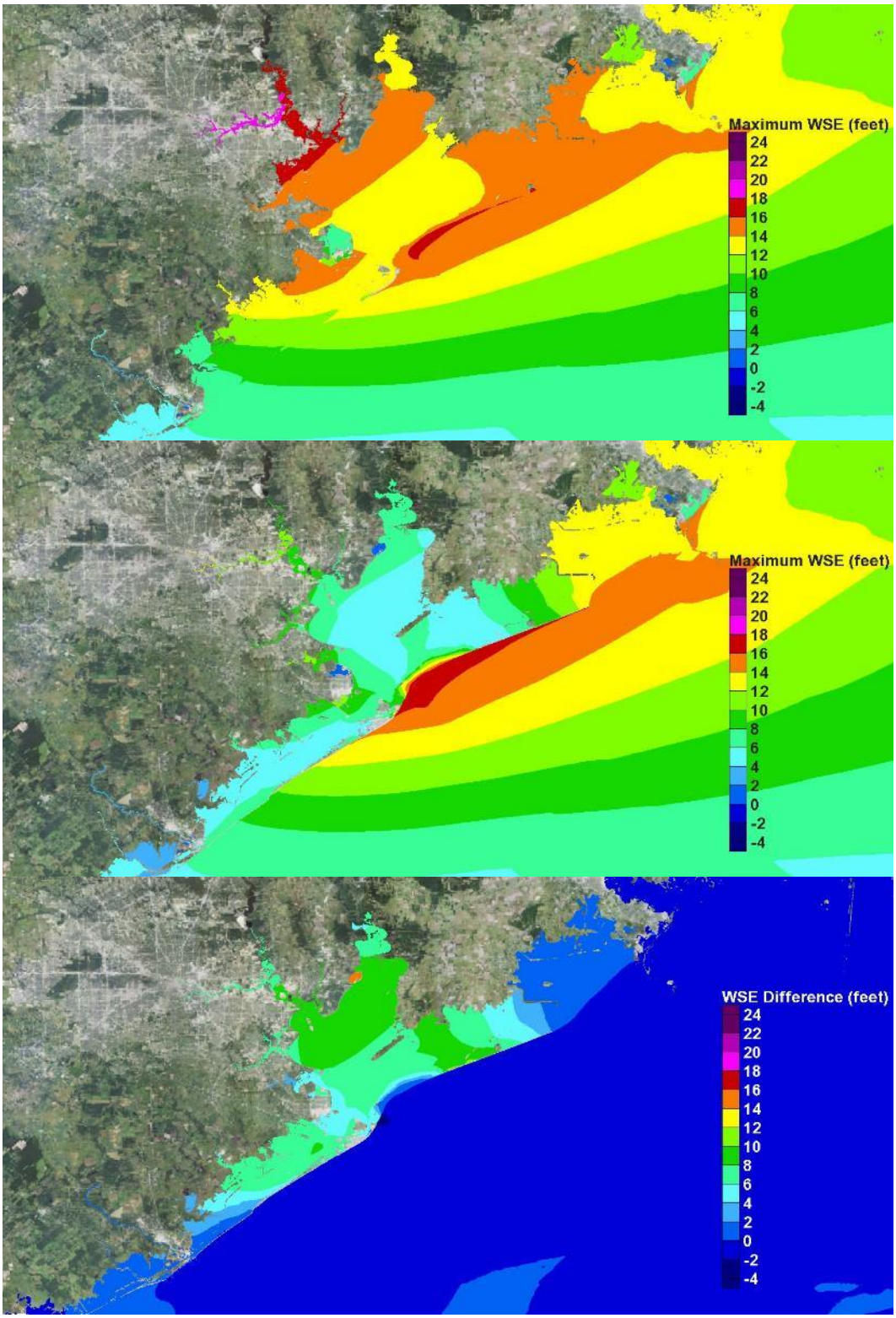

Figure 86. Maximum water surface elevation maps for storm 128. Existing conditions (top); With-dike conditions (middle); Difference in maximum water surface elevation (bottom)

Table 18. Summary of Maximum Storm Surge Conditions for Storm 128

Location	Existing Condition	With-Dike Condition	Changes
Galveston (Gulf side)	14 to 14.5 ft	14 to 16.5 ft	Increase of 0 to 2 ft. Increase in overtopping of the seawall expected.
Galveston (Bay side)	13.5 to 14 ft	7 to 12 ft	Reduction of 4 to 7 ft
Rest of Galveston Island	8 to 13.5 ft, increasing from west to east	6 to 7 ft	Reduction of 1 to 7 ft
Bolivar Peninsula	15 to 16.5 ft	6 to 13 ft	Increase of 1 ft at the dike. Overflow and overtopping of the dike. Reduction of 2 to 10 ft
Texas City area	13 to 15.5 ft	7 to 9 ft	Reduction of 6 to 7 ft. Eliminates interior flooding.
Clear Lake Area	15 to 16 ft	7 to 7.5 ft	Reduction of 7.5 to 8 ft
Bayport Area	16 ft	7 ft	Reduction of 8 ft
Upper reaches of Houston Ship Channel	18 to 19 ft	10 to 11 ft	Reduction of 8 ft

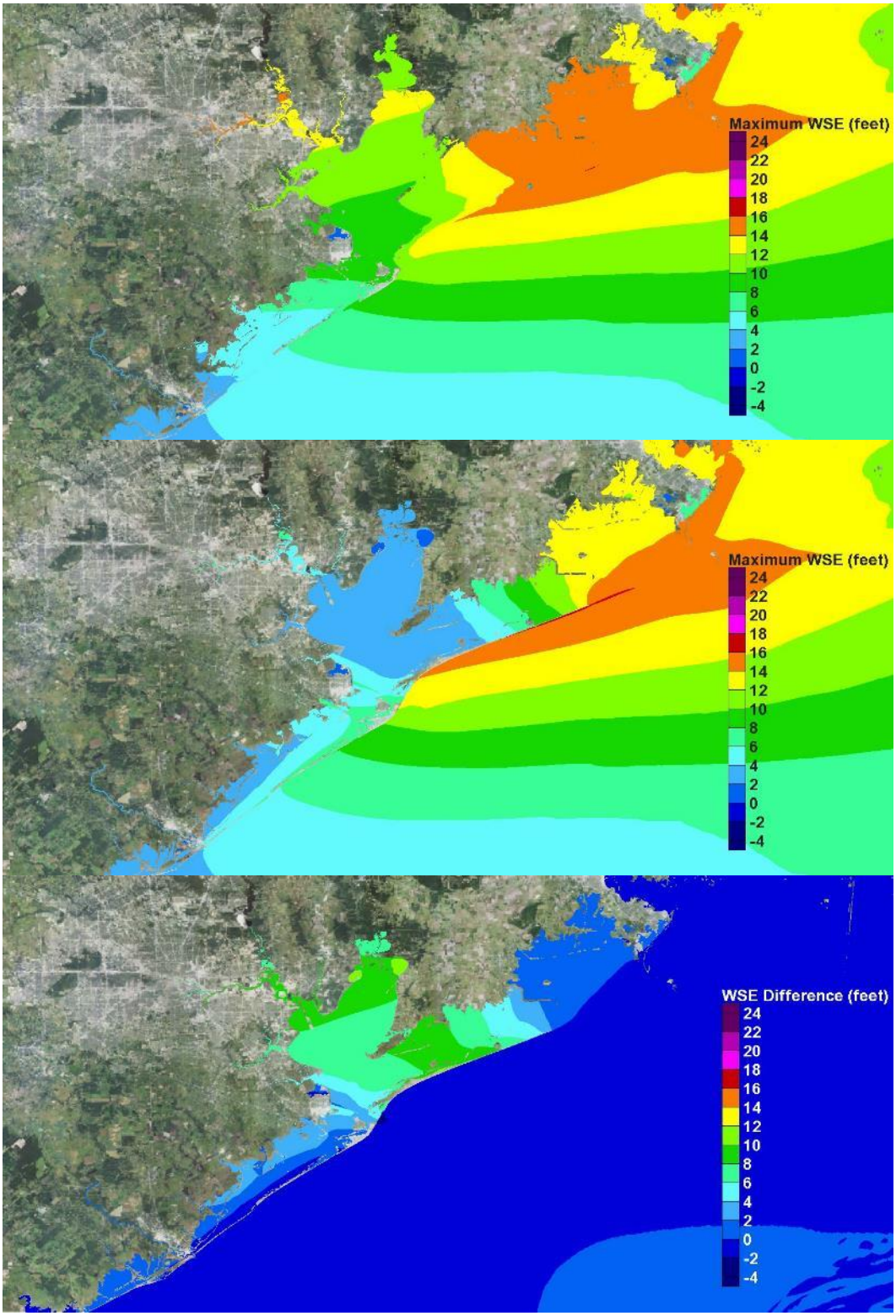

Figure 87. Maximum water surface elevation maps for storm 061. Existing conditions (top); With-dike conditions (middle); Difference in maximum water surface elevation (bottom)

Table 19. Summary of Maximum Storm Surge Conditions for Storm 061

Location	Existing Condition	With-Dike Condition	Changes
Galveston (Gulf side)	8 to 11 ft	9 to 12 ft	Increase of 1 ft
Galveston (Bay side)	8 to 10 ft	6 to 7 ft	Reduction of 2 to 4 ft
Rest of Galveston Island	4 to 7 ft	4 to 7 ft	Increase of 0 to 0.5 ft
Bolivar Peninsula	14 to 16 ft	3 to 10 ft	Reduction of 4 to 9 ft
Texas City area	8.5 to 9.5 ft	6 to 7 ft	Reduction of 2 to 4 ft
Clear Lake Area	10 to 11 ft	3 ft	Reduction of 7 to 8 ft
Bayport Area	11 to 11.5 ft	3 ft	Reduction of 8 to 8.5 ft
Upper reaches of Houston Ship Channel	14 ft	6 ft	Reduction of 8 ft

9 Placing Hurricane-Induced Water Levels in a Probabilistic Context

Introduction

The 25-storm bracketing set of tropical cyclones (TCs) was mostly comprised of very severe hurricanes having extremely low minimum central pressures of 900 mb and different land-falling tracks. Hurricanes that have a central pressure of 900 mb and make landfall in the Houston-Galveston region, like many of the bracketing set of storms, are exceedingly rare events. The Houston-Galveston region has not experienced a 900-mb hurricane in the most recent 140 years; however, the possibility exists that such a severe hurricane can directly impact the region. The probability of peak storm surge produced by such an occurrence is of great interest, with and without the proposed Ike Dike.

A few less intense storms also were considered in the bracketing storm set, having minimum central pressures of 930-, 960-, and 975-mb, all on a single direct-hit track. The 1900 Galveston Hurricane had a central pressure of 936 mb at landfall. Hurricane Ike had a central pressure of 950 mb at landfall. Both of these storms directly and adversely impacted the Houston-Galveston area. The probabilities of peak surge that produced these types of less intense, but more likely, events also is of great interest.

The Ike Dike concept reduced storm surge throughout Galveston Bay for all the bracketing-set TCs, including the very severe 900-mb storms. The dike showed considerable reduction in storm surge for the 930-mb storms and even more reduction for the less intense 960 and 975-mb storms, all of which have a much greater probability of occurrence compared to 900-mb storms. However, several of the 900-mb TCs, and the 930-mb direct hit storm, produced very high storm surge which overtopped the proposed Ike Dike at various locations. These extreme storms still produced substantial surge and inundation within Galveston Bay as a result of both overtopping and the effect of strong winds within the Bay. It is important to determine the frequency of occurrence of water levels for these types of rare TCs as well as the more likely storms. A full probabilistic approach is

essential for accurately determining the risk of both flooding and damage/losses associated with TCs for the existing condition and for determining the reduction in risk associated with the Ike Dike concept.

An initial approach, which is informative, relatively simple and much less resource intensive than a full probabilistic approach, was taken to gain insight on the inundation and damage/losses prevented by the dike in a probabilistic context. Although simple and not rigorous from a probability and statistics perspective, it sheds some initial light for TCs that produce water levels having certain frequencies of occurrence. This approach is based on the idea of a proxy storm, in which a single storm is selected to best represent a certain annual exceedance probability (AEP), or alternatively the average recurrence interval (ARI), water surface elevation throughout the corridor of greatest potential economic damage/loss. This corridor encompasses the City of Galveston, follows the western shoreline of Galveston Bay including Texas City and the Clear Lake area, and extends into the upper reaches of the Houston Ship Channel. The process for selecting proxy storms and results from the proxy storm analysis are presented later in this chapter.

A final approach will involve simulation of a large set of TCs for both existing conditions and with Ike Dike conditions, to assess risk of flooding and economic damages, without and with the proposed project.

Approach for Statistical Analysis of Water Surface Elevation

To provide a basis for proxy storm selection and to fully and accurately characterize the probability of extreme water surface elevations for existing conditions, a full joint probability analysis was conducted by the U.S. Army Engineer Research and Development Center (ERDC) using joint probability methods. The analysis produced water surface elevation statistics for a set of points, or save locations, in the Houston-Galveston region, including the key corridor for potential economic damage and losses, for existing conditions. The approach used by the ERDC differs slightly, in some aspects, from the approach used in the FEMA Region VI Risk Map study of the Texas coast (FEMA 2011). Differences in the joint probability analyses are noted later in this chapter.

Joint Probability Analysis

To quantify and estimate probabilities of hurricane-induced water levels, a probabilistic model of TCs was first built based on the historical storm climatology; and then the model was used to determine the probability of previously simulated synthetic tropical cyclones. For the present study, a new Joint Probability Analysis (JPA) was applied which takes advantage of more rigorous methods recently developed by the ERDC, which were applied to a recent study of the coastal storm hazard for the northeast United States, the North Atlantic Coast Comprehensive Study (Nadal-Caraballo, et al. 2015).

The present JPA model was built based on the historical storm climatology of tropical cyclones developed in the FEMA Region VI Risk MAP study (FEMA 2011). It also utilized high fidelity hydrodynamic modeling of TCs which was done as part of the Risk MAP study (FEMA 2011), in which the wind, pressure, surge and waves were modeled for each cyclone. The Risk MAP study included specification and modeling of 223 tropical cyclones for the northern Texas region, comprised of 152 high-intensity cyclones and 71 low-intensity cyclones. All hydrodynamic responses were stochastic because storms are random in both recurrence and intensity.

The statistical analysis of the storm surge responses of the 223 simulated TCs produced response statistics including average recurrence interval (ARI) water surface elevations. In addition, epistemic uncertainty was quantified and represented as confidence limits.

Joint Probability Method

Statistical analysis of water level response resulting from TCs in most cases suffers from a lack of historical observations, which results in a small sample size. Moreover, some of the characteristics of the TCs that impact a particular area may make it necessary to consider them as belonging to different populations, further reducing the sample sizes. Storm intensity has been identified as such a characteristic (Resio et al., 2007) since intense TCs tend to behave differently from weak ones.

The Joint Probability Method (JPM) overcomes this problem by focusing on the forcing instead of the response. In broad terms, TCs are defined by a number of forcing parameters which are used to generate the corresponding wind and pressure fields required for the simulation of

storm water level and waves. Therefore, the JPM has become the dominant probabilistic model used to assess the coastal storm hazard in hurricane-prone areas.

Although the details in the application of the JPM can vary significantly by study, the different approaches typically follow a common general methodology, depending on the dominant processes and respective solution strategies.

The JPM methodology generally includes the following steps:

- Characterization of historical storm climatology.
- Computation of historical spatially-varying storm recurrence rate (SSR).
- Storm parameterization and development of probability distributions of historical storm parameters.
- Discretization of probability distributions of storm parameters.
- Development of a synthetic storm set.
- Meteorological and hydrodynamic simulation of synthetic storms.
- Estimation of errors and other secondary terms.
- Integration of joint probability of storm responses (e.g., storm surge or waves)

The AEP of coastal storm hazards at a given site is a function of three main components: the storm recurrence rate (SRR), the joint probability of characteristic storm parameters, and the storm responses (e.g., water surface elevation in the present study).

The JPA of coastal storm hazards can be summarized by means of the JPM integral:

$$\lambda_{r(\hat{x})>r} = \lambda \int P[r(\hat{x}) + \varepsilon > r|\hat{x}, \varepsilon]\, f_{\hat{x}}(\hat{x}) f_{\varepsilon}(\varepsilon) d\hat{x} d\varepsilon \approx \sum_i^n \lambda_i\, P[r(\hat{x}) + \varepsilon > r|\hat{x}, \varepsilon] \quad (9\text{-}1)$$

where $\lambda_{r(\hat{x})>r}$ = AEP of storm response r due to forcing vector $\hat{x}$; ε = unbiased error or epsilon term; $P[r(\hat{x}) + \varepsilon > r|\hat{x}, \varepsilon]$ = conditional probability that storm i with parameters $\hat{x}_i$ generates a response larger than r. The storm parameters commonly used in a JPM for the characterization of TCs and included in the forcing vector $\hat{x}$ are: track location (x_0), heading direction (θ), central pressure deficit (Δp), radius of

maximum winds (R_{max}), and translational speed (V_t). Secondary parameters may include: epsilon, or error, term (ε); Holland B , which characterizes the peakedness or radial shape of the wind field; and astronomical tide.

In order to develop the set of synthetic storms, each parameter is treated as a correlated random variable and either a marginal or a conditional probability density function (PDF) is sought for each parameter based on the TCs observed in the historical record. The probability distributions are then discretized and the corresponding weights are assigned to the range of discrete values. Synthetic storms are developed as possible combinations of samples from the marginal or conditional distributions. Each synthetic storm must consist of a physically- and meteorologically-realistic combination of the aforementioned parameters. The parameterized TCs are used as inputs to the PBL wind/pressure model. This model is used as part of the JPM methodology to estimate the time-histories of the wind and pressure fields that drive high-fidelity storm surge and wave numerical hydrodynamic models such as ADCIRC and WAM/STWAVE, respectively.

A central issue surrounding application of the JPM is the number of storm parameters required to adequately represent TCs and their forcing. In current practice, it has been shown that the five parameters listed above are sufficient to characterize TCs and their wind and pressure fields for the purpose of quantifying coastal storm hazards. Sources of epistemic uncertainty often accounted for in the JPM include:

1. Hydrodynamic modeling errors potentially arising from unresolved physical processes, inadequate grid resolution, and bathymetry inaccuracy.
2. Meteorological modeling errors due to use of idealized wind and pressure fields, and wind variations not captured by the PBL model.
3. Track variations not captured in the synthetic storm set.
4. Random variations in the peakedness of the wind fields represented by the Holland B parameter.

The AEP of a particular storm hazard is computed by integration of Equation (9-1). Epistemic uncertainty is quantified and incorporated in the JPM as confidence limits (e.g., 84%, 90%, 95%, and 98% are considered in the present study).

Joint Probability Method with Optimal Sampling

Although the JPM approach has been implemented since the 1970s, recent advancements in sampling techniques and the development of the JPM with Optimal Sampling (JPM-OS) have made it possible to reduce the necessary number of synthetic storms, more efficiently characterizing the parameter and probability spaces. The main accomplishment of these new developments was the reduction in number of storms required for populating the parameter space, from thousands, or even tens of thousands, down to hundreds of storms. This reduction was accomplished by optimizing the sampling of the storm parameters (Resio et al. 2007; Toro 2008; Vickery and Blanton 2008).

Different implementations of the JPM-OS methodology emerged as a result of several studies done in the aftermath of Hurricane Katrina after 2005, which led to the proliferation of surge hazard studies that brought further improvements to the JPM. Different approaches include the JPM-OS by Bayesian Quadrature (JPM-OS-BQ), the JPM with augmented sampling by means of Response Surface (JPM-OS-RS), and other JPM applications that use hybrid optimal sampling techniques.

Of particular importance was the work done by the Interagency Performance Evaluation Taskforce (IPET 2009) in which JPM-OS methods were developed for the statistical analysis of water level extremes to evaluate the performance of the Southeast Louisiana hurricane surge reduction system. This study provided the basic framework for the storm surge and modeling approaches used in later works, including the Texas Risk MAP study (FEMA 2011). This effort, led by a team of USACE, FEMA, NOAA, and private sector and academic researchers, was documented in the IPET (2009) report.

Regional studies conducted after Hurricane Katrina that stood out included the Louisiana Coastal Protection and Restoration (LACPR) (USACE 2009a), the Mississippi Coastal Improvements Program (MSCIP) (USACE 2009b), the Mississippi Coastal Analysis Project (FEMA 2008a) and the Risk MAP Study for the Coastal Counties in Texas (FEMA 2011). The JPM-OS-RS approach was applied in the Texas Risk MAP study (FEMA 2011).

The JPM-OS-BQ was adopted as part of FEMA's National Flood Insurance Program Risk MAP program best practices, as documented in the

Operating Guidance No. 8-12 (FEMA 2012). The JPM-OS-BQ approach was adopted for the present analysis.

JPM-OS-BQ Implementation for the Present Study

Tropical Cyclone Data Sources

The first step in implementing a JPA is characterization of the historical storm climatology, TCs in this case. Characterization requires identification of a TC data source and selection of a period of record for which the analysis will be performed.

For TC s, the main data source was HURDAT2 (Landsea and Franklin, 2013). HURDAT2 is a product of NOAA's National Hurricane Center (NOAA-NHC) and consists of the reanalysis of all historical TCs recorded in the North Atlantic basin (i.e., North Atlantic Ocean, Gulf of Mexico, and the Caribbean Sea) from 1851 to the present. This same basic data source was used in the Texas Risk MAP study (FEMA 2011).

The JPA performed in this study focused on TCs with $\Delta p \geq 28$ hPa. The Δp were computed as the difference between a far-field atmospheric pressure of 1,013 hPa and central pressure (c_p). TCs of this intensity are expected to be classified, on average, as category 1 hurricanes based on the Saffir-Simpson hurricane wind scale (SSHWS), but generally fall within the tropical storm to category 2 range.

Period of Record

Prior to the selection of historical TCs, the specific period of record to be used for the JPA must be defined. The SRR and the marginal distributions of storm parameters are sensitive to the historical record length. The 1940s decade marked the dawn of modern aircraft reconnaissance missions to measure hurricane parameters, resulting in much more reliable estimates of storm characteristics, including frequency and intensity.

Prior to 1944, the main data sources were land stations and ship reports (Jarvinen et al. 1984). During this period it was typical for relatively weak storms to go undetected and for the intensity of strong storms to be underestimated. After 1944 and as a consequence of World War II, aerial reconnaissance led to increased data collection incidence and

measurement accuracy, including storm position, track, wind speed and pressure. The use of satellite imagery was introduced during the 1964 hurricane season (Neumann et al., 1985) and was considered one of the major advances in TC tracking (Jarvinen et al., 1984).

The high frequency of unsampled TCs prior to the 1940s has been well documented. Mann et al. (2007) estimated an undercount in the pre-aircraft reconnaissance era (1870–1943) ranging from 0.5 to 2.0 TC/yr, with a mean of 1.2 TC/yr. Landsea et al. (2010) discussed that the increase in reported TCs during the 1940s and until about 1960 had been interpreted as a result of climate change. This increase, however, is likely to be a consequence of improved observing and recording of short-lived TCs coinciding with the advent of aircraft reconnaissance and satellite imagery.

Worley et al. (2005) identified spikes in the number of unrecorded moderate to long-lived TCs during the 1910s and 1940s as due to reduced ship observations during World War I and World War II, respectively. Vecchi and Knutson (2011), after adjusting HURDAT data for unrecorded TCs, concluded that the mid-twentieth century was a high activity period that extended from the 1940s to the 1960s.

In recent flood hazard studies where the JPM-OS methodology has been used, the period of record that was considered started in the early 1940s (FEMA 2008a, 2012; Resio et al., 2007). For the present study, the period of record was 1940-2013. For the Texas Risk Map study (FEMA 2011), the period of record considered was 1940-2007.

Computation of Spatially-Varying Storm Recurrence Rate

A second step in conducting a JPA is computation of the historical spatially-varying storm recurrence rate (SSR) for the area of interest. Calculation of the SRR requires sampling of historic TC occurrences for the region. The computation method adopted in the present study is different from that used in the Texas Risk MAP study (FEMA 2011), and slightly different rates are calculated.

Efficient storm sampling from the historical record and statistical computation of the SRR can be achieved using several different approaches. In recent studies some of the approaches used to compute the spatial variation of SRR have included: area-crossing, line-crossing,

Gaussian Kernel Function (GKF), and other combined methods. Both area-crossing and line-crossing are examples of capture zone methods. In the area-crossing approach only storms passing through a particular area are counted in the computation of the SRR. The line-crossing approach usually consists of an idealized coastline, or a reference line representing a segment of coastline. Only storms making landfall along the chosen segment of coastline are captured and counted towards the computation of the SRR.

Capture zones can also be defined in other ways, such as a rectangular or circular window, or any other finite spatial region. In past studies, the standard had been to apply any of the capture zone methods in order to count the storms and to assign uniform weights to all captured storms. The main limitation of the capture zone approach is that, while all storms within the chosen capture zone are given uniform weights, storms outside this zone are given a weight of zero. The conundrum lies in establishing a capture zone large enough to reduce the uncertainty associated with sample size by capturing an adequate number of storms from which significant statistics can be derived, but small enough to balance the uncertainty associated with spatial variability and population heterogeneity.

The use of the Gaussian Kernel Function (GKF) method, developed by Chouinard and Liu (1997), can overcome the main limitations of capture zone approaches. The standard application of the GKF consists of establishing a grid of nodes where estimates of the SRR are sought. All storms within this gridded space can be counted at any given node, but the weight assigned to each storm decreases with increasing distance from storm to node. The distance-adjusted weights are computed using a Gaussian probability density function (PDF) with an optimal kernel size.

The GKF equations are as follows:

$$\lambda = \frac{1}{T}\sum_i^n w(d_i) \qquad (9\text{-}2)$$

$$w(d_i) = \frac{1}{\sqrt{2\pi}h_d} exp\left[-\frac{1}{2}\left(\frac{d_i}{h_d}\right)^2\right] \qquad (9\text{-}3)$$

where, λ = SRR in storms/yr/km; T = record length in (yr); $w(d_i)$ = distance-adjusted weights from the Gaussian PDF (km^{-1}); d_i = distance

from location of interest to a storm data point (km); h_d = optimal kernel size (km). Use of the GKF weights minimizes sample size uncertainty by taking full advantage of all available storm data, while significantly reducing the uncertainty associated with spatial variability and potentially heterogeneous populations.

Optimal Gaussian Kernel Size

For purposes of this study, the optimal kernel size was determined from a series of sensitivity analyses performed using all tropical cyclones in the HURDAT2 database with $\Delta p \geq 28$ hPa within the 1940–2013 period. For validation purposes, the SRR computed from the GKF were compared to the observed SRR estimated using the capture zone approach. The analysis consisted of first estimating the observed SRR using circular capture zones with radii ranging from 100 km to 500 km, and then computing the mean observed SRR corresponding to this range of radii; second, the squared error of the GKF results was computed from the difference between the mean observed SRR and GKF estimates using kernel sizes from 100 km to 500 km. For each cyclone, only track data points with $\Delta p \geq 28$ hPa were accounted for in this analysis.

Figure 9-1 shows the variation of SRR as a function of capture zone radius (blue curve), as well as the mean observed SRR (red line), for a coastal reference location in Galveston, Texas. The observed SRR for Galveston varied from roughly 4.5E-4 to 7.0E-4 storms/year/km, depending on the capture zone radius, and had a mean of 5.5E-4 storms/year/km.

The squared error of the difference between the GKF and the observed SRR for Galveston is presented in Figure 9-2. This difference decreases to almost zero for kernel sizes between 150 km and 200 km, and remains close to zero for the remaining of the evaluated kernel sizes (up to 500 km). While the optimal kernel size for the Galveston location evidently lies within the 150-200 km range, it reaches a plateau after roughly 250 km. For this study, an optimal kernel size of 200 km was adopted for the Galveston, TX and surrounding area.

This optimal kernel size is in agreement with the kernel size of 200 km selected in a FEMA study of coastal Mississippi (FEMA 2008a; Toro 2008). A 200-km kernel size was found to be optimal by Nadal-Caraballo et al. (2015) in the North Atlantic Coast Comprehensive Study.

The weights computed using the GKF with a kernel size of 200 km are illustrated in Figure 9-3. These weights are shown relative to the weight of a storm track point located right on the coastal reference line (CRL), (d_i = 0 km), or

$$\text{Relative weight} = \frac{w(d_i)}{w(d_i{=}0)} \tag{9-3}$$

Data from such a storm track point would have a relative weight of 1.0, whereas, a track point located at a distance 200 km away from the CRL would have a relative weight of 0.6. The weights decrease as distance from the CRL increases, based on the Gaussian pdf, until becoming negligible. The relative weight of track points located at 600 km and 850 km from the CRL, for example, will have relative weights of roughly 1.0E-2 and 1.0E-4, respectively.

For the present study, further analyses were performed to determine the SRR corresponding to both high intensity ($\Delta p \geq 48$ hPa) and low intensity (28 hPa $\leq \Delta p <$ 48 hPa) storms for the 1940-2013 period. The SRR of high intensity storms computed for locations in the Galveston region varied from 1.6E-4 to 2.2E-4 storms/year/km. For low intensity storms in the same area, the computed SRR ranges from 4.2E-4 to 5.1E-4 storms/year/km.

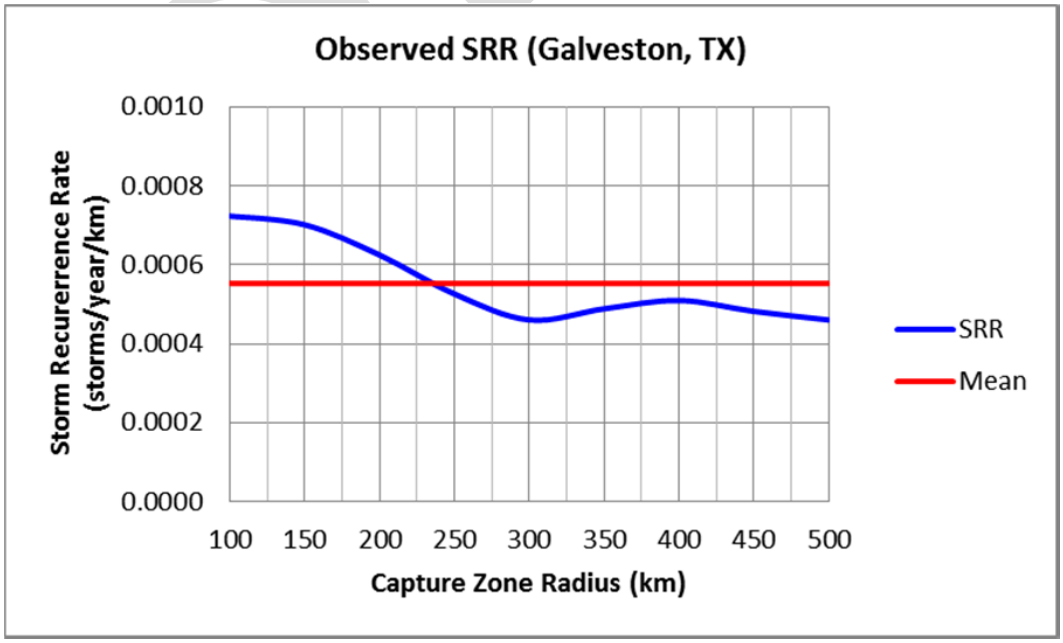

Figure 9-1. Observed SRR for Galveston, Texas.

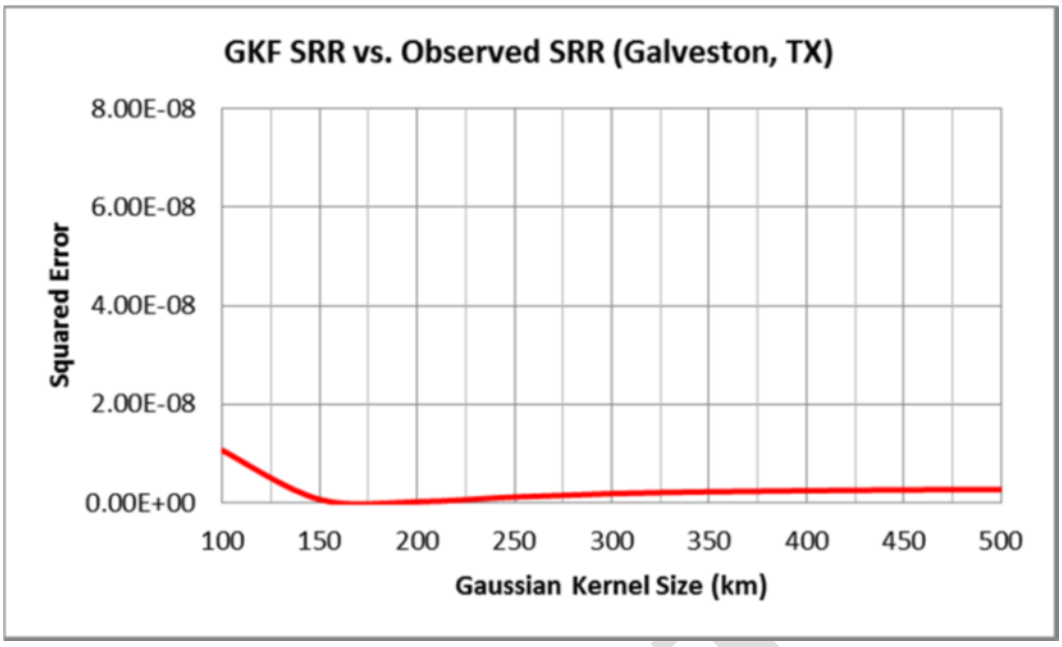

Figure 9-2. Comparison of GKF SRR vs. Mean Observed SRR for Galveston, Texas.

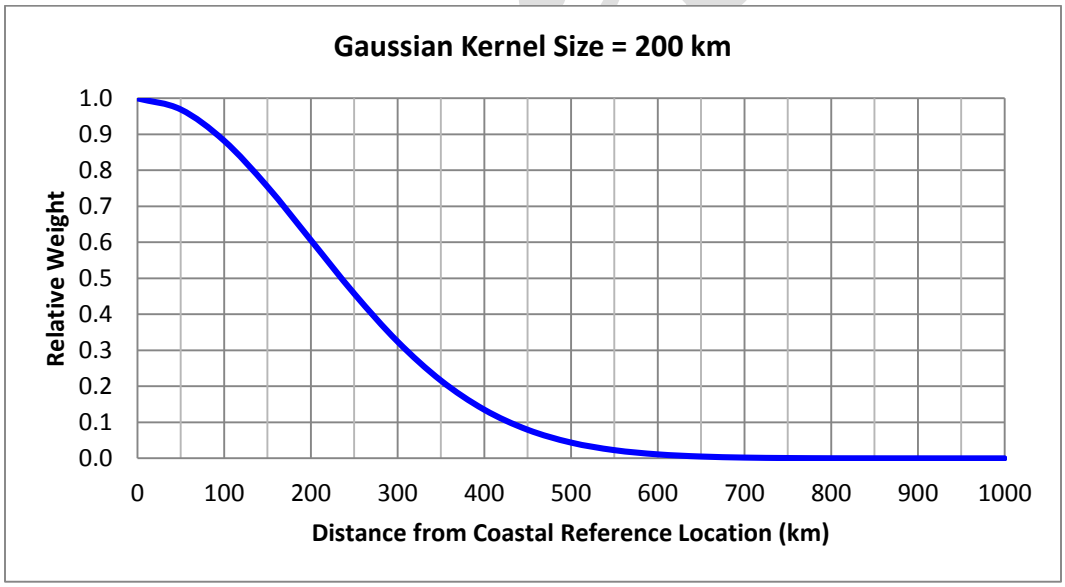

Figure 9-3. Relative weight of storm parameters as a function of distance from CRL.

The GKF SRR results corresponding to high intensity storms ($\Delta p \geq 48$ hPa) in the entire Atlantic basin for the 1940–2013 period are shown in Figure 9-4. SRR of low intensity storms (28 hPa $\leq \Delta p < 48$ hPa) for the same period are presented in Figure 9-5. The Δp values were determined based on a far-field pressure of 1,013 hPa. The SRR depicted in these figures is SRR_{200km}, with units of storms/yr, and represents the annual chance of a TC passing within 200 km.

Estimates of SRR from Other Studies

For comparison purposes, the SRR of high intensity storms in previous FEMA studies (Resio et al., 2007; FEMA, 2009a, 2009b; FEMA, 2011) for the Galveston area have been determined to be around 0.02 storms/year/deg, or roughly 2.0E-4 storms/year/km.

The SRR analyses in the present study were performed using the standard GKF method developed by Chouinard and Liu (1997) with an optimal kernel size of 200 km. However, in the Resio et al. (2007) work, the SRR was estimated using a hybrid method which employed a line-crossing approach to sample only landfalling storms, then using GKF weights with kernel size of 250 km for the actual computation of SRR. Figure 9-6 shows the coastal reference line that was used. The Resio et al. (2007) results are shown in Figure 9-7 with units of storms/year/deg.

In FEMA (2008a) and Toro 92008), another hybrid method was used that included a rectangular window capture zone. The results, which were based on a kernel size of 160 km, are illustrated in Figure 9-8 with units also in storms/year/deg.

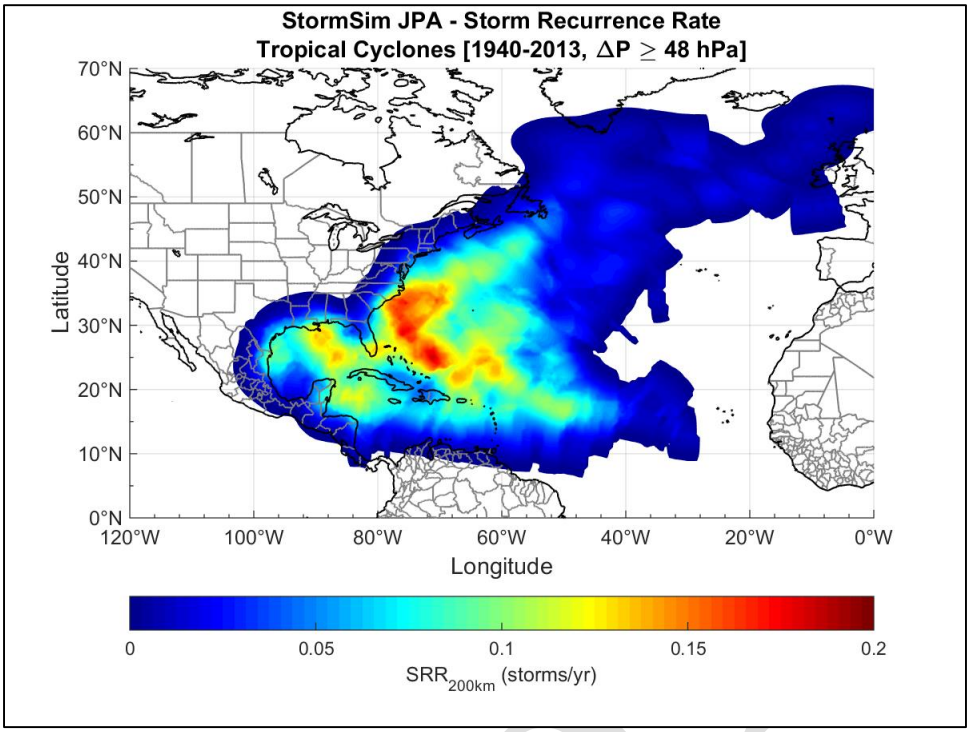

Figure 9-4. SRR for high intensity tropical cyclones recorded in the Atlantic basin from 1940–2013.

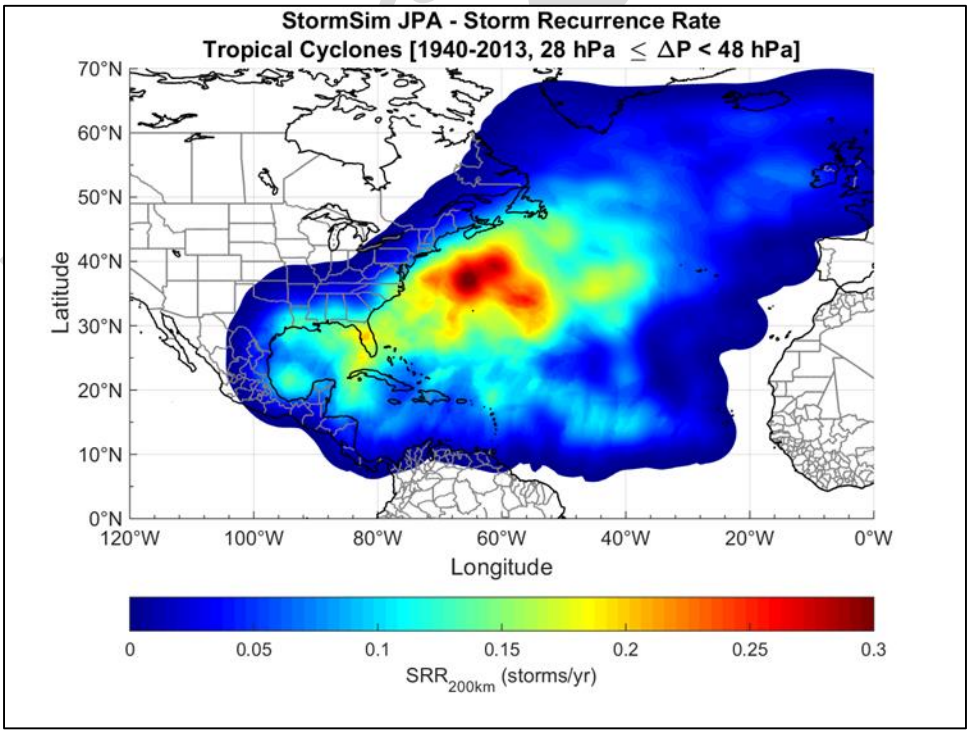

Figure 9-5. SRR for low intensity tropical cyclones recorded in the Atlantic basin from 1940–2013.

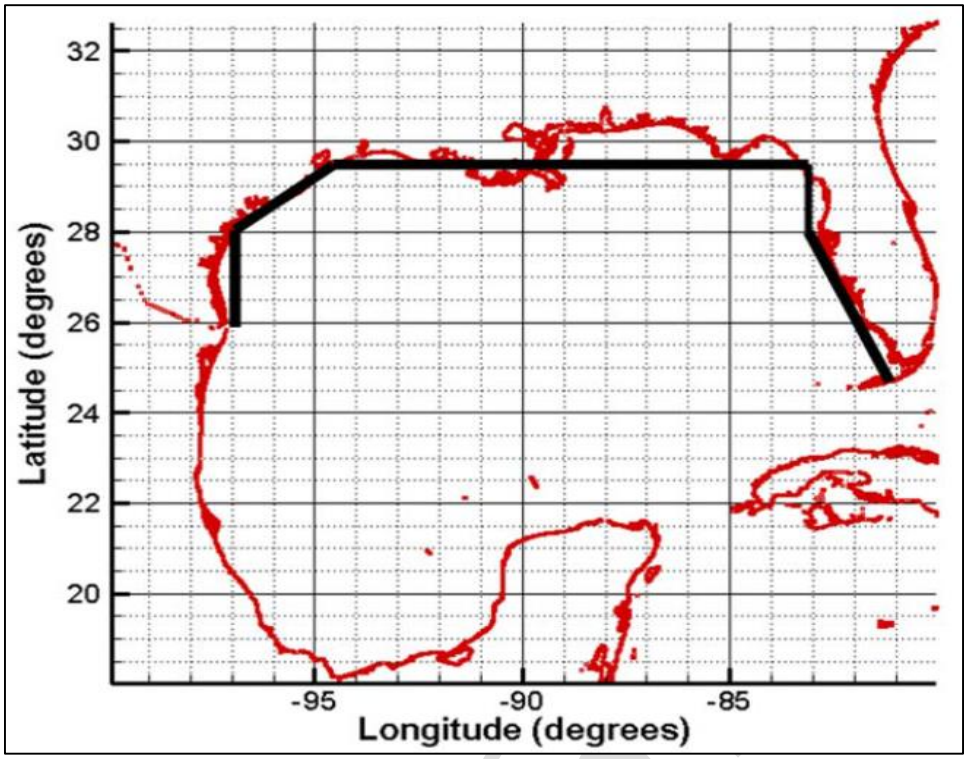

Figure 9-6. Coastal reference line used by Resio (2007) in determining the SRR.

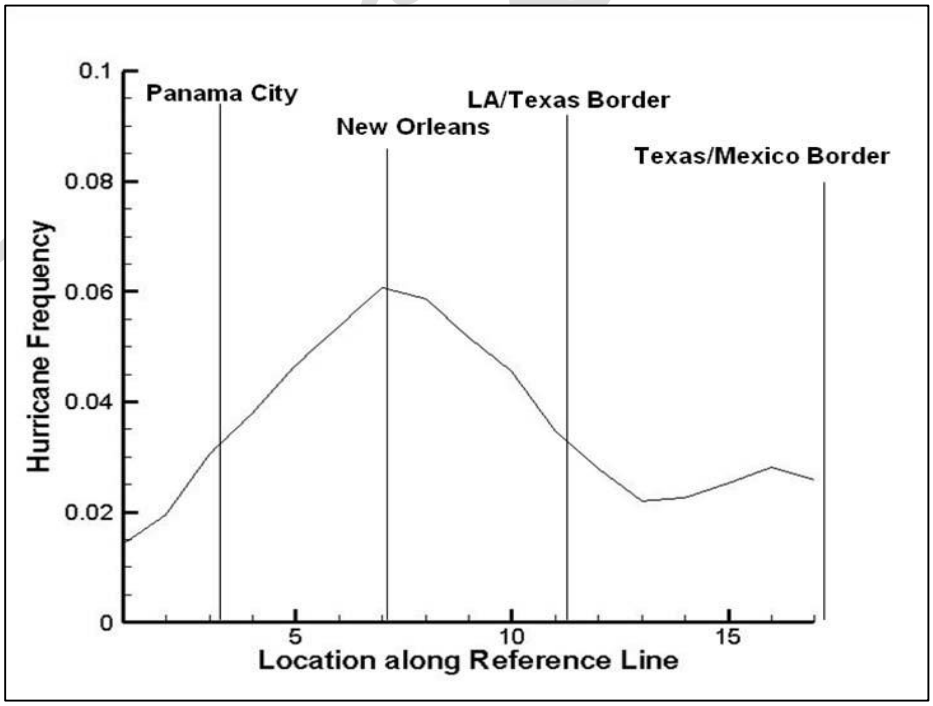

Figure 9-7. SRR estimated for the Gulf coast region by Resio et al (2007).

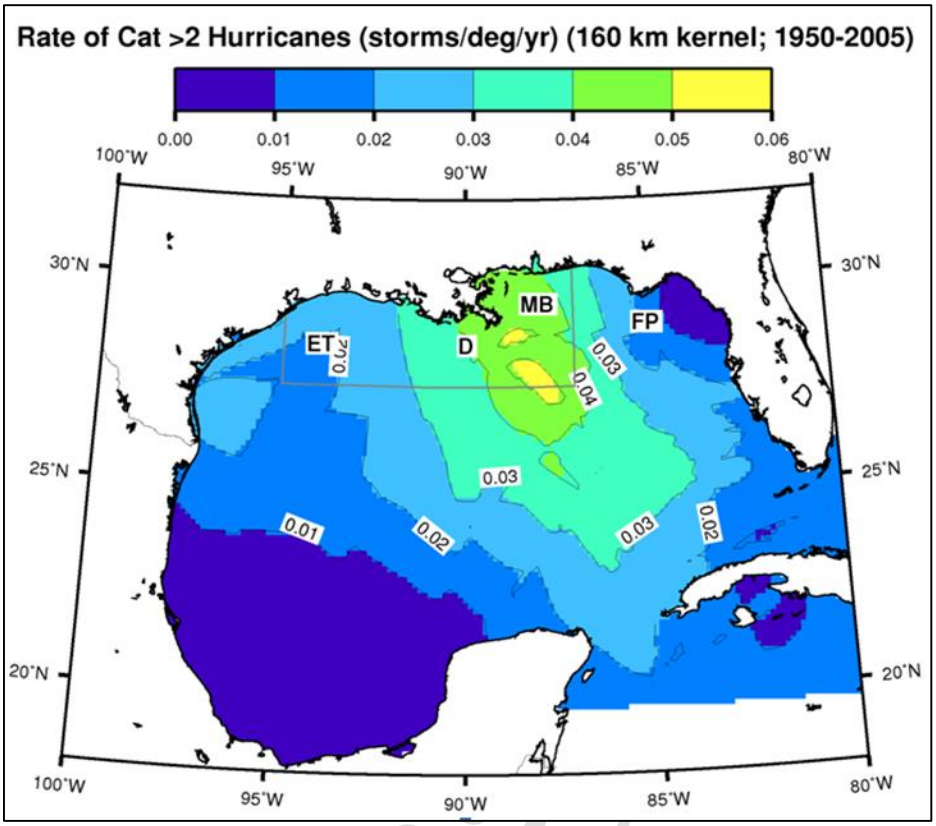

Figure 9-8. SRR computed from GKF for the Gulf of Mexico in FEMA (2008a).

Probability Distributions of Tropical Storm Parameters

In general, the next steps in conducting a JPA are: storm parameterization and development of probability distributions of historical TC parameters, discretization of probability distributions of TC parameters, and development of a synthetic storm set. The storm set adopted for use in the present study is the same storm set that was developed for the FEMA Risk MAP study of the Texas Coast (FEMA 2011). Compared to the method used in the Texas Risk MAP study (FEMA 2011), the present study adopted a different approach for discretizing probability distribution of storm parameters and optimizing the discrete weights assigned to each TC parameter combination.

Most recent FEMA studies of hurricane-prone coastal areas have been based on some implementation of JPM-OS methodology for sampling distributions of TC parameters. The two most well established JPM-OS methods are the JPM-OS Response Surface approach (Resio et al., 2007) and the JPM-OS Bayesian Quadrature approach (Toro et al., 2010). The Response Surface approach (JPM-OS-RS) has been used in studies

throughout the Gulf Coast, including Louisiana (IPET 2009) and Texas (FEMA 2011). The Bayesian Quadrature Approach (JPM-OS-BQ) has been used in areas of the Gulf Coast region such as Mississippi (FEMA 2008a).

The focus of the JPM-OS-RS is to augment the storm sampling by interpolating intermediate parameter values from response surfaces. The interpolated values have been shown to introduce additional uncertainty in water surface elevations with root-mean-square deviation on the order of 0.70 m (CPRA 2013). The added uncertainty is seldom quantified in these studies. The JPM-OS-RS also requires expert judgment for the selection of the storm parameters and associated discrete weights.

The JPM-OS-BQ approach employs a quadrature scheme that selects the optimal storm parameters and assigns the appropriate discrete weights. The JPM-OS-BQ was adopted as part of FEMA's Risk MAP program best practices, as documented in the Operating Guidance No. 8-12 (FEMA 2012). In the present study, the Bayesian Quadrature (Diaconis 1988; O'Hagan 1991; Minka 2000; Toro 2008, Toro et al., 2008) algorithm was used to optimize the discrete weights assigned to each parameter combination corresponding to the synthetic storm set developed as part of the Texas Risk MAP study (FEMA 2011).

Estimation of Errors and Other Secondary Terms

The error or epsilon (ε) term that is considered in the JPM integral (Equation 9-1) is a combination of multiple epsilons that are considered to be probabilistically independent and aggregated accordingly. Following is a list of epsilons that have been estimated and accounted for in recent JPM-OS studies:

1) Errors in hydrodynamic modeling and grids associated with epistemic uncertainty.
2) Errors in meteorological modeling associated with simplified PBL winds.
3) Random variations in the Holland *B* parameter.
4) Storm track variations not captured in synthetic storm set.
5) Random astronomical tide phase.

The uncertainty associated with each epsilon is assumed to be unbiased and normally distributed. This allows the epsilons to be represented as standard deviations and their effects to be combined additively. The total uncertainty associated with the combined epsilon (σ_ε) is computed as the square root of the sum of the squares of the standard deviations of each individual epsilon (σ_i):

$$\sigma_\varepsilon = \sqrt{\sum_i^n (\sigma_i^2)} \quad (9\text{-}4)$$

where σ_ε is the total standard deviation of errors and σ_i is the standard deviation of error i.

Errors in Hydrodynamic Modeling

The epsilon related to hydrodynamic modeling errors, σ_{hyd}, has been estimated in substantially different ways in recent FEMA studies. For example, in FEMA (2008), σ_{hyd} was computed as follows:

$$\sigma_{hyd} = \sqrt{\sigma_{cal}^2 - \sigma_{meas}^2} \quad (9\text{-}5)$$

where σ_{cal} = calibration error; σ_{meas} = measurement error. The calibration error was estimated as the standard deviation of the difference between simulated and measured storm surge elevations. The measurement error was estimated as a standard deviation representing the variability in high water marks. The epsilons σ_{cal} and σ_{meas} were estimated to be 0.46 m and 0.40 m, respectively, resulting in σ_{hyd} = 0.23 m. Other studies (Resio et al. 2007; FEMA 2011) have estimated σ_{hyd} for the Louisiana-Mississippi coast to be in the range of 0.53–0.76 m. This same range for σ_{hyd}, 0.53– 0.76 m (mean of 0.645 m), was adopted in the present study.

Errors in Meteorological Modeling

The epsilon associated with errors in meteorological modeling, σ_{met}, is estimated from the variability in water levels when comparing levels simulated using best winds to those simulated with PBL winds. The wind and pressure fields derived from "best winds" employs techniques that combine inputs from a variety of meteorological sources. In Resio et al. (2007) and FEMA (2011) values of σ_{met} are not explicitly provided. However, it is stated that the range of $\sigma_{hyd+met}$ for the Louisiana-Mississippi coast is estimated to be 0.61–1.07 m. In FEMA (2008a), σ_{met}

for coastal Mississippi was estimated at 0.36 m. For the present study, values of 0.07 to 0.30 (mean of 0.185 m) were adopted, the same as values adopted in FEMA (2011).

In the Texas Risk MAP study (FEMA 2011), regional biases were evident in comparisons that were made between maximum water surface elevation results from historic storms run using handcrafted Oceanweather "best winds" and runs using a PBL-model representation of the same historic storms. The same bias correction adopted by FEMA (2011) for the region encompassing Galveston Bay was applied in the present study.

Variations in Holland B Parameter

Regarding the epsilon associated with random variations in the Holland B parameter, σ_B, the storm surge elevation has been found to vary almost linearly with changes in the Holland B parameter. The epsilon σ_B is typically assumed to be in the range of 10–20% of the storm surge (Resio et al. 2007). More recent studies have adopted σ_B = 0.15 × storm surge elevation FEMA (2008a, 2011). This same epsilon term was adopted in the present study, σ_B = 0.15 × storm surge elevation.

Storm Track Variations

The epsilon related to storm track variations not accounted for in the synthetic storm set, σ_{track}, was estimated to be 0.20% of the wave setup contribution to the storm surge elevation (Resio 2007; FEMA 2011). The wave setup is estimated to be roughly 15–30% of the storm surge (Resio 2007; FEMA 2011). Other FEMA (2008a) studies have not explicitly accounted for σ_{track}.

Errors due to track variation were excluded from the present study. The way it was computed in FEMA (2011) resulted in a fairly insignificant magnitude.

Random Astronomical Tide Phase

There are locations where the magnitude of the astronomical tide is small enough that it can be treated as an uncertainty associated with the total water level response. This has been the approach followed for the Gulf of Mexico (e.g., FEMA 2008a, FEMA 2011). In cases where the tide amplitude is relatively small compared to the storm surge, the purpose of

this uncertainty is to capture the aleatory variability arising from the fact that the arrival of a TC can occur at any tide phase. This uncertainty is sometimes computed as the standard deviation of the predicted tide at any given location. FEMA (2008a) estimated the uncertainty associated with the astronomical tide to be 0.20 m for coastal Mississippi. In FEMA (2014), the adopted approach differed and consisted of simulating each storm with a random tide phase.

In the present study, the maximum surge values for each of the 223 FEMA North Texas storms, which were each modeled on a mean sea level with wave effects but without astronomical tides, was linearly superimposed with 96 random tide values. The tide values were obtained from NOAA gage 8771450 (http://tidesandcurrents.noaa.gov/stationhome.html?id=8771450). The period of record considered for the tide was '1904 Jan 01' to '2013 Dec 31'. Only tide values corresponding to hurricane season months (June-November) were used. This approach followed that taken in the North Atlantic Coast Comprehensive Study, NACCS, (Nadal-Caraballo et al., 2015)

Summary of Estimated Errors

The values of the error terms used in the present study along with the previous JPM-OS studies for Mississippi (FEMA 2008a), Texas (FEMA 2011), New York/New Jersey (FEMA 2014) and the NACCS, (Nadal-Caraballo et al., 2015) are listed in Table 9-2.

Table 9-2. Comparison of uncertainty estimates in JPM studies.

Uncertainty	Present Study	FEMA 2008a (m)	FEMA 2011 (m)	FEMA 2014 (m)	NACCS (m)
Hydrodynamic modeling	0.53 to 0.76	0.23	0.53 to 0.76	0.39	0.48
Meteorological modeling	0.07 to 0.30	0.36	0.07 to 0.30	0.54	0.38
Storm track variation	n/a	n/a	0.20* × wave setup	n/a	0.25
Holland B	0.15* x surge elevation	0.15* × surge elevation	0.15* × surge elevation	n/a	0.15* × surge elevation
Astronomical tide	variable	0.20	0.20	n/a	variable

*Factor on storm surge elevation is dimensionless.

Summary of Differences in JPM-OS Studies for the Houston-Galveston Region

For the present study, the JPM of hurricane parameters was recomputed and the probabilities of each of the previously modeled storms were recomputed in order to take advantage of new, more rigorous methods recently developed by the ERDC. The joint probability of coastal storm hazards was performed following a methodology similar to that described in FEMA (2011), but using a revised probabilistic model based on Bayesian Quadrature techniques (FEMA 2012). A re-analysis of the joint probability statistics was done using the new probabilistic model, which also incorporates additional data from tropical cyclones that have affected the Gulf of Mexico coast since 2007, including Hurricane Isaac in 2012. As part of the present study, storm recurrence rates, storm parameter statistics, and the probabilities of extreme water levels were recomputed.

The main differences between the FEMA (2011) JPM effort and the present JPM study are the following:

1) Period of record – FEMA (2011) considered the period of record 1940-2007. The present study considered the period 1940-2013.

2) Storm population – FEMA (2011) only considered landfalling hurricanes. The present study accounted for bypassing tropical storms as well.

3) Storm Recurrence Rate (SRR) – FEMA (2011) used a hybrid approach consisting of land-crossing sampling of storms and GKF weights to compute the SRR. The present study used a standard GKF approach that accounted for all tropical cyclones in the NOAA-HURDAT historical record within a given range of intensity and a limited time period (e.g. 1940–2013).

4) Storm frequency – FEMA (2011) estimated frequency of landfalling hurricanes at 1-degree increments of longitude starting at latitude 29.5. For the present study, all statistics including SRR were individually computed at 200 locations along the Gulf of Mexico U.S. coastline, for increased spatial coherence and fidelity.

5) Discretization method for storm parameters– The discretization method employed in FEMA (2011) and the weights used for the discrete storm parameter values were based on expert judgment. In the present

study, the weights were assigned to the synthetic storm set which was developed as part of FEMA (2011) in an optimal manner based on the Bayesian Quadrature algorithm.

6) Optimal kernel size – FEMA (2011) settled on a kernel size of 333 km. The present study used a kernel size of 200 km.

7) Epsilon terms – The epsilons used in the present study, shown in Table 9-2, were based on the knowledge gathered from previous FEMA (2008a, 2011) studies and from the USACE NACCS study. Differences in epsilon values between the present study and FEMA (2011) are noted in the table.

Existing Condition Water Surface Elevation Statistics

Based on the JPA approach described above and the maximum water surface elevation fields computed for each of the 223 North Texas storms that were simulated by FEMA (2011), water surface elevation statistics (WSE) were computed for a series of 43 locations that are shown in Figure 9-9 and in Table 9-3. These statistics represent existing conditions. Estimates of WSE having average recurrence intervals of 10, 20, 50, 100, 200, 500 and 1,000 years are shown for the mean value (Table 9-4) and for the upper value associated with the following confidence limits (CL), 84%, 90%, 95% and 98%, which are shown in Tables 9-5, 9-6 , 9-7 and 9-8, respectively. At a given location, compared to the mean values, WSE values for successively greater confidence intervals are increasingly higher.

As seen in Tables 9-4 through 9-8, some general spatial patterns are evident in the WSE associated with each ARI. Along the open Gulf coast, WSE for a particular ARI are similar in magnitude along both Galveston Island and Bolivar Peninsula, with values being slightly greater along Bolivar Peninsula compared to those along Galveston Island. WSE on the bay sides of both Galveston Island and Bolivar Peninsula are slightly less than WSE on the open Gulf sides of both barriers.

Along the western shoreline of Galveston Bay, WSE for a particular ARI generally increases from the City of Galveston northward toward the upper reaches of the Houston Ship Channel; and along most of the western Bay shoreline they are higher than WSE along the open Gulf coast. The highest WSE values occur in the upper reaches of the Ship Channel for any particular ARI. This overall trend for increasing WSE along the western Bay shoreline is due to the predominance of onshore-directed core winds

associated with those hurricanes that tend to produce the greatest storm surges in the Houston-Galveston region. Strong winds having an onshore component within the shallow Bay tend to set up the water surface from south to north, or southeast to northwest, which act to increase water surface elevations in the northern and northwestern parts of the bay.

Within the interior tidal channels and creeks of the Clear Lake and Dickinson Bay areas, WSE are generally slightly higher than WSE at the entrances to these same areas. This pattern generally arises due to the prevalence of winds that have an east-to-west component, which are associated with the counterclockwise rotating wind circulation about the eye of those approaching hurricanes that cause the highest surges in the Bay. Winds blowing from the east tend to produce higher surge on the west side of the Bay compared to the east side, establishing a water surface gradient. This gradient also is forced within the creeks and tidal channels, which serve as conduits through which the storm surge can propagate into the more interior parts of the system. This gives rise to slightly higher WSE in the western interior parts of the Clear Lake and Dickinson Bay areas, compared to the WSE at the entrances to these areas.

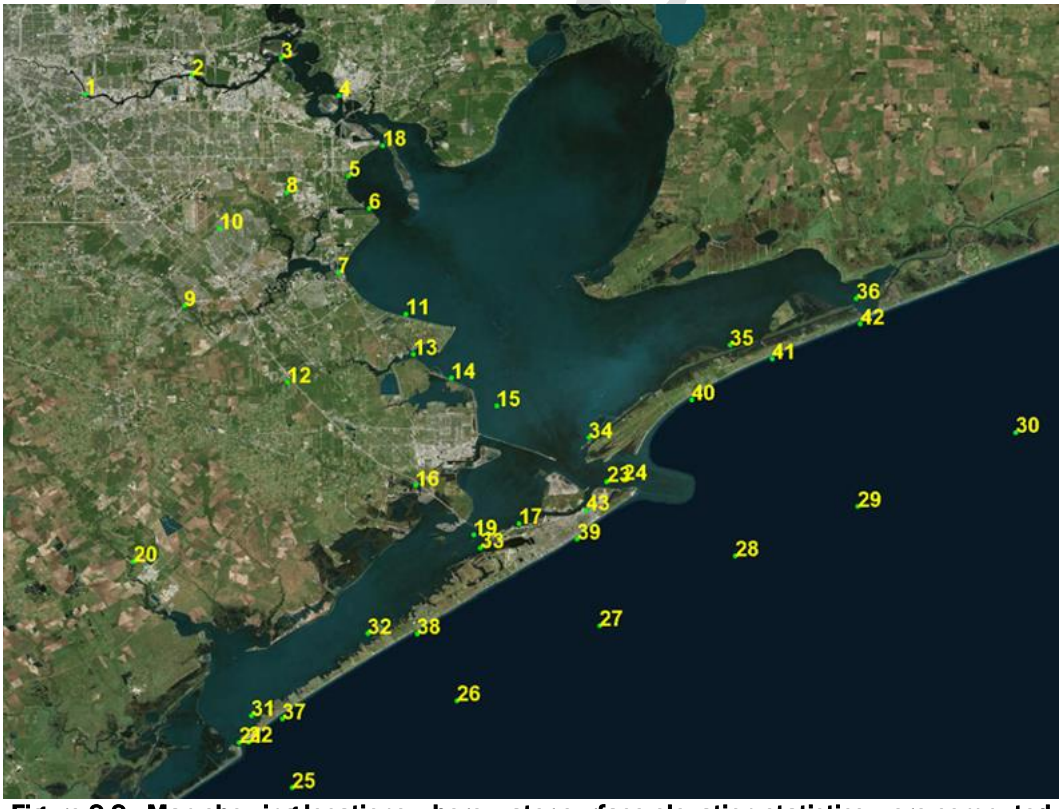

Figure 9-9. Map showing locations where water surface elevation statistics were computed for the present study. Station numbers correspond to the locations listed in Table 9-3.

Table 9-3. Locations where water surface elevation statistics were computed

No.	Location	Latitude (°N)	Longitude(°W)	Bottom Elevation (m, NAVD88)
1	Houston Ship Channel (upper)	29.7275	95.275	-13.3
2	Houston Ship Channel (mid)	29.7469	95.1688	-13.3
3	Houston Ship Channel (lower)	29.7635	95.0801	-15.8
4	Alexander Island	29.7261	95.0228	-15.8
5	LaPorte	29.6461	95.0127	-1.5
6	Bayport	29.6137	94.9925	-13.3
7	Clear Lake (east)	29.5494	95.0233	-6.5
8	Clear Lake (north)	29.6296	95.0743	-1
9	Clear Lake (west)	29.5177	95.1788	-2.7
10	Clear Lake (northwest)	29.5936	95.1414	-0.1
11	San Leon	29.5091	94.9584	-0.6
12	Dickinson	29.4416	95.0763	-0.5
13	Dickinson Bay entrance	29.4692	94.951	-3.5
14	Texas City (north)	29.4456	94.9131	-0.5
15	Texas City (east)	29.4178	94.8679	-2.1
16	Texas City (south)	29.3386	94.9486	-0.4
17	Galveston (bay)	29.3004	94.8458	-1
18	Morgan's Point	29.67603	94.97897	-15.8
19	West Bay (east)	29.2894	94.8908	-4.3
20	West Bay (north)	29.2628	95.2295	-0.6
21	San Luis Pass (throat-bay)	29.08236	95.12465	-4.6
22	San Luis Pass (throat-ocean)	29.08284	95.11508	-4.6
23	Bolivar Roads (throat-bay)	29.34213	94.75846	-15.4
24	Bolivar Roads (throat-ocean)	29.34424	94.74177	-14.6
25	San Luis Pass (offshore)	29.0376	95.0716	-14
26	Galveston Is (offshore mid west)	29.124	94.9075	-14
27	Galveston Is (offshore mid east)	29.1989	94.7654	-14
28	Bolivar Roads (offshore)	29.2684	94.6304	-14
29	Bolivar Pen (offshore mid)	29.3177	94.5085	-14
30	Bolivar Pen (offshore east)	29.3912	94.3511	-14
31	Galveston Is (bay west)	29.1092	95.1121	-0.7
32	Galveston Is (bay mid)	29.1911	94.9963	-0.4
33	Galveston Is (bay east)	29.2763	94.8843	-0.7
34	Bolivar Pen (bay west)	29.3863	94.7761	-0.5
35	Bolivar Pen (bay mid)	29.4785	94.6355	-0.5
36	Bolivar Pen (bay east)	29.5246	94.51	-0.5
37	Galveston Is (nearshore west)	29.106	95.0814	-2.6
38	Galveston Is (nearshore mid)	29.1906	94.947	-2.6
39	Galveston (Pleasure Pier)	29.2853	94.7878	-2.6
40	Bolivar Pen (nearshore west)	29.4236	94.6737	-2.6
41	Bolivar Pen (nearshore mid)	29.4646	94.5936	-2.6
42	Bolivar Pen (nearshore east)	29.4994	94.506	-2.6
43	Univ Texas Medical Branch	29.313816	94.778801	-8

Table 9-4. Average Recurrence Interval WSEs, Mean.

Location		Average Recurrence Interval in years (mean WSE in ft, NAVD88)						
		10	20	50	100	200	500	1,000
1	Houston Ship Channel (upper)	7.0	9.5	12.8	15.2	17.4	19.8	21.3
2	Houston Ship Channel (mid)	6.6	9.0	12.2	14.5	16.5	18.6	20.1
3	Houston Ship Channel (lower)	6.3	8.6	11.7	13.9	15.8	17.9	19.3
4	Alexander Island	6.0	8.2	11.0	13.1	14.8	16.8	18.2
5	LaPorte	6.0	8.1	10.6	12.6	14.3	16.2	17.4
6	Bayport	5.8	7.8	10.1	12.0	13.7	15.6	16.8
7	Clear Lake (east)	5.9	7.9	10.1	11.9	13.6	15.7	16.9
8	Clear Lake (north)	6.4	8.6	11.3	13.3	15.1	16.8	17.9
9	Clear Lake (west)	6.6	8.8	11.3	13.4	15.4	17.6	18.9
10	Clear Lake (northwest)	6.6	8.8	11.5	13.6	15.6	17.7	18.9
11	San Leon	5.4	7.2	9.2	10.8	12.4	14.3	15.5
12	Dickinson	6.9	9.2	11.6	13.3	14.9	16.6	17.6
13	Dickinson Bay entrance	5.8	7.7	10.0	11.7	13.4	15.3	16.5
14	Texas City (north)	5.3	7.1	9.1	10.8	12.4	14.2	15.3
15	Texas City (east)	4.9	6.7	8.8	10.5	12.0	13.8	14.9
16	Texas City (south)	4.4	6.3	8.8	10.9	12.8	15.2	16.8
17	Galveston (bay)	4.8	6.6	8.7	10.5	12.1	14.0	15.1
18	Morgan's Point	5.7	7.8	10.3	12.3	14.0	15.8	17.1
19	West Bay (east)	4.4	6.1	8.1	9.8	11.4	13.2	14.3
20	West Bay (north)	5.3	7.8	10.3	12.5	14.8	17.2	18.7
21	San Luis Pass (throat-bay)	4.3	5.9	8.2	10.0	11.5	13.2	14.6
22	San Luis Pass (throat-ocean)	4.3	6.0	8.4	10.2	11.7	13.4	14.9
23	Bolivar Roads (throat-bay)	4.6	6.5	9.2	10.9	12.4	14.2	15.6
24	Bolivar Roads (throat-ocean)	4.6	6.5	9.3	11.0	12.5	14.4	15.8
25	San Luis Pass (offshore)	4.0	5.6	8.0	9.6	11.0	12.7	14.1
26	Galveston Is (offshore mid west)	4.0	5.8	8.3	9.8	11.2	13.0	14.5
27	Galveston Is (offshore mid east)	3.8	5.4	7.9	9.4	10.7	12.6	14.2
28	Bolivar Roads (offshore)	3.9	5.7	8.4	9.9	11.2	13.0	14.6
29	Bolivar Pen (offshore mid)	3.8	5.6	8.2	9.7	11.1	12.8	14.3
30	Bolivar Pen (offshore east)	3.6	5.3	8.0	9.5	10.9	12.9	14.3
31	Galveston Is (bay west)	3.9	5.1	7.0	8.8	10.4	12.1	13.4
32	Galveston Is (bay mid)	3.8	5.0	7.0	8.8	10.5	12.2	13.3
33	Galveston Is (bay east)	4.2	5.8	7.7	9.5	11.1	12.9	14.0
34	Bolivar Pen (bay west)	4.3	6.0	8.3	9.9	11.3	13.1	14.2
35	Bolivar Pen (bay mid)	2.8	4.2	6.0	7.6	9.0	10.6	11.7
36	Bolivar Pen (bay east)	2.5	4.0	6.2	8.0	9.5	11.4	12.8
37	Galveston Is (nearshore west)	4.4	6.2	8.8	10.6	12.1	14.0	15.4
38	Galveston Is (nearshore mid)	4.4	6.4	9.2	10.9	12.4	14.4	15.9
39	Galveston (Pleasure Pier)	4.4	6.2	8.9	10.6	12.1	14.1	15.9
40	Bolivar Pen (nearshore west)	4.9	7.1	10.2	12.2	13.8	15.7	17.4
41	Bolivar Pen (nearshore mid)	4.6	6.8	9.9	11.7	13.3	15.3	16.9
42	Bolivar Pen (nearshore east)	4.5	6.6	9.7	11.6	13.1	15.1	16.7
43	Univ Texas Medical Branch	4.6	6.5	9.0	10.7	12.3	14.0	15.2

Table 9-5. Average Recurrence Interval WSEs, 84% Confidence Limit.

Location		Average Recurrence Interval in years (84% CL WSE in ft, NAVD88)						
		10	20	50	100	200	500	1,000
1	Houston Ship Channel (upper)	9.2	11.7	15.0	17.4	19.6	22.0	23.5
2	Houston Ship Channel (mid)	8.8	11.2	14.4	16.7	18.7	20.8	22.3
3	Houston Ship Channel (lower)	8.5	10.8	13.9	16.1	18.0	20.1	21.5
4	Alexander Island	8.2	10.4	13.2	15.3	17.0	19.0	20.4
5	LaPorte	8.2	10.2	12.8	14.8	16.5	18.4	19.6
6	Bayport	8.0	10.0	12.3	14.2	15.9	17.8	19.0
7	Clear Lake (east)	8.1	10.1	12.3	14.1	15.8	17.9	19.1
8	Clear Lake (north)	8.5	10.8	13.4	15.5	17.3	19.0	20.1
9	Clear Lake (west)	8.8	11.0	13.5	15.6	17.6	19.8	21.1
10	Clear Lake (northwest)	8.8	11.0	13.7	15.8	17.8	19.9	21.1
11	San Leon	7.6	9.4	11.4	13.0	14.6	16.5	17.7
12	Dickinson	9.1	11.4	13.8	15.5	17.1	18.8	19.8
13	Dickinson Bay entrance	8.0	9.9	12.2	13.9	15.6	17.5	18.7
14	Texas City (north)	7.5	9.2	11.3	13.0	14.6	16.4	17.5
15	Texas City (east)	7.1	8.9	11.0	12.7	14.2	16.0	17.1
16	Texas City (south)	6.6	8.5	11.0	13.1	15.0	17.4	19.0
17	Galveston (bay)	6.9	8.8	10.9	12.7	14.3	16.2	17.3
18	Morgan's Point	7.9	10.0	12.5	14.5	16.2	18.0	19.3
19	West Bay (east)	6.6	8.3	10.3	12.0	13.6	15.4	16.5
20	West Bay (north)	7.5	10.0	12.5	14.7	17.0	19.4	20.9
21	San Luis Pass (throat-bay)	6.5	8.1	10.4	12.2	13.7	15.4	16.8
22	San Luis Pass (throat-ocean)	6.5	8.2	10.6	12.4	13.9	15.6	17.1
23	Bolivar Roads (throat-bay)	6.8	8.7	11.4	13.1	14.6	16.4	17.8
24	Bolivar Roads (throat-ocean)	6.8	8.7	11.5	13.2	14.7	16.6	18.0
25	San Luis Pass (offshore)	6.2	7.8	10.2	11.8	13.2	14.9	16.3
26	Galveston Is (offshore mid west)	6.2	8.0	10.5	12.0	13.4	15.2	16.7
27	Galveston Is (offshore mid east)	6.0	7.6	10.1	11.6	12.9	14.8	16.4
28	Bolivar Roads (offshore)	6.1	7.9	10.6	12.1	13.4	15.2	16.8
29	Bolivar Pen (offshore mid)	6.0	7.8	10.4	11.9	13.3	15.0	16.5
30	Bolivar Pen (offshore east)	5.8	7.5	10.2	11.7	13.1	15.1	16.5
31	Galveston Is (bay west)	6.1	7.3	9.2	11.0	12.6	14.3	15.6
32	Galveston Is (bay mid)	6.0	7.2	9.2	11.0	12.7	14.4	15.5
33	Galveston Is (bay east)	6.4	8.0	9.9	11.7	13.3	15.1	16.2
34	Bolivar Pen (bay west)	6.5	8.2	10.5	12.1	13.5	15.3	16.4
35	Bolivar Pen (bay mid)	5.0	6.4	8.2	9.8	11.2	12.8	13.9
36	Bolivar Pen (bay east)	4.7	6.2	8.4	10.2	11.7	13.6	15.0
37	Galveston Is (nearshore west)	6.6	8.4	11.0	12.8	14.3	16.2	17.6
38	Galveston Is (nearshore mid)	6.6	8.6	11.4	13.1	14.6	16.6	18.1
39	Galveston (Pleasure Pier)	6.6	8.4	11.1	12.8	14.3	16.3	18.1
40	Bolivar Pen (nearshore west)	7.1	9.3	12.4	14.4	16.0	17.9	19.6
41	Bolivar Pen (nearshore mid)	6.8	9.0	12.1	13.9	15.5	17.5	19.1
42	Bolivar Pen (nearshore east)	6.7	8.7	11.9	13.8	15.3	17.3	18.9
43	Univ Texas Medical Branch	6.8	8.7	11.2	12.9	14.5	16.2	17.4

Table 9-6. Average Recurrence Interval WSEs, 90% Confidence Limit.

Location		Average Recurrence Interval in years (90% CL WSE in ft, NAVD88)						
		10	20	50	100	200	500	1,000
1	Houston Ship Channel (upper)	9.8	12.3	15.6	18.0	20.3	22.6	24.2
2	Houston Ship Channel (mid)	9.4	11.9	15.1	17.3	19.3	21.5	22.9
3	Houston Ship Channel (lower)	9.1	11.5	14.5	16.7	18.6	20.7	22.2
4	Alexander Island	8.8	11.0	13.9	15.9	17.7	19.6	21.0
5	LaPorte	8.8	10.9	13.4	15.4	17.2	19.1	20.2
6	Bayport	8.6	10.6	12.9	14.8	16.6	18.4	19.6
7	Clear Lake (east)	8.7	10.7	12.9	14.7	16.5	18.5	19.7
8	Clear Lake (north)	9.2	11.4	14.1	16.1	17.9	19.6	20.7
9	Clear Lake (west)	9.4	11.6	14.1	16.2	18.2	20.4	21.7
10	Clear Lake (northwest)	9.4	11.7	14.3	16.5	18.5	20.5	21.7
11	San Leon	8.3	10.0	12.0	13.6	15.3	17.1	18.3
12	Dickinson	9.7	12.0	14.4	16.1	17.7	19.4	20.5
13	Dickinson Bay entrance	8.6	10.5	12.8	14.5	16.2	18.1	19.3
14	Texas City (north)	8.1	9.9	11.9	13.6	15.2	17.0	18.1
15	Texas City (east)	7.7	9.5	11.6	13.3	14.8	16.6	17.8
16	Texas City (south)	7.2	9.2	11.6	13.7	15.6	18.0	19.6
17	Galveston (bay)	7.6	9.4	11.5	13.3	15.0	16.8	17.9
18	Morgan's Point	8.6	10.6	13.2	15.1	16.8	18.7	19.9
19	West Bay (east)	7.3	8.9	10.9	12.6	14.3	16.0	17.1
20	West Bay (north)	8.1	10.6	13.1	15.3	17.6	20.0	21.5
21	San Luis Pass (throat-bay)	7.1	8.7	11.1	12.8	14.3	16.0	17.4
22	San Luis Pass (throat-ocean)	7.1	8.8	11.3	13.0	14.5	16.3	17.7
23	Bolivar Roads (throat-bay)	7.4	9.3	12.0	13.7	15.2	17.1	18.4
24	Bolivar Roads (throat-ocean)	7.4	9.3	12.1	13.8	15.3	17.2	18.6
25	San Luis Pass (offshore)	6.8	8.4	10.8	12.4	13.8	15.5	16.9
26	Galveston Is (offshore mid west)	6.8	8.6	11.1	12.6	14.0	15.9	17.3
27	Galveston Is (offshore mid east)	6.6	8.2	10.7	12.2	13.6	15.4	17.0
28	Bolivar Roads (offshore)	6.7	8.5	11.2	12.7	14.0	15.8	17.4
29	Bolivar Pen (offshore mid)	6.6	8.4	11.0	12.6	13.9	15.7	17.1
30	Bolivar Pen (offshore east)	6.4	8.1	10.8	12.4	13.8	15.7	17.2
31	Galveston Is (bay west)	6.8	8.0	9.8	11.6	13.2	14.9	16.2
32	Galveston Is (bay mid)	6.6	7.8	9.8	11.7	13.3	15.0	16.1
33	Galveston Is (bay east)	7.0	8.6	10.6	12.3	13.9	15.7	16.8
34	Bolivar Pen (bay west)	7.1	8.9	11.2	12.7	14.2	15.9	17.0
35	Bolivar Pen (bay mid)	5.6	7.0	8.8	10.4	11.9	13.4	14.5
36	Bolivar Pen (bay east)	5.3	6.8	9.0	10.8	12.3	14.2	15.6
37	Galveston Is (nearshore west)	7.2	9.0	11.6	13.4	14.9	16.8	18.2
38	Galveston Is (nearshore mid)	7.2	9.2	12.0	13.7	15.2	17.2	18.8
39	Galveston (Pleasure Pier)	7.2	9.0	11.7	13.5	14.9	17.0	18.7
40	Bolivar Pen (nearshore west)	7.7	9.9	13.1	15.0	16.6	18.6	20.3
41	Bolivar Pen (nearshore mid)	7.4	9.6	12.7	14.5	16.1	18.1	19.7
42	Bolivar Pen (nearshore east)	7.3	9.4	12.5	14.4	15.9	17.9	19.5
43	Univ Texas Medical Branch	7.4	9.3	11.8	13.5	15.1	16.9	18.0

Table 9-7. Average Recurrence Interval WSEs, 95% Confidence Limit.

Location		Average Recurrence Interval in years (95% CL WSE in ft, NAVD88)						
		10	20	50	100	200	500	1,000
1	Houston Ship Channel (upper)	10.6	13.1	16.4	18.8	21.0	23.4	25.0
2	Houston Ship Channel (mid)	10.2	12.7	15.9	18.1	20.1	22.3	23.7
3	Houston Ship Channel (lower)	9.9	12.3	15.3	17.5	19.4	21.5	23.0
4	Alexander Island	9.6	11.8	14.6	16.7	18.5	20.4	21.8
5	LaPorte	9.6	11.7	14.2	16.2	18.0	19.8	21.0
6	Bayport	9.4	11.4	13.7	15.6	17.4	19.2	20.4
7	Clear Lake (east)	9.5	11.5	13.7	15.5	17.3	19.3	20.5
8	Clear Lake (north)	10.0	12.2	14.9	16.9	18.7	20.4	21.5
9	Clear Lake (west)	10.2	12.4	14.9	17.0	19.0	21.2	22.5
10	Clear Lake (northwest)	10.2	12.5	15.1	17.3	19.3	21.3	22.5
11	San Leon	9.1	10.8	12.8	14.4	16.0	17.9	19.1
12	Dickinson	10.5	12.8	15.2	16.9	18.5	20.2	21.3
13	Dickinson Bay entrance	9.4	11.3	13.6	15.3	17.0	18.9	20.1
14	Texas City (north)	8.9	10.7	12.7	14.4	16.0	17.8	18.9
15	Texas City (east)	8.5	10.3	12.4	14.1	15.6	17.4	18.6
16	Texas City (south)	8.0	10.0	12.4	14.5	16.4	18.8	20.4
17	Galveston (bay)	8.4	10.2	12.3	14.1	15.8	17.6	18.7
18	Morgan's Point	9.4	11.4	14.0	15.9	17.6	19.5	20.7
19	West Bay (east)	8.1	9.7	11.7	13.4	15.1	16.8	17.9
20	West Bay (north)	8.9	11.4	13.9	16.1	18.4	20.8	22.3
21	San Luis Pass (throat-bay)	7.9	9.5	11.8	13.6	15.1	16.8	18.2
22	San Luis Pass (throat-ocean)	7.9	9.6	12.1	13.8	15.3	17.1	18.5
23	Bolivar Roads (throat-bay)	8.2	10.1	12.8	14.5	16.0	17.9	19.2
24	Bolivar Roads (throat-ocean)	8.2	10.1	12.9	14.6	16.1	18.0	19.4
25	San Luis Pass (offshore)	7.6	9.2	11.6	13.2	14.6	16.3	17.7
26	Galveston Is (offshore mid west)	7.6	9.4	11.9	13.4	14.8	16.6	18.1
27	Galveston Is (offshore mid east)	7.4	9.0	11.5	13.0	14.4	16.2	17.8
28	Bolivar Roads (offshore)	7.5	9.3	12.0	13.5	14.8	16.6	18.2
29	Bolivar Pen (offshore mid)	7.4	9.2	11.8	13.4	14.7	16.5	17.9
30	Bolivar Pen (offshore east)	7.2	8.9	11.6	13.1	14.6	16.5	18.0
31	Galveston Is (bay west)	7.6	8.8	10.6	12.4	14.0	15.7	17.0
32	Galveston Is (bay mid)	7.4	8.6	10.6	12.5	14.1	15.8	16.9
33	Galveston Is (bay east)	7.8	9.4	11.4	13.1	14.7	16.5	17.6
34	Bolivar Pen (bay west)	7.9	9.6	11.9	13.5	14.9	16.7	17.8
35	Bolivar Pen (bay mid)	6.4	7.8	9.6	11.2	12.7	14.2	15.3
36	Bolivar Pen (bay east)	6.1	7.6	9.8	11.6	13.1	15.0	16.4
37	Galveston Is (nearshore west)	8.0	9.8	12.4	14.2	15.7	17.6	19.0
38	Galveston Is (nearshore mid)	8.0	10.0	12.8	14.5	16.0	18.0	19.5
39	Galveston (Pleasure Pier)	8.0	9.8	12.5	14.3	15.7	17.8	19.5
40	Bolivar Pen (nearshore west)	8.5	10.7	13.9	15.8	17.4	19.4	21.1
41	Bolivar Pen (nearshore mid)	8.2	10.4	13.5	15.3	16.9	18.9	20.5
42	Bolivar Pen (nearshore east)	8.1	10.2	13.3	15.2	16.7	18.7	20.3
43	Univ Texas Medical Branch	8.2	10.1	12.6	14.3	15.9	17.7	18.8

Table 9-8. Average Recurrence Interval WSEs, 98% Confidence Limit.

Location		Average Recurrence Interval in years (98% CL WSE in ft, NAVD88)						
		10	20	50	100	200	500	1,000
1	Houston Ship Channel (upper)	11.4	13.9	17.2	19.6	21.8	24.2	25.7
2	Houston Ship Channel (mid)	11.0	13.4	16.6	18.9	20.9	23.0	24.5
3	Houston Ship Channel (lower)	10.7	13.0	16.1	18.3	20.2	22.3	23.7
4	Alexander Island	10.4	12.6	15.4	17.5	19.2	21.2	22.6
5	LaPorte	10.4	12.4	15.0	17.0	18.7	20.6	21.8
6	Bayport	10.2	12.2	14.5	16.4	18.1	20.0	21.2
7	Clear Lake (east)	10.3	12.3	14.5	16.3	18.0	20.1	21.3
8	Clear Lake (north)	10.7	13.0	15.6	17.7	19.4	21.2	22.3
9	Clear Lake (west)	11.0	13.2	15.7	17.8	19.8	22.0	23.3
10	Clear Lake (northwest)	11.0	13.2	15.9	18.0	20.0	22.1	23.3
11	San Leon	9.8	11.6	13.6	15.2	16.8	18.7	19.9
12	Dickinson	11.3	13.6	16.0	17.7	19.3	21.0	22.0
13	Dickinson Bay entrance	10.2	12.1	14.4	16.1	17.8	19.7	20.9
14	Texas City (north)	9.7	11.4	13.5	15.2	16.8	18.6	19.7
15	Texas City (east)	9.3	11.1	13.2	14.9	16.4	18.2	19.3
16	Texas City (south)	8.8	10.7	13.2	15.3	17.2	19.6	21.2
17	Galveston (bay)	9.1	11.0	13.1	14.9	16.5	18.4	19.5
18	Morgan's Point	10.1	12.1	14.7	16.7	18.4	20.2	21.5
19	West Bay (east)	8.8	10.5	12.5	14.2	15.8	17.6	18.7
20	West Bay (north)	9.7	12.2	14.7	16.9	19.2	21.6	23.1
21	San Luis Pass (throat-bay)	8.7	10.3	12.6	14.4	15.9	17.6	19.0
22	San Luis Pass (throat-ocean)	8.7	10.4	12.8	14.6	16.1	17.8	19.3
23	Bolivar Roads (throat-bay)	9.0	10.9	13.6	15.3	16.8	18.6	20.0
24	Bolivar Roads (throat-ocean)	9.0	10.9	13.6	15.4	16.9	18.8	20.2
25	San Luis Pass (offshore)	8.4	10.0	12.4	14.0	15.4	17.1	18.5
26	Galveston Is (offshore mid west)	8.4	10.2	12.7	14.2	15.6	17.4	18.9
27	Galveston Is (offshore mid east)	8.2	9.8	12.3	13.8	15.1	17.0	18.6
28	Bolivar Roads (offshore)	8.3	10.1	12.8	14.3	15.6	17.4	19.0
29	Bolivar Pen (offshore mid)	8.2	10.0	12.6	14.1	15.5	17.2	18.7
30	Bolivar Pen (offshore east)	8.0	9.7	12.4	13.9	15.3	17.3	18.7
31	Galveston Is (bay west)	8.3	9.5	11.4	13.2	14.8	16.5	17.8
32	Galveston Is (bay mid)	8.2	9.4	11.4	13.2	14.9	16.5	17.7
33	Galveston Is (bay east)	8.6	10.2	12.1	13.9	15.5	17.3	18.4
34	Bolivar Pen (bay west)	8.7	10.4	12.7	14.3	15.7	17.5	18.6
35	Bolivar Pen (bay mid)	7.2	8.6	10.4	12.0	13.4	15.0	16.1
36	Bolivar Pen (bay east)	6.9	8.4	10.6	12.4	13.9	15.8	17.2
37	Galveston Is (nearshore west)	8.8	10.6	13.2	15.0	16.5	18.4	19.8
38	Galveston Is (nearshore mid)	8.8	10.8	13.6	15.3	16.8	18.8	20.3
39	Galveston (Pleasure Pier)	8.8	10.6	13.3	15.0	16.5	18.5	20.3
40	Bolivar Pen (nearshore west)	9.3	11.5	14.6	16.6	18.1	20.1	21.8
41	Bolivar Pen (nearshore mid)	9.0	11.2	14.3	16.1	17.7	19.7	21.3
42	Bolivar Pen (nearshore east)	8.9	10.9	14.1	16.0	17.5	19.5	21.1
43	Univ Texas Medical Branch	9.0	10.9	13.4	15.1	16.6	18.4	19.6

Probabilistic Context for Hurricane Ike's Maximum Water Surface Elevations

Within the Houston-Galveston region, the geographic corridor having the greatest potential for substantial flood-induced economic damages/losses runs from the City of Galveston, northward along the western shoreline of Galveston Bay, and into the upper reaches of the Houston Ship Channel.

Table 9-4 showed expected values for the various ARI water surface elevations. Using these values, the maximum water surface elevations observed during Hurricane Ike can be placed in a probabilistic context, within this corridor having the greatest potential for economic losses that runs along the western shoreline of Galveston Bay an into the upper reaches of the Houston Ship Channel.

At Galveston Pleasure Pier, on the Gulf side, the maximum water surface elevation observed during Ike was 10.6 ft NAVD88. This value is equal to the 100-yr ARI value at this location (10.6 ft) from Table 9-4, i.e., this value has a 1% chance of occurring each and every year. On the bay side of Galveston, the observed maximum water surface elevation reached 10.7 ft, which is also approximately equal to the 100-yr ARI value at this location (10.5 ft).

In the vicinity north of Texas City, near the entrance to Dickinson Bay, and at San Leon, the maximum water surface elevation was slightly higher, approximately 11 ft (11.3 ft was recorded at the Eagle Point gage, and 10.8 ft near San Leon). These values are also approximately equal to the 100-yr ARI values in this vicinity (10.8 ft north of Texas City and at San Leon, and 11.7 ft at the entrance to Dickinson Bay).

At the entrance to Clear Lake and in the vicinity of Morgan's Point, maximum water surface elevations during Ike were slightly higher, 12 to 12.5 ft, NAVD88. These are roughly equal to the expected 100-yr ARI values at the entrance to Clear Lake (11.9 ft) and Morgan's Point (12.3 ft).

In the upper reaches of the Houston Ship Channel, maximum water surface elevations during Ike were higher, approximately 13 to nearly 15 ft, increasing slightly from east to west along the channel. Within the economic corridor, the water surface elevations reached their highest values along this section of the Ship Channel during Ike. The 100-yr ARI values also increase in this section of the channel, from east to west,

ranging from 13.9 ft in the east to 15.2 ft in the west. Conditions during Ike were similar to the expected 100-yr ARI values in the upper reaches of the ship channel.

Throughout this economic corridor, the maximum water surface elevations experienced during Ike were approximately equal to the expected 100-yr ARI values. These conditions have a 1% chance of occurring each and every year.

The Proxy Storm Concept

This economic corridor is generally oriented in a shore-perpendicular direction relative to the open Gulf shorelines of Galveston Island and Bolivar Peninsula. The corridor is relatively narrow in alongshore extent compared to the entire Galveston Bay region.

Because of the corridor's location and orientation, extreme WSEs that can severely impact this area, such as those associated with the 100-yr and 500-yr ARIs, are expected to be principally dictated by the most severe hurricanes which make landfall within a particular stretch of coast. That coastal landfall zone extends from near Bolivar Roads pass (like the "direct-hit" track for some of the bracketing set storms) to a point that is 20 to 30 nm southwest of the pass (like storms 128 and 036 from the bracketing set). The extreme water surface elevation fields associated with the 100-yr and 500-yr ARIs are expected to have a general pattern of variability that is dictated in large part by the extreme bracketing set storms that approach from the south-southeast or southeast directions and make landfall in this critical zone. Tracks from the south-southeast and southeast also are the most common tracks for severe storms that have impacted the Texas coast, historically.

A field of 100-yr WSE (in feet) is shown in Figure 9-10. The figure is based upon the FEMA (2011) JPA approach. To generate this figure, 100-yr ARI WSEs were computed at each node of the storm surge model, color-coded based upon magnitude, and plotted at each model grid node. Elevations shown in Figure 9-10 are draft results from the FEMA (2011) study; and they are considered to be draft results until finalized by FEMA. The "still" WSE in Figure 9-10 only reflect the contributions of storm surge, tide and other sources of uncertainty. It is important to note that these elevations are <u>not</u> FEMA Base Flood Elevations (BFEs); they do not include the

effects of wind wave crests on top of the "still" water surface. The different color contour bands reflect 1-ft changes in WSE.

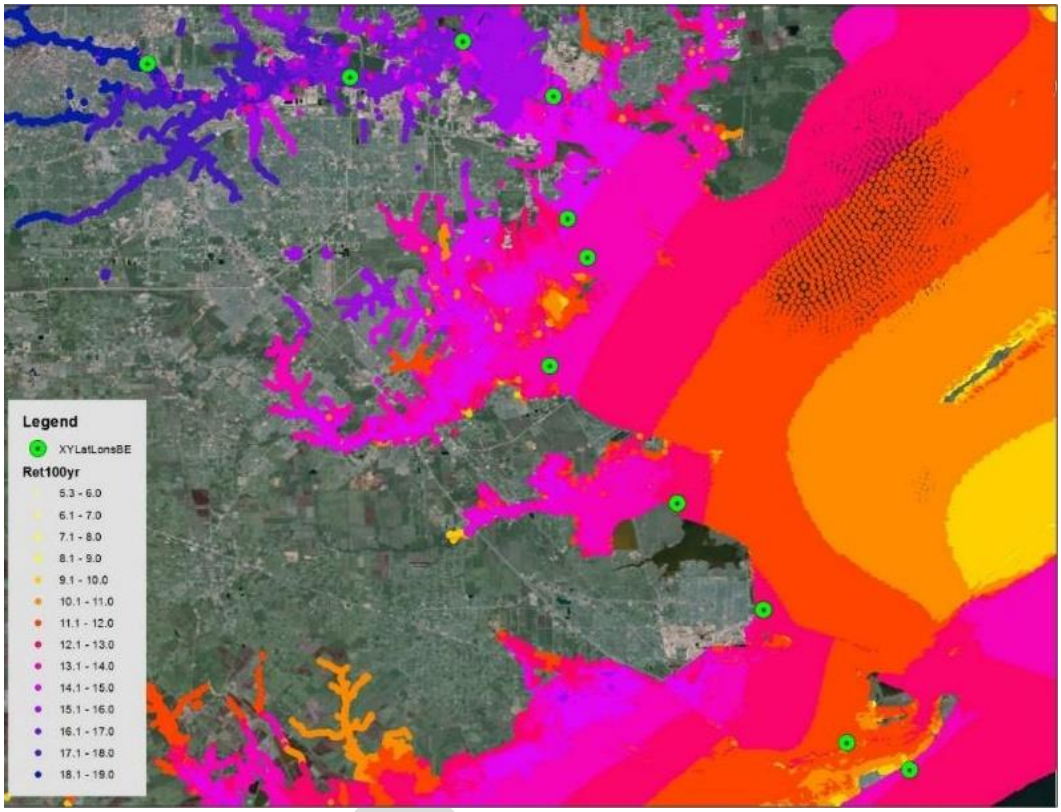

Figure 9-10. Field of water surface elevations (in feet) reflecting the 100-yr average recurrence interval, based on the draft FEMA (2011) results.

Table 9-9 shows the FEMA (2011) "still" WSEs at a few discrete locations within the key economic corridor for both the 100-yr and 500-yr ARIs. These locations are shown as green dots in Figure 9-10. The locations are listed in geographical order, starting with the upper reaches of the Houston Ship Channel, moving toward the south, and ending at the open Gulf coast at Galveston Pleasure Pier.

A sloping water elevation surface, with values increasing from southeast to northwest, is evident in the tabular results for both the 100-yr and 500-yr ARIs. The same pattern also is clearly evident in the graphical results for the 100-yr ARI shown in Figure 9-10; as reflected by the WSE color contours in the Bay which are roughly parallel to the open Gulf shoreline. The sloping surface is evident in the Bay proper, the upper reaches of the Houston Ship Channel, and along the western shoreline of the Bay. This WSE pattern is quite similar to that seen for some of the bracketing set

storms that approach from the southeast and south-southeast directions and make landfall just to the southwest of the City of Galveston.

Table 9-9. 100-yr and 500-yr average recurrence interval "still" water surface elevations at selected locations based upon the JPA approach and North Texas storm simulations from FEMA (2011).

			100-yr ARI WSE (ft)	500-yr ARI WSE (ft)
Location	Latitude (N)	Longitude (W)		
Houston Ship Channel	29° 44' 52''	95° 17' 12''	18.1	22.7
Houston Ship Channel	29° 44' 20''	95° 09' 14''	16.7	21.2
Houston Ship Channel	29° 45' 44''	95° 04' 48''	15.9	20.5
Alexander Island	29° 43' 35''	95° 01' 15''	14.9	19.2
La Porte	29° 38' 46''	95° 00' 42''	14.1	18.1
Bayport	29° 37' 14''	94° 59' 55''	13.6	17.4
Clear Lake (Seabrook)	29° 32' 59''	95° 01' 24''	13.4	16.8
Texas City levee (north)	29° 27' 35''	94° 56' 24''	12.6	16.1
Texas City levee (east)	29° 23' 24''	94° 53' 00''	12.4	16.2
Galveston (bay side)	29° 18' 10''	94° 49' 44''	11.8	14.8
Galveston (ocean side)	29° 17' 07''	94° 47' 16''	13.1	17.7

Because of the similarity between the ARI WSE pattern and the maximum WSE pattern for individual storms, it was anticipated that there might be a "proxy" storm from among the 223-storm FEMA set, one of the synthetic hypothetical hurricanes that were simulated, which produced a WSE field that was quite similar to the WSE field corresponding to a particular ARI WSE field throughout the key economic corridor. If so, then a with-dike storm simulation could be made for this same FEMA storm and then compared to the FEMA storm that was run for existing conditions as part of the FEMA (2011) study. In this way, without-dike and with-dike results could be compared to assess the effectiveness of the dike in reducing damages/losses for a storm that produces WSEs that have a particular ARI throughout the economic corridor. Based on this preliminary analysis using the FEMA (2011) results, the proxy storm concept seemed to have merit, as a first step to placing water surface elevations and economic damages/losses in a probabilistic context.

Identification and Selection of Proxy Storms

Using the existing condition water surface elevation statistics computed as part of the present study and presented earlier in this chapter, proxy

storms were defined for the 10-yr, 100-yr and 500-yr ARI WSE. With-dike simulations were made for each proxy storm, then the without-dike and with-dike maximum WSE fields were provided to the study economics team for analysis. The following approach, described for the 10-yr ARI proxy storm, was used to identify and select the three proxy storms.

First, based on the statistical analysis results shown in Table 9-8 for the 90% CL WSE values, the 10-yr ARI WSE was identified at each of the eighteen locations within the corridor of high economic value that are shown in Figure 9-11 and listed in Table 9-10. Second, individual storms from the 223-storm FEMA set were examined as potential proxies, based on their track and other hurricane parameters, and on their maximum WSE fields. Third, for each candidate proxy storm, the maximum WSE for that storm was extracted for each of the locations used to make the selection. Fourth, differences and absolute differences were computed between the ARI WSE and the storm-specific WSE at each of the eighteen locations, and average differences were computed for the entire set of locations. Fifth, the proxy storm was selected as the storm that minimized the average differences between it and the ARI WSE values, and minimized any bias.

Figure 9-11. Locations of water surface elevations used to identify and select proxy storms.

Table 9-10. Locations of water surface elevations used to identify and select proxy storms.

	Location	Latitude (°N)	Longitude (°W)
1	Houston Ship Channel (upper)	29.7275	95.275
2	Houston Ship Channel (mid)	29.7469	95.1688
3	Houston Ship Channel (lower)	29.7635	95.0801
4	Alexander Island	29.7261	95.0228
5	LaPorte	29.6461	95.0127
6	Bayport	29.6137	94.9925
7	Clear Lake (east)	29.5494	95.0233
8	Clear Lake (north)	29.6296	95.0743
9	Clear Lake (west)	29.5177	95.1788
10	Clear Lake (northwest)	29.5936	95.1414
11	San Leon	29.5091	94.9584
12	Dickinson	29.4416	95.0763
13	Dickinson Bay entrance	29.4692	94.951
14	Texas City (north)	29.4456	94.9131
15	Texas City (east)	29.4178	94.8679
16	Texas City (south)	29.3386	94.9486
17	Galveston (bay)	29.3004	94.8458
18	Galveston (Pleasure Pier)	29.2853	94.7878

10-yr Proxy Storm

Storm 535 from the original FEMA set was selected to be the 10-yr proxy storm. Storm 535 is a 975-mb storm that approaches from the southeast (TXN Fan set, Track 4, in FEMA storm set jargon) and makes landfall near San Luis Pass. It has the following characteristics:

Minimum central pressure - 975 mb

Central pressure at landfall - 987 mb

Maximum wind speed - 35 m/sec (68 kts)

Max wind speed at landfall - 26 m/sec (50 kts)

Radius to maximum winds - varies from 17.7 to 25.7 n mi

Variable Holland B parameter

Forward speed of 6 kts

The maximum wind speed and wind speed at landfall cited for each of the three proxy storms reflect 30-min average winds at a 10-m elevation.

Results for the 10-yr proxy storm are shown in Table 9-11. Some added precision was retained in the analyses done to identify and select proxy storms, and it is reflected in Table 9-11 and in subsequent tables in this section. However, the added precision is not indicative of overall accuracy of the computed WSEs; the computed WSE are no more accurate than tenths of a foot, at best. In the "Difference" column, green numbers indicate locations where the actual storm maximum WSE exceeded the ARI WSE value; red numbers indicate where the actual storm WSE was less than the ARI WSE value.

In Table 9-11, WSE differences for Storm 535 show a very small negative bias of approximately 0.1 ft; the average absolute difference is about 0.4 ft. The average absolute difference reflects an "error" of about 4% to 6%, in light of the 10-yr ARI WSE range of 7.2 to 9.8 ft.

Table 9-11. Water surface elevations for the 10-yr proxy storm, Storm 535.

10-yr Proxy Storm Water Surface Elevations		10-yr WSE 90% CL (ft)	Storm 535 WSE (ft)	Difference (ft)	Absolute Difference (ft)
1	Houston Ship Channel (upper)	9.78	10.53	0.75	0.75
2	Houston Ship Channel (mid)	9.42	10.04	0.62	0.62
3	Houston Ship Channel (lower)	9.12	9.61	0.49	0.49
4	Alexander Island	8.86	9.06	0.20	0.20
5	LaPorte	8.83	8.79	-0.03	0.03
6	Bayport	8.63	8.37	-0.26	0.26
7	Clear Lake (east)	8.73	8.50	-0.23	0.23
8	Clear Lake (north)	9.15	9.38	0.23	0.23
9	Clear Lake (west)	9.42	9.48	0.07	0.07
10	Clear Lake (northwest)	9.38	9.65	0.26	0.26
11	San Leon	8.27	7.64	-0.62	0.62
12	Dickinson	9.68	9.55	-0.13	0.13
13	Dickinson Bay entrance	8.63	8.14	-0.49	0.49
14	Texas City (north)	8.10	7.38	-0.72	0.72
15	Texas City (east)	7.74	6.92	-0.82	0.82
16	Texas City (south)	7.19	7.45	0.26	0.26
17	Galveston (bay)	7.58	6.76	-0.82	0.82
18	Galveston (Pleasure Pier)	7.19	6.50	-0.69	0.69
	Average	8.65	8.54	-0.108	0.428

Figure 9-12 shows the maximum WSE field for Storm 525. The WSE pattern is very similar to the pattern shown in Figure 9-10, with highest surges in the northwest part of Galveston Bay and the upper reaches of the Houston Ship Channel.

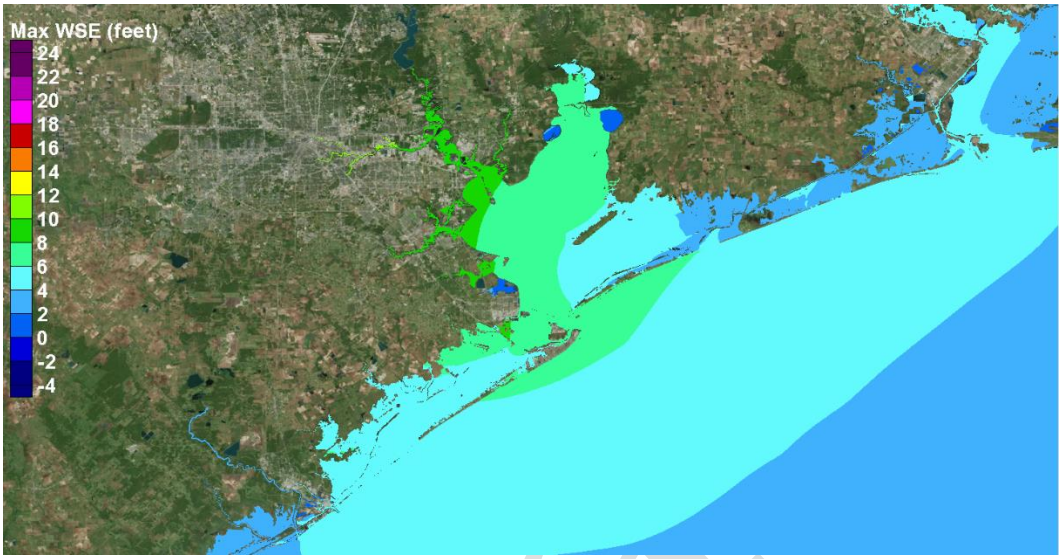

Figure 9-12. Maximum water surface elevation field for Storm 535, from FEMA (2011), the 10-yr proxy storm.

100-yr Proxy Storm

Storm 033 from the original FEMA set was selected to be the 100-yr proxy storm. Storm 033 is a 930-mb storm that approaches from the southeast (also has the TXN Fan set, Track 4) and makes landfall near San Luis Pass. It has the following characteristics:

Minimum central pressure - 930 mb

Central pressure at landfall - 948 mb

Maximum wind speed - 51 m/sec (100 kts)

Max wind speed at landfall - 40 m/sec (78 kts)

Radius to maximum winds - varies from 25.8 to 37.4 n mi

Variable Holland B parameter

Forward speed of 11 kts

Results for the 100-yr proxy storm are shown in Table 9-12. WSE differences for Storm 033 show no significant bias, overall; however, there are small regional biases, with Storm 033 WSEs being higher than the 100-yr ARI values in the northern and southern portions of the corridor

and Storm 033 WSEs being lower than the ARI WSEs in the central portion of the corridor in the Clear Lake and Dickinson Bay areas. The overall average absolute difference is about 0.9 ft. The average absolute difference reflects an "error" of about 5% to 7%, in light of the 100-yr ARI WSE range of 13.3 to 18.1 ft.

Figure 9-13 shows the maximum WSE field for Storm 033. The WSE pattern is very similar to the pattern shown for the 10-yr proxy storm and the 100-yr ARI WSE shown in Figure 9-10, with the highest surges in the northwest part of Galveston Bay and the upper reaches of the Houston Ship Channel. The similarity tween the two proxy storms is strongly influenced by the identical track that they both have.

Table 9-12. Water surface elevations for the 100-yr proxy storm, Storm 033.

100-yr Proxy Storm Water Surface Elevations		100-yr WSE 90% CL (ft)	Storm 033 WSE (ft)	Difference (ft)	Absolute Difference (ft)
1	Houston Ship Channel (upper)	18.05	18.34	0.30	0.30
2	Houston Ship Channel (mid)	17.36	18.05	0.69	0.69
3	Houston Ship Channel (lower)	16.70	17.62	0.92	0.92
4	Alexander Island	15.88	16.73	0.85	0.85
5	LaPorte	15.39	15.49	0.10	0.10
6	Bayport	14.80	14.83	0.03	0.03
7	Clear Lake (east)	14.70	13.94	-0.75	0.75
8	Clear Lake (north)	16.14	14.83	-1.31	1.31
9	Clear Lake (west)	16.24	14.34	-1.90	1.90
10	Clear Lake (northwest)	16.47	15.13	-1.35	1.35
11	San Leon	13.65	13.12	-0.52	0.52
12	Dickinson	16.14	14.17	-1.97	1.97
13	Dickinson Bay entrance	14.53	14.44	-0.10	0.10
14	Texas City (north)	13.62	13.48	-0.13	0.13
15	Texas City (east)	13.26	13.88	0.62	0.62
16	Texas City (south)	13.68	15.68	2.00	2.00
17	Galveston (bay)	13.32	13.42	0.10	0.10
18	Galveston (Pleasure Pier)	13.48	15.68	2.20	2.20
	Average	15.19	15.18	-0.013	0.880

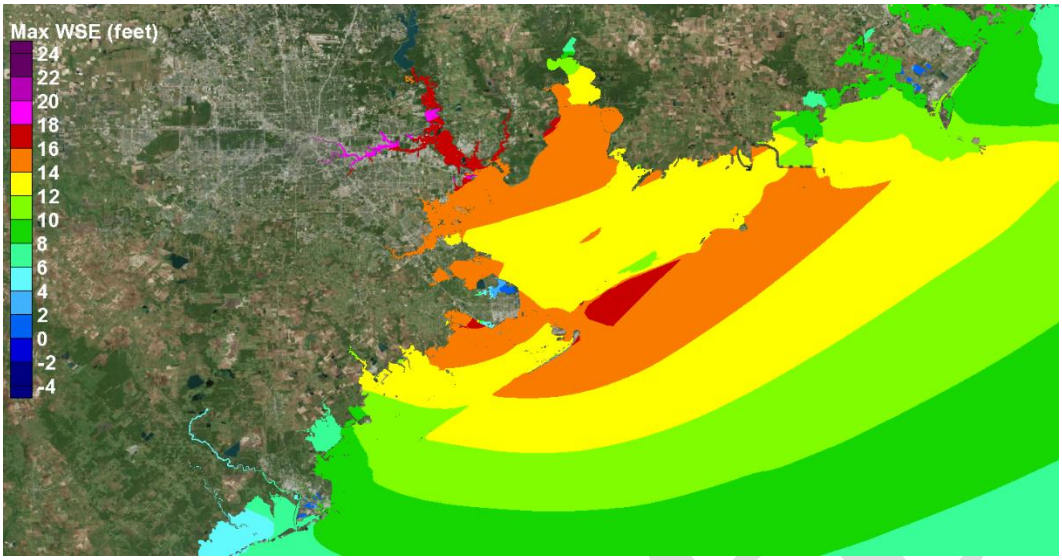

Figure 9-13. Maximum water surface elevation field for Storm 033, from FEMA (2011), the 100-yr proxy storm.

500-yr Proxy Storm

Storm 036 from the original FEMA set was selected to be the 500-yr proxy storm. Storm 036 is a 900-mb storm that approaches from the southeast (it also has the TXN Fan set, Track 4) and makes landfall near San Luis Pass. It has the following characteristics:

Minimum central pressure - 900 mb

Central pressure at landfall - 916 mb

Maximum wind speed – 58 m/sec (112 kts)

Max wind speed at landfall - 48 m/sec (93 kts)

Radius to maximum winds - varies from 21.8 to 31.6 n mi

Variable Holland B parameter

Forward speed of 11 kts

Results for the 500-yr proxy storm are shown in Table 9-13. WSE differences for Storm 036 show a negative bias of approximately 1 ft, overall, with Storm 036 WSEs being lower than the 500-yr ARI values at most locations. In the Clear Lake and Dickson Bay areas, Storm 036 maximum WSEs are 1 to 4 ft lower than the 500-yr ARI values. Storm 036 produces the largest storm surges in Galveston Bay, among all the 223 FEMA (2011) storms. The overall average absolute difference is about 1.3 ft. The average absolute difference reflects an "error" of about 6% to 8%, in light of the 500-yr ARI WSE range of 16.6 to 22.6 ft.

Figure 9-14 shows the maximum WSE field for Storm 036. The WSE pattern is very similar to the pattern shown for the other proxy storms and the 100-yr ARI WSE shown in Figure 9-10. All three proxy storms had the same track, which contributes to the similarity in maximum WSE patterns exhibited by all three storms. Again, the highest surges occurred in the northwest part of Galveston Bay and the upper reaches of the Houston Ship Channel.

Table 9-13. Water surface elevations for the 500-yr proxy storm, Storm 036.

500-yr Proxy Storm Water Surface Elevations		500-yr WSE 90% CL (ft)	Storm 036 WSE (ft)	Difference (ft)	Absolute Difference (ft)
1	Houston Ship Channel (upper)	22.64	21.46	-1.18	1.18
2	Houston Ship Channel (mid)	21.46	21.29	-0.16	0.16
3	Houston Ship Channel (lower)	20.74	20.80	0.07	0.07
4	Alexander Island	19.65	19.82	0.16	0.16
5	LaPorte	19.06	18.41	-0.66	0.66
6	Bayport	18.44	17.68	-0.75	0.75
7	Clear Lake (east)	18.50	16.63	-1.87	1.87
8	Clear Lake (north)	19.62	17.68	-1.94	1.94
9	Clear Lake (west)	20.41	16.54	-3.87	3.87
10	Clear Lake (northwest)	20.47	17.88	-2.59	2.59
11	San Leon	17.13	15.65	-1.48	1.48
12	Dickinson	19.39	15.72	-3.67	3.67
13	Dickinson Bay entrance	18.08	17.03	-1.05	1.05
14	Texas City (north)	17.03	16.04	-0.98	0.98
15	Texas City (east)	16.63	16.70	0.07	0.07
16	Texas City (south)	18.01	19.19	1.18	1.18
17	Galveston (bay)	16.80	16.34	-0.46	0.46
18	Galveston (Pleasure Pier)	16.96	18.90	1.94	1.94
	Average	18.95	17.99	-0.959	1.338

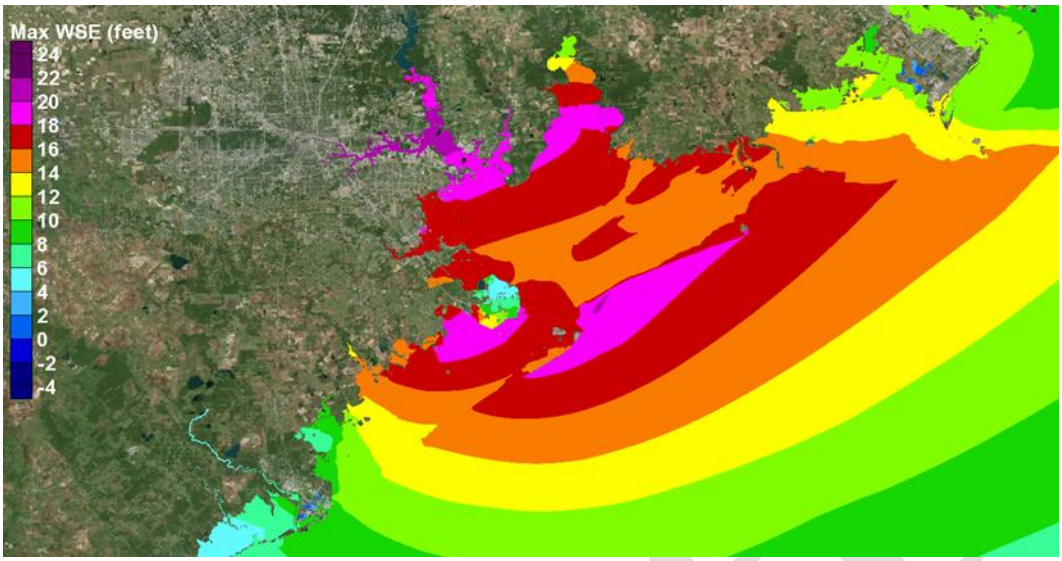

Figure 9-14. Maximum water surface elevation field for Storm 036, from FEMA (2011), the 500-yr proxy storm.

Proxy Storm Simulations With and Without an Extended Ike Dike

For certain hurricanes in the original bracketing set of storms, surge model results indicated that a significant amount of water flowed around the northeast end of the unterminated conceptual Ike Dike. The dike, as implemented in the bracketing-set with-dike simulations, ended near the northeast end of Bolivar Peninsula and the dike was not tied into higher ground. This flanking flow contributing to elevated water levels within Galveston Bay, which were judged to be not indicative of water surface elevations associated with a dike having an effective termination scheme. A plan for terminating the coastal dike to higher natural ground, or to some other man-made feature, such as an elevated road, has not yet been formulated; so the dike has been represented as an unterminated structure.

In the revised modeling approach, for the with-dike conditions, the dike was treated as an overtopping weir section, instead of a three-dimensional morphologic feature; and, it was extended in length toward the northeast, all the way to Sabine Pass. The change to a weir representation was done to promote model stability, avoiding the supercritical flows that would occur on the back side of the dike that is being overtopped. The dike modifications required changes to both the storm surge and wave model grid meshes as well as changes to how the dike was represented within both meshes. The lengthened dike was expected to better reflect surge conditions within Galveston Bay, for a dike having an effective termination

scheme, by greatly reducing the contribution of flanking flow to water elevations in the Bay. These mesh changes are being refined further, and results from the simulations reported here reflect work-in-progress.

The 100-yr and 500-yr proxy storms were simulated, both with and without the extended dike, to further examine the effectiveness of the conceptual Ike Dike in reducing storm surge levels within the Bay. These draft results were provided to the economics team for further analysis.

Effect of the Extended Ike Dike for the 100-yr Proxy Storm

The computed maximum water surface elevation fields for the without-dike and with-dike conditions, for the 100-yr proxy storm, are shown in Figures 9-15 and 9-16, respectively. For the existing conditions, a peak storm surge of approximately 16 ft was generated along the Gulf side of the City of Galveston, slightly less than the 17-ft crest elevation of the Galveston Seawall. Significant wave overtopping of the seawall would be expected at this surge level. Peak surge approached 17 ft was computed along the open coast of Bolivar Peninsula.

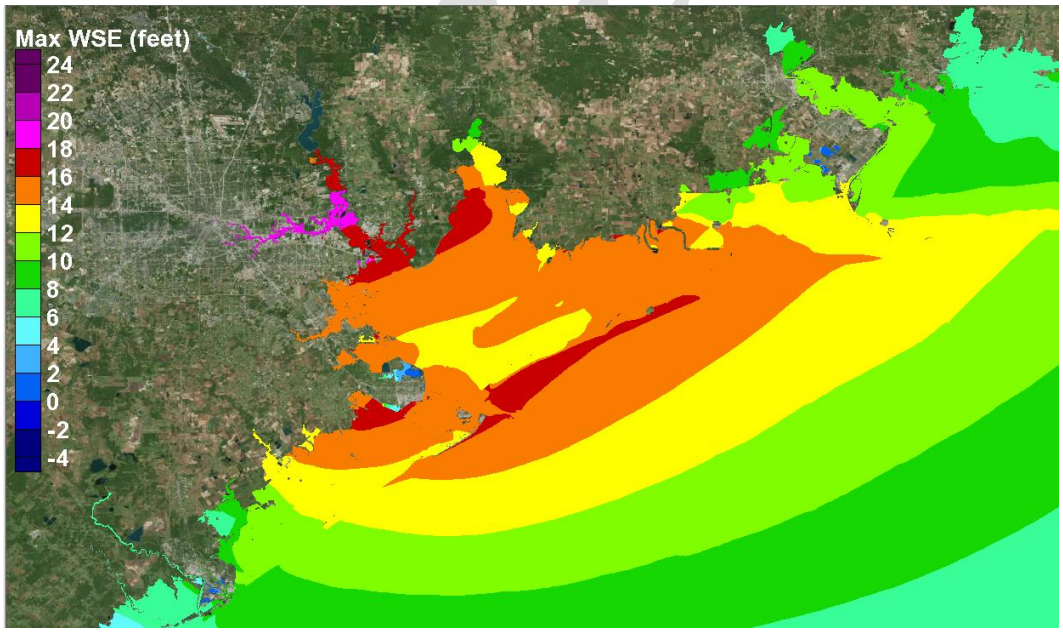

Figure 9-15. Maximum water surface elevation field for the 100-yr proxy storm, existing conditions.

Within the bays, from the bay side of the City of Galveston to the north side of Texas City and near San Leon, the peak surge was fairly constant, ranging from 14 to 15 ft. From San Leon northward, peak surge steadily increased to levels ranging from 15 ft to 17 ft along the northwest shoreline of Galveston Bay. Peak surges were even higher in the uppermost parts of the Bay, increasing to nearly 20 ft in the upper reaches of the Houston Ship Channel.

Figure 9-16 shows the maximum water surface elevation field for with-dike conditions. The extended dike produces a considerable reduction in storm throughout Galveston and West Bays. Along the bay side of the City of Galveston, peak surges are reduced from 14-15 ft to 10-12 ft. Along the western shoreline of Galveston Bay, peak surges are generally in the 6-8 ft range; but they are slightly higher, approaching 10-12 ft, in some of the isolated areas of the interior back channels of Dickinson Bay and Clear Lake. Peak surges in the upper reaches of the Houston Ship Channel are reduced to levels less than 12 ft, roughly an 8-ft reduction in peak surge in this area due to the dike. Along the eastern shoreline of the Bay, the presence of the dike reduces peak surge levels to elevations of 3 to 6 ft.

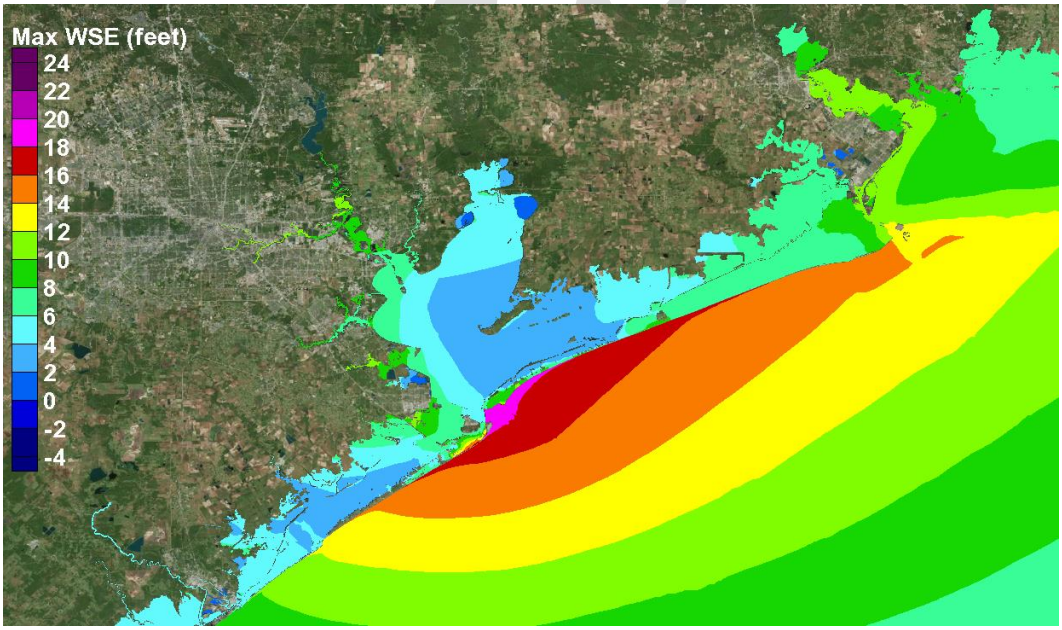

Figure 9-16. Maximum water surface elevation field for the 100-yr proxy storm, extended-dike conditions.

For the 100-yr proxy storm, the extended dike reduces surge levels within most of the Bay system to levels that are significantly less than the peak surges observed for Hurricane Ike, less by several feet in most places. The extended dike also lowered peak surges around Texas City, in such a way as to greatly reduce of the protective dike surrounding Texas City.

However, unlike the significant reductions in peak surge achieved by the dike throughout most of the Bay, peak surge along the Gulf side of Galveston Bay is actually increased by amounts of 0.5 to 1.5 ft, to peaks of 16 to 18 ft, associated with the presence of the dike, i.e., the "long dike effect." The increased open coast surge leads to an increased magnitude of overtopping and increased potential for overflow in the immediate vicinity of the dike. The same is true along Bolivar Peninsula.

A long impermeable coastal dike that is built to retard surge penetration will locally increase the surge by a small amount on the open coast side of the dike. The long dike effect is essentially this: the presence of the barrier serves as an obstacle to the wind-driven surge, something for the wind-driven surge to pile up against, that would otherwise not be present if the dike were not there. But the dike will dramatically reduce the surge for a much larger region behind the barrier, by drastically curtailing the storm propagation and penetration past the dike.

Effect of the Extended Ike Dike for the 500-yr Proxy Storm

Figures 9-17 and 9-18 show the computed maximum water surface elevation fields for the existing and with-dike conditions, respectively, for the 500-yr proxy storm. For existing conditions (Figure 9-17), a peak storm surge exceeding 18 ft was generated along the Gulf side of the City of Galveston, higher than the 17-ft crest elevation of the Galveston Seawall. Substantial overflow of the seawall occurs at this elevation. Peak surge approached 19 to 20 ft along open coast of Bolivar Peninsula.

Within the bays, along the south side of Texas City the peak surge reached approximately 19 ft, and considerable overflow of its surrounding protective levee occurred, along with considerable interior flooding of Texas City. North of Texas City, peak surge along the western shoreline of Galveston Bay peak surge steadily increased toward the north, from 17 ft to about 20 ft at the northern parts of the main Galveston Bay. Into the

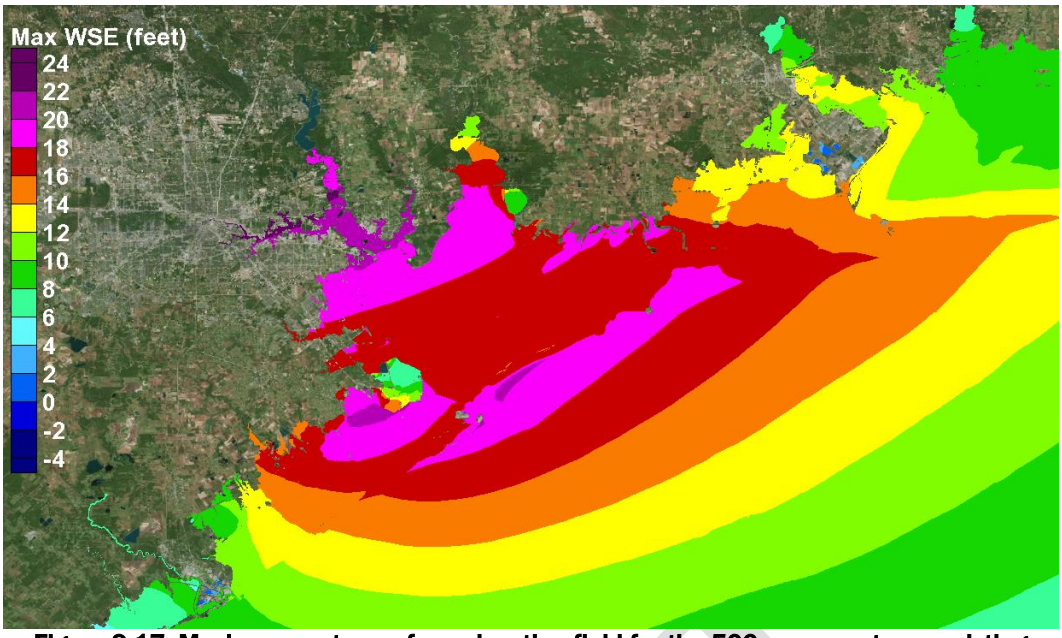

Figure 9-17. Maximum water surface elevation field for the 500-yr proxy storm, existing conditions.

upper reaches of the Houston Ship Channel, peak surges increased further, to levels reaching approximately 22 ft. Throughout Galveston Bay, surges exceeded 16 ft.

Figure 9-18 shows that the extended dike also produces a considerable reduction in storm surge throughout the Bay for the 500-yr proxy storm. Along the bay side of the City of Galveston, peak surges are reduced from 17-18 ft to 12-14 ft. Along the western shoreline of Galveston Bay, peak water surface elevations approached 13 ft in some of the isolated areas of the interior back channels of Dickinson Bay, but they generally ranged from 10-12 ft. Peak surges in the upper reaches of the Houston Ship Channel are reduced to levels less than 14 ft, roughly an 8-ft reduction in peak surge in this area. Along the eastern shoreline of the Bay, the presence of the dike reduces peak surge levels to elevations of 6 to 8 ft NAVD88.

For the 500-yr proxy storm, the extended dike significantly reduces surge levels along the western shoreline of the Bay to levels that are approximately equal to peak surges that were observed for Hurricane Ike. The dike significantly reduced overflow of the protective dike surrounding Texas City, greatly reducing the depth of inundation for a large portion of Texas City that was inundated by this storm, without the coastal dike in place.

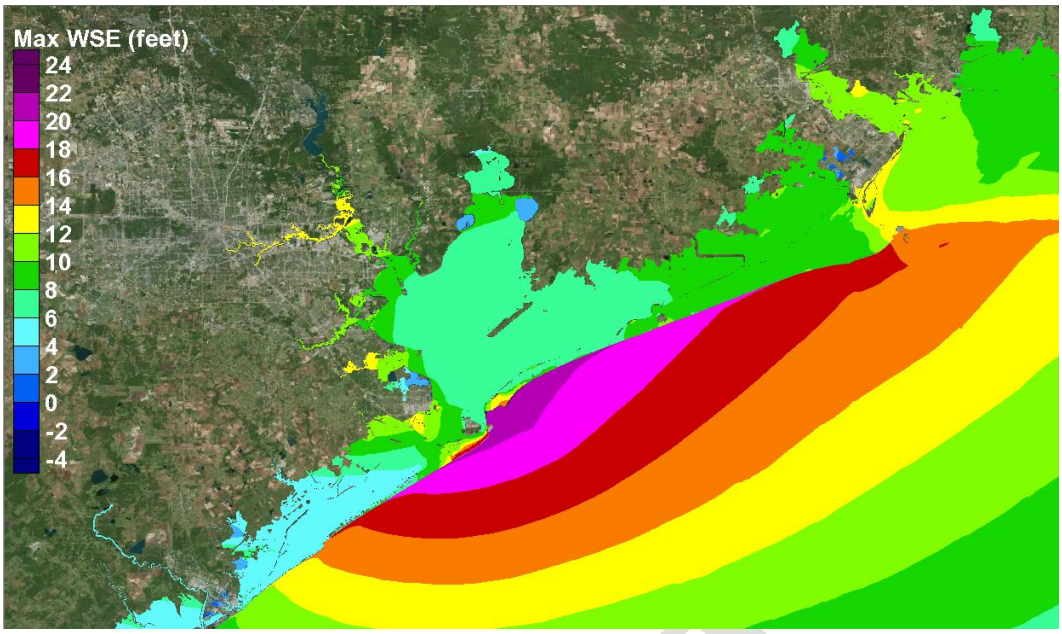

Figure 9-18. Maximum water surface elevation field for the 500-yr proxy storm, extended-dike conditions.

10 Influence of Sea Level Rise on Storm Surge

Introduction

As part of the proposed work, the sensitivity of storm surge to sea level rise will be investigated for the Houston-Galveston region. A single sea level rise scenario will be used in simulations involving three historic storms and three proxy storms. The sea level rise scenario will be consistent with that used for the New Orleans surge barrier design. Existing conditions and with-dike conditions will be simulated for the single sea level rise scenario. The sea level rise scenario will only consider a global sea level rise contribution; it will not consider the effect of subsidence on relative sea level rise. As part of this feasibility study, the influence of sea level rise is only being considered as a sensitivity test. It is not intended as a rigorous analysis of the effects of relative sea level rise on dike design and performance. The information below was developed to define the sea level rise scenario that would be adopted at this initial stage of the feasibility study.

Design and construction of the hurricane risk reduction system for New Orleans was done at the same time the U.S. Army Corps of Engineers (USACE) was developing an approach for treating sea level change in its design guidance for coastal flood risk reduction projects. The USACE adopts a 50-year time span for its economic analysis. Current USACE guidance requires analysis of three different sea level rise scenarios: low, intermediate and high rates of rise. Figure 89 shows the three sea level rise projections for the Galveston Bay vicinity during the 50-year period from 2020 to 2070. Generation of the three curves utilizes the 99-year record of sea level data from the Galveston Pier 21 gage. The figure was generated using the USACE sea level change curve calculator: *http://www.corpsclimate.us/ccaceslcurves.cfm* .

For Galveston, over the 50 years following an assumed construction year of 2020, the projected sea level changes are approximately 1, 1.5 and 3 ft for the low, intermediate, and high scenarios, respectively. For this feasibility study, the intermediate sea level change scenario value of 1.5 ft will be used to examine the influence of sea level change on project feasibility.

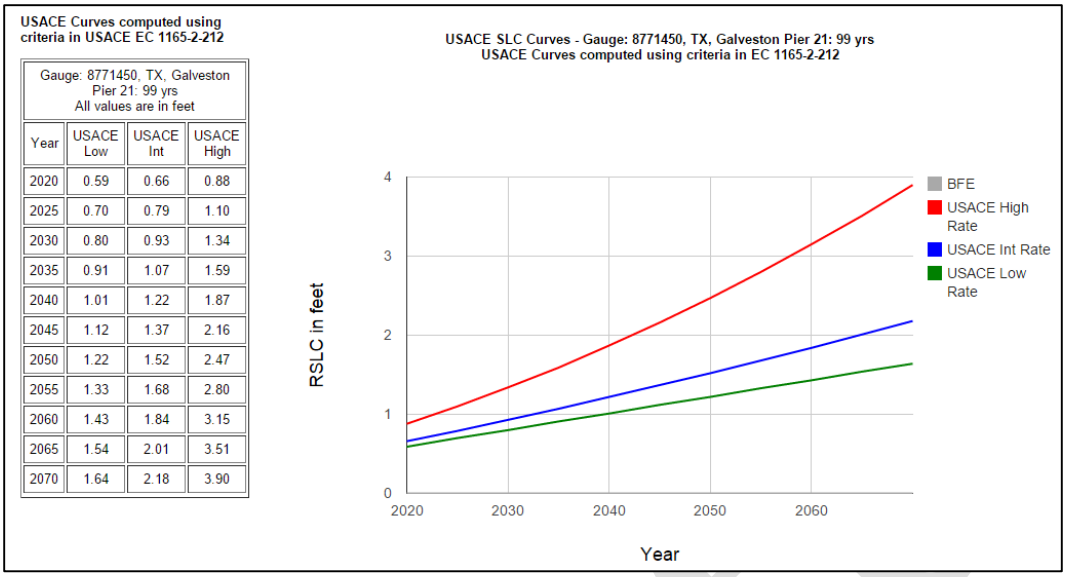

USACE Curves computed using criteria in USACE EC 1165-2-212

Gauge: 8771450, TX, Galveston Pier 21: 99 yrs All values are in feet			
Year	USACE Low	USACE Int	USACE High
2020	0.59	0.66	0.88
2025	0.70	0.79	1.10
2030	0.80	0.93	1.34
2035	0.91	1.07	1.59
2040	1.01	1.22	1.87
2045	1.12	1.37	2.16
2050	1.22	1.52	2.47
2055	1.33	1.68	2.80
2060	1.43	1.84	3.15
2065	1.54	2.01	3.51
2070	1.64	2.18	3.90

Figure 89. Sea level change scenarios for Galveston and vicinity, following USACE guidance.

11 Summary of Key Findings to Date

Generation of the Open Coast Storm Surge

Hurricane storm surge along the north Texas coast is primarily influenced by two contributors. One is the development of a wind-driven surge forerunner, an Ekman wave, which is forced on the Louisiana-Texas continental shelf. The forerunner is created by water moving along the shelf that is forced by the hurricane's peripheral winds; the alongshore moving water is then directed onshore by the Coriolis force. The counterclockwise rotating wind circulation about the hurricane's eye creates winds that are directed to the west and southwest along the shelf in the northwest Gulf of Mexico as a hurricane approaches the region. Forerunner development begins while the storm is well offshore in the deep waters of the Gulf. The forerunner is manifested as a slowly rising water surface elevation at the coast which can propagate into the Galveston Bay through the passes. This contribution can be as much as 6 feet in magnitude, as was observed by Kennedy et al (2011) during Hurricane Ike (2008). The second contributor is the direct effect of the highest winds in the core of the hurricane as it crosses the continental shelf and pushes the accumulated shelf waters toward the coast. The largest open coast surge computed for the 22 major hurricanes simulated thus far (those having a very low central pressure of 900 mb) was 18 to 19 ft at Galveston Pleasure Pier.

Surge Generation within Galveston Bay

Within the Bay, storm surge is highly dependent upon filling that occurs from several sources. The most significant source is surge propagation over Galveston Island and Bolivar Peninsula. A second source is surge propagation through Bolivar Roads and San Luis Pass which connect the Gulf to the Bays. A third contributor is the local wind-set up due to strong winds within the Bay which create a gradient or tilt to the water surface. The tilting action is in the direction of the wind; higher water surface elevation on the downwind side, lower water surface on the upwind side. Within Galveston Bay the largest surge computed for the major hurricanes simulated thus far was 18 to 20 ft on the Bay side of Galveston, 18 to 20 ft in the Texas City area, 19 ft in the Clear Lake area, 21 ft in the Bayport area and 24 to 25 feet in the upper reaches of the Houston Ship Channel.

Influence of Storm Track on Surge Development

Three storms were selected to examine the influence of track on development of the surge forerunner. Each storm had a different track and landfall location, but they all had the same minimum central pressure, forward speed and radius-to-maximum-winds.

Far field winds for the hurricane that approached from the south were directed onshore during the forerunner development period. These onshore winds were the primary contributor to formation of a significant open-coast surge forerunner. Movement of water along both the wide Louisiana continental shelf and the narrower north Texas shelf was a lesser contributor to the forerunner for this storm track. For the storm that approached from the south-southeast, the alongshore movement of water along the Louisiana and north Texas shelves was much stronger. This movement of water is then turned to the right or toward shore by the Coriolis force to raise the water level at the coast. This process was the primary contributor to the significant forerunner that developed for this storm track. For the storm that approached from the southeast, the alongshore movement of water was the primary contributor to forerunner development. However, as the storm approached the edge of the shelf, winds were directed more offshore along the Louisiana coast. These offshore winds reduced the alongshore movement of water from the Louisiana shelf toward the north Texas shelf, thereby reducing the forerunner amplitude.

Three storms were selected to examine the influence of storm track on surge development by the hurricane's core winds. Core winds are those nearest the eye, particularly on the right hand side of the storm where the wind speeds are typically highest. Whereas, the storm's far field winds dominate the forerunner development process, the storm's core winds begin to dominate surge development once the storm moves onto the continental shelf. Each of the three storms had the same minimum central pressure and radius-to-maximum-winds, but their tracks differed; and the storm from the south had a higher forward speed than the other two. All three storms made landfall at a different location along Galveston Island.

With storm parameters being the same, or nearly so, and for these particular landfall locations for each storm, the hurricane that approached from the south generated a maximum storm surge zone that first developed at the City of Galveston, The zone then migrated northeast to

Bolivar Peninsula as the storm approached and made landfall. For the other two storms which approached from the south-southeast and southeast directions, storm surge built up from the east and northeast. For both storms, maximum surge zones developed along Bolivar Peninsula, and they persisted at that location through the time of landfall.

Peak surge along the open coast was greatest for the storm which approached from the south-southeast. This storm developed a significant forerunner as a result of considerable movement of water from the Louisiana shelf to the north Texas shelf. This large accumulated volume of water was they driven ashore by the core winds. Peak surge for the storm from the south was less; this storm did not have the same volume of water moving along the Louisiana shelf and onto the north Texas shelf. The storm from the southeast produced the least amount of open coast surge. This occurred primarily because of the offshore directed winds along the Louisiana coast which reduced the forerunner and drew down the surge before it increased with arrival of the core winds. The same prevalence of offshore winds did not occur for storms on the south and south-southeast tracks.

Within Galveston Bay, at landfall, all three storms produced maximum surges at the southwest corner of the Bay, at the bay side of the City of Galveston. This high surge at the southwest corner forced water from Galveston Bay into West Bay, and prevailing winds set up the western side of West Bay.

For all three storms wind directions shifted rapidly for the few hours after landfall, first pushing water toward the western shoreline of Galveston Bay and then toward the northern shoreline. After landfall, the storm from the south transited through the center of Galveston Bay. This movement created times of relatively lower wind speeds within the Bay, as the hurricane's eye was positioned over the Bay. Wind directions near the eye changed very rapidly with passage of the eye. Coupled with the lower wind speeds, the lack of a persistent wind direction resulted in formation of no substantial water surface elevation gradient in addition to filling of the Bay. For all three storms, significant filling of Galveston and West Bays occurred due to forerunner penetration through the passes and by flow over the barrier islands. When the storm from the south did move away from the Bay, winds from the west persisted and set up the east side of Galveston and West Bays.

The eye of the storm from the south-southeast transited along the western side of Galveston Bay; and the eye for the storm from the southeast passed well to the west of the Bay. For both storms, once the eye moved away from the Bay, persistent winds from the south formed a substantial water surface gradient within the Bay, which was superimposed on the significant filling of the Bay. This substantial south-to-north gradient was established by persistent winds from the south that pushed water into the northern parts of the system.

Dependence of Peak Surge on Hurricane Intensity

A direct-hit set of four storms was simulated, each having a different central pressure (900 mb, 930 mb, 960 mb and 975 mb), but all following the same track, direction of approach from the south-southeast, landfall at the City of Galveston, and subsequent transit inland along the western shoreline of Galveston Bay. Open coast surges at Galveston for the four storms, listed from greatest to least intensity, were 13.5 to 16.5 ft, 11 ft to 15 ft, 7.5 to 10.5 ft, and 7 to 8.5 ft, respectively. In the Texas City area, peak surges for the four storms were 11 to 15 ft, 11.5 to 12.5 ft, 8.5 to 11 ft, and 8 to 8.5 ft, respectively. In the Clear Lake and Bayport areas, peak surges were 15 to 16.5 ft, 13 to 13.5 ft, 10 to 10.5 ft, and 8 to 8.5 ft, respectively, for the four storms. In the upper reaches of the Houston Ship Channel, peak surges were 19 to 20 ft, 15 ft, 12 to 12.5 ft, and 9 to 10 ft, respectively.

Results confirm that peak surge is strongly influenced by storm intensity; i.e., the greater the intensity (i.e., the lower the central pressure) the greater the peak surge. Central pressure is positively and well correlated with maximum wind speed, wind speed is nonlinearly related to surface wind stress, and wind stress is linearly related to water surface slope and storm surge.

Within Galveston Bay, peak surges tended to increase from the lower parts along the western shoreline to the upper parts, and then into the Houston Ship Channel where surge levels tended to be the highest for each storm. The counterclockwise wind circulation tended to force water into the upper reaches of the Houston Ship Channel.

Dependence of Peak Surge on Storm Track

The 21 major hurricanes (those having a 900-mb central pressure) that have been simulated approached the Houston-Galveston region from one of three general directions, from the south, the south-southeast and the

southeast. Each of the storms in each group had a unique track and a different landfall location. Within each of the three directional groupings, hurricanes had different but parallel tracks. Tracks for the storms, and thus landfall locations, in each grouping were separated by about 20 miles. For each of the different groupings, results suggest that hurricanes which make landfall in the zone that extends from San Luis Pass to a location 20 miles west of Bolivar Roads, will produce the greatest peak surges in the Houston-Galveston region, assuming all other hurricane parameters are the same and they only differ by track. Storms that made landfall at Bolivar Roads or to the east of Bolivar Roads tended not to generate nearly as high peak surges within the Bay; and for these hurricanes, the farther the landfall positon was from Bolivar Roads, the more peak surges in the Bay decreased significantly.

Putting Storm Surge in the Context of Probability

To provide a basis for proxy storm selection and to fully and accurately characterize the probability of extreme water surface elevations for existing conditions, a full joint probability analysis was conducted by the U.S. Army Engineer Research and Development Center (ERDC) using joint probability methods. The analysis produced water surface elevation statistics for a set of points, or save locations, in the Houston-Galveston region, including the key corridor for potential economic damage and losses, for existing conditions. The approach used by the ERDC differs slightly, in some aspects, from the approach used in the FEMA Region VI Risk Map study of the Texas coast (FEMA 2011); however the FEMA (2011) storm surge archive was used as the underlying storm surge data source for the statistical analysis.

Based on the statistical analysis, Table 11-1 summarizes several extreme water level statistics for the following key locations within the economic corridor: the upper reaches of the Houston Ship Channel, Morgan's Point, the entrance to Clear Lake, the east side of Texas City, bay side of the City of Galveston, and the Gulf side of the City of Galveston. For each location, the mean, or expected value, of water surface elevations corresponding to the 100-yr and 500-yr ARIs are shown (these correspond to water levels having a 1% and 0.2% chance of occurring each and every year, respectively). The water surface elevations listed in Table 11-1 account for the astronomical tide, wave contributions to the still water level, and a number of sources of uncertainty arising from various sources.

In addition to expected values, water levels for the 100-yr and 500yr ARIs also shown for two different confidence levels, 90% and 95% (the 90%CL and 95C%CL values, respectively). We recommend that the 90%CL ARI values be adopted for use in the feasibility assessment of the Ike Dike concept. They provide a much higher level of confidence than use of the mean, or expected values. Values in the table show that at all locations, for both the 100-yr and 500-yr ARIs, the 90%CL values are about 3 ft higher than the expected values; and the 95%CL values are about 3.5 ft higher than the expected values.

Table 11-1. Water Surface Elevation Statistics for Select Key Locations

Location	Extreme Water Surface Elevations (ft, NAVD88)					
	100-yr ARI mean	100-yr ARI 90%CL	100-yr ARI 95%CL	500-yr ARI mean	500-yr ARI 90C%CL	500-yr ARI 95%CL
Houston Ship Chan (upper)	15.2	18.0	18.8	19.8	22.6	23.4
Morgan's Point	12.3	15.1	15.9	15.8	18.7	19.5
Clear Lake Entrance	11.9	14.7	15.5	15.7	18.5	19.3
Texas City (east side)	10.5	13.3	14.1	13.8	16.6	17.4
Galveston (bay side)	10.5	13.3	14.1	14.0	16.8	17.6
Galveston (Gulf side)	10.6	13.5	14.3	14.1	17.0	17.8

For comparison purposes, Hurricane Ike produced maximum water surface elevations of 10.5 to 12 ft NAVD88 for much of the main portion of Galveston Bay and at the City of Galveston. In the upper reaches of the Houston Ship Channel Ike produced maximum water levels of 13 to 15 ft.

A crest elevation of 17 ft for the conceptual Ike Dike, which is equal to the present crest elevation of the Galveston Seawall, corresponds to a 500-yr ARI water surface elevation at a 90% confidence level at the Galveston Pleasure Pier.

Because of the similarity between the ARI water surface elevation pattern in Galveston Bay and the maximum water surface elevation pattern in the Bay for individual storms, it was thought that "proxy" storms could be identified from among the 223-storm FEMA storms, such that one of the synthetic hypothetical hurricanes that were simulated in the FEMA study (2011) produced a water surface elevation field that was quite similar to the field corresponding to a particular ARI water surface elevation field throughout the key economic corridor within the Bay. Based on this preliminary analysis using the FEMA (2011) results, the proxy storm

concept seemed to have merit, as a first step to placing water surface elevations and economic damages/losses in a probabilistic context. Proxy storms were identified for 10-yr, 100-yr and 500-yr ARI water surface elevations. The proxy storms enable reductions in inundation attributed to the Ike Dike to be placed in a probabilistic context prior to simulating a large set of hurricanes and performing a more rigorous analysis on that much larger set of results.

Surge Reduction Achieved with the Ike Dike Concept

The primary benefit of the Ike Dike concept is to greatly reduce or eliminate the sources of Bay filling, the greatest one being flow over the barrier islands. This eliminates, or nearly so, a major contributor to the storm surge and subsequent flooding within Galveston Bay. Reduction of storm surge in the Bay also can lead to a reduction in the amount of wave energy generated within the Bay by reducing the water depth.

The dike also acts to eliminate or reduce storm surge and wave attack along the coastal barrier islands, preventing surge and waves from damaging buildings and infrastructure. Damages are reduced or prevented as long as the dike is not overtopped or subjected to steady overflow. If overtopping and overflow occurs, damages and losses behind the dike can accrue on the barrier islands. Barrier islands can also flood from the backside or bay side; and by reducing surge level in Galveston Bay, the Ike Dike can reduce flooding of the barrier islands from the Bay side.

Results from Original Bracketing Set of Storms and Initial Modeling Approach

Based on an analysis of modeled water surface elevations for the original bracketing set of storms (25 storm simulations made for both without- and with-dike conditions), which were run with the initial surge and wave model model set up and modeling approach, even for these major bracketing-set storms, significant flood reduction benefits will accrue throughout the region. For the direct-hit set of four storms, having central pressures of 900, 930, 960 and 975 mb, the Ike Dike concept reduced storm surge within the Bay by these approximate amounts: 4.5 to 7 ft, 7 to 10 ft, 6 to 9 ft, 5 to 7 ft, respectively. The dike limited storm surge levels within the Bay to 4 to 7 ft for the 930-mb storm, 2 to 4 ft for the 960-mb storms, and 2 to 4 ft for the 975-mb storm. This indicates that the Ike

Dike concept will have considerable storm surge and flooding reduction benefits for all storms, particularly for the most frequently occurring, less intense, hurricanes.

The dike significantly reduced storm surge in Galveston Bay for the rare but possible 900-mb storm, by 4.5 to 7 ft, and the 930-mb storm by 7 to 10 ft, so considerable flood reduction benefits will accrue for many locations within the region even for major storms. However, the 900- and 930-mb direct-hit storms did produce flow over the dike in some areas, extensively in places, which would result in flood damage along the barrier islands in these areas. Overtopping and overflow occurred for some of the other 900-mb storms that produced substantial open coast storm surge which exceeded the crest height of the dike. Unless the dike is overwhelmed, it would reduce damages even in these overtopping and overflow situations, compared to the existing condition.

For all the 900-mb storms, the Ike Dike significantly reduces storm surge throughout Galveston Bay and the Houston Ship Channel, by amounts of up to 14 ft, depending on storm track. Reductions achieved with the dike were most often in the 6 ft to 12 ft range, which are significant reductions that will lead to significantly smaller damage/losses.

Results from 100-yr and 500-yr Proxy Storms and Revised Modeling Approach

The 500-yr and 100-yr proxy storms were simulated for existing conditions and with- extended dike conditions, using a revised and improved model setup and modeling approach. The extended dike ended at Sabine Pass; whereas the original dike considering in the bracketing set runs ended at the northeast end of Bolivar Peninsula. Results were provided to the economics team for their analysis.

For the 100-yr proxy storm, the extended dike produces a considerable reduction in storm throughout Galveston and West Bays. Along the bay side of the City of Galveston, peak surges are reduced from 14-15 ft to 10-12 ft. Along the western shoreline of Galveston Bay, peak surges are generally in the 6-8 ft range; but they are slightly higher, approaching 10-12 ft, in some of the isolated areas of the interior back channels of Dickinson Bay and Clear Lake. Peak surges in the upper reaches of the Houston Ship Channel are reduced to levels less than 12 ft, roughly an 8-ft reduction in peak surge in this area due to the dike. Along the eastern

shoreline of the Bay, the presence of the dike reduces peak surge levels to elevations of 3 to 6 ft.

For the 100-yr proxy storm, the extended dike reduces surge levels within most of the Bay system to levels that are significantly less than the peak surges observed for Hurricane Ike, less by several feet in most places. The extended dike also lowered peak surges around Texas City, in such a way as to greatly reduce of the protective dike surrounding Texas City.

For the 500-yr proxy storm, along the bay side of the City of Galveston, peak surges are reduced from 17-18 ft to 12-14 ft. Along the western shoreline of Galveston Bay, peak water surface elevations approached 13 ft in some of the isolated areas of the interior back channels of Dickinson Bay, but they generally ranged from 10-12 ft. Peak surges in the upper reaches of the Houston Ship Channel are reduced to levels less than 14 ft, roughly an 8-ft reduction in peak surge in this area. Along the eastern shoreline of the Bay, the presence of the dike reduces peak surge levels to elevations of 6 to 8 ft NAVD88.

For the 500-yr proxy storm, the extended dike significantly reduces surge levels along the western shoreline of the Bay to levels that are approximately equal to peak surges that were observed for Hurricane Ike. The dike significantly reduced overflow of the protective dike surrounding Texas City, greatly reducing the depth of inundation for a large portion of Texas City that was inundated by this storm, without the coastal dike in place.

Future Work

It is important in future work to define the probability of these rare extreme storms and all the storms that have been simulated. Future work will involve a more rigorous assessment of hurricane probability, risk of flooding, and reductions in the risk of flooding associated with the dike. The more rigorous statistical approach will require simulations of 150 to 200 hypothetical hurricanes of varying characteristics, including intensity, track, forward speed, and radius to maximum winds (a measure of storm size), with the Ike Dike concept implemented into the modeling.

12 References

Blain, C.A., J.J. Westerink, R.A. Luettich, Jr. and N.W. Scheffner, 1994, ADCIRC: an advanced three-dimensional circulation model for shelves coasts and estuaries, report 4: hurricane storm surge modeling using large domains, Dredging Research Program Technical Report, DRP-92-6, U. S. Army Engineers Waterways Experiment Station.

Bunpapong, M., Reid, R.O., and Whitaker, R.E., "An Investigation of Hurricane-Induced Forerunner Surge in the Gulf of Mexico," Technical Report CERC-85-5, Coastal Engineering Research Center, U.S. Army Corps of Engineers, September 1985.

Bunpapong, M., Reid, R.O., and Whitaker, R.E., "An Investigation of Hurricane-Induced Forerunner Surge in the Gulf of Mexico," Technical Report CERC-85-5, Coastal Engineering Research Center, U.S. Army Corps of Engineers, September 1985.

Cardone, V. J., C.V. Greenwood, and J. A. Greenwood. 1992. Unified program for the specification of tropical cyclone boundary layer winds over surfaces of specified roughness. Contract Rep. CERC 92-1. Vicksburg, MS: U.S. Army Corps of Engineers Waterways Experiment Station.

Cardone, V.J., A.T. Cox, J.A. Greenwood, and E.F. Thompson. 1994. Upgrade of tropical cyclone surface wind field model. Misc. Paper CERC-94-14, Vicksburg, MS: U.S. Army Corps of Engineers Waterways Experiment Station.

Cardone, V.J. and A.T. Cox. 2009. Tropical cyclone wind field forcing for surge models: critical issues and sensitivities. *Nat Hazards* 51: 29–47.

Chouinard, L.M. and C. Liu. 1997. Model for Recurrence Rate of Hurricanes in Gulf of Mexico. Journal of Waterway, Port, Coastal and Ocean Engineering 123(3): 113-119.

Coastal Protection and Restoration Authority (CPRA). 2013. Greater New Orleans Flood Protection System Notice of Completion – Design Assessment by Non-Federal Sponsor. Bell City, LA: Lonnie G. Harper & Associates.

Diaconis, P. (1988). Bayesian numerical analysis. Statistical Decision Theory and Related Topics IV.

Dietrich, J.C., S. Bunya, J.J. Westerink, B.A. Ebersole, J.M. Smith, J.H. Atkinson, R. Jensen, D.T. Resio, R.A. Luettich, C. Dawson, V.J. Cardone, A.T. Cox, M.D. Powell, H.J. Westerink, H.J. Roberts. 2010a. A High-Resolution Coupled Riverine Flow, Tide, Wind, Wind Wave and Storm Surge Model for Southern Louisiana and Mississippi: Part II – Synoptic Description and Analysis of Hurricanes Katrina and Rita. Monthly Weather Review, Volume 138, 378-404.

Dietrich, J.C., S. Bunya, J.J. Westerink, B.A. Ebersole, J.M. Smith, J.H. Atkinson, R. Jensen, D.T. Resio, R.A. Luettich, C. Dawson, V.J. Cardone, A.T. Cox, M.D. Powell, H.J. Westerink, H.J. Roberts. 2010b. A High-Resolution Coupled Riverine Flow, Tide, Wind, Wind Wave and Storm Surge Model for Southern Louisiana and Mississippi: Part II – Synoptic Description and Analysis of Hurricanes Katrina and Rita. Monthly Weather Review, Volume 138, 378-404.

East, J.W., Turco, M.J., and Mason, Jr., R.R., "Monitoring Inland Storm Surge and Flooding from Hurricane Ike in Texas and Louisiana, " Open File Report 2008-1365, March 2009.

Federal Emergency Management Agency (FEMA). 2008a. Mississippi coastal analysis project. Final Report: HMTAP Task Order 18, prepared for the Federal Emergency Management Agency, Department of Homeland Security. Gaithersburg, MD: URS Group, Inc.

Federal Emergency Management Agency (FEMA). 2008b. Hurricane Ike in Texas and Louisiana, High Water Marks, FEMA Mitigation Assessment Team Report (October 2008).

Federal Emergency Management Agency (FEMA). 2011. *Flood Insurance Study: Coastal Counties, Texas: Scoping and Data Review*. Denton, TX: Federal Emergency Management Agency, Region 6 (draft, in review).

Federal Emergency Management Agency (FEMA). 2012. Operating Guidance No. 8-12 for use by FEMA staff and Flood Mapping Partners: Joint probability – optimal sampling method for tropical storm surge.

Washington, DC: Federal Emergency Management Agency, Department of Homeland Security.

Federal Emergency Management Agency (FEMA). 2014. Redefinition of the Coastal Flood Hazard Zones in FEMA Region II: Analysis of the Coastal Storm Surge Flood Frequencies. Final Report prepared for the Federal Emergency Management Agency, Department of Homeland Security. Fairfax, VA: Risk Assessment, Mapping, and Planning Partners.

Günther, H. 2005. WAM cycle 4.5 version 2.0. Institute for Coastal Research, GKSS Research Centre, Geesthacht, Germany, 38 pp.

Interagency Performance Evaluation Task Force (IPET). 2009. Performance evaluation of the New Orleans and Southeast Louisiana Hurricane Protection System. Final Report of the Interagency Performance Evaluation Task Force. Washington, DC: U.S. Army Corps of Engineers, Department of the Army.

Jarvinen, B.R., C.J. Neumann, and M.A.S. Davis. 1984. A tropical cyclone data tape for the North Atlantic Basin, 1886–1983: contents, limitations, and uses. NOAA Tech. Memo 22. Miami, Florida: National Hurricane Center, National Weather Service.

Kennedy, A.B., Gravois, U., Zachry, B., Luettich, R., Whipple, T. Weaver, R., Reynolds, Fleming, J. Chen, Q., and Avissar, R. (2010). “Rapidly installed temporary gauging for waves and surge, and application to Hurricane Gustav”, Continental Shelf Research 30, 1743-1752.

Kennedy, A.B., Gravois, U., Zachry, B.C., Westerink, J.J., Hope, M.E., Dietrich, J.C., Powell, M.D., Cox, A.T., Luettich, R.L., and Dean, R.G. (2011). “Origin of the Hurricane Ike forerunner surge”, Geophys. Res. Lett., L08805, doi:10.1029/2011GL047090.

Komen, G. J., L. Cavaleri, M. Donelan, K. Hasselmann, S. Hasselmann, and P.A.E.M. Janssen. 1994. Dynamics and modelling of ocean waves. Cambridge, UK: Cambridge University Press, 560 pages.

Landsea, C.W., G.A. Vecchi, L.Bengtsson, and T.R. Knutson. 2010. Impact of Duration Thresholds on Atlantic Tropical Cyclone Counts. Journal of Climate 23 (10): 2508–19.

Landsea, C.W. and J.L. Franklin. 2013. Atlantic hurricane database uncertainty and presentation of a new database format. Monthly Weather Review 141(10): 3576–3592.

Luettich, R.A., Jr., J.J. Westerink, and N.W. Scheffner, 1992, ADCIRC: an advanced three-dimensional circulation model for shelves coasts and estuaries, report 1: theory and methodology of ADCIRC-2DDI and ADCIRC-3DL, Dredging Research Program Technical Report DRP-92-6, U.S. Army Engineers Waterways Experiment Station.

Mann, M.E., T.A. Sabbatelli, and U. Neu. 2007. Evidence for a Modest Undercount Bias in Early Historical Atlantic Tropical Cyclone Counts. Geophysical Research Letters 34(22): L22707.

Massey, T.C., Anderson, M.E., Smith, J.M., Gomez, J., and Jones, R., 2011. STWAVE: Steady-State Spectral Wave Model User's Manual for STWAVE. Version 6.0. ERDC/CHL SR-11-1, U.S. Army Engineer Research and Development Center.

Minka, T. P. (2000) Deriving quadrature rules from Gaussian processes. Technical Report, Statistics Department, Carnegie Mellon University.

Nadal-Caraballo, N.C., Melby, J.A., Gonzalez, V.M., and Cox, A.T., 2015. North Atlantic Coast Comprehensive Study (NACCS), Coastal Storm Hazards from Virginia to Maine, ERDC/CHL TR-15-5, U.S. Army Engineer Research and Development Center. (draft, under review)

National Oceanic and Atmospheric Administration (NOAA), Tides and Currents web site,
http://tidesandcurrents.noaa.gov/stations.html?type=Water+Levels

Neumann, C.J., G.W. Cry, E.L. Caso, and B.R. Jarvinen. 1985. Tropical Cyclones of the North Atlantic Ocean, 1871-1980. Asheville, NC: National Climatic Center.

O'Hagan, A. (1991). Bayes-Hermite quadrature. Journal of Statistical Planning and Inference, No. 29.

Resio, D.T., S.J. Boc, L. Borgman, V. Cardone, A.T. Cox, W.R. Dally, R.G. Dean, D. Divoky, E. Hirsh, J.L. Irish, D. Levinson, A. Niedoroda, M.D.

Powell, J.J. Ratcliff, V. Stutts, J. Suhada, G.R. Toro, and P.J. Vickery. 2007. White Paper on estimating hurricane inundation probabilities. Consulting Report prepared by USACE for FEMA. Vicksburg, MS: U.S. Army Engineer Research and Development Center.

Smith, J. M., A. R. Sherlock, and D. T. Resio. 2001. STWAVE: Steady-state spectral wave model user's manual for STWAVE, Version 3.0. ERDC/CHL SR-01-1. Vicksburg, MS. U.S. Army Engineer Research and Development Center.

Smith, J.M. 2007. Full-plane STWAVE with bottom friction: II. Model overview. CHETN-I-75. U.S. Army Engineer Research and Development Center.

Smith, J.M., Jensen, R.E., Kennedy, A.B., Dietrich, J.C., and Westerink, J.J. Waves in Wetlands: Hurricane Gustav. Proceedings of the 32nd Conference on Coastal Engineering. 2010.

Texas Coastal Ocean Observation Network (TCOON) web site, http://www.cbi.tamucc.edu/TCOON/

Thompson, E. F., and V. J. Cardone. 1996. Practical modeling of hurricane surface wind fields. ASCE J. of Waterway, Port, Coastal and Ocean Engineering, **122(**4): 195-205.

Toro, G.R. 2008. Joint probability analysis of hurricane flood hazards for Mississippi – Final URS Group Report in support of the FEMA-HMTAP flood study of the State of Mississippi. Boulder CO: Risk Engineering.

Toro, G.R., D.T. Resio, D.D., A.W. Niedoroda, and C. Reed. 2010. Efficient joint-probability methods for hurricane surge frequency analysis. *Ocean Engineering* 37(1): 125–34.

U.S. Army Corps of Engineers (USACE). 2009a. *Louisiana Coastal Protection and Restoration* (LACPR). Final Technical Report. New Orleans, LA: New Orleans District, Mississippi Valley Division, USACE.

U.S. Army Corps of Engineers (USACE). 2009b. *Mississippi Coastal Improvements Program (MSCIP), Hancock, Harrison, and Jackson*

Counties, Mississippi. Mobile, AL: Mobile District, South Atlantic Division, USACE.

U.S. Weather Bureau. Monthly Weather Review, September 1900, Vol. XXXVIII, No. 9.

Vecchi, G.A. and T.R. Knutson. 2011. Estimating Annual Numbers of Atlantic Hurricanes Missing from the HURDAT Database (1878–1965) Using Ship Track Density. *Journal of Climate* 24(6): 1736–1746.

Vickery, P.J., and B.O. Blanton. 2008. *North Carolina coastal flood analysis system hurricane parameter development*. Technical Report TR-08-06. Chapel Hill, NC: RENCI Renaissance Computing Institute.

WAMDI Group, 1988. The WAM Model - A Third Generation Ocean Wave Prediction Model. Journal of Physical Oceanography, 18, 1775-1810

Westerink, J.J., R.A. Luettich, A.M. Baptista, N.W. Scheffner and P. Farrar, 1992, Tide and storm surge predictions using finite element model, ASCE Journal of Hydraulic Engineering, 118(10):1373-1390.

Worley, S.J., S.D. Woodruff, R.W. Reynolds, S.J. Lubker, and N. Lott. 2005. ICOADS Release 2.1 Data and Products. *Journal of Climatology* 25:823-842.